

## I. SYLLABUS AND INTRODUCTION

The course is taught on basis of lecture notes which are supplemented by the textbook Ashcroft and Mermin. Some practical information:

- Professor: Michel van Veenendaal
- Office: Faraday West 223
- Tel: 815-753-0667 (NIU), 630-252-4533 (Argonne)
- e-mail: veenendaal@niu.edu
- web page: [www.niu.edu/~veenendaal](http://www.niu.edu/~veenendaal)
- Office hours: I am at NIU Tu/Th. Feel free to walk into my office at any time. You can always make an appointment if you are worried that I might not be there. Official office hours will be established if you feel that the “open door” policy does not work.
- Prerequisites: there are no official prerequisites for the course. However, a knowledge of quantum mechanics at the 560/561 level is recommended. Mathematical concepts that will be used are calculus, vector algebra, Fourier transforms, differential equations, linear algebra (in particular matrices and eigenvalues problems).
- Homework: several homework sets will be given. They will be posted on the web site.
- Midterm: one midterm will be given.
- Attendance: There is no required attendance.
- Additional further reading  
F. Wooten, *Optical Properties of Solids* (Academic Press, New York, 1972).

## CONTENTS

- *Background:* A sort background and history of solid-state physics is given.
- *The electronic structure: tight-binding method (1D).* First, we study a diatomic molecule starting from hydrogen wavefunctions. We create an understanding why two atoms prefer to form a molecule. The molecule is then made longer until an infinitely long one-dimensional molecule is formed. The eigenenergies of the chain are calculated analytically. As an additional example we consider the benzene molecule.
- *The electronic structure: nearly free-electron model (1D).* In this section, we start from the opposite limit and consider free electrons moving in one dimension. A periodic potential representing the presence of nuclei is then added.
- *Comparison of results for tight-binding and nearly-free electron model.* The results of the two opposite limits are compared and their connections are shown.
- *Other ways of keeping atoms together.* Different forms of crystal binding are discussed: covalent bonds, ionic crystals, and van der Waals forces.
- *Formalization: Bloch theorem.* The Bloch theorem and its connection to the periodicity of the lattice is discussed.
- *Phonons in one dimension.* In this section, nuclear vibrations are introduced. Collective nuclear motion leads to phonons. We first consider a monoatomic linear chain.
- *Periodicity and basis.* A linear chain is introduced consisting of alternating atoms of a different kind. This is known as a lattice plus a basis.
- *Effect of a basis on the electronic structure.* The effects of introducing two different types of atoms on the electronic structure is demonstrated. It is shown that a change in the periodicity can change the conductive properties from metallic to semiconducting.

- *Effect of a basis on the phonon dispersions.* For the phonon dispersion, the effect of introducing a basis is the creation of optical phonon modes in addition to the acoustical modes.
- *Crystal structures.* After introducing several concepts in one dimension, we have a closer look at crystal structures in two and three dimension. We look at the symmetry of crystals and their effects on the material properties.
- *Measuring crystal structure: Diffraction.* This section describes how neutrons, electron, and, in particular, X-rays are scattered from a crystal lattice. The focus on the conceptual understanding of diffraction. Bragg's law is derived.
- *The reciprocal lattice.* The reciprocal lattice (the Fourier transform of the lattice in real space) is introduced. The concepts of diffraction and Brillouin zone are formalized.
- *Free electron in two and three dimensions.* The free electron model is studied in two dimensions. Special attention is paid to the Brillouin zones, the Fermi surface for different electron fillings, the density of states,
- *Nearly-free electron in two dimensions.* A periodic potential is introduced in the free-electron model in two dimensions. The effects on the electronic structure and the Fermi surface are studied.
- *Tight-binding in two dimensions.* As in one dimension, the nearly free-electron model is compared to the tight-binding model and its differences and, in particular, the similarities are discussed.
- *The periodic table.* We now look at more realistic systems and see what electronic levels are relevant for the understanding of the properties of materials. The filling of the different atomic levels is discussed.
- *Band structure of selected materials: simple metals and noble metals.* We apply the concepts that we have learned in one and two dimensions to the band structure of real materials. First, aluminium is studied, which is a good example of a nearly free-electron model. We then compare the noble metals, such as copper and gold. Here, the  $s$  and  $p$  like electrons behave as nearly-free electrons. However, the  $d$  electrons behave more like tightly bound electrons.
- *Thermal properties.* In this section, we study the thermal properties of solids. In particular, we discuss the temperature dependence of the specific heat due to electrons and phonons. For phonons, we distinguish between acoustical and optical phonons.
- *Optical spectroscopy.* The optical properties of solids are discussed in a semi-classical model. Using the dielectric properties of materials, it is explained why metals reflect optical light, whereas insulators do not. The different colors of aluminium, gold, and silver are discussed.
- *Quantum-mechanical treatment of optical spectroscopy.* The relationship between the semiclassical approach of the optical properties of solids and their electronic structure is discussed. It is shown that the classical oscillators correspond to interband transitions.
- *Relation to absorption.* A relation is made between the dielectric function and absorption (Fermi's Golden Rule) as derived in quantum mechanics.
- *Thomas-Fermi screening.* Using the concepts of dielectric properties introduced in the previous section, it is explained why many systems behave like metals, despite the presence of strong Coulomb interactions. The idea is known as screening.
- *Many-particle wavefunctions.* It is shown how to construct many-particle wavefunctions. Many-particle effects become important when electrons and phonons can no longer be treated as independent particles due to electron-electron and electron-phonon interactions.
- *Magnetism.* Different types of magnetism are discussed. In diamagnetism, a local moment is created by the magnetic field. For paramagnetism, local moments are already present due to the presence of electron-electron interactions. The effect of the magnetic field is the alignment of the local moments.
- *Ferromagnetism.* In ferromagnetism, the magnetic moments in a materials align parallel spontaneously below a certain temperature.
- *Antiferromagnetism.* Antiferromagnetism is similar to ferromagnetism. However, the magnetic moments align in the opposite direction.

- *Phonons.* Phonons in three dimensions are formally derived. The phonons are quantized making them effective particles.
- *Electron-phonon interaction.* The interactions between the electrons and the phonons is derived.
- *Attractive potential.* It is shown how the interaction between the electrons and the phonons can lead to an attractive potential between the electrons.
- *Superconductivity and the BCS Hamiltonian.* Using an effective Hamiltonian including the attractive interaction between the electron, it is shown how a superconducting ground state can be made. This theory is known as BCS theory after Bardeen, Cooper, and Schrieffer.
- *BCS ground state wavefunction and energy gap.* The ground-state wavefunction and the energy gap of the BCS model are described.
- *Transition temperature.* The temperature where a solid becomes superconducting is calculated and its relation to the superconducting gap is derived.
- *Ginzburg-Landau theory.* This section describes a phenomenological model, known as Ginzburg-Landau theory, to describe superconductivity.
- *Flux quantization and the Josephson effect.* It is shown how magnetic flux is quantized due to the superconducting current. This quantization leads to peculiar effects in the current across an insulating barrier. This is known as the Josephson effect.

## II. BACKGROUND

*From Hoddesson, Braun, Teichamn, Weart, Out of the crystal maze, (Oxford University Press, 1992).*

Obviously, people have been interested in the properties of solids since the old ages. The ancient Greeks (and essentially all other cultures) classified the essential elements as earth, wind, air, and fire or in modern terms: solids, liquids, gases, and combustion (or chemical reactions in general). Whole periods have been classified by the ability to master certain solids: the stone age, the bronze age, the iron age. And even our information age is based for a very large part on our ability to manipulate silicon. Many attempts have been made to understand solids: from Greek philosophers via medieval alchemists to cartesian natural philosophers. Some macroscopic properties could be framed into classical mechanics. Optical conductivity in solids was worked out in the theories of Thomas Young and Jean Fresnel in the late eighteenth and early nineteenth century. Elastical phenomena in solids had a long history. Macroscopic theories for electrical conductivity were developed by, e.g. Georg Ohm and Ludwig Kirchhoff. Another good example of a mechanical model for a solid are the theories of heat conductivity developed in the early nineteenth century by Joseph Fourier. Franz Ernst Neumann developed a mechanical theory for the interaction between elasticity and optics, allowing him to understand anisotropy in materials such as the birefringence that occurs when an isotropic medium is subjected to pressure or uneven heating.

Another important ingredient to understanding solids is symmetry. Already in 1690, it was suggested by Huygens that the regular form of solids is intricately related to their physics. The first scientific theory of crystal symmetry was set up by René-Just Haüy in 1801-2, based on atomistic principles. This was extended upon by mineralogist Christian Samuel Weiss, who, however, completely rejected the atomistic approach. He introduced the concepts of crystallographic axis. The crowning achievement is the classification by Auguste Bravais that there are only 14 ways to order a set of points so that the neighborhood of any individual lattice point looks the same. In 1901, Woldemar Voigt published his book on crystallography classifying the 230 different space groups (and was shocked by the large number).

Another important nineteenth century development is the reemergence of the atomistic theories. The success of continuum theories (classical mechanics, electricity and magnetism, thermodynamics) had pushed atomistic thought to the background, in particular in physics (remember the trials and tribulation Ludwig Boltzmann went through in the acceptance of his statistical approach to thermodynamics which was often considered a nice thought experiment, but hopelessly complicated). However, chemical reactions clearly indicated the discrete nature of matter.

A microscopic theory proved elusive until the advent of quantum mechanics in the early twentieth century. Quantum mechanics is crucial in understanding condensed matter. For example, gases can be reasonably well described in a classical framework due to their low density. This means that we do not require quantum (Fermi-Dirac) statistics and we do not have to deal with atomic levels.

Theories started accelerating after the discovery of the electron by J. J. Thompson and Hendrik Lorentz (and mind you, Lorentz and Zeeman determined the  $e/m$  ratio before Thompson). The classical theory of solids essentially treats a solid as a gas of electrons in the same fashion as Boltzmann's theory of gases. This model was developed by Paul Drude (who, inexplicably, committed suicide at age 42, only a few days after his inauguration as professor at the University of Berlin). The theory was elaborated by Hendrik Lorentz. Although a useful attempt, the use of Maxwell-Boltzmann statistics as opposed to Fermi-Dirac statistics leads to gross errors with the thermal conductivity  $\kappa$  and the conductivity  $\sigma$  off by several orders of magnitude. The theory gets a lucky break with the Wiedemann-Franz law that the ratio  $\kappa/\sigma$  is proportional to the temperature  $T$ . (It is not quite clear to me why AM wants to start out with an essentially incorrect theory, apart from historic reasons... Then again, we also do not teach the Ptolemean system anymore). However, it was very important in that it was one of the first microscopic theories of a solid.

Early attempts to apply quantum mechanics to solids focused on specific heat as measured by Nernst. Specific heat was studied theoretically by Einstein and Debye. The difference in their approaches lies in their assumption on the momentum dependence of the oscillators. Einstein assumed one particular oscillator frequency representing optical modes. Debye assumed sound waves where the energy is proportional to the momentum. Phonon dispersion curves were calculated in 1912 by Max Born and Theodore von Kármán. However, again, this can again be done from Newton's equations.

However, further progress had to wait the development of quantum statistics which were not developed until 1926. In the meantime, the number of experimental techniques to study condensed matter was increasing. In 1908, Kamerlingh-Onnes and his low-temperature laboratory managed to produce liquid Helium. This led to the discovery of superconductivity in mercury (and in some ways the onset of "big" physics).

After discussions with Peter Paul Ewald in 1912, who was working on his dissertation with Sommerfeld on optical birefringence, Max von Laue successfully measured the diffraction of X-rays from a solid. The experiments were interpreted by William Henry Bragg and his son William Lawrence opening up the way for x-ray crystal analysis.

In 1926-7, Enrico Fermi and Paul Dirac established independently a statistical theory that included Wolfgang

Pauli's principle that quantum states can be occupied by only one electron. This property is inherently related to the antisymmetry of the wavefunctions for fermions. In 1927, Arnold Sommerfeld attempted a first theory of solids using Fermi-Dirac statistics. It had some remarkable improvements over the Drude-Lorentz model. The specific heat was significantly lower due to the fact that not all electrons participate in the conductive properties, but only the ones with the highest energies (i.e. the ones close to the Fermi level). However, the model still completely ignores the effect of the nuclei leading to significant discrepancies with various experiments including resistivity. Werner Heisenberg also had an interest in metals and proposed the problem to his doctoral student Felix Bloch. The first question that he wanted Bloch to address was how to deal with the ion in metals? Bloch assumed that the potential of the nuclei was more important than the kinetic energy. A tight-binding model as opposed to Sommerfeld's free-electron model and ended up with the theorem that the wavefunction can be written as  $\psi = e^{i\mathbf{k}\cdot\mathbf{r}}u(\mathbf{r})$ , plane wave modulated by a function that has the periodicity of the lattice. Another important development Rudolf Peierls and Léon Brillouin was the effect of the periodic potential in the opening of gaps at particular values of the momentum  $k$ , now known as Brillouin zones.

### III. THE ELECTRONIC STRUCTURE: TIGHT-BINDING METHOD (1D)

#### *AM Chapter 10*

A solid has many properties, such as crystal structure, optical properties (i.e. whether a crystal is transparent or opaque), magnetic properties (magnetic or antiferromagnetic), conductive properties (metallic, insulating), etc. Apart from the first, these properties are related to what is known as the electronic structure of a solid. The electronic structure essentially refers to the behavior of the electrons in the solid. Whereas the nuclei of the atoms that form the solid are fixed, the electronic properties vary wildly for different systems. Unfortunately, the electronic structure is complicated and needs to be often approximated using schemes that sometimes work and at other times fail completely. The behavior of the electrons is, as we know from quantum mechanics, described by a Hamiltonian  $H$ . In general, this Hamiltonian contains the kinetic energy of the electron, the potential energy of the nuclei, and the Coulomb interactions between the electrons. Especially, the last one is very hard to deal with. Compare this with a running competition. For the 100 m, the runners have their own lane and the interaction between the runners is minimal. One might consider each runner running for him/herself (obviously, this is not quite correct). However, for larger distances, the runners leave their lanes and start running in a group. We can no longer consider the runners as running independently, since they have to avoid each other, they might bump into each other, etc. This is a much more complicated problem. The same is true for solids. In some solids, we can treat the electrons as being more or less independent. In some solids, we have to consider the interactions between the electrons explicitly. For the moment, we will neglect the interactions between the electrons, even though for some systems, they can turn the conductive properties from metallic to insulating. Systems with strong electron-electron interactions are an important (and still largely unsolved) topic in current condensed-matter physics research. The enormous advantage is that we do not have a problem with  $N$  particles (where  $N$  is of the order of  $10^{23}$ ), but  $N$  times a one-particle problem. Of course, this is what you were used to so far. You probably remember the free-electron model (to which we will return later on). First, the bands were obtained (pretty easy since  $\varepsilon_{\mathbf{k}} = \hbar^2 k^2 / 2m$ ), and in the end you just filled these eigenstates up to the Fermi level. So far, you might not have realized that this was actually an approximation. This is the type of system we will be considering at the moment. So we are left with a Hamiltonian containing the kinetic energy of the electron, the potential to the nuclei, and some average potential due to the other electrons in the solid.

This is essentially an extension on the quantum-mechanical model of particles in a box with the periodic potential of the nuclei added later. We will come back to that in a while, but we start with a model that puts in the atoms explicitly (known as the tight-binding model). This allows us to start thinking about the crystal immediately, instead of putting it in as some afterthought. In general, we can write the Hamiltonian for the electron in a crystal as

$$H = H_{\text{el}} = \sum_i \frac{\mathbf{p}_i^2}{2m} + \frac{1}{4\pi\varepsilon_0} \sum_{ij} \frac{Z_j e^2}{|\mathbf{r}_i - \mathbf{R}_j|} + \frac{1}{2} \frac{1}{4\pi\varepsilon_0} \sum_{i \neq i'} \frac{e^2}{|\mathbf{r}_i - \mathbf{r}_{i'}|}. \quad (1)$$

This leaves out the kinetic energy of the nuclei and their interaction. We will come back to that later. Our first assumption is that the nuclei are fixed charges in space. The electrons move so fast that they do not notice the motion of the nuclei. This is not true and the interaction between electrons and the motion of the nuclei can lead to exciting phenomena such as superconductivity, but it is a good starting point. The first term in the equation is the kinetic energy of the electrons. The second term is the interaction between the electrons and the nuclei, where  $i$  sums over all the electrons in the solid and  $j$  sums over all the nuclei with charge  $Z_j e$ . The last term is the Coulomb interaction between the electrons. The factor  $1/2$  avoid double counting. Including this term makes it impossible to

solve the problem, except for very small systems. We need to simplify something. Option number one is to ignore it all together. This is a gross simplification, but doing that will help us to understand solids better. What is left is essentially electrons moving around in a potential landscape built up by the potentials of the nuclei.

Why can we still get a good idea when neglecting something not particularly negligible such as interaction between electrons. The trick is that we should not consider real nuclei, but effective nuclei. Consider lithium metal. Li has a configuration  $1s^2 2s$ . The electrons in the  $2s$  orbitals do not feel the  $3+$  nucleus of Li. Instead, they feel a potential which is closer to a  $\text{Li}^{1+}$  ion, i.e. the nucleus plus the two  $1s$  electrons. Therefore, there is an effective  $Z_{\text{eff}} \cong 1$  nucleus as opposed to a  $Z = 3$  nucleus. This concept of treating the electrons as an effective background potential is very important in condensed-matter physics. However, it should be noted that often it fails miserably.

Crystals can be very complicated, so let us start with something simple: a chain of atoms. Although some materials can indeed be described as a one-dimensional chain, we are more interested in the concepts, which are very similar in any dimension. Unfortunately, even a chain is rather complicated to start out with, so let us begin with just two atoms and later add more atoms to it to form the chain.

### 1. The hydrogen molecule

Let us also consider the simplest system: a system of Hydrogen-like atoms (again not very practical, since Hydrogen forms  $\text{H}_2$  molecules at room temperature, but still a model often used in theoretical physics). For each site, we only consider one orbital (in our Hydrogen example, this would be the  $1s$  orbital). So in total, we have two orbitals  $\varphi_1(\mathbf{r})$  and  $\varphi_2(\mathbf{r})$ , since we have two sites. However, this creates the impression that we have two different orbitals, whereas we only have one type of orbital but located at two different sites. We can therefore also write  $\varphi(\mathbf{r} - \mathbf{R}_1)$  and  $\varphi(\mathbf{r} - \mathbf{R}_2)$ , where  $\varphi(\mathbf{r})$  is the atomic orbital at the origin. With two orbitals in our basis set, we have a total of four matrix elements

$$\varepsilon = \int d\mathbf{r} \varphi^*(\mathbf{r} - \mathbf{R}_1) H \varphi(\mathbf{r} - \mathbf{R}_1) = \int d\mathbf{r} \varphi^*(\mathbf{r} - \mathbf{R}_2) H \varphi(\mathbf{r} - \mathbf{R}_2) \quad (2)$$

and

$$-t = \int d\mathbf{r} \varphi^*(\mathbf{r} - \mathbf{R}_1) H \varphi(\mathbf{r} - \mathbf{R}_2) = \left( \int d\mathbf{r} \varphi^*(\mathbf{r} - \mathbf{R}_1) H \varphi(\mathbf{r} - \mathbf{R}_2) \right)^*, \quad (3)$$

where we use vector notation to allow easy generalization to arbitrary dimension even though we are considering only problems in one dimension for the moment.

In the end, we only have two parameters  $\varepsilon$  and  $t$ . Note that for  $\varepsilon$  the two matrix elements are equivalent, since the on-site energy does not depend on the position in space. Note that for Hydrogen atoms, if  $|\mathbf{R}_1 - \mathbf{R}_2| \rightarrow \infty$ , we obtain  $\varepsilon = -13.6$  eV. The wavefunction  $\varphi(\mathbf{r} - \mathbf{R})$  would be a  $1s$  orbital. Since the nuclei are far apart the electron in the wavefunction at site  $\mathbf{R}_1$  will not feel the potential of the nucleus at site  $\mathbf{R}_2$  (this is basically the assumption when solving the Hydrogen atom, where the potential is that of a single nucleus). For  $t$ , the matrix elements are just each others conjugate.  $t$  is known as the transfer matrix element or hopping integral. We take put a minus sign here so that  $t$  will be a positive number. This matrix element will go to zero in the limit  $|\mathbf{R}_1 - \mathbf{R}_2| \rightarrow \infty$ . Note that  $t$  involves an integral of an orbital at site  $\mathbf{R}_1$  and one at  $\mathbf{R}_2$ . The orbitals are localized (generally, their size is of the order of the Bohr radius). If the nuclei are far apart, the product  $\varphi^*(\mathbf{r} - \mathbf{R}_1)\varphi(\mathbf{r} - \mathbf{R}_2)$  is very small everywhere in space. Hence, the matrix will be very small.

Let us take  $t$  to be a real number (which it is for Hydrogen atoms, since everything is real when using  $1s$  orbitals). We can also write this in a bra-ket notation

$$\varepsilon = \langle \mathbf{R}_1 | H | \mathbf{R}_1 \rangle = \langle \mathbf{R}_2 | H | \mathbf{R}_2 \rangle \quad (4)$$

$$t = -\langle \mathbf{R}_1 | H | \mathbf{R}_2 \rangle = -\langle \mathbf{R}_2 | H | \mathbf{R}_1 \rangle, \quad (5)$$

where  $|\mathbf{R}_i\rangle$  denotes the atomic wavefunction at site  $\mathbf{R}_i$ . For  $s$ -like orbitals, the matrix element would be negative, so  $t$  would be a positive number. This allows us to write the Hamiltonian for the two orbitals in the basis set as a matrix

$$H = \begin{pmatrix} \varepsilon & -t \\ -t & \varepsilon \end{pmatrix}. \quad (6)$$

Any vector can now be written as a linear combination of

$$|\mathbf{R}_1\rangle = \begin{pmatrix} 1 \\ 0 \end{pmatrix} \quad \text{and} \quad |\mathbf{R}_2\rangle = \begin{pmatrix} 0 \\ 1 \end{pmatrix}. \quad (7)$$

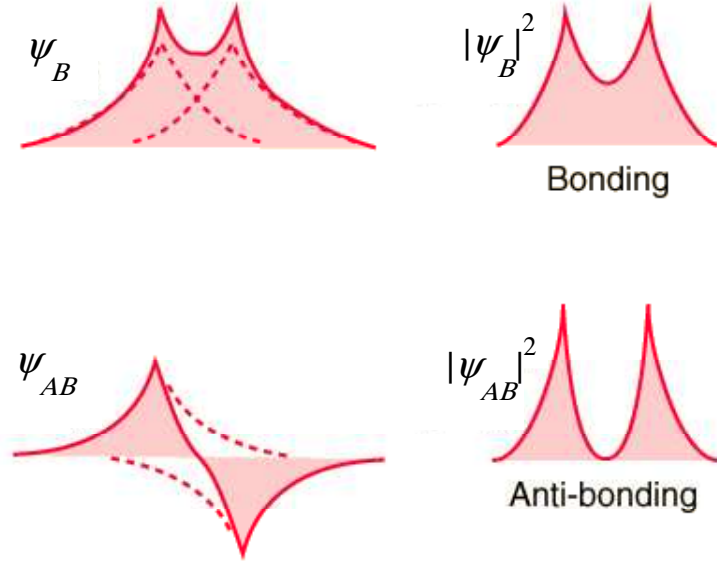


FIG. 1: The bonding  $\psi_B$  and  $\psi_{AB}$  wavefunctions for the hydrogen  $H_2$  are given on the left. The probabilities are on the right.

Let us work with the Hamiltonian on  $|\mathbf{R}_1\rangle$

$$H = \begin{pmatrix} \varepsilon & -t \\ -t & \varepsilon \end{pmatrix} \begin{pmatrix} 1 \\ 0 \end{pmatrix} = \begin{pmatrix} \varepsilon \\ -t \end{pmatrix} = \varepsilon|\mathbf{R}_1\rangle - t|\mathbf{R}_2\rangle \quad (8)$$

Therefore if  $t = 0$ ,  $H|\mathbf{R}_1\rangle = \varepsilon|\mathbf{R}_1\rangle$ , i.e.  $|\mathbf{R}_1\rangle$  would be an eigenstate of the Hamiltonian. However, the matrix element  $t$  brings the electron from atom 1 to site 2. The matrix element  $t$  is therefore often called a transfer matrix element or a hopping matrix element. Note that the Hamiltonian is not diagonal and eigenstates will be of the form  $|\psi\rangle = a_1|\mathbf{R}_1\rangle + a_2|\mathbf{R}_2\rangle$ . We would like to solve the Schrödinger equation

$$H|\psi\rangle = E|\psi\rangle. \quad (9)$$

We can split this out into different components as

$$\langle \mathbf{R}_i | H | \psi \rangle = E \langle \mathbf{R}_i | \psi \rangle, \quad (10)$$

with  $i = 1, 2$ . There is a complication in that the overlap matrix elements  $S = \langle \mathbf{R}_1 | \mathbf{R}_2 \rangle = \int d\mathbf{r} \varphi^*(\mathbf{r} - \mathbf{R}_1) \varphi(\mathbf{r} - \mathbf{R}_2) \neq 0$ . Taking this into account, we obtain

$$\begin{pmatrix} \varepsilon & -t \\ -t & \varepsilon \end{pmatrix} |\psi\rangle = E \begin{pmatrix} 1 & S \\ S & 1 \end{pmatrix} |\psi\rangle \quad (11)$$

Note that  $\langle \mathbf{R}_1 | \mathbf{R}_1 \rangle = \langle \mathbf{R}_2 | \mathbf{R}_2 \rangle = 1$ . The eigenvalues can be found by solving the determinant

$$\begin{vmatrix} \varepsilon - E & -t - ES \\ -t - ES & \varepsilon - E \end{vmatrix} = 0. \quad (12)$$

This gives the equation

$$(\varepsilon - E)^2 - (-t - ES)^2 = 0 \quad \Rightarrow \quad \varepsilon - E = \pm(-t - ES) \quad \Rightarrow \quad E_{B/AB} = \frac{\varepsilon \mp t}{1 \pm S}. \quad (13)$$

In this case, the overlap simply renormalizes the energies. The calculation becomes simpler if we forget about the overlap between the orbitals, which we will do in the remainder, and take  $S = 0$ . This gives  $E_{B/AB} = \varepsilon \mp t$ . The eigenstates are also easily obtained and are

$$|\psi_{B/AB}\rangle = \frac{1}{\sqrt{2}}(|\mathbf{R}_1\rangle \pm |\mathbf{R}_2\rangle). \quad (14)$$

Note that for  $\langle \mathbf{R}_1 | H | \mathbf{R}_2 \rangle < 0$  the bonding ( $B$ ) combination is the lowest (the antibonding ( $AB$ ) is the lowest for  $\langle \mathbf{R}_1 | H | \mathbf{R}_2 \rangle > 0$ ). An electron spends an equal amount of time on atom 1 as it does on atom 2, as it should, because there is atom 1 is equivalent to atom 2. In the bonding orbital, the wavefunction is a lot smoother (note that the anti bonding orbital has a node between the two atoms). This reduces the kinetic which is proportional to the gradient of the wavefunction through to the  $\nabla^2 \psi$  term in the Hamiltonian. The lowering of the kinetic energy due to the delocalization of the wavefunction is also important in keeping solids together. These are the well-known bonding-antibonding combinations of a  $H_2$  molecule. Each atom contributes one electron. The two electrons will go into the bonding orbital, giving

$$|\psi_{B\uparrow}\psi_{B\downarrow}\rangle = \frac{1}{2}(|\mathbf{R}_1 \uparrow \mathbf{R}_1 \downarrow\rangle + |\mathbf{R}_1 \uparrow \mathbf{R}_2 \downarrow\rangle + |\mathbf{R}_2 \uparrow \mathbf{R}_1 \downarrow\rangle + |\mathbf{R}_2 \uparrow \mathbf{R}_2 \downarrow\rangle), \quad (15)$$

where we can put two electrons in the bonding orbital due to the spin degree of freedom. Note that the probability of finding the two electrons on the same atom equal that of finding one electron on each atom. This would be surprising if electrons really interacted strongly with each other. However, we neglected that. As said, the energy gain is a result of the delocalization of the wave function. This does not always work. Note that the antibonding states are actually higher in energy. For example, a Helium atom has two electrons in the  $1s$ . When bringing two He atoms together two form a  $He_2$  molecule, we can in principle form the same bonding and antibonding wavefunctions. However, since we now have four electrons in total we have to fill up both the bonding and antibonding states gives an energy of  $2(\varepsilon - t) + 2(\varepsilon + t) = 4\varepsilon$ . Therefore, He cannot take any energetic gain from the formation of the bonding and antibonding combinations and no real bonding is formed. There is another way to look at this. The  $2s$  electrons from one helium atom cannot delocalize to the neighboring helium atom, since the  $2s$  orbital of that atom is full and Pauli's principle forbids the delocalization. Therefore,  $He_2$  does not bond and that is why He is a noble element.

## 2. A linear chain of $1s$ orbitals

Obviously, this is not much of a solid. However, it is straightforward to extend this procedure to chains of arbitrary length  $N$ . Let us take the atoms on a chain to be numbered  $1, 2, 3, \dots, N$ . General wavefunctions for  $N$  sites can then be written as

$$\psi(\mathbf{r}) = \sum_{\mathbf{R}} a_{\mathbf{R}} \phi(\mathbf{r} - \mathbf{R}) \quad \text{or} \quad |\psi\rangle = \sum_{\mathbf{R}} a_{\mathbf{R}} |\mathbf{R}\rangle. \quad (16)$$

Again, we want to solve the Schrödinger equation  $H|\psi\rangle = E|\psi\rangle$ . For the  $\mathbf{R}'$ 'th component, we obtain

$$\langle \mathbf{R}' | H | \psi \rangle = E \langle \mathbf{R}' | \psi \rangle \quad \Rightarrow \quad \sum_{\mathbf{R}} \langle \mathbf{R}' | H | \mathbf{R} \rangle a_{\mathbf{R}} = E \sum_{\mathbf{R}} \langle \mathbf{R}' | \mathbf{R} \rangle a_{\mathbf{R}} = E a_{\mathbf{R}'}, \quad (17)$$

where we have assumed  $\langle \mathbf{R}' | \mathbf{R} \rangle = \delta_{\mathbf{R}, \mathbf{R}'}$ . We can write this in matrix form as

$$\begin{pmatrix} H_{11} & \cdots & H_{1N} \\ \vdots & & \vdots \\ H_{N1} & \cdots & H_{NN} \end{pmatrix} \begin{pmatrix} a_1 \\ \vdots \\ a_N \end{pmatrix} = E \begin{pmatrix} a_1 \\ \vdots \\ a_N \end{pmatrix}, \quad (18)$$

where  $H_{ij} = \langle \mathbf{R}_i | H | \mathbf{R}_j \rangle$ . As before, we have  $H_{nn} = \varepsilon$ . If atoms are on neighboring sites, we have  $H_{n, n+1} = -t$ . In principle,  $H_{n, n+2}$ ,  $H_{n, n+3}$ , etc. are nonzero (known as next-nearest neighbor and next-next nearest neighbor hopping matrix elements), but we will take them zero for simplicity. This gives a matrix

$$H = \begin{pmatrix} \varepsilon & -t & 0 & 0 & \cdots & & & & & & \\ -t & \varepsilon & -t & 0 & 0 & \cdots & & & & & \\ 0 & -t & \varepsilon & -t & 0 & 0 & \cdots & & & & \\ 0 & 0 & -t & \varepsilon & -t & 0 & 0 & \cdots & & & \\ \cdots & 0 & 0 & -t & \varepsilon & -t & 0 & 0 & \cdots & & \\ & \cdots & 0 & 0 & -t & \varepsilon & -t & 0 & 0 & \cdots & \\ & & & & & & \cdot & \cdot & \cdot & \cdot & \end{pmatrix} \quad (19)$$

Although, not easily solvable by hand, the energies can be found using some computer program that solves eigenvalue problems. For different lengths  $N$ , the eigenvalues are given in Fig. 2. We have taken the constant shift  $\varepsilon = 0$ . The



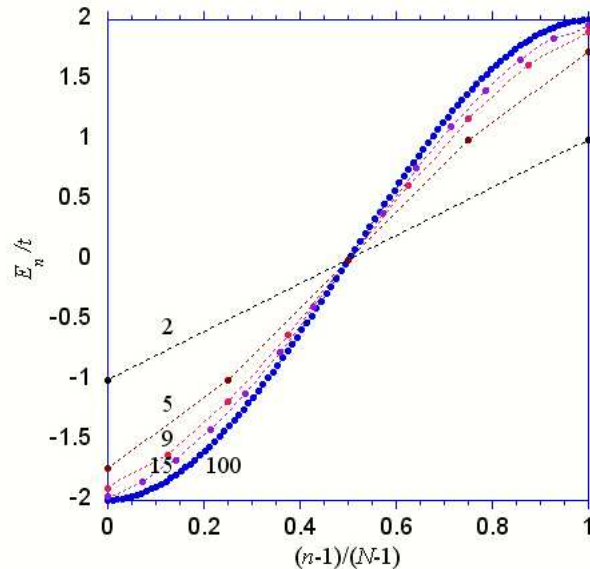


FIG. 2: The eigenvalues of a linear chain of 2, 5, 9, 15, 100 atoms with a hopping matrix element  $t$  between neighboring atoms.

eigenvalues  $E_n$  with  $n = 1, \dots, N$  are ordered and plotted as a function of  $(n-1)/(N-1)$ , i.e. from 0 to 1. As we have seen before, for  $N = 2$ , the eigenvalues are  $\pm t$ . However, if we increase the length of the chain, we see that the eigenvalues approach a continuous curve. The extrema of the curve are  $\pm 2t$ . The question is what is this curve and can we obtain this curve in different fashion apart from solving the matrix by brute force?

First, we have to realize that we want to study bulk systems or systems that are essentially infinity. The study of surfaces is a whole field in itself but not our focus at the moment. For small chains the number of atoms close to the edge of the chain is relatively large. So we can study a large system, but we can also introduce a mathematical trick. Note, that none of the atoms in the chain is equivalent, since they all have a different distance to the end of the chain. However, if we connect the two ends of the chain to each other, all the atoms become equivalent. This is known as periodic boundary conditions. Although, this is essentially a mathematical trick, in some systems this is physically realized. The best known example would be a benzene ring consisting of six carbon atoms. However, in two and three dimensions, this is more difficult to realize. In two dimensions, the system would be a torus (which could be achieved, maybe, with a carbon nanotube), but in three dimension, it is impossible to realize. Let us go back to the diatomic molecule. Applying periodic boundary condition implies that 1 is connected to 2, but 2 is again connected to 1. This leads to a doubling of the transfer matrix element, giving a Hamiltonian:

$$H = \begin{pmatrix} \varepsilon & -2t \\ -2t & \varepsilon \end{pmatrix}. \quad (20)$$

The eigenvalues are  $E_{1,2} = \mp 2t$ . Note that this is equal to the extrema in the continuous curve we obtained for large  $N$ . This is a significant difference from the  $\pm t$ , we obtained earlier. We could expect that, because all atoms in the “chain” are at the end of the chain. For larger

$$H = \begin{pmatrix} \varepsilon & -t & 0 & 0 & \dots & & & 0 & -t \\ -t & \varepsilon & -t & 0 & 0 & \dots & & 0 & 0 \\ 0 & -t & \varepsilon & -t & 0 & 0 & \dots & & \\ 0 & 0 & -t & \varepsilon & -t & 0 & 0 & \dots & \\ \dots & 0 & 0 & -t & \varepsilon & -t & 0 & 0 & \dots \\ & \dots & 0 & 0 & -t & \varepsilon & -t & 0 & 0 & \dots \\ & & & & \cdot & \cdot & \cdot & \cdot & & \\ 0 & 0 & & & \cdot & \cdot & 0 & -t & \varepsilon & -t \\ -t & 0 & & & \cdot & \cdot & \cdot & 0 & -t & \varepsilon \end{pmatrix} \quad (21)$$

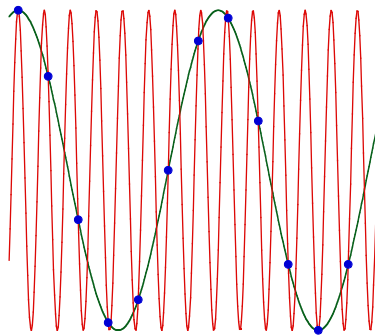


FIG. 3: The lines give the values of  $e^{ikx}$  and  $e^{(k+K)x}$  as a function of  $x$ . We have taken  $k = 0.3\pi$  and  $K = 2\pi$ . The dots indicate the values at the atomic positions. Note that the Fourier transform only includes these values.

Obviously, when  $N$  is very large (and number of atoms are generally very large numbers), this one extra matrix element will not affect the majority of the eigenvalues, so the eigenvalues with and without periodic boundary conditions should be virtually identical. If you solve this matrix you find out that the eigenvalues always lie on the curve that is obtained when  $N \rightarrow \infty$ . This curve is known as a band. The electronic structure is quite often known as the band structure.

So what is missing here? The essential ingredient is translational symmetry. Although we are all attached to real space, it is the periodicity that is really important. When there are milemarkers along the road, you do not say there is a mile marker at 1 mile, and one at 2 miles, and one at 3 miles. You say there is a mile marker every 1 mile. In a more mathematical term, we should be considering Fourier transforms. The quantity that is related to space by Fourier transform is momentum (the other important dimension is time, which is related to frequency by Fourier transform, which, in quantum mechanics is directly related to energy). In free space, space is continuous, and therefore the momentum is continuous as well. Conservation of momentum in classical mechanics is inherently related to the translational symmetry of space. When we go to a solid, the translational symmetry of space is no longer continuous, but related to the interatomic distances and therefore discrete. We applied periodic boundary conditions so we need to satisfy:

$$e^{ik(x+L)} = e^{ikx} \quad (22)$$

where the length of the chain is  $L = Na$ , with  $a$  the distance between the atoms. This means if we displace ourselves by  $L$  (the length of the chain), we end up at the same position due to the periodic boundary conditions. This implies that

$$kL = \pm 2n\pi \Rightarrow k = \pm \frac{2n\pi}{L}, \quad (23)$$

where  $n$  is an integer. This would lead to an infinite amount of wavenumbers  $k$ . This is not entirely correct. Before doing a Fourier transform, we had  $N$  orbitals, one for each site. After the Fourier transform, we should still end up with the same number of states. Therefore, since we have positive and negative numbers, the maximum  $n$  is  $N/2$ . The allowed  $k$  values are therefore

$$k = 0, \pm \frac{2\pi}{L}, \pm \frac{4\pi}{L}, \dots, \pm \frac{\pi}{a}. \quad (24)$$

So we only have  $k$  values in the region  $[-\frac{\pi}{a}, \frac{\pi}{a}]$ . You might wonder what happened to all the other  $k$  values. From a point of view of periodicity, they are exactly equivalent. Figure 3 shows a comparison between  $e^{ikx}$  and  $e^{i(k+2\pi/a)x}$  (where for the example  $k$  is taken  $0.3\pi$ ). Although the functions are of course different, they have the same values at the sites of the atoms (indicated by the blue dots). However, you might remember from Fourier analysis that you often need all  $k$  values to build special functions (e.g. a square or a delta function) and there might be structure in the wavefunction that Fourier components with a larger  $k$  value. However, the  $k$  is only related to the periodic part of the wavefunction. These smaller structures are related to the atomic part of the wavefunction

$$\varphi_{\mathbf{k}}(\mathbf{r}) = \frac{1}{\sqrt{N}} \sum_{\mathbf{R}} e^{i\mathbf{k}\cdot\mathbf{R}} \varphi(\mathbf{r} - \mathbf{R}). \quad (25)$$

Note that the Fourier transform only includes the values of the exponentials at the atomic positions. Therefore, any  $k + 2\pi n$ , with  $n$  an integer, is equivalent to  $k$ . Essentially, this is a unitary transformation of  $N$  wavefunctions in real

space to a  $\mathbf{k}$  dependent basis. We can also inverse this procedure

$$\varphi(\mathbf{r} - \mathbf{R}) = \frac{1}{\sqrt{N}} \sum_{\mathbf{k}} e^{-i\mathbf{k}\cdot\mathbf{R}} \varphi_{\mathbf{k}}(\mathbf{r}). \quad (26)$$

We can also write this in bra-ket notation

$$|\mathbf{k}\rangle = \frac{1}{\sqrt{N}} \sum_{\mathbf{R}} e^{i\mathbf{k}\cdot\mathbf{R}} |\mathbf{R}\rangle \quad \text{and} \quad |\mathbf{R}\rangle = \frac{1}{\sqrt{N}} \sum_{\mathbf{k}} e^{-i\mathbf{k}\cdot\mathbf{R}} |\mathbf{k}\rangle. \quad (27)$$

We now want to understand what the Hamiltonian looks like in this new basis set. Let us first rewrite the Hamiltonian in bra-ket notation in real space. Note that

$$|\mathbf{R}_i\rangle\langle\mathbf{R}_j| = i \rightarrow \begin{pmatrix} 0 \\ \cdot \\ \cdot \\ 0 \\ 1 \\ 0 \\ \cdot \end{pmatrix} (0, 0, \dots, 0, 1, 0, \dots) = i \rightarrow \begin{pmatrix} \cdot & \cdot & \cdot \\ \dots & 0 & 0 & 0 & \dots \\ \dots & 0 & 1 & 0 & \dots \\ \dots & 0 & 0 & 0 & \dots \\ \cdot & \cdot & \cdot \end{pmatrix} \quad (28)$$

$\uparrow$   
 $j$

using this we can rewrite the matrix in Eqn. (21)

$$H = \sum_{\mathbf{R}, \mathbf{R}'} |\mathbf{R}'\rangle\langle\mathbf{R}'| H |\mathbf{R}\rangle\langle\mathbf{R}| = -t \sum_{\mathbf{R}, \boldsymbol{\delta}} |\mathbf{R} + \boldsymbol{\delta}\rangle\langle\mathbf{R}|, \quad (29)$$

where  $\boldsymbol{\delta}$  is a vector connecting  $\mathbf{R}$  to its nearest neighbors (the atoms left and right of the atom in a chain). The Fourier transform can be made by inserting the definitions into the Hamiltonian:

$$H = -t \sum_{\mathbf{R}, \boldsymbol{\delta}} \frac{1}{N} \sum_{\mathbf{k}, \mathbf{k}'} e^{-i\mathbf{k}\cdot(\mathbf{R}+\boldsymbol{\delta})} |\mathbf{k}\rangle\langle\mathbf{k}'| e^{i\mathbf{k}'\cdot\mathbf{R}} \quad (30)$$

$$= -t \sum_{\mathbf{k}, \mathbf{k}'} \left( \frac{1}{N} \sum_{\mathbf{R}} e^{i(\mathbf{k}'-\mathbf{k})\cdot\mathbf{R}} \right) \left( \sum_{\boldsymbol{\delta}} e^{-i\mathbf{k}\cdot\boldsymbol{\delta}} \right) |\mathbf{k}\rangle\langle\mathbf{k}'| \quad (31)$$

$$= \sum_{\mathbf{k}, \mathbf{k}'} \delta_{\mathbf{k}, \mathbf{k}'} \varepsilon_{\mathbf{k}} |\mathbf{k}\rangle\langle\mathbf{k}'|. \quad (32)$$

We see that the Hamiltonian is diagonal in  $\mathbf{k}$  due to the delta function. The diagonal matrix elements (which are directly the eigenvalues) are given by

$$\varepsilon_{\mathbf{k}} = -t \sum_{\boldsymbol{\delta}} e^{-i\mathbf{k}\cdot\boldsymbol{\delta}}. \quad (33)$$

The nearest-neighbor vectors for a chain in the  $x$ -direction are given by  $\boldsymbol{\delta} = \pm a\hat{\mathbf{x}}$ , where  $\hat{\mathbf{x}}$  is a unit vector in the  $x$ -direction.

$$\varepsilon_{\mathbf{k}} = -t(e^{ika} + e^{-ika}) = -2t \cos ka, \quad (34)$$

where  $\mathbf{k} = k\hat{\mathbf{x}}$ . Since  $k$  goes from  $-\frac{\pi}{a}$  to  $\frac{\pi}{a}$ , the eigenvalues lie on a cosine between  $-2t$  and  $2t$ , see Fig. 4.

### 3. The benzene molecule

The Benzene molecule ( $\text{C}_6\text{H}_6$ ) consists of 6 carbon atom that form a hexagon, see Fig. 5. The hydrogen atoms are attached to the carbons. Since the atomic number of carbon is six, we have a total of  $6 \times (1 + 6) = 42$  electrons. However, 12 of these are strongly bound in the Carbon  $1s$  orbitals (with a binding energy of more than 280 eV). For molecular bonding, we can ignore those. The more important ones are the  $2s$  and  $2p$  orbitals of carbon and the  $1s$

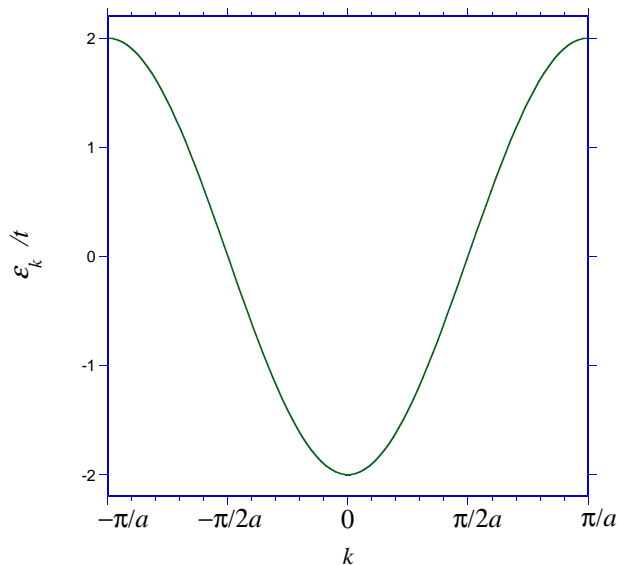


FIG. 4: The eigenenergies for a single tight-binding band  $\varepsilon_k = -2t \cos k$  as a function of  $k$ .

orbitals of hydrogen. Some of these form strong covalent bonds including so-called  $sp^2$  hydrids. We will deal with covalent bonding later. However, from Fig. 5, we can see that there are 12 covalent bonds, known as  $\sigma$  (sigma) bonds. These are comparable to the bonding states of the hydrogen molecule. We can see six bonds between the carbon atoms and six between the carbon and hydrogen atoms. Since each bond can contain two electrons (again, compare the  $H_2$  molecule), this accounts for another 24 electrons. This leaves us with  $42 - 12 - 24 = 6$  electrons. In a model based on bonding this allows for three more bonds, known as pi ( $\pi$ ) bonding. These should be between the carbon since the hydrogen already have their bond (related to the  $1s$  orbitals) and each carbon needs four bonds (one for the  $2s$  and three for the  $2p$ ). However, this leaves us with two possible configurations, see Fig. 5. The idea developed in the nineteenth century by Kekulé i is that the molecule switches between the two configurations.

However, we can apply the ideas from the previous sections to the benzene molecule. We can define the matrix element between  $p_z$  orbitals on carbon atoms on neighboring sites  $i$  and  $j$  as

$$t = -\langle p_{zi} | h | p_{zj} \rangle = \int d\mathbf{r} \varphi_{p_z}(\mathbf{r} - \mathbf{R}_i) H \varphi_{p_z}(\mathbf{r} - \mathbf{R}_j). \quad (35)$$

Note that  $t > 0$ . We do not need the conjugate, since the  $p_z$  are real orbitals. The determinant is given by

$$\begin{vmatrix} E_0 - E & -t & 0 & 0 & 0 & -t \\ -t & E_0 - E & -t & 0 & 0 & 0 \\ 0 & -t & E_0 - E & -t & 0 & 0 \\ 0 & 0 & -t & E_0 - E & -t & 0 \\ 0 & 0 & 0 & -t & E_0 - E & -t \\ -t & 0 & 0 & 0 & t & E_0 - E \end{vmatrix}, \quad (36)$$

where  $E_0$  is the binding energy of the  $p_z$  orbital. Note the presence of the  $-t$  in the upper-right and bottom-left corner. This is the matrix element completing the hexagon, i.e. connecting carbon atoms 1 and 6. This matrix element would be absent when studying a linear hydrocarbon with six carbon atoms (hexadiene). The eigenvalues are found to be

$$E = E_0 - 2t, E_0 - t, E_0 - t, E_0 + t, E_0 + t, E_0 + 2t. \quad (37)$$

The 6  $\pi$  electrons go into the lowest molecular orbitals giving a total energy of  $E = 6E_0 - 8t$ .

The wavefunction for the eigenstate with energy  $E_0 - 2t$  is completely symmetric

$$\psi_1 = \frac{1}{\sqrt{6}}(\psi_{p_{1z}} + \psi_{p_{2z}} + \psi_{p_{3z}} + \psi_{p_{4z}} + \psi_{p_{5z}} + \psi_{p_{6z}}), \quad (38)$$

and contains two electrons. This gives a different picture than that suggested by that of molecular bonds. An electron in the  $\psi_1$  orbital is delocalized over all the six carbon atoms and not localized in bonds between two carbon atoms.

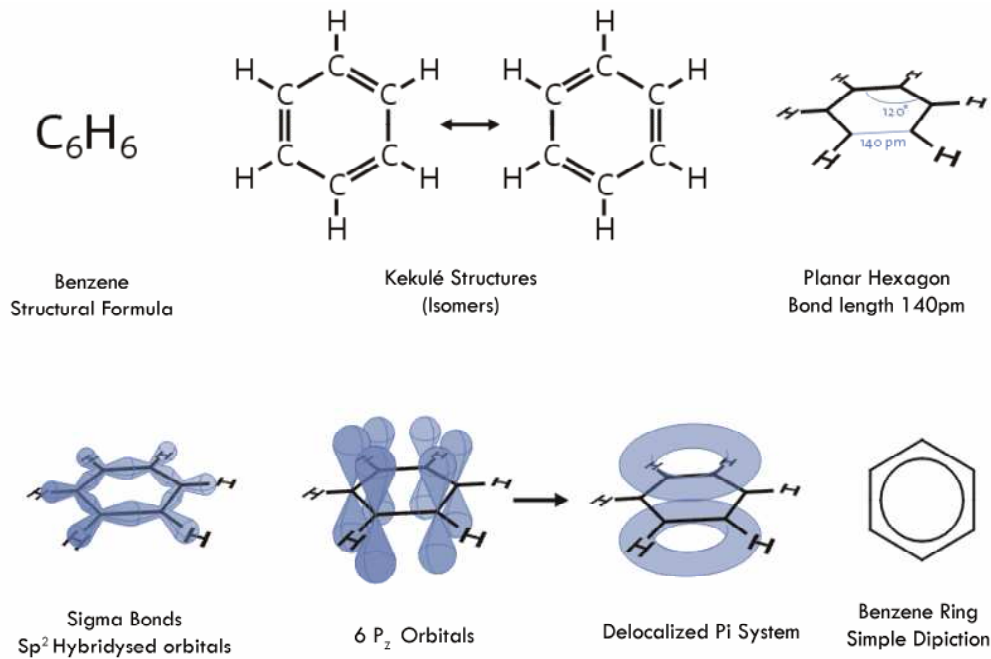


FIG. 5: The benzene molecule  $C_6H_6$  forms a hexagon. In the electronic structure of a benzene molecule there are strong covalent bonds formed by the  $sp^2$  hybrids. The  $p_z$  orbitals that stick out of the plane of the molecule bond less strongly and the electrons delocalize. Already in the nineteenth century, it was recognized by Kekulé, that there are two different possibilities for bonding which are both equivalent. A more modern way is considering the electrons delocalized in molecular bonds.

This is the reason why in modern notations of the benzen molecule, the  $\pi$  states are indicated by a circle, see Fig. 5. The two wavefunctions at energy  $E_0 - t$  are

$$\psi_2 = \frac{1}{\sqrt{3}}\left(\frac{1}{2}\psi_{p_{1z}} - \frac{1}{2}\psi_{p_{2z}} - \psi_{p_{3z}} - \frac{1}{2}\psi_{p_{4z}} + \frac{1}{2}\psi_{p_{5z}} + \psi_{p_{6z}}\right), \quad (39)$$

and

$$\psi_3 = \frac{1}{2}(\psi_{p_{1z}} + \psi_{p_{2z}} - \psi_{p_{4z}} - \psi_{p_{5z}}). \quad (40)$$

Since their energies are degenerate, any linear combination of  $\psi_2$  and  $\psi_3$  is also an eigenfunction. These two wavefunctions contain the other four electrons. The wavefunctions for  $E_0 + t$  are

$$\psi_4 = \frac{1}{\sqrt{3}}\left(\frac{1}{2}\psi_{p_{1z}} + \frac{1}{2}\psi_{p_{2z}} - \psi_{p_{3z}} + \frac{1}{2}\psi_{p_{4z}} + \frac{1}{2}\psi_{p_{5z}} - \psi_{p_{6z}}\right), \quad (41)$$

and

$$\psi_5 = \frac{1}{2}(\psi_{p_{1z}} - \psi_{p_{2z}} + \psi_{p_{4z}} - \psi_{p_{5z}}). \quad (42)$$

Finally the wavefunction at energy  $E_0 + 2t$  is given by

$$\psi_6 = -\frac{1}{\sqrt{6}}(\psi_{p_{1z}} - \psi_{p_{2z}} + \psi_{p_{3z}} - \psi_{p_{4z}} + \psi_{p_{5z}} - \psi_{p_{6z}}). \quad (43)$$

The last three orbitals are empty. Note that they look very similar to the first three wavefunction except that the signs have changed. Instead of having bonding between neighboring atoms we have antibonding states.

Although at first sight this might seem like some coefficients which just happen to come out of a calculation, on further inspection you can see that there is some system to the coefficients. A rather trivial one is

$$\psi_1 = \frac{1}{\sqrt{6}} \sum_n \psi_{p_{nz}}. \quad (44)$$

But  $\psi_6$  we can write as

$$\psi_6 = \frac{1}{\sqrt{6}} \sum_n \psi_{p_{nz}} \cos n\pi. \quad (45)$$

Looking more carefully at the wavefunctions, we see that

$$\psi_2 = \frac{1}{\sqrt{3}} \sum_n \psi_{p_{nz}} \cos n\frac{\pi}{3} \quad (46)$$

and

$$\psi_3 = \frac{1}{\sqrt{3}} \sum_n \psi_{p_{nz}} \sin n\frac{\pi}{3}. \quad (47)$$

The same thing we can do for  $\psi_4$  and  $\psi_5$ , but now using  $2\pi/3$ . In addition, since  $\psi_2$  and  $\psi_3$  are degenerate, we can make linear combinations of them that are still eigenfunctions

$$\psi_{2,3}^+ = \frac{1}{\sqrt{2}}(\psi_2 + i\psi_3) = \frac{1}{\sqrt{6}} \sum_n \psi_{p_{nz}} e^{in\frac{\pi}{3}}, \quad (48)$$

and

$$\psi_{2,3}^- = \frac{1}{\sqrt{2}}(\psi_2 - i\psi_3) = \frac{1}{\sqrt{6}} \sum_n \psi_{p_{nz}} e^{-in\frac{\pi}{3}}. \quad (49)$$

The same can be done for  $\psi_4$  and  $\psi_5$ . So it appears that the eigenstates look like a Fourier transform  $\varphi_{k'}$  of the states  $\psi_{p_{nz}}$  in real space

$$\varphi_{k'} = \frac{1}{\sqrt{6}} \sum_n \psi_{p_{nz}} e^{-ik'n}, \quad k' = 0, \pm\frac{\pi}{3}, \pm\frac{2\pi}{3}, \pi. \quad (50)$$

In fact, even the eigenvalues can be written as  $E_k = E_0 + 2t \cos k$ . Note that we have an effective lattice spacing of  $a \equiv 1$ . We can always go back to the real lattice spacing by taking  $k = \frac{k'}{a}$  and wherever we have  $k'$  we have to replace it by  $ka$ . This all corresponds nicely to what we observed before that when applying periodic boundary conditions, we could solve the eigenstates exactly. Here the periodic boundary conditions are not an artificial construction, but a physical reality due to the closed loop.

#### IV. THE ELECTRONIC STRUCTURE: NEARLY FREE-ELECTRON MODEL (1D)

##### *AM Chapter 9*

In the previous chapter, we started from atoms and atomic orbitals. The potential of the nucleus played a dominant role. When bringing the atoms together, we observed the formation of “bands”. The gain in bringing the atoms together was the delocalization of the wavefunction, giving rise to a lowering of the kinetic energy. We can also directly start from the opposite end and assume the kinetic energy is the most important part in the formation of a solid and add the potential of the nuclei only later.

In free space in the Schrödinger equation is given by

$$-\frac{\hbar^2}{2m} \nabla^2 \psi(\mathbf{r}) = E \psi(\mathbf{r}). \quad (51)$$

The solution is well known and the eigenfunction are simple plane waves

$$\psi(\mathbf{r}) = \frac{1}{\sqrt{V}} e^{i\mathbf{k}\cdot\mathbf{r}}, \quad (52)$$

where  $V$  is the size of the system. The eigenvalues are

$$\epsilon_{\mathbf{k}} = \frac{\hbar^2 \mathbf{k}^2}{2m} \quad (53)$$

Note that we directly have bands (although generally one does not call them bands for free electrons). Again, we can apply periodic boundary condition, see Eqn. (24), giving

$$k_i = \pm \frac{2\pi n}{L} \quad \text{with } n \text{ integer.} \quad (54)$$

Note that so far there is no restriction on the  $k$  values to the range  $[-\frac{\pi}{a}, \frac{\pi}{a}]$ . The only thing we have done so far is put the particles in a box, which is not yet a solid. The system becomes a solid by introducing the potential  $U(r)$  due to the nuclei that are arranged in a periodic structure. In general, we can express any arbitrary potential in a Fourier series

$$U(\mathbf{r}) = \sum_{\mathbf{k}} U_{\mathbf{k}} e^{i\mathbf{k}\cdot\mathbf{r}}. \quad (55)$$

However, we want to impose that the potential satisfies the periodicity of the lattice. Therefore, the potential should be equivalent when moving to a different lattice site by the vectors  $\mathbf{R}$  that indicate the lattice sites:

$$U(\mathbf{r} + \mathbf{R}) = \sum_{\mathbf{k}} U_{\mathbf{k}} e^{i\mathbf{k}\cdot(\mathbf{r}+\mathbf{R})} = \sum_{\mathbf{k}} e^{i\mathbf{k}\cdot\mathbf{R}} U_{\mathbf{k}} e^{i\mathbf{k}\cdot\mathbf{r}} \quad (56)$$

This is not going to work for any arbitrary wavevector  $\mathbf{k}$ . The vectors  $\mathbf{K}$  that satisfy this are known as reciprocal lattice vectors

$$e^{i\mathbf{K}\cdot\mathbf{R}} = 1. \quad (57)$$

These vectors return again and again since they are intimately related to the translational symmetry of the crystal. We will discuss in more detail later on how to obtain these reciprocal lattice vectors and discuss various cases for different crystals. Let us just satisfy ourselves that these vectors exist and only consider the case of one dimension

$$e^{iKa} = 1 \quad \Rightarrow \quad K = \pm \frac{2\pi n}{a}. \quad (58)$$

Note that since  $a$  is much smaller than  $L$ , the  $K$  are much larger the separation between the  $k$  values. In general, the periodic potential is therefore given by

$$U(\mathbf{r}) = \sum_{\mathbf{K}} U_{\mathbf{K}} e^{i\mathbf{K}\cdot\mathbf{r}}. \quad (59)$$

The matrix elements between different running waves are given by

$$\langle \mathbf{k}' | U | \mathbf{k} \rangle = \sum_{\mathbf{K}} \frac{1}{V} \int dx e^{-i\mathbf{k}'\cdot\mathbf{r}} U_{\mathbf{K}} e^{i\mathbf{K}\cdot\mathbf{r}} e^{i\mathbf{k}\cdot\mathbf{r}} = \sum_{\mathbf{K}} U_{\mathbf{K}} \frac{1}{V} \int d\mathbf{r} e^{-i(\mathbf{k}' - \mathbf{K} - \mathbf{k})\cdot\mathbf{r}} = \sum_{\mathbf{K}} U_{\mathbf{K}} \delta_{\mathbf{k}', \mathbf{k} + \mathbf{K}}. \quad (60)$$

In bra-ket notation, we can write the potential as

$$U = \sum_{\mathbf{K}} U_{\mathbf{K}} |\mathbf{k} + \mathbf{K}\rangle \langle \mathbf{k}| \quad (61)$$

This has the important consequence that a running wave with wavevector  $k$  is coupled to the running waves with wavevectors  $k \pm 2\pi n/a$  with  $n = 0, 1, 2, 3, \dots$ , see Fig. 6. However, this also means that  $k$  is no longer a good quantum number. The periodic potential reduces the  $k$  values that are good quantum numbers. Although we are free to choose the  $k$  values, generally the region  $[-K/2, K/2] = [-\pi/a, \pi/a]$  is chosen. The wavevectors inside this region do not couple to each other with the periodic potential. In addition, any wavevector outside this region is coupled to one inside by a reciprocal lattice vector  $K$ . The allowed  $k$  values are therefore equivalent to those found in Eqn. (24) when discussing the tight-binding model.

Since only the  $\mathbf{k}$  values separated by a reciprocal lattice vector  $\mathbf{K}$  couple, we can write the eigenfunctions as a linear combination of these running waves

$$\psi_{\mathbf{k}}(\mathbf{r}) = \sum_{\mathbf{K}} c_{\mathbf{k}-\mathbf{K}} e^{i(\mathbf{k}-\mathbf{K})\cdot\mathbf{r}}, \quad (62)$$

where  $c_{\mathbf{k}-\mathbf{K}}$  is a coefficient. For each  $\mathbf{k}$ , we find a set of coupled equations

$$\epsilon_{\mathbf{k}-\mathbf{K}} c_{\mathbf{k}-\mathbf{K}} + \sum_{\mathbf{K}'} U_{\mathbf{K}'} c_{\mathbf{k}-\mathbf{K}+\mathbf{K}'} = E c_{\mathbf{k}-\mathbf{K}}. \quad (63)$$

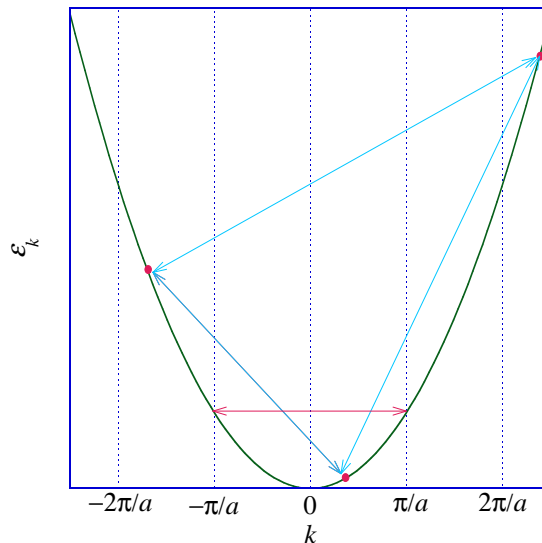


FIG. 6: The scattering of electrons between different running waves  $e^{ikx}$  due to a periodic potential resulting from nuclei in a chain at a distance  $a$  from each other. The potential couples  $k$  values with each other that are  $K = \pm 2\pi n/a$  apart. The blue arrows show this scattering for an arbitrary  $k$  value (Note that only three  $k$  points are included). The red arrow shows the particular case for  $k = \pm \frac{\pi}{a}$ . This is a Bragg reflection and the electrons scatters to  $k = \mp \frac{\pi}{a}$  which has exactly the same energy  $\varepsilon_k$ .

Note that this reproduces to  $E = \varepsilon_{\mathbf{k}-\mathbf{K}}$  in the absence of a periodic potential.

This model is known as the nearly-free electron model and is generally use only in the case the the periodic potential is weak (such as K, Na, and Al metals). However, even a weak potential can have a large influence if the energy separation of the states that if couples is small (or even zero). For the energy difference to be zero we require

$$\varepsilon_{\mathbf{k}} = \varepsilon_{\mathbf{k}-\mathbf{K}} \quad \Rightarrow \quad k^2 = (\mathbf{k} - \mathbf{K})^2 = k^2 - 2\mathbf{k} \cdot \mathbf{K} + K^2, \quad (64)$$

or

$$\mathbf{k} \cdot \mathbf{K} = \frac{1}{2}K^2. \quad (65)$$

Some of you might recognize this as the Laue condition for x-ray diffraction (which, of course is equivalent to the Bragg condition). In principle, this should not be a surprise. X-rays are scattered by a lattice through repeated interaction with the nuclei. The same applies to electrons. In one dimension,  $\mathbf{k}$  and  $\mathbf{K}$  are either parallel or antiparallel and we find  $k = \pm \frac{1}{2}K$ . Let us consider  $K = 2\pi/a$ , for which  $k = K/2 = \pi/a$  should have the same energy as  $k - K = -\pi/a$ , which is indeed correct. The effects are therefore strongest close to the  $k$  values indicated by the dotted lines in Fig. 6. In this region, we can neglect the coupling to other running waves if  $|\varepsilon_{\mathbf{k}} - \varepsilon_{\mathbf{k}-\mathbf{K}}| \gg U$ . We are then left with solving the determinant

$$\begin{vmatrix} \varepsilon_{\mathbf{k}} - E & U_{\mathbf{K}} \\ U_{\mathbf{K}}^* & \varepsilon_{\mathbf{k}-\mathbf{K}} - E \end{vmatrix} = 0. \quad (66)$$

This leads to the quadratic equation

$$(\varepsilon_{\mathbf{k}} - E)(\varepsilon_{\mathbf{k}-\mathbf{K}} - E) - |U_{\mathbf{K}}|^2 = 0, \quad (67)$$

which has the solutions

$$E = \frac{\varepsilon_{\mathbf{k}} + \varepsilon_{\mathbf{k}-\mathbf{K}}}{2} \pm \sqrt{\left(\frac{\varepsilon_{\mathbf{k}} - \varepsilon_{\mathbf{k}-\mathbf{K}}}{2}\right)^2 + |U_{\mathbf{K}}|^2}. \quad (68)$$

In the limit that  $\varepsilon_{\mathbf{k}} \cong \varepsilon_{\mathbf{k}-\mathbf{K}}$ , we obtain

$$E = \varepsilon_{\mathbf{k}} \pm |U_{\mathbf{K}}|. \quad (69)$$



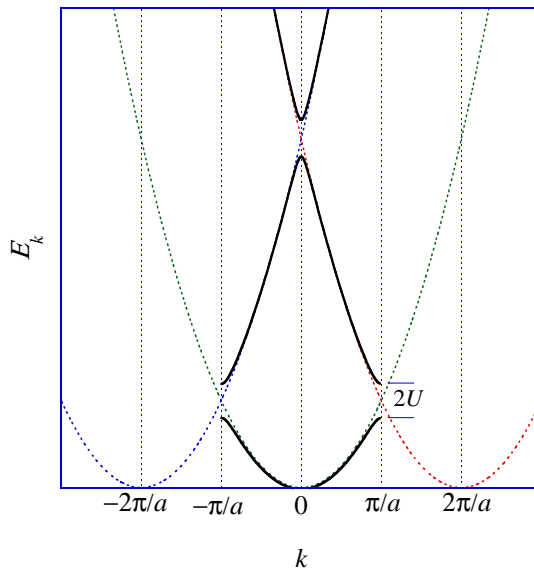


FIG. 7: Calculation of the bands in a nearly-free electron model. Shown are the energies  $\varepsilon_k$  and  $\varepsilon_{k+K}$  with  $K = \pm \frac{2\pi}{a}$ . The calculated nearly-free electron bands are shown for the region  $[-K/2, K/2] = [-\frac{\pi}{a}, \frac{\pi}{a}]$

We see that an energy gap opens at the  $k = \pm \frac{1}{2}K$ . We can also verify that in this limit around  $\mathbf{k} = \frac{1}{2}\mathbf{K}$ , we have

$$\frac{\partial E}{\partial \mathbf{k}} = \frac{\hbar^2}{m} \left( \mathbf{k} - \frac{1}{2}\mathbf{K} \right), \quad (70)$$

i.e. the derivative is zero on the Bragg planes and the bands are therefore flat. (Not entirely surprising since we just demonstrated that a gap opens, so the bands must be either in a maximum or a minimum).

We can extend this procedure to include additional reciprocal lattice vectors  $K$ . Let us consider the situation in one dimension for  $K = 0$  and  $K_{\pm} = \pm \frac{2\pi}{a}$ . We can also use the following properties of the potential. Since the potential is real, we have

$$U_{-\mathbf{K}} = U_{\mathbf{K}}^*. \quad (71)$$

If in addition, we have inversion symmetry (meaning that the system is unchanged when  $\mathbf{r} \rightarrow -\mathbf{r}$ , which is the case for a linear chain), we also have

$$U_{-\mathbf{K}} = U_{\mathbf{K}} = U_{\mathbf{K}}^*. \quad (72)$$

Using this we can write down the Hamiltonian.

$$H = \begin{pmatrix} \varepsilon_k & U_K & U_K \\ U_K & \varepsilon_{k-K_-} & U_{2K} \\ U_K & U_{2K} & \varepsilon_{k-K_+} \end{pmatrix}. \quad (73)$$

The results are given in Fig. 7. Note that the energies  $\varepsilon_{k-K_{\pm}} = \hbar^2(k - K_{\pm})^2/2m$  look in the region  $[-K/2, K/2]$  as parabolas centered around  $K_{\pm}$ . The eigenvalues of  $H$  can be easily solved numerically. The values for  $E_{kn}$ , where  $n = 1, 2, 3$  is the bandindex are plotted in the region  $[-K/2, K/2]$ . We have taken  $U_K = U_{2K}$ . This is known as the reduced-zone scheme, see AM Fig. 9.4). This is the scheme commonly used in the scientific literature. Figure 9.4 also shows the extended-zone scheme and the repeated-zone scheme. In particular, the extended-zone scheme looks natural at first. It looks like the original parabola with gaps opened at the reciprocal lattice vectors  $K$ . However, this clings too much to the free-electron like picture and in some sense is slightly misleading. It is important to note that in a chain of  $N$  atoms, there are only  $N$   $k$ -values that are good quantum numbers. Convention dictates that these  $N$   $k$ -values are chosen in the region  $[-K/2, K/2]$ . This region is known as the first Brillouin zone. All the other  $k$ -values are not good quantum number. For example,  $k = 2.3\pi/a$  is not a good  $k$  value since it is coupled by the periodic potential to  $k = 0.3\pi/a$ . This directly implies that we have more eigenstates than  $k$ -values. This is why there is another quantum number, the band index  $n$ . All eigenstates  $E_{kn}$  are identified by the value of  $k$  in

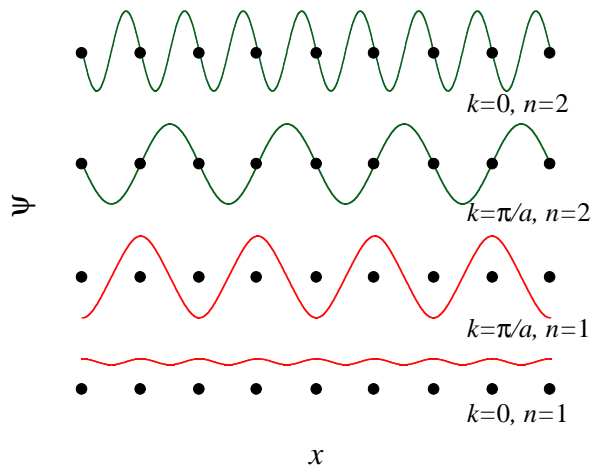


FIG. 8: The wavefunction of the nearly-free electron eigenstates for four eigenvalues  $E_{0,1}$ ,  $E_{\frac{\pi}{a},1}$ ,  $E_{\frac{\pi}{a},2}$ , and  $E_{0,2}$ . We have assumed  $U_K < 0$  and  $U_{2K} > 0$ .

the region  $[-K/2, K/2]$  and the band index  $n$ . Because of the mixing, we can no longer identify eigenstates with the free-electron bands. Even at  $k = 0$ , we have, for the lowest eigenfunction in Fig. 7,

$$|E_{k=0,1}\rangle = a|k\rangle - \sqrt{1-a^2}(|k-K_- \rangle + |k-K_+ \rangle), \quad (74)$$

where the coefficient  $a \cong 1$  (actually  $a = 0.9978$  for the example in the figure). Indeed close to  $|k\rangle$ , but still mixed with  $|k-K_{\pm}\rangle$ . The repeated-zone scheme has its uses from time to time, as long as you keep in mind that it just repeats the same information as is already contained in the first Brillouin zone and nothing new is added.

## V. COMPARISON OF RESULTS FOR TIGHT-BINDING AND NEARLY-FREE ELECTRON MODEL

In this section, we will compare the results from tight-binding and the nearly-free electron model. At first, this looks like a pointless exercise. For tight-binding we find a single band given  $E_k = -2t \cos ka$ . For the nearly-free electron model we have several bands which originate from free electron parabolas. Although, we are not going to make the claim that the two are exactly equivalent, they have more in common than you might think at first sight. The tight-binding model starts from atomic states which include the potential of the nucleus fully and then starts adding the kinetic energy due to the delocalization of the electrons when the solid is formed. The nearly-free electron model starts from completely delocalized electron and starts adding the effect of the potential of the nuclei. Somewhere along the way to two must have something in common. (They will never be entirely equivalent, since the treatment of the potential in the nearly-free electron is somewhat oversimplified. The inclusion of only two Fourier components,  $U_K$  and  $U_{2K}$ , is obviously insufficient to describe the much more complicated shape of the potential.

Let us start by looking at the eigenfunctions in the nearly-free electron model. Let us start with the one with the lowest energy. The eigenfunction is given in Eqn. (74). This gives a wave in real space for  $k = 0$  and  $n = 1$ ,

$$\psi_{0,1}(x) = \frac{1}{\sqrt{L}}(a - 2\sqrt{1-a^2} \cos Kx). \quad (75)$$

In the case that  $a = 1$  (i.e., the limit  $U = 0$ ), we just obtain that  $\psi_{0,1} = \frac{1}{\sqrt{L}}$  constant throughout the system. The higher-order oscillation are a result of the (small) mixing in of the  $K_{\pm}$  terms.

Effect are more drastic around  $k = K_{\pm}/2$ . Let us take  $k = K_+/2 = \frac{\pi}{a}$ . Here we obtain mixing of the free-electron states  $\varepsilon_k$  and  $\varepsilon_{k-K_+/2}$ , as we have solved in Eqn. (66) (we can neglect  $\varepsilon_{k+K/2}$  which is at higher-energies). The wavefunction are

$$\psi_{\frac{\pi}{2},i}(x) = \frac{1}{2\sqrt{L}}(e^{i\frac{\pi}{a}x} \mp \text{sgn}(U_K)e^{i\frac{\pi}{a}x}). \quad (76)$$

with  $i = 1, 2$ . The wavefunctions depend on the sign of the coupling. Let us consider the situation  $U_K < 0$ , shown in

Fig. 8, which gives

$$\psi_{\frac{\pi}{2},n}(x) = \begin{cases} \sqrt{\frac{2}{L}} \cos \frac{\pi}{a} x & n = 1 \\ i\sqrt{\frac{2}{L}} \sin \frac{\pi}{a} x & n = 2, \end{cases} \quad (77)$$

where  $n$  is the band index which simply numbers the band with the lowest number assigned to the band lowest in energy. We see that  $\psi_{\frac{\pi}{2},1}(x)$  has extrema on the positions of the nuclei, whereas  $\psi_{\frac{\pi}{2},2}(x)$  has nodes on the positions of the nuclei. This is reminiscent of atomic physics:  $s$  orbitals have their maxima at the nucleus, whereas, for example the  $p_x$  orbital has a node at the nucleus. From this we can understand one origin of the discrepancy between our tight-binding and nearly-free electron calculation. In our tight-binding calculation, we only included  $s$  orbitals, so we only get one band which resembles the lowest band of the nearly-free electron calculation, but not the higher-lying band. On the other hand, we also see that the effect of folding the free-electron bands is to create “orbital-like” structure related to the nuclei. For the highest energy of the second band ( $n = 2$ ), the wavefunction has nodes not only at the nuclei, but also between the nuclei, see Fig. 8.

However, we see that we can create a better connection between the two approaches by including  $p$  type orbitals. Let us try to extend our tight-binding approach, following the approach by Slater and Koster, Phys. Rev. B **94**, 1498 (1954). We adjust Eqn. (25) to allow the inclusion of more orbitals

$$\varphi_{\mathbf{k},s}(\mathbf{r}) = \frac{1}{\sqrt{N}} \sum_{\mathbf{R}} e^{i\mathbf{k}\cdot\mathbf{R}} \varphi_s(\mathbf{r} - \mathbf{R}). \quad (78)$$

The dispersion for these states, we found to be

$$\varepsilon_k^{ss} = 2(ss\sigma) \cos ka \quad \text{with} \quad (ss\sigma) = \int d\mathbf{r} \varphi_s(\mathbf{r} - \mathbf{R}') H \varphi_s(\mathbf{r} - \mathbf{R}) \quad (79)$$

where  $\mathbf{R}$  and  $\mathbf{R}'$  are nearest neighbors and  $(ss\sigma) = -t$  (using the notation by Slater and Koster indicating that the matrix element is between two  $s$  orbitals; the  $\sigma$  indicates the type of bonding. There are also  $\pi$  and  $\delta$  bonding, but that is not relevant for the discussion here). We can repeat this approach for  $p$  orbitals giving

$$\varphi_{\mathbf{k},p}(\mathbf{r}) = \frac{1}{\sqrt{N}} \sum_{\mathbf{R}} e^{i\mathbf{k}\cdot\mathbf{R}} \varphi_p(\mathbf{r} - \mathbf{R}) \quad (80)$$

with energies

$$\varepsilon_{\mathbf{k}}^{pp} = 2(pp\sigma) \cos ka. \quad \text{with} \quad (pp\sigma) = \int d\mathbf{r} \varphi_p(\mathbf{r} - \mathbf{R}') H \varphi_p(\mathbf{r} - \mathbf{R}) \quad (81)$$

This looks similar, but there is an important difference. For typical Hamiltonians  $H$ , the matrix elements are negative when the positive lobes are pointing to each other. This is always the case for the  $s$  orbital which is positive everywhere

$$\cdots (+)(+)(+)(+)(+)(+)(+)(+) \cdots, \quad (82)$$

where  $(+)$  schematically indicates an  $s$  orbital at a certain site. This is the state found for  $k = 0$  (and energy  $\varepsilon_k = 2(ss\sigma) < 0$ ). Note that this is positive everywhere just as the nearly-free electron wavefunction for  $k = 0$  and  $n = 1$  in Fig. 8. For  $k = \frac{\pi}{a}$  (and energy  $\varepsilon_k = -2(ss\sigma) > 0$ ), the exponential changes sign at each site, giving

$$\cdots (+)(-)(+)(-)(+)(-)(+)(-) \cdots. \quad (83)$$

This has nodes between the nuclei, just as the wavefunction for  $k = \frac{\pi}{a}$  and  $n = 1$ .

The  $p$  orbital on the other hand have a node

$$\cdots (-+)(-+)(-+)(-+)(-+)(-+)(-+)(-) \cdots \quad (84)$$

The convention we choose is that the positive lobe of the  $p$  orbital  $(-+)$  is in the positive  $x$  direction (we can choose any convention that we like, but in the end it should lead to the same results). In this convention, we see that the positive lobes are pointing towards the negative lobes. The matrix elements are therefore negative. This also has as a consequence that the solution with the lowest energy is the one where the sign changes for each sites, i.e.

$$\cdots (-+)(+-)(-+)(+-)(-+)(+-)(-+)(+-) \cdots \quad (85)$$

However, this looks nice since the positive lobes are pointing towards the positive lobes and the negative lobes are pointing towards the negative lobes. This is essentially the bonding state with no nodes between the nuclei (but with nodes on the nuclei). This corresponds well with the lowest  $n = 2$  nearly-free electrons solution for  $k = \frac{\pi}{a}$  (alternating signs), which also has no nodes between the nuclei. The state with the higher energy is given in Eqn. (84), where there are nodes between the nuclei, comparable to the nearly-free electron wavefunction for  $k = 0$  and  $n = 2$  in Fig. 8.

We can also compare the dispersion. In order to do this, we need to overcome one more hurdle, namely the matrix elements between  $s$  and  $p$  are not zero,

$$(sp\sigma) = \int d\mathbf{r} \varphi_s(\mathbf{r} - \mathbf{R}') H \varphi_p(\mathbf{r} - \mathbf{R}). \quad (86)$$

The dispersion does not follow a cosine dependence since an  $s$  orbital, in our convention, couples differently to the left and the right

$$\dots (-+)(+)(-+), \quad (87)$$

a problem that did not arise when dealing with just  $s$  orbitals. Following Eqns. (33) and (34), we find

$$\varepsilon_k^{sp} = (sp\sigma)(e^{ika} - e^{-ika}) = 2i(sp\sigma) \sin ka. \quad (88)$$

We now have a basis  $(\psi_{k,s}, \psi_{k,p})$  giving a matrix

$$H = \begin{pmatrix} \varepsilon_k^{ss} & \varepsilon_k^{sp} \\ (\varepsilon_k^{sp})^* & \varepsilon_k^{pp} \end{pmatrix} \quad (89)$$

Figure 9 gives a comparison between the lowest two bands ( $n = 1, 2$ ) in the nearly-free electron model and the  $s$  and  $p$  tight-binding model. The fit has been done by eye. Although a perfect fit cannot be expected due to the different approximations, it is clear that they are giving comparable physics.

Although, at first sight, it might seem surprising that similar physics comes out of a model starting with free electrons and a model starting from atomic orbitals. A comparison between tight-binding and nearly-free electron model can be given as follows:

	<b>tight binding</b>	<b>nearly free electron model</b>
starting point	atomic properties	kinetic energy of the electrons
basis functions	atomic orbitals	plane waves
$k = \pm n \frac{2\pi}{L}$	periodic boundary conditions	periodic boundary conditions
$k \in [-\frac{\pi}{a}, \frac{\pi}{a}]$	$N$ atoms give $N$ $k$ values or $\frac{N}{2} \frac{2\pi}{L} \leq k \leq \frac{N}{2} \frac{2\pi}{L}$	periodic potential couples $k$ values that differ by $K = n \frac{2\pi}{a}$
number of bands	equals number of atomic orbitals	equal number of reciprocal lattice vectors
approximations	neglect orbitals	$U_K = 0$ for large $K$

However, when you think more of it, in principle it should not make a difference. The starting wavefunctions are just a basis. If my basis is complete (i.e. you can express any arbitrary wavefunction in your basis, a statement you might remember from Fourier analysis) then solving the same Hamiltonian should give the same eigenfunction and eigenenergies, regardless of the basis we started with. Differences do arise because we start making approximations along the way:

- The free-electron model is beautiful as a basis (exponentials are the foundation of Fourier analysis): they are orthogonal and complete. The tight-binding basis set is more problematic. In principle, the solutions of the Hydrogen atom for one atom form a complete basis which is orthogonal. However, this is not what we are doing. We are taking the solution for one atom and putting them on different sites. This basis set is not even orthogonal.
- The potential of the nuclei is much better treated in the tight-binding model. There is one important caveat: in general we are not dealing with Hydrogen atom. The potential is treated much more poorly in the nearly-free electron model. So far, we have included only two Fourier terms. Obviously, this will give a sinusoidal potential and not the  $1/r$  potential that one would expect from the nuclei. However, in principle nothing prevents us from including all Fourier components. Then again, this defeats the purpose of a nearly-free electron model.

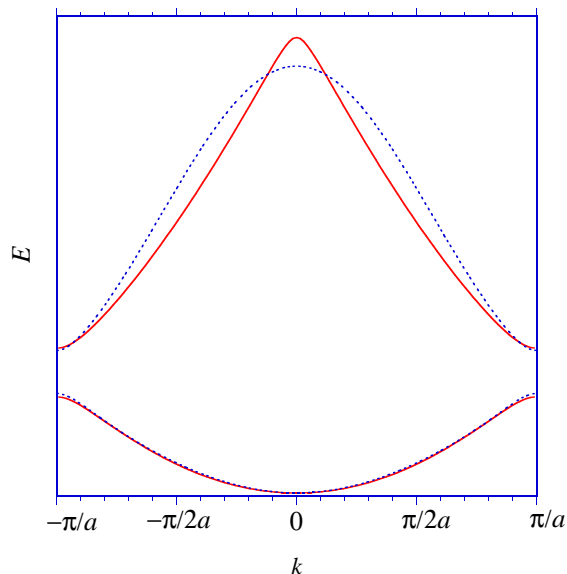


FIG. 9: Comparison of the two bands lowest in energy ( $n = 1, 2$ ) in a nearly-free electron (red) with a tight-binding calculation (blue dotted) including an  $s$  and a  $p$  orbital.

Summarizing, although the nearly-free electron usually takes pride of place in most textbooks over the tight-binding model (in that it is usually treated in an earlier chapter), the tight-binding model wins out in practicality. Tight-binding is often used in the scientific literature. The electronic structure is nowadays generally calculated with complex codes that have been developed over many years. However, one often would like to use the output of such calculations as the input for other calculations (for the experts, for example, many-body calculations or molecular dynamics). This is usually done by making a tight-binding fit to the more sophisticated electronic structure calculations. Nearly-free electron models are used much less often (typing in tight-binding on Physical Review online yielded more 3500 papers, whereas nearly-free electron gave less than 300 papers). One of the reasons is that it works well for only a few systems, usually involving  $s$  and sometimes  $p$  orbitals. One might actually wonder why it works at all. One needs that the nucleus is very well screened. One has to realize that most electrons in a solid are very strongly bound to the nucleus and only the electrons in the outer shells really form bands. However, this inner shell electrons can effectively screen the nucleus. They are effectively a negative charge compensating the positive charge of the nucleus.

## VI. OTHER WAYS OF KEEPING ATOMS TOGETHER

### A. Covalent bonds

Covalent bonds are strong bonds with a clear direction. The concepts are very important conceptually for organic chemistry. In solids, the ideas become somewhat less clearly defined. The most straightforward covalent bond is the hydrogen bond of the  $\text{H}_2$  atom. There are two electrons in the molecule that both reside in the bonding states. This is a typical situation for covalent bonding, where a bond between two atoms is shared by two electrons.

When we consider carbon, the situation becomes a bit more complex. Suppose we want to make a linear chain of carbon atoms. Let us take the chain in the  $z$  direction. The configuration of the Carbon atom is given by  $(1s)^2(2s)^2(2p_x)^1(2p_y)^1$ . The  $1s$  electrons are strongly bound and do not contribute to the bonding. These are known as core electrons. The  $2s$  and  $2p$  orbitals are close in energy. The strongest bonding occurs for the bonding between the orbitals along the chain: the  $2s$  orbital (which does not point in any particular direction) and the  $2p_z$ , which lies along the chain. Their coupling is known as  $\sigma$ -bonding. The  $2p_x$  and  $2p_y$  orbitals, which are perpendicular to the chain, bond as well (known as  $\pi$ -bonding) but this is weaker since the orbitals are further apart. Let us return to the  $\sigma$ -bonding. Now we have a problem since we have two orbitals along the chain, so which one forms the bonding. The solution is that they form hybrids that can be expressed as

$$\phi_1 = a_1\psi_s + a_2\psi_{p_z} \quad \text{and} \quad \phi_2 = b_1\psi_s + b_2\psi_{p_z}. \quad (91)$$

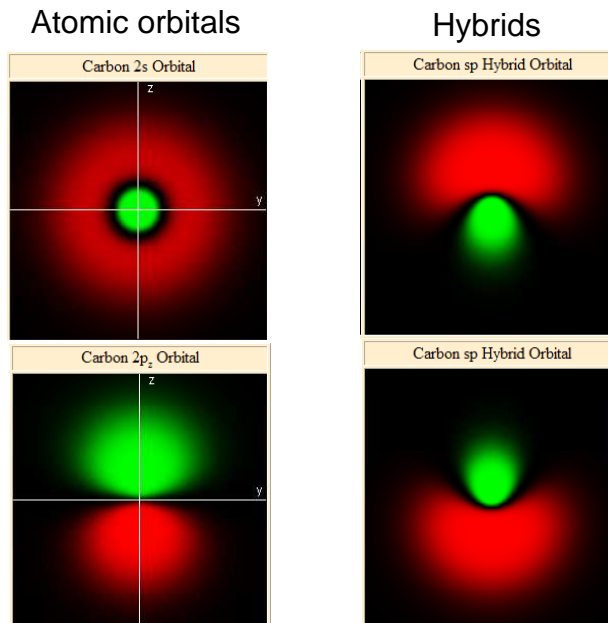


FIG. 10: The  $sp$ -hybrids in Carbon are formed by combining the  $2s$  and  $2p$  orbitals.

The coefficients are determined such that the wavefunctions are orthogonal and normalized

$$\int \psi_1^* \psi_1 d\mathbf{r} = 1 \quad \text{and} \quad \int \psi_2^* \psi_2 d\mathbf{r} = 1 \quad \text{and} \quad \int \psi_1^* \psi_2 d\mathbf{r} = 0 \quad (92)$$

We want that the new wavefunctions contain both an equal amount of  $s$  character. Combining all the equations leads to the solution

$$\phi_1 = \frac{1}{\sqrt{2}}(\psi_s + \psi_{p_z}) \quad \text{and} \quad \phi_2 = \frac{1}{\sqrt{2}}(\psi_s - \psi_{p_z}). \quad (93)$$

This process is depicted in Fig. 10. What we obtain are two  $sp$  hybrids one pointing predominantly in the positive  $z$  direction, whereas the other is pointing in the negative  $z$  direction. An example of an  $sp$  hybrid is acetylene ( $C_2H_2$ ). Acetylene is a linear molecule with the two carbon atoms in the center and the two hydrogen atoms at the ends of the molecules. The two  $sp$  hybrids of the Carbon atoms pointing between the carbon atoms form a  $\sigma$  bonding molecular orbital between the two carbon atoms. The  $sp$  hybrids pointing to the outside of the molecule form molecular bonds with the hydrogen atoms. In addition to the  $\sigma$  bonding, we have the  $\pi$  bonding orbitals, where the  $p_x$  and  $p_y$  orbital of one carbon atom connect to the  $p_x$  and  $p_y$  orbital of the other carbon atom, respectively. This creates a total of three bonds between the two carbon atoms. This is often denoted as

$$H - C \equiv C - H. \quad (94)$$

Each carbon atom has four bonds corresponding to the four valence electrons of carbon. The amazing thing about carbon is the enormous flexibility of making covalent bonds. In addition to linear bonds, planar bonds can be made, known as  $sp^2$  hybrids. Following the same procedure as described above, we can find three new wavefunction consisting of  $s$ ,  $p_x$ , and  $p_y$  orbitals:

$$\psi_1 = \frac{1}{\sqrt{3}}\psi_s + \sqrt{\frac{2}{3}}\psi_{p_x} \quad (95)$$

$$\psi_2 = \frac{1}{\sqrt{3}}\psi_s - \frac{1}{\sqrt{6}}\psi_{p_x} + \frac{1}{\sqrt{2}}\psi_{p_y} \quad (96)$$

$$\psi_2 = \frac{1}{\sqrt{3}}\psi_s - \frac{1}{\sqrt{6}}\psi_{p_x} - \frac{1}{\sqrt{2}}\psi_{p_y}. \quad (97)$$

These hybrids are depicted in Fig. 11. Note that every orbital has  $1/3$   $s$  orbital and  $2/3$   $p$  orbital character. The first hybrid has on the positive  $x$  side both the positive  $s$  orbital and the positive part of the  $p$  orbital. There the wave

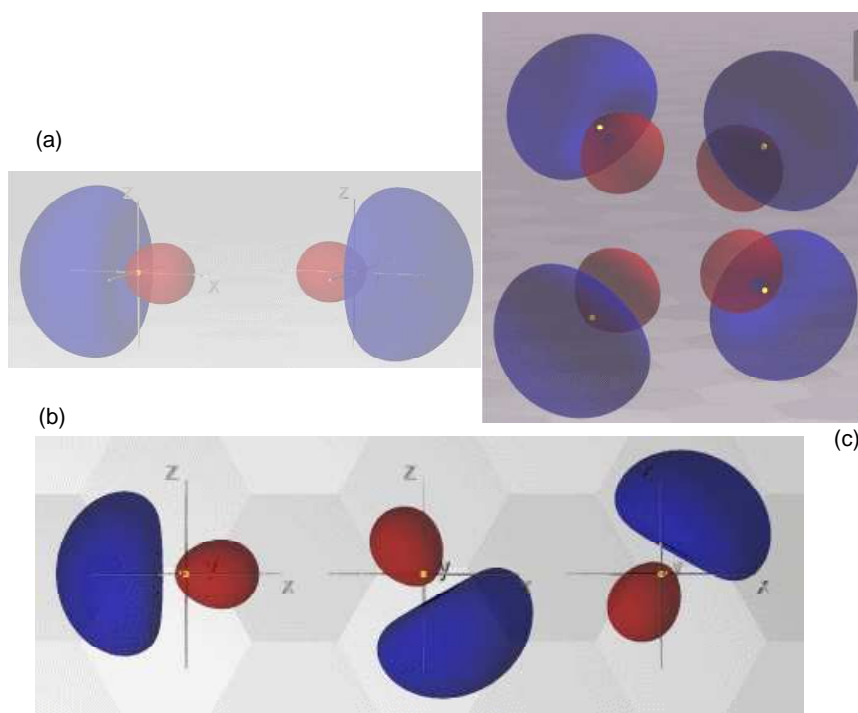


FIG. 11: Hybrids that are formed by combining  $s$  and  $p$  orbitals: (a)  $sp$ , (b)  $sp^2$ , and (c)  $sp^3$  hybrids. From <http://www.chm.davidson.edu/vce/AtomicOrbitals/hybrid.html>.

functions add up. On the negative  $x$  side, we have a positive  $s$  orbital and the negative lobe of the  $p$  orbital. There the wavefunction partially cancel each other. For the second hybrid, the situation is very similar. Note that the wave function can be written as

$$\psi_2 = \frac{1}{\sqrt{3}}\psi_s + \sqrt{\frac{2}{3}} \left\{ -\frac{1}{2}\psi_{p_x} + \frac{1}{2}\sqrt{3}\psi_{p_y} \right\} \quad (98)$$

$$= \frac{1}{\sqrt{3}}\psi_s + \sqrt{\frac{2}{3}} \left\{ \cos 120^\circ \psi_{p_x} + \sin 120^\circ \psi_{p_y} \right\} = \frac{1}{\sqrt{3}}\psi_s + \sqrt{\frac{2}{3}}\psi_{p_{120^\circ}}. \quad (99)$$

The combination of  $p_x$  and  $p_y$  orbital is effectively a  $p$  orbital at  $120^\circ$  degrees with respect to the  $x$ -axis. This  $sp^2$  hybrid is therefore equivalent to the first hybrid except it is rotated by  $120^\circ$  around the  $z$ -axis.

A typical example of an  $sp^2$  hybrid is Ethylene ( $C_2H_4$ ). One  $2s$  and two  $2p$  orbitals form three  $sp^2$  hybrids at a  $120^\circ$  degree angle with each other. Two of those couple two the Hydrogen atom, the other connects the two Carbon atoms, forming a planar molecule. The remaining  $p$  is perpendicular to the plane of the molecule (the  $p_z$  orbital). The two  $p_z$  orbitals of the Carbon atoms form a  $\pi$  bonding with each other. Another example we have seen before namely benzene  $C_6H_6$ , see Fig. 5. The six carbon atoms form a hexagon with  $120^\circ$  angles. The bonds along the ring occupy two electrons of each carbon. There are also six  $sp^2$  hybrids sticking to the outside of the ring that bind with the hydrogen atoms. We already discussed earlier what happened to the fourth electron of each carbon. They occupy the  $p_z$  orbitals perpendicular to the plane. Originally, it was also attempted to describe the  $p_z$  orbitals as covalent bonds. However, it was realized quickly that there is an ambiguity in describing the  $p_z$  orbitals as covalent bonds, see Fig. 5. This process can also be extended to solids. The best known example is graphite where the carbon atoms form an hexagonal plane.

In addition, carbon can form three-dimensional bonds. In an  $sp^3$  hybrid, all the orbitals assume equivalent roles,

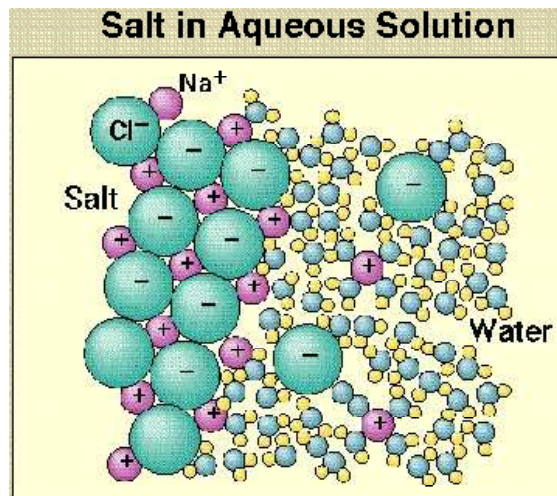


FIG. 12: Since the binding in ionic crystals is due to the electrostatic interaction and not through covalency, the opposite charge can often be easily replaced by other charges or polarized molecules, such as water.

this leads to wavefunctions of the type

$$\psi_1 = \frac{1}{2}(\psi_s + \psi_{p_x} + \psi_{p_y} + \psi_{p_z}) \quad (100)$$

$$\psi_2 = \frac{1}{2}(\psi_s + \psi_{p_x} - \psi_{p_y} - \psi_{p_z}) \quad (101)$$

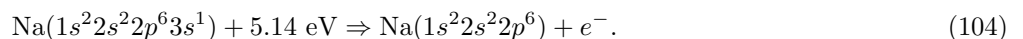
$$\psi_3 = \frac{1}{2}(\psi_s - \psi_{p_x} + \psi_{p_y} - \psi_{p_z}) \quad (102)$$

$$\psi_4 = \frac{1}{2}(\psi_s - \psi_{p_x} - \psi_{p_y} + \psi_{p_z}). \quad (103)$$

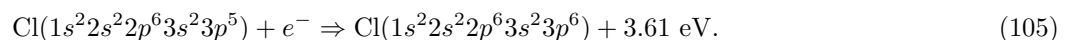
The orbitals form a tetrahedron and have mutual angles of  $109^\circ.28'$ , see Fig. 11. One of the simplest examples of an  $sp^3$  hybrid can be found in Methane ( $\text{CH}_4$ ). The four single bonds form  $\sigma$  bonding with the Hydrogen  $s$  orbitals. A somewhat more complicated example is Ethane ( $\text{C}_2\text{H}_6$ ). Four  $sp^3$  orbitals are formed at each C atom. One of these connects the two Carbon atoms, the other three connect to the Hydrogen  $s$  orbitals. One can also form a solid of carbon atoms with  $sp^3$  hybrids: diamond. Since all the bonds are  $\sigma$  bonding and therefore strong, diamond is one of the hardest materials in the world. The  $sp^3$  hybrids are also important for silicon, which is just below carbon in the periodic table.

## B. Ionic crystals

Until now, we have looked at systems where the kinetic energy was mainly responsible for the binding of the solid. This is known as covalent bonding or metallic bonding. However, as we saw the two can actually be quite close. However, in many cases the electrostatic potential can play an important role. A prototypical example is rocksalt NaCl. The idea behind ionic crystals is that an electron transfer takes place between the atoms giving rise to positively and negatively charged atoms that attract each other. Just as for the covalent bonding for hydrogen, let us first start with considering a molecule and then look at a chain. The sodium atom gives up its electron



Obviously, this costs energy, since the electron was bound to the sodium nucleus. The chloride atom accepts the electron



Although we gain energy in the latter process, it still costs 1.52 eV in total. However, now we have a positive and a negative charge that should have an electrostatic attraction. The energy separation in crystalline NaCl is  $2.81 \times 10^{-10}$



m. A naive estimate gives an attractive energy of 5.1 eV. The real cohesive energy is somewhat higher



This gives a total energy gain of  $7.9 - 5.1 + 3.6 = 6.4$  eV.

One should realize that the distinction between ionic and covalent is in the end somewhat arbitrary. Let us take a somewhat generic “molecule” consisting of atoms  $A$  and  $B$ . The atoms prefer to be monovalent  $A^+$  and  $B^-$  (we can do the same thing for divalent ions or more complicated systems). The energy difference is given by  $\Delta = E(AB) - E(A^+B^-)$ . Now let us also introduce a coupling  $-t$  (with  $t > 0$ ) between the two configurations. We then obtain a matrix

$$H = \begin{pmatrix} 0 & -t \\ -t & \Delta \end{pmatrix} \begin{array}{l} |A^+B^- \rangle \\ |AB \rangle \end{array} \quad (107)$$

The eigenvalues are given by

$$E_{\pm} = \frac{\Delta}{2} \pm \frac{1}{2} \sqrt{\Delta^2 + 4t^2}. \quad (108)$$

The eigenvectors are

$$|E_{-}\rangle = \cos \theta |A^+B^- \rangle + \sin \theta |AB \rangle \quad (109)$$

$$|E_{+}\rangle = \sin \theta |A^+B^- \rangle - \cos \theta |AB \rangle, \quad (110)$$

where  $\tan 2\theta = 2t/\Delta$ . In the limit  $\Delta \ll t$ ,  $\theta \rightarrow 0$  and we have the ionic limit  $|E_{-}\rangle = |A^+B^- \rangle$  and  $|E_{+}\rangle = |AB \rangle$ . However, when  $t/\Delta$  increases the system becomes more covalent and the eigenvectors are mixtures of both configurations (note that we cannot let  $\Delta \rightarrow 0$ , since in this limit we also need to take fluctuations to  $|A^-B^+ \rangle$  into account). So in real systems, there is a continuous change from covalent to ionic. Numerical programs to calculate structure do not make a difference when calculating metals, covalent, or ionic materials.

Now that we understand a molecule, let us extend it to a linear chain. First we need to introduce an additional term in the Hamiltonian. If we just had positive and negative ions the minimum distance between the ions will be zero. Obviously, this does not happen because at some distance the electron clouds start to overlap and the ions will start to repel each other. The total interaction energy on a particular ion is then

$$U_i = \sum_{i \neq j} U_{ij}, \quad (111)$$

with

$$U_{ij} = \lambda e^{-r_{ij}/\rho} \pm \frac{1}{4\pi\epsilon_0} \frac{e^2}{r_{ij}}. \quad (112)$$

The dependence of the repulsive potential is empirical where  $\lambda$  and  $\rho$  are parameters;  $\lambda$  indicates the strength and  $\rho$  is the effective range of the repulsive potential. The second term is the potential between the ions where the  $+$  sign is for like charges and the  $-$  is for unlike charges. The total energy is determined by summing over the other ions. The result we can multiply by  $N$  to account for the number of pairs (assuming we are dealing with an ionic crystal with two different ions). This gives

$$U_{\text{tot}} = NU_i = Nz\lambda e^{-R/\rho} - \frac{N}{4\pi\epsilon_0} \frac{\alpha q^2}{R} \quad (113)$$

where  $R$  is the interatomic distance and  $z$  is the number of nearest neighbors. For a linear chain  $z = 2$ . The constant  $\alpha$  is known as the Madelung potential. This constant follows from the summation over the ions in the chain

$$\sum_{j \neq i} \frac{(-1)^{j-i}}{r_{ij}} = -\frac{2}{R} \sum_{n=1}^{\infty} \frac{(-1)^n}{n}. \quad (114)$$

The Madelung constant is then

$$\alpha = 2 \left( 1 - \frac{1}{2} + \frac{1}{3} - \frac{1}{4} + \dots \right) = 2 \ln 2 \cong 1.386. \quad (115)$$

So for a linear chain we obtain

$$U_{\text{tot}} = NU_i = 2N\lambda e^{-R/\rho} - \frac{2N \ln 2}{4\pi\epsilon_0} \frac{q^2}{R}. \quad (116)$$

Note that there is no additional factor two because we do not want to double count the bonds. Therefore,  $N$  should be the number of pairs and not the number of ions. The evaluation for a chain is relatively easy. However, even for a relatively simple structure, such as NaCl, finding  $\alpha$  is complicated since the series do not converge properly. However, this is more a mathematical problem which can be solved and gives 1.7476 for NaCl.

The expression in Eqn. (113) can be used to find the equilibrium distance. The minimum in energy is found for

$$\frac{dU_{\text{tot}}}{dx} = -\frac{Nz\lambda}{\rho} e^{-R/\rho} + \frac{\alpha}{4\pi\epsilon_0} \frac{q^2}{R^2} = 0. \quad (117)$$

This can also be written as

$$z\lambda e^{-R_0/\rho} = \frac{\rho}{R_0} \frac{1}{4\pi\epsilon_0} \frac{\alpha q^2}{R_0}. \quad (118)$$

This allows us to write the total energy as

$$U_{\text{tot}} = -\frac{N}{4\pi\epsilon_0} \frac{\alpha q^2}{R_0} \left(1 - \frac{\rho}{R_0}\right). \quad (119)$$

The range of  $\rho$  is approximately  $0.1R_0$ .

Since the binding is mainly due to electrostatic forces and not through covalent bonding, the charges can often be easily replaced by something else. For example, water molecules have a dipole moment and can effectively replace the positive and negative charges, see Fig. 12. This has as a result that many ionic crystals dissolve in water. Obviously, not every ionic crystal dissolves in every liquid. The ionic binding can be too strong. For example, monovalent ionic crystals dissolve more easily than those with a higher valency. In addition, covalency could play a role in the binding. Also, it depends strongly on the polarizability of the solvent.

### C. Van der Waals forces

Van der Waals forces are important for the creation of solids of noble elements. As we saw when discussing the  $\text{H}_2$  molecule, a noble element, such as helium, cannot take advantage of bonding since the  $1s$  orbitals is full. Binding can still occur between helium atoms due to polarization effects. The electric charge of one helium atom induces a dipole in another helium atoms creating an effective binding. The binding is very weak and solids of noble elements occur only at very low temperature. In fact, He only becomes a solid when applying pressure at very low temperatures. We shall not further discuss the Van der Waals forces here.

## VII. FORMALIZATION: BLOCH THEOREM

### AM Chapter 8

In the chapter on the nearly-free electron model we saw that the wavefunction can be written as, copying Eqn. (62),

$$\psi_{\mathbf{k}}(\mathbf{r}) = \sum_{\mathbf{K}} c_{\mathbf{k}-\mathbf{K}} e^{i(\mathbf{k}-\mathbf{K})\cdot\mathbf{r}}. \quad (120)$$

Since the exponentials form a complete basis set (which means we should be able to express any function in them), this is a general statement. We can therefore express all eigenstates with eigenenergies  $E_{n\mathbf{k}}$  in this fashion. We also saw that  $\mathbf{k}$  is a good quantum number in a crystal. Let us therefore separate the part related to  $\mathbf{k}$

$$\psi_{n\mathbf{k}}(\mathbf{r}) = e^{i\mathbf{k}\cdot\mathbf{r}} \sum_{\mathbf{K}} c_{\mathbf{k}-\mathbf{K}}^n e^{-i\mathbf{K}\cdot\mathbf{r}} = e^{i\mathbf{k}\cdot\mathbf{r}} u_{n\mathbf{k}}(\mathbf{r}) \quad \text{with} \quad u_{n\mathbf{k}}(\mathbf{r}) = \sum_{\mathbf{K}} c_{\mathbf{k}-\mathbf{K}}^n e^{-i\mathbf{K}\cdot\mathbf{r}}. \quad (121)$$

This shows that the eigenfunction can be expressed in a plane-wave part  $e^{i\mathbf{k}\cdot\mathbf{r}}$  and a function  $u_{n\mathbf{k}}(\mathbf{r})$ . The interesting property of the latter is that it has the periodicity of the lattice

$$u_{n\mathbf{k}}(\mathbf{r} + \mathbf{R}) = \sum_{\mathbf{K}} c_{\mathbf{k}-\mathbf{K}}^n e^{-i\mathbf{K}\cdot(\mathbf{r}+\mathbf{R})} = u_{n\mathbf{k}}(\mathbf{r}), \quad (122)$$

since  $e^{-i\mathbf{K}\cdot\mathbf{R}} = 1$ . This is related to the orbital structure that we obtained when folding  $k$  values back into the first Brillouin zone (in one dimension, the region  $[-K/2, K/2]$ ). An alternative way of expressing Bloch's theorem is

$$\psi_{n\mathbf{k}}(\mathbf{r} + \mathbf{R}) = e^{i\mathbf{k}\cdot(\mathbf{r}+\mathbf{R})} u_{n\mathbf{k}}(\mathbf{r} + \mathbf{R}) = e^{i\mathbf{k}\cdot\mathbf{R}} \psi_{n\mathbf{k}}(\mathbf{r}). \quad (123)$$

That is nice you might say, but what does it physically mean? Let us consider free space. We know that the solutions are given by plane waves

$$\psi_{\mathbf{k},\text{free}}(\mathbf{r}) = \frac{1}{\sqrt{V}} e^{i\mathbf{k}\cdot\mathbf{r}}. \quad (124)$$

Free space is uniform. Therefore, we expect that the probability of finding an electron is equal everywhere. This is the case since  $|\psi_{\mathbf{k},\text{free}}|^2 = 1/V$  everywhere (some of you might say that the probability does not have to be constant: we can make wavepackages. This is correct, but you might also remember that wave packages are not eigenstates in free space). However, even though the probability is constant, the wavefunction can still pick up a phase. Under a displacement  $\boldsymbol{\tau}$ , we have

$$\psi_{\mathbf{k},\text{free}}(\mathbf{r} + \boldsymbol{\tau}) = \frac{1}{\sqrt{V}} e^{i\mathbf{k}\cdot(\mathbf{r}+\boldsymbol{\tau})} = e^{i\mathbf{k}\cdot\boldsymbol{\tau}} \psi_{\mathbf{k},\text{free}}(\mathbf{r}). \quad (125)$$

In a solid, we do not expect the probability to be uniform in space. On the contrary, it is very natural to expect that the probability is higher closer to the nuclei where the electron feel and attractive potential. So we do not expect something for an arbitrary vector  $\boldsymbol{\tau}$ . However, we do expect that the probability is exactly the same when we displace ourselves by a lattice vector  $\mathbf{R}$ . After all, the solid looks exactly the same again. This is the underlying physics of Eqn. (123). In a solid, under displacement of  $\mathbf{R}$ , the only change to the wavefunction can be a phase factor.

Does the Bloch theorem also hold for tight-binding wavefunctions that look different from Eqn. (120), see Eqn. (25). Let us check

$$\begin{aligned} \varphi_{\mathbf{k}}(\mathbf{r} + \mathbf{R}') &= \frac{1}{\sqrt{N}} \sum_{\mathbf{R}} e^{i\mathbf{k}\cdot\mathbf{R}} \varphi(\mathbf{r} + \mathbf{R}' - \mathbf{R}) \\ &= \frac{1}{\sqrt{N}} e^{i\mathbf{k}\cdot\mathbf{R}'} \sum_{\mathbf{R}-\mathbf{R}'} e^{i\mathbf{k}\cdot(\mathbf{R}-\mathbf{R}')} \varphi(\mathbf{r} + \mathbf{R}' - \mathbf{R}) = e^{i\mathbf{k}\cdot\mathbf{R}'} \varphi_{\mathbf{k}}(\mathbf{r}), \end{aligned} \quad (126)$$

which is Bloch's theorem.

## VIII. PHONONS IN ONE DIMENSION

### A. Monoatomic basis

A phonon is a lattice vibration. It is called a collective excitation, since atoms move at the same time. The easiest way to derive the phonon dispersion is to start from Newton's equation of motion. The potential between the atoms are considered to behave like springs. Or in other terms, the assumption is that the potential of the atom around its equilibrium position is given by a parabola. In one dimension, the equation of motion for atom at site  $R = na$  where  $n$  is an integer and  $a$  the distance between the atoms. is then given by

$$M \frac{d^2 x_R}{dt^2} = K [(x_{R+a} - x_R) - (x_R - x_{R-a})] \quad (127)$$

$$= K (x_{R+a} + x_{R-a} - 2x_R), \quad (128)$$

We can look for normal modes of oscillation if we assume that

$$x_R \sim e^{ikR - i\omega t}. \quad (129)$$

Inserting gives

$$-\omega^2 M = K(e^{ika} + e^{-ika} - 2) = 2K(\cos ka - 1) \quad (130)$$

Using that  $\cos 2x = 1 - 2\sin^2 x$  or  $1 - \cos 2x = 2\sin^2 x$ , we find

$$\omega = \sqrt{\frac{4K}{M}} \sin \frac{1}{2}ka. \quad (131)$$

Unlike electrons, the phonon dispersion is zero for  $k = 0$ . This can be understood by visualizing what the displacements are in this limit. For  $k = 0$ , all atoms are moving in the same direction. Basically, this is a displacement of the lattice which does not cost and elastic energy since the distance between the atoms does not change. This is known as a Goldstone mode. The velocity of a wave packet is given by its group velocity

$$v_g = \frac{d\omega}{dk}. \quad (132)$$

(remember that for a free electron, we have

$$v_g = \frac{d\omega}{dk} = \frac{d(\hbar\omega)}{d(\hbar k)} = \frac{d\varepsilon_k}{dp} = \frac{d}{dp} \frac{p^2}{2m} = \frac{p}{m}, \quad (133)$$

so the definition makes sense). For the dispersion in Eqn. (131), we find

$$v_g = \sqrt{\frac{Ka^2}{M}} \cos \frac{1}{2}ka. \quad (134)$$

The group velocity is zero at the zone boundary  $k = \frac{\pi}{a}$ . For this wavevector, we have a standing wave. For small wavevectors, we can use  $\cos x \cong 1$ , to obtain

$$v_g = \sqrt{\frac{Ka^2}{M}}. \quad (135)$$

The group velocity in the limit  $ka \ll 1$  is independent of the wavevector  $k$ . In the same limit, we can use  $\sin x \cong x$ , and write the dispersion relation as

$$\omega \cong \sqrt{\frac{4K}{M}} \frac{1}{2}ka = \sqrt{\frac{Ka^2}{M}} k = v_g k \quad (136)$$

## IX. PERIODICITY AND BASIS

### *AM Chapters 4-7*

In the previous sections, we studied a simple one-dimensional chain consisting of one type of atom. Taking this chain along the  $x$ -direction, we can build up this chain by taking multiples of a primitive vector that gives the vector needed to go from lattice site into another

$$\mathbf{a}_1 = a\hat{\mathbf{x}} \quad \Rightarrow \quad \mathbf{R} = n\mathbf{a}_1 \quad \text{with} \quad n = \dots, -2, -1, 0, 1, 2, \dots \quad (137)$$

However, more important for our considerations of the periodic potential was not so much the real space position of the atoms, but their effect on reciprocal space. This is directly related to the fact that momentum  $\mathbf{k}$  is a good quantum number. Translational symmetry of the potential imposed, reproducing Eqn. (57),

$$e^{i\mathbf{K}\cdot\mathbf{R}} = 1. \quad (138)$$

In one dimension this gives reciprocal lattice vectors, which again can be expressed in a unit vector

$$\mathbf{b}_1 = \frac{2\pi}{a}\hat{\mathbf{x}} \quad \Rightarrow \quad \mathbf{K} = n\mathbf{b}_1 \quad \text{with} \quad n = \dots, -2, -1, 0, 1, 2, \dots \quad (139)$$

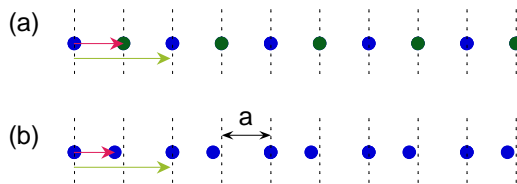


FIG. 13: Examples of one-dimensional chains that cannot be described by a single vector. For both (a) and (b), the green vector is the lattice vector that describes the periodicity.

It is easy to see that  $\mathbf{R}$  and  $\mathbf{K}$  satisfy the condition  $e^{i\mathbf{K}\cdot\mathbf{R}} = 1$ .

*Basis.*— So far, we have considered one-dimensional systems with only one atom in the unit cell. Let us consider for example a chain with alternating atoms at the lattice positions  $n\mathbf{a}_1$ , see Fig. 13(a). It can be easily seen that the periodicity is now  $2a$  instead of  $a$ . We therefore need a new primitive vector

$$\mathbf{a}'_1 = 2a\hat{\mathbf{x}} \quad \Rightarrow \quad \mathbf{R} = n\mathbf{a}'_1 \quad \text{with} \quad n = \dots, -2, -1, 0, 1, 2, \dots \quad (140)$$

Using the vectors

$$\mathbf{r}_1 = 0 \quad \text{and} \quad \mathbf{r}_2 = a\hat{\mathbf{x}}. \quad (141)$$

This is known as a basis of atoms. We can build the chain by putting atoms of type 1 at sites  $\mathbf{R} + \mathbf{r}_1$  and atoms of type 2 at sites  $\mathbf{R} + \mathbf{r}_2$ .

An alternative way to obtain a doubling of the primitive vector is by a displacement of the atom, as done, for example, in Fig. 13(b). The basis is now  $\mathbf{r}_1 = 0$  and  $\mathbf{r}_2 = \alpha a\hat{\mathbf{x}}$  with  $0 < \alpha < 1$ . In this situation we place equivalent atoms at the vectors  $\mathbf{R} + \mathbf{r}_i$  with  $i = 1, 2$ . This is known as a Peierls distortion.

## X. EFFECTS OF A BASIS ON THE ELECTRONIC STRUCTURE

In this section, we study the effects that the introduction of a basis can have on the electronic structure. Let us consider the situation of two inequivalent atoms, see Fig. 13(a), which is slightly easier than the situation for displaced atoms. We already saw that the one-dimensional chain is given by  $\varepsilon_{\mathbf{k}} = -2t \cos ka$ , see Eqn. (34). Now one of the atoms is replaced by a different atom. First, this could affect the hopping matrix element  $t$ . However, this effect is not that interesting since it does not really make the atoms different and we ignore it. The next effect is the difference in on-site energy that an electron feels when it is on site. Let us take this difference in on-site energy to be  $\Delta$ . We can now write down the  $2 \times 2$  tight-binding Hamiltonian for the chain

$$H = \begin{pmatrix} 0 & \varepsilon_{\mathbf{k}} \\ \varepsilon_{\mathbf{k}} & \Delta \end{pmatrix} \begin{array}{l} |1\rangle \\ |2\rangle \end{array} \quad (142)$$

Note that atoms of type 1 only couple to atoms of type 2. Atom of the same type do not couple to each other. However, in principle, we could include next-nearest neighbor matrix elements, which leads to terms of the form  $\varepsilon_{\mathbf{k}}^i = -2t_i \cos 2ka$  for  $i = 1, 2$  on the diagonal. This matrix is solved straightforwardly giving eigenvalues

$$E_{\pm} = \frac{\Delta}{2} \pm \frac{1}{2} \sqrt{\Delta^2 + 4\varepsilon_{\mathbf{k}}}. \quad (143)$$

The solutions are given in Fig. 14. The first thing to note is that the increase of the periodicity from  $a$  to  $2a$  leads to a reduction of the size Brillouin zone from  $\pi/a$  to  $\pi/2a$ . Second, in the region  $[-\pi/a, \pi/a]$ , we now have two bands which is directly related to the fact that we now have two atoms in the basis. However, since the states are strongly mixed we cannot identify a particular band with a particular atom. Third, at the edges of the new Brillouin zone at  $\pm\pi/2a$ , we see that a gap opens. In the limit  $\Delta \rightarrow 0$ , this gap disappears and the eigenvalues are  $E_{\pm} = \pm\varepsilon_{\mathbf{k}}$ . We recover the original band, but folded back inside the smaller Brillouin zone.

For the distorted system, see Fig. 13(b), a similar thing happens. This result can have surprising effects. Let us suppose we had an undistorted system with a half-filled band  $\varepsilon_{\mathbf{k}}$ . Since the Fermi level lies nicely inside a band, this system is a metal. Now if the system for some reason distorts (and it is not unusual to have lattice distortions as a function of temperature), then a gap opens. The lower band in Fig. 14 is then full, whereas the upper band is empty. Therefore, an energy of  $\Delta$  is necessary to excite an electron from the occupied states to the unoccupied states. The system is now an insulator/semiconductor.

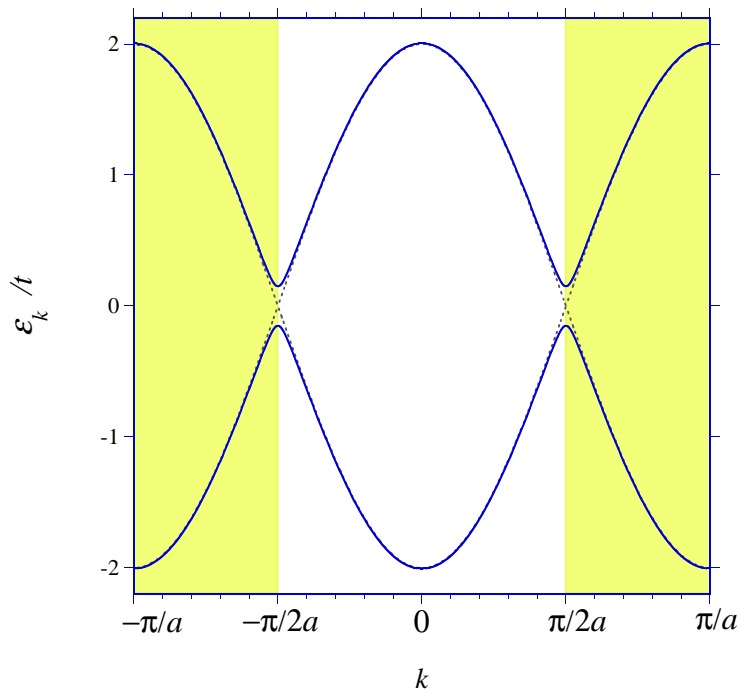


FIG. 14: The effect of having alternating atoms 1 and 2 on the electronic structure for a one-dimensional chain. First, the increase of the periodicity from  $a$  to  $2a$  leads to a reduction of the Brillouin zone from  $\pi/a$  to  $\pi/2a$ . Second, at the edges of the new Brillouin zone at  $\pm\pi/2a$  a gap opens up (for clarity, the new bands have been shifted down by  $\Delta/2$ ).

## XI. EFFECTS OF A BASIS ON THE PHONON DISPERSIONS

We now consider what the effect is of the presence of two atom in the basis on the phonon dispersion. We can extend Eqn. (128) by considering two atoms

$$M_1 \frac{d^2 u_R}{dt^2} = K(v_{R+a} + v_{R-a} - 2u_R) \quad (144)$$

$$M_2 \frac{d^2 v_{R+a}}{dt^2} = K(u_{R+2a} + u_R - 2v_{R+a}), \quad (145)$$

where  $u_R$  and  $v_R$  are deviations from the equilibrium position  $R$ . Again, we look for solutions in the form of travelling waves

$$u_R = u e^{ikR - i\omega t} \quad \text{and} \quad v_{R+a} = v e^{ikR - i\omega t}. \quad (146)$$

Inserting in the equations of motion gives

$$-\omega^2 M_1 u = K v (1 + e^{-2ika}) - 2K u \quad (147)$$

$$-\omega^2 M_2 v = K u (e^{2ika} + 1) - 2K v. \quad (148)$$

We can find the solutions of these two equations by solving the determinant

$$\begin{vmatrix} 2K - \omega^2 M_1 & K(1 + e^{-2ika}) \\ K(1 + e^{2ika}) & 2K - \omega^2 M_2 \end{vmatrix} = 0. \quad (149)$$

This gives

$$M_1 M_2 \omega^4 - 2K(M_1 + M_2)\omega^2 + 2K^2(1 - \cos 2ka) = 0. \quad (150)$$

The solutions are given by

$$\omega^2 = \frac{K(M_1 + M_2)}{M_1 M_2} \pm \frac{1}{2M_1 M_2} \sqrt{4K^2(M_1 + M_2)^2 - 8M_1 M_2 K^2(1 - \cos 2ka)}. \quad (151)$$

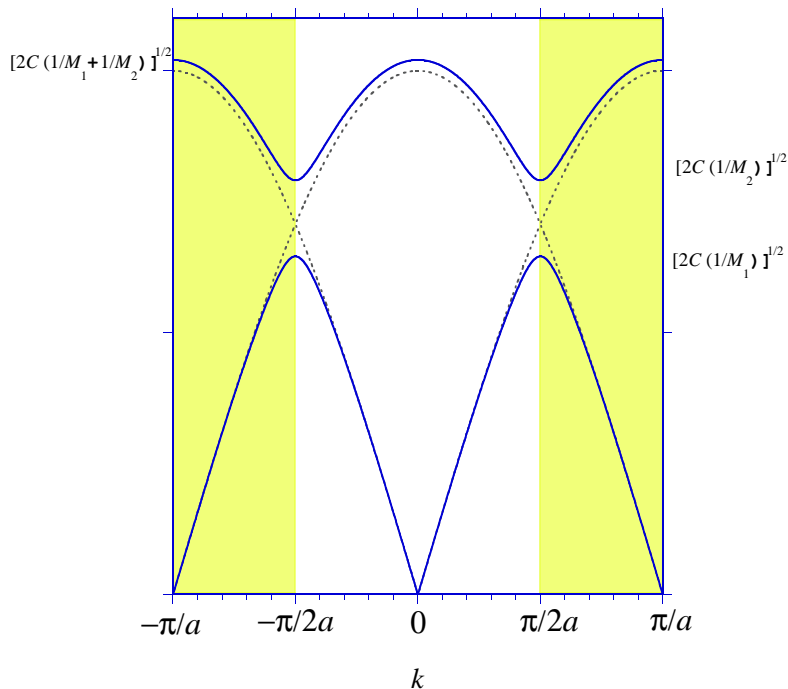


FIG. 15: Optical and acoustical branches of the phonon dispersion for a diatomic chain with  $M_1 > M_2$ . The limiting frequencies at  $k = 0$  and  $k = \pi/2a$  are indicated.

We can also look at the limiting values for  $k \rightarrow 0$  and  $k = \pi/2a$ . For  $k \rightarrow 0$ , we have  $\cos 2ka \cong 1 - \frac{1}{2}(2ka)^2$ , giving two roots

$$\omega = \sqrt{2K\left(\frac{1}{M_1} + \frac{1}{M_2}\right)} \quad (152)$$

$$\omega = \sqrt{\frac{K}{2(M_1 + M_2)}} 2ka. \quad (153)$$

As in the previous section, the doubling of the unit cell from  $a$  to  $2a$  leads to a reduction of the Brillouin zone from  $k = \pi/a$  to  $\pi/2a$ . At the edge of the Brillouin zone the eigenvalues are

$$\omega = \sqrt{\frac{2K}{M_1}} \quad \text{and} \quad \omega = \sqrt{\frac{2K}{M_2}}. \quad (154)$$

Although one-dimensional materials (or materials that act one-dimensional) are less common than three-dimensional systems, the effects described here already give a good idea of the consequences of inclusion of more atoms in a basis. Also in three-dimensional systems there are different reason to have two atoms in the basis. Obviously, one can have two different atoms in the compounds, such as, e.g. NaCl. However, some crystals cannot be simply described by the primitive vectors, but require a basis. Examples are silicon and diamond.

If the chain was really one-dimensional then the atoms can only move in one direction, i.e. along the chain. However, for a one-dimensional chain in three dimensions the atoms can move in three directions, not only along the chain, but also perpendicular to the chain. The vibrations along the chain give rise to longitudinal phonons. The modes perpendicular to the chain lead to the transverse branches. Since there are two directions perpendicular to the chain, there are two transverse modes. The corresponds to the notion that for a chain of  $N$  atoms, there are  $3N$  degrees of freedom. The splitting is clearly observed experimentally, see for example the phonon dispersions for silicon in Fig. 17. The longitudinal vibrations, being towards the neighboring atoms, cost more energy.

## XII. CRYSTAL STRUCTURES

In one dimension, we do not have too many choices. We can change  $a$ , the difference between the atoms. One might think that we can also change something by taking the vector not along the  $\hat{x}$  but in a different direction.

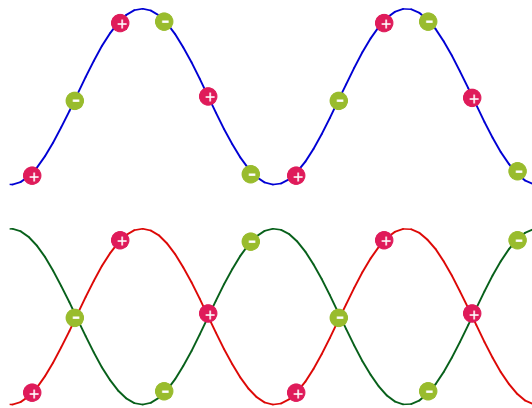


FIG. 16:

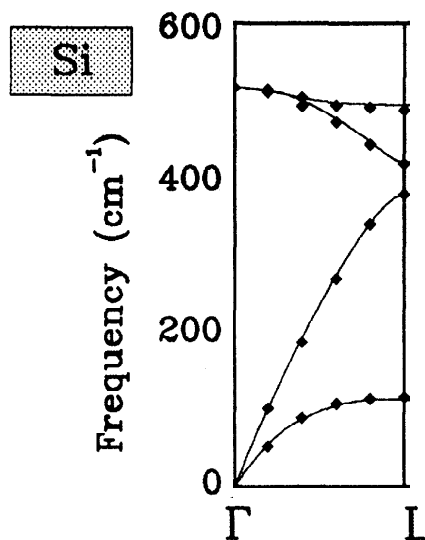


FIG. 17: The phonon dispersion in Si in a high-symmetry direction in the Brillouin zone. Along other directions the transverse modes split. Note that  $100 \text{ cm}^{-1} \cong 12.4 \text{ meV}$ .

However, this would not change the one-dimensional crystal, but simply rotate the whole crystal. When going to two dimensions there are many more possibilities. We can take two vectors  $\mathbf{a}_1$ ,  $\mathbf{a}_2$ . Obviously, we have the condition that the vectors are not parallel. However, they can have different lengths and the angle between the vectors can change. The lattice can be constructed via

$$\mathbf{R} = n_1 \mathbf{a}_1 + n_2 \mathbf{a}_2 \quad (155)$$

When studying crystal structures, the lattice is assumed to stretch to infinity. This means that  $u_1$  and  $u_2$  assume any integer value. From each lattice point, the lattice looks entirely equivalent. There is not one particular choice to reproduce a lattice, see Fig. 18(a) and (b). Some vectors can produce part of the lattice points, but do not reproduce the entire lattice, see Fig. 18(c). They are therefore not proper lattice vectors.

The lattice points created by the vectors  $\mathbf{a}_1$  and  $\mathbf{a}_2$  do not directly correspond to atoms. For a simple system, one can have a simple one to one correspondence between the lattice points and the atoms, see Fig. 19(a). However, this is not necessary and we can simply displace the atoms from the lattice points, see Fig. 19(b). The two vectors  $\mathbf{a}_1$  and  $\mathbf{a}_2$  build up a parallelogram. Each parallelogram contains exactly the same number of atoms (in this simple case one atom). This parallelogram is a primitive lattice cell. But generally, several atoms can be related to each lattice point, see Fig. 19(c). These can be equivalent atoms, different atoms, and, in a molecular crystal, correspond to entire molecules. Again, there is no unique choice to create primitive lattice cells. There are an infinite number of ways to create primitive cells. However, they should all have the same area (or in three dimensions, the same volume) and built up the plane (space) without leaving any empty space.



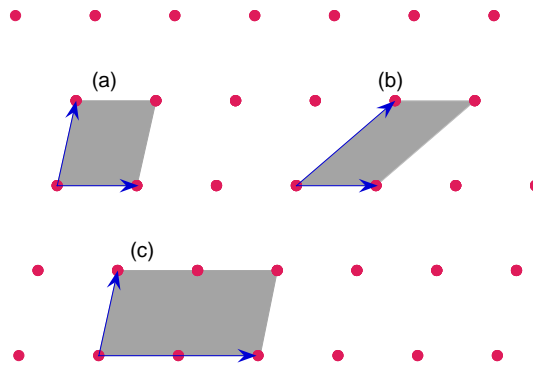


FIG. 18: Lattice points in two dimensions. The choice of vectors is not unique. The vectors given in (a) and (b) both reproduce the same lattice points. On the other hand, the vectors given in (c) do not reproduce the lattice points.

With two arbitrary vectors, an infinite number of lattices can be built. However, for lattice vectors of unequal length and with an arbitrary angle between them, there is not a lot of symmetry. Only rotations of  $\pi$  and  $2\pi$  about any lattice point bring the lattice back onto itself. This is called an oblique lattice. However, special lattices can be invariant under rotation of  $2\pi/3$ ,  $2\pi/4$ , or  $2\pi/6$ . To achieve this invariance, stricter conditions must be imposed onto the lattice vector, such as equal length or specific angles between the vectors, such as  $90^\circ$  and  $120^\circ$ . We can distinguish five distinct lattices, known as Bravais lattices, see Fig. 20. The most straightforward is the square lattice, comparable with a two-dimensional Cartesian coordinate system. This is the lattice with the highest symmetry. We can change the vectors to obtain lattice of lower symmetry. For example, by making their lengths unequal, we obtain a rectangular lattice. Note that we could rotate the square lattice under  $45^\circ$  and obtain the same lattice. However, this is no longer possible for the rectangular lattice. We can also make the angle between the vectors different from  $90^\circ$ . Again, this lowers the symmetry. In the end, one might wonder why we care that one lattice is more symmetric than another lattice. The answer lies in the fact that the different symmetries manifest themselves into their different electronic structure and macroscopic properties. For example, different lattice parameters in different directions can lead to a different resistivity.

In condensed-matter physics, one is dealing more often with three-dimensional systems. Again, we can build up a crystal starting from the primitive vectors  $\mathbf{a}_1$ ,  $\mathbf{a}_2$ , and  $\mathbf{a}_3$ . For a simple cubic system, these are given by  $\mathbf{a}_1 = a\hat{x}$ ,  $\mathbf{a}_2 = a\hat{y}$ , and  $\mathbf{a}_3 = a\hat{z}$ . Often however the crystal structures are more complicated, such as face-centered cubic or body-centered cubic. (This is for a large part related to the fact that simple cubic is not close packed. Try obtaining a simple cubic lattice by throwing marbles in a box ...). Let us look at the different lattices in more detail. We can

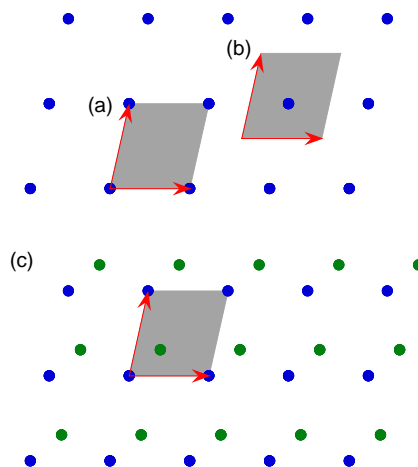


FIG. 19: Lattice vectors can build up different lattices. Figures (a) and (b) shows that lattice points do not necessarily coincide with the position of the atoms. However, each primitive lattice cell contains the same number of atoms. Although it might appear that there are more atoms in the primitive lattice cell in (a). This is because the atoms are shared by several primitive lattice cells. Figure (c) shows an example of a lattice with a basis of two atoms.

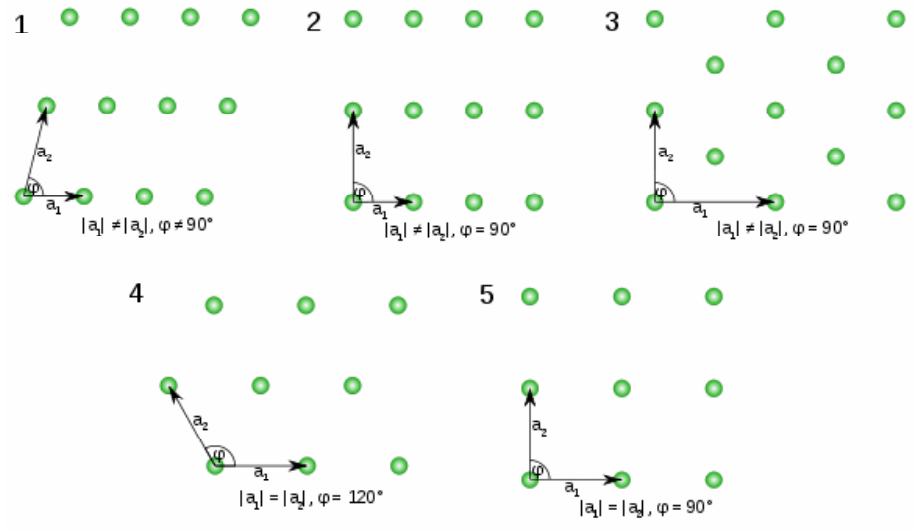


FIG. 20: The five fundamental two-dimensional Bravais lattices: 1: oblique, 2: rectangular, 3: centered rectangular, 4: hexagonal, and 5: square. Source: wikipedia

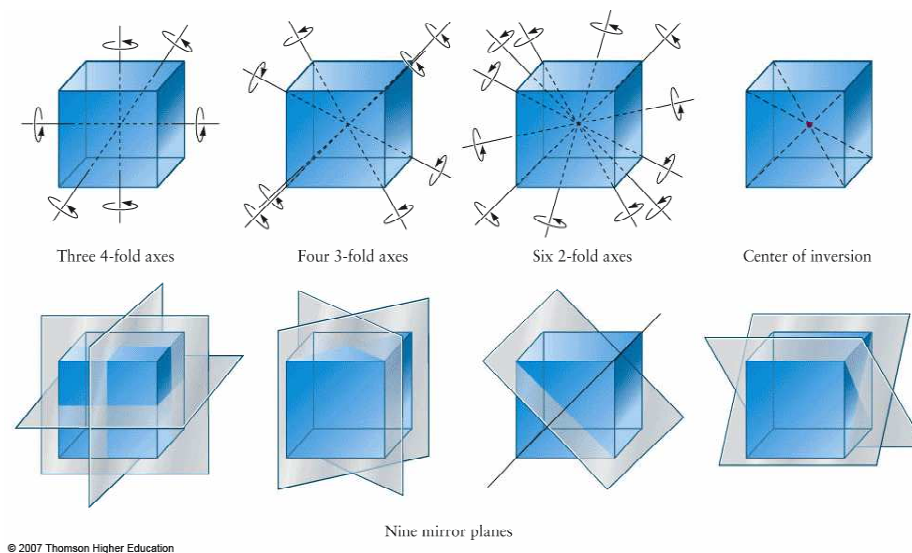


FIG. 21: The symmetry operations of a cube.

classify the different lattice according to their different symmetry operations. These symmetry operations can include translation, rotation, reflections and inversion. We can separate two sets of operations for the Bravais lattices

- Translations through Bravais lattice vectors.
- Operations that leave a particular point of the lattice fixed (point group operations).
- A combination of the above.

Let us again look at the simple cube. The symmetry operations of a cube are shown in Fig. 21. A cube can be brought onto itself by two-, three-, and four-fold rotations, nine mirror planes, and by inversion. The cube is the basic shapes with the largest number of point group operations. In total, there are seven different basic shapes, see Fig. basicshapes, that define seven different lattice systems. Why do we care about the change in symmetry. The reason for that is that the symmetry can teach us a lot about the splitting of the energy levels of different orbitals. When we only look at the local point group operations, this is generally known as crystal field splitting, see Fig. 23. In quantum mechanics, we are taught the hydrogen atom, where the orbitals with the same  $n$  and  $l$  have the same

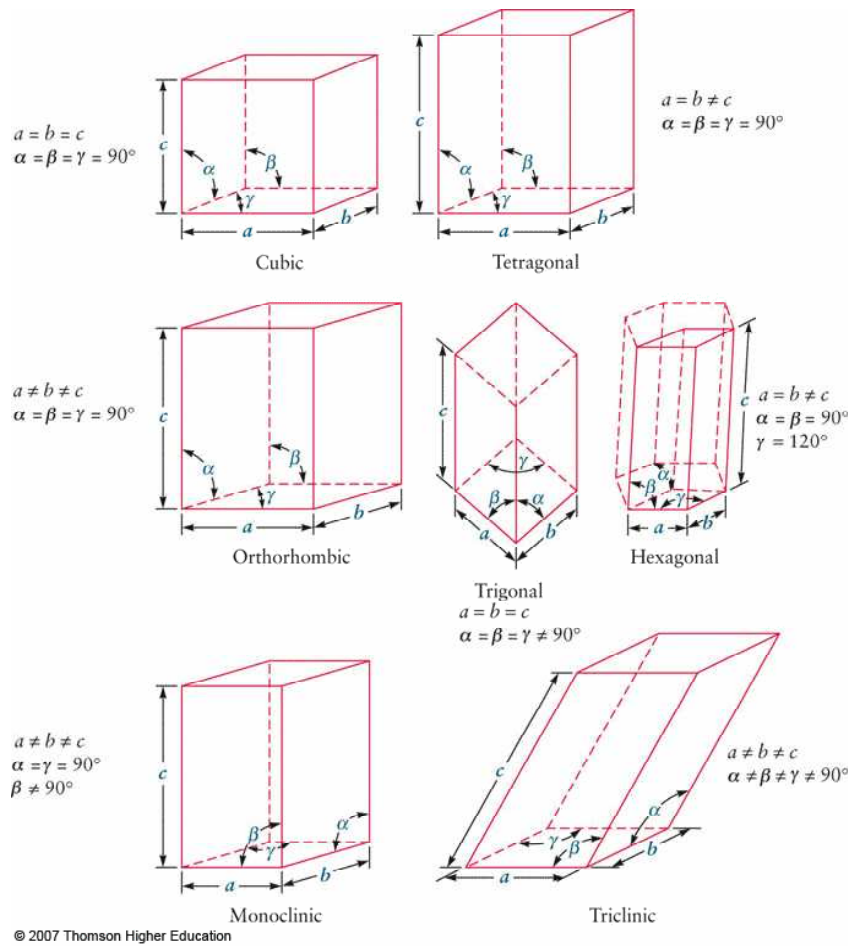


FIG. 22: The seven basic shapes that define the seven lattice systems.

TABLE I: Real orbitals as a combination of the atomic orbitals  $\psi_{lm}$ .

$l = 0$	$s$	$\psi_{00}$	$\sim 1$
$l = 1$	$p_x$	$-\frac{1}{\sqrt{2}}(\psi_{11} - \psi_{1,-1})$	$\sim x$
	$p_y$	$\frac{i}{\sqrt{2}}(\psi_{11} + \psi_{1,-1})$	$\sim y$
$l = 2$	$p_z$	$\psi_{10}$	$z$
	$d_{yz}$	$\frac{i}{\sqrt{2}}(\psi_{21} + \psi_{2,-1})$	$\sim \sqrt{3}yz$
	$d_{zx}$	$-\frac{1}{\sqrt{2}}(\psi_{21} - \psi_{2,-1})$	$\sim \sqrt{3}zx$
	$d_{xy}$	$-\frac{i}{\sqrt{2}}(\psi_{22} - \psi_{2,-2})$	$\sim \sqrt{3}xy$
	$d_{x^2-y^2}$	$\frac{1}{\sqrt{2}}(\psi_{22} + \psi_{2,-2})$	$\sim \frac{\sqrt{3}}{2}(x^2 - y^2)$
	$d_{3z^2-r^2}$	$\psi_{20}$	$\sim (\frac{3}{2}z - \frac{1}{2}r^2)$

energy (although you probably also learnt that they can be split by the spin-orbit coupling, which we will not consider here). The quantum number  $l$  with its orbital components  $m = -l, -l + 1, \dots, l - 1, l$  can be seen as a symmetry classification for spherical symmetry. Symmetry tells you that different  $l$  can have different energies, but there is no reason that the  $2l + 1$  different levels classified with  $m$  should have different energies. The spherical group is known as  $SO_3$ . The 3 essentially indicates that all three axes are equivalent. This is no longer the case when one applies a magnetic field. When taking the field along the  $z$ -axis, the  $x$  and  $y$  axis are still equivalent to each other, but the  $z$  axis is different. This group is known as  $SO_2$ . Symmetry considerations that are beyond the scope of this course tell that this splits all the different levels for a particular  $l$ , i.e. all the  $m$  have different energies. The theory behind this is known as group theory. Symmetry considerations can teach you many things. For example, many of the theory on quarks in high-energy physics are based on group-theoretical considerations (in this case the  $SU_3$  group).

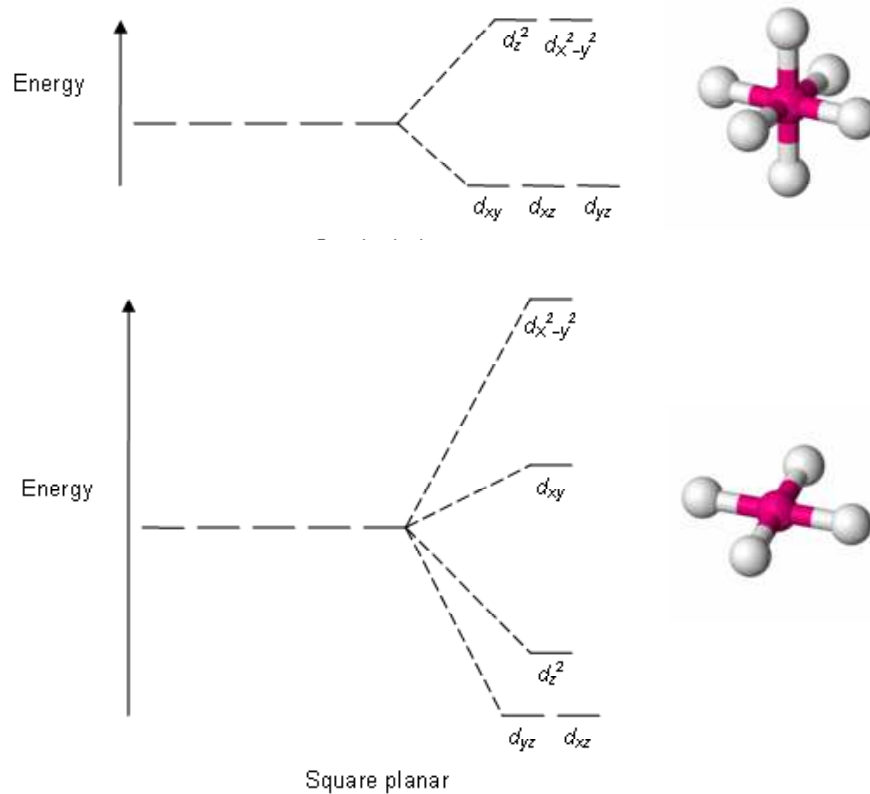


FIG. 23: The effect of the lowering of the symmetry on the energy levels of the  $3d$  electrons.

The same ideas hold for point-group symmetries. If a system has a higher symmetry (i.e. more symmetry operations bring the lattice onto itself) then more levels are degenerate. If the symmetry is lowered, the levels split. Let us consider an atom in a cubic environment. The atom has six nearest-neighbors at equal distances, see Fig. 23. We know that an  $s$  level in this surrounding does not split, simply it is just one state and it is impossible to split one state. When we consider the  $p$  orbitals, again nothing changes. We can imagine the  $p_x$ ,  $p_y$ , and  $p_z$  orbitals and one can easily verify that they have the same surroundings. Table I shows how to obtain these orbitals from the atomic orbitals and Fig. 24 gives an idea of the size of the wavefunction. However, this is no longer the case when considering  $d$  orbitals. The  $d$  orbitals have  $l = 2$  and are therefore fivefold degenerate (neglecting spin). Group symmetry tells you that the  $d$  orbitals split into two groups, one twofold degenerate and one threefold degenerate. These are generally known as  $e_g$  and  $t_{2g}$  orbitals, respectively. Although group theory tells you that this is the way they should split in this symmetry, it does not tell you what the energies are (compare high-energy physics. The symmetry tells you what quarks there are not their masses). The symmetry tells you how things will split, but the Hamiltonian of the system causes the actual splitting. In fact, the splitting can be due to different effects. If there is nothing in the Hamiltonian of the six surrounding atoms that affect the atom in the center, see Fig. 23, the splitting is zero and all the  $d$  levels are degenerate. Essentially from an electronic point of view, the symmetry is still spherical. The levels can split because the neighboring atoms are not neutral (for example, in an ionic crystal, they have a real charge). These arguments also hold for more complicated systems. Figure 23 shows a typical situation for the  $d$  orbitals, where the  $t_{2g}$  levels  $d_{xy}$ ,  $d_{yz}$ , and  $d_{zx}$  are lower in energy than the  $e_g$  levels  $d_{x^2-y^2}$  and  $d_{3z^2-r^2}$ . Generally, in a compound, the transition metal ions are positively charged. For example, the formal valency of nickel in NiO is  $\text{Ni}^{2+}$ . NiO has a NaCl structure, so the nickel atom is surrounded by six oxygen ions. This is a cubic surrounding as shown in Fig. 23 (the formal notation is  $O_h$ ). The surrounding oxygens are negatively charged,  $\text{O}^{2-}$ . This means that the  $3d$  orbitals of nickel experience a potential of the six oxygens. Since this potential is not nicely spherical, the orbitals split. The electrons in the  $e_g$  orbitals feel the repulsive potential of the oxygens more strongly, since the lobes of the orbitals are pointing towards the neighboring oxygens, see Fig. 24. An alternative way to split the orbitals is due to the formation of covalent bonds between the transition metal and the oxygens. Even though the mechanism is different, the splitting is the same. The symmetry can be lowered by, for example, removing the atoms in the  $z$  direction, see Fig. 23. This surrounding has tetragonal symmetry, see Fig. basicshapes. When doing this, the  $p$  orbitals split in energy. Just by looking at the surrounding ions, it is clear that the  $p_z$  orbital is now different from the  $p_x$  and  $p_y$  orbitals. For the  $d$

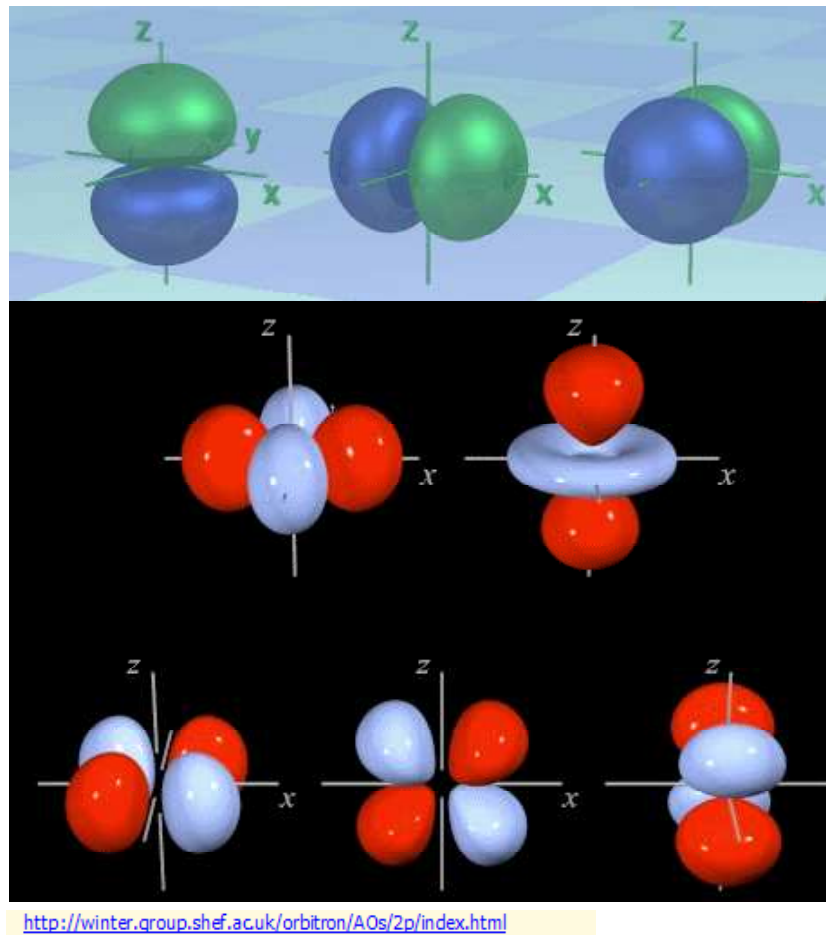


FIG. 24: Top: the three  $p$  orbitals ( $p_z$ ,  $p_x$ ,  $p_y$ ). Bottom: the five  $d$  orbitals ( $x^2 - y^2$ ,  $3z^2 - r^2$ ,  $xy$ ,  $zx$ ,  $yz$ ).

orbitals, we see that the levels split further. Only the  $yz$  and  $zx$  orbitals are now equivalent from a symmetry point of view. In a solid where all the axes are different, known as orthorhombic symmetry, see Fig. basicshapes, also the energies of these two orbitals will be different.

The point group symmetries lead to seven basic shapes, see Fig. basicshapes, which correspond to seven lattice systems. However, we have considered now only the point group. We can also include the translational properties. The combination of point group and translational operations is called the space group. Inclusion of these lead to a total of fourteen Bravais lattices, see Fig. 25. For the cubic system, there are three inequivalent lattices: the simple cube, the body-centered cube (bcc), and the face-centered cube (fcc). Although part of the cubic point group, the primitive vectors of the simple cube do not produce the fcc and bcc lattices. We could build these lattices using the primitive vectors of a simple cube plus a basis. For example, for bcc, the basis would be  $\mathbf{0}$  and  $\frac{a}{2}(\hat{x} + \hat{y} + \hat{z})$  if the sides of the cube have length  $a$ . However, although this might bring out the point group better, they are not the primitive vectors of the bcc lattice. One choice that reproduces the bcc lattice is

$$\mathbf{a}_1 = \hat{x} \quad \mathbf{a}_2 = \hat{y} \quad \mathbf{a}_3 = \frac{a}{2}(\hat{x} + \hat{y} + \hat{z}), \quad (156)$$

see the left side of Fig. 26. However, generally there are more choices. A more symmetric set is

$$\mathbf{a}_1 = \frac{a}{2}(-\hat{x} + \hat{y} + \hat{z}) \quad \mathbf{a}_2 = \frac{a}{2}(\hat{x} - \hat{y} + \hat{z}) \quad \mathbf{a}_3 = \frac{a}{2}(\hat{x} + \hat{y} - \hat{z}), \quad (157)$$

see the right side of Fig. 26. We cannot do this for all lattice systems since some of them are equivalent to other Bravais lattices. This can already be seen in two dimensions. Whereas there is a centered rectangular Bravais lattice, there is no centered square lattice. It is easily verified that a centered square lattice is in fact a square lattice with a smaller lattice constant.

### XIII. MEASURING CRYSTAL STRUCTURE: DIFFRACTION

The most common method to study crystal structure is X-ray diffraction (although it can also be done with electrons and neutrons). The X-rays scatter through repeated interactions with the atomic nuclei plus their surrounding electron cloud. This scattering is very similar to the scattering of electrons on the periodic potential as we have seen earlier.

The 7 lattice systems	The 14 Bravais lattices			
triclinic	P $\alpha, \beta, \gamma \neq 90^\circ$			
monoclinic	P $\alpha \neq 90^\circ$ $\beta, \gamma = 90^\circ$		C $\alpha \neq 90^\circ$ $\beta, \gamma = 90^\circ$	
orthorhombic	P $a \neq b \neq c$	C $a \neq b \neq c$	I $a \neq b \neq c$	F $a \neq b \neq c$
	a	b	c	c
	b	b	b	b
tetragonal	P $a \neq c$		I $a \neq c$	
rhombohedral	P $\alpha, \beta, \gamma \neq 90^\circ$			
hexagonal	P $a \neq c$			
cubic	P (fcc)	I (bcc)	F (fcc)	
	a	a	a	

FIG. 25: The fourteen three-dimensional Bravais lattices. Source: wikipedia

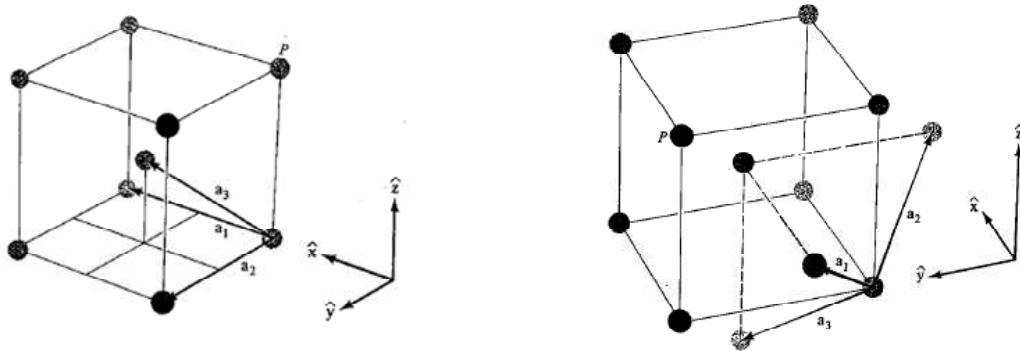


FIG. 26: Two ways of choosing the primitive vectors for a bcc lattice.

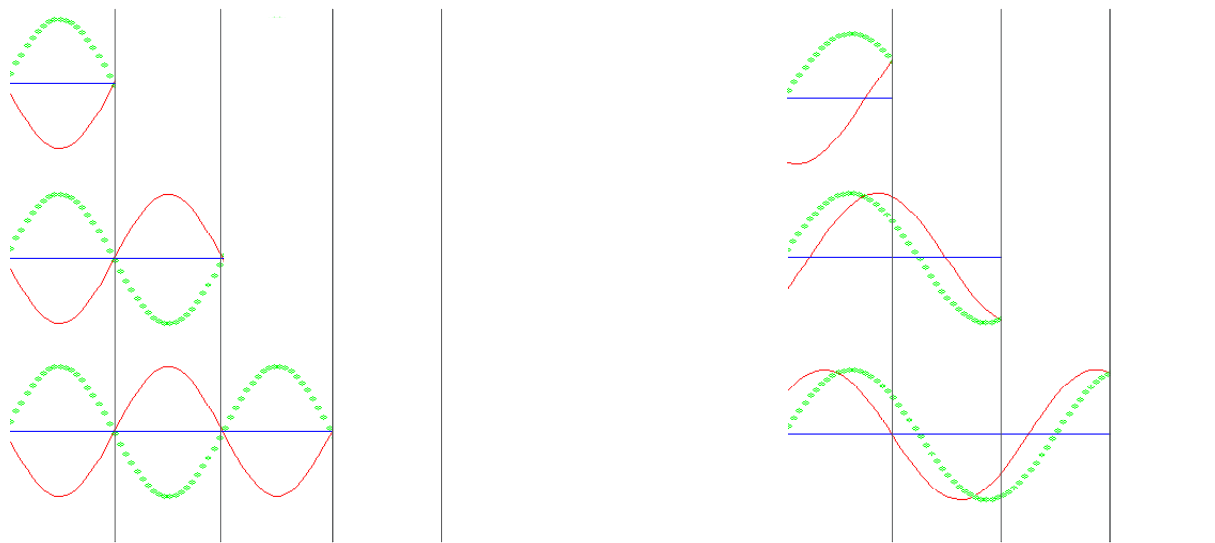


FIG. 27: Bragg reflection in back-scattering for a three-dimensional crystal (or a chain). The left side shows the condition for which Bragg scattering occurs. The light coming in from the left (green dots) is the same. From top to bottom, the red line shows the reflection from the first, second, and third crystal plane. The outgoing waves are all the same again and therefore interfere constructively. The wavevector  $k = \pi/a$ , with  $a$  the distance between the planes, corresponding to a wavelength of  $\lambda = 2a$  satisfies the Bragg condition. The right side shows what happens for a wavevector that does not satisfy the Bragg condition. Again, all the incoming waves are equivalent. However, since the scattered waves are different, there is a destructive interference.

In fact, we already derived the conditions for the scattering of X-rays, see Eqn. (65),

$$\mathbf{k} \cdot \mathbf{K} = \frac{1}{2}K^2, \quad \text{or} \quad \mathbf{k} \cdot \hat{\mathbf{K}} = \frac{1}{2}K, \quad (158)$$

where  $\hat{\mathbf{K}}$  is a unit vector in the direction of the reciprocal lattice vector  $\mathbf{K}$ . When  $\mathbf{k}$  is parallel to  $\mathbf{K}$ , we have  $k = \frac{1}{2}K$ . This is effectively like a one-dimensional case, where the reciprocal lattice vectors are given by  $K = 0, \pm \frac{2\pi}{a}, \frac{4\pi}{a}, \dots$ . The smallest nonzero wavevector for which we have Bragg reflection is then  $k = \frac{\pi}{a}$ . This corresponds to a wavelength of  $2a$ , where  $a$  is the distance between the lattice planes. This situation is depicted in the left side of Fig. 27. We see that the scattered waves have all the same phase and therefore interfere constructively. On the right side of Fig. 27, we see that for an arbitrary wavevector scattered waves from different crystal planes, the waves interfere destructively. We can also see what happens if the planes are inequivalent. Figure 28 shows the situations for a wavevector  $k = \pi/2a$  or a wavelength of  $\lambda = 4a$ . If the planes were equivalent, one would not expect any constructive interference, which can be seen from Fig. 28, where the scattered waves have opposite sign when going out of the crystal. This is expected since  $k = \pi/2a$  does not satisfy the condition  $k = \frac{1}{2}K$ . However, if there are alternating planes of different atoms, the amplitude of the scattered waves are different and, although they still interfere destructively, the cancellation is not complete and one still observes scattered intensity. This is expected since making alternating planes of different atoms

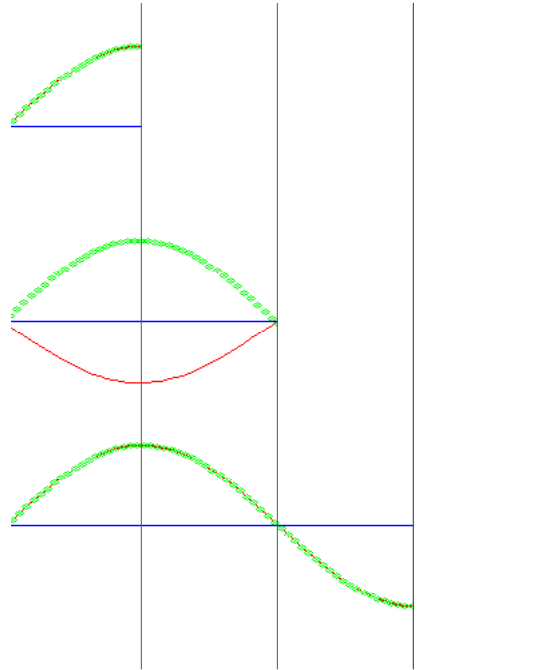


FIG. 28: Bragg reflection in back-scattering for a three-dimensional crystal with  $k = \pi/2a$  or a wavelength of  $\lambda = 4a$ , where  $a$  is the distance between the planes. If the planes were equivalent, this wavevector would not satisfy the Bragg condition and the scattered waves would interfere destructively. However, if the planes are inequivalent (for example, different atoms or the atoms in one plane are slightly displaced) then there is not a complete cancellation and one can still observe a Bragg peak.

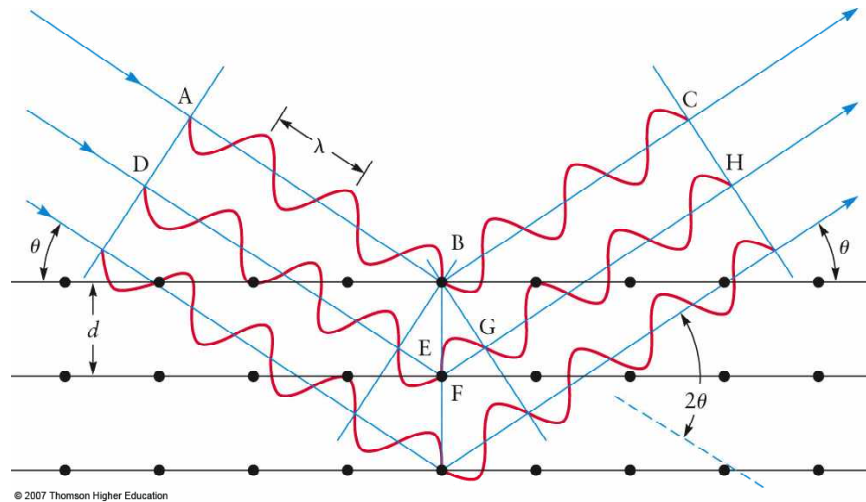


FIG. 29: The scattering of X-rays from a solid with lattice planes separated by  $d$ . The angle between the X-ray beam and the planes is  $\theta$ . The scattered angle is  $2\theta$ .

increases the periodicity from  $a$  to  $2a$ . Therefore the lowest nonzero reciprocal lattice vector is  $K = 2\pi/2a = \pi/a$  and therefore  $k = \pi/2a$  does satisfy the condition  $k = \frac{1}{2}K$ .

Although we had already obtained the Bragg condition  $\mathbf{k} \cdot \mathbf{K} = \frac{1}{2}K^2$ , it is instructive to look at a slightly different derivation. Let us suppose there are X-rays coming in at an angle  $\theta$  with respect to the lattice planes, see Fig. 29. As we saw in the one-dimensional case, in order to obtain constructive interference, the difference in path length needs to be a multiple of the wavelengths of the x-rays. It is straightforward to obtain the difference in pathlength, which is  $2d \sin \theta$ . Equating this to a multiple of the wavelengths gives Bragg's law

$$2d \sin \theta = n\lambda. \quad (159)$$



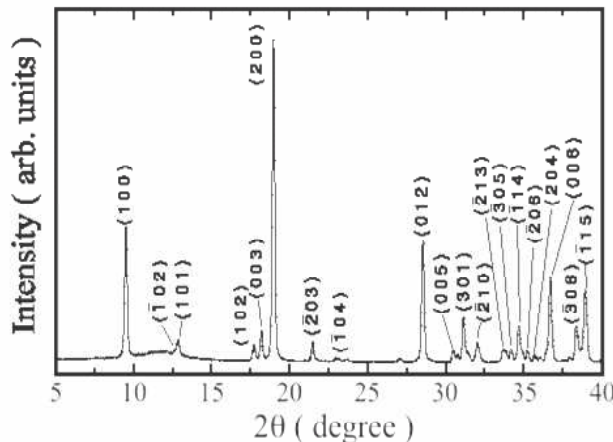


FIG. 30: A typical powder diffraction pattern where the scattering angle is scanned (a  $\theta$ - $2\theta$  scan). The sample is a NbSe<sub>3</sub> powder. From Zhili Xiao.

This is equivalent to the result that we obtained before, which in X-ray diffraction is called the Von Laue condition. For scattering it basically states that for elastic scattering, the difference between the incoming and outgoing wavevectors should be equal to a reciprocal lattice vector

$$\mathbf{k} - \mathbf{k}' = \mathbf{K} \quad \text{or} \quad \mathbf{k}' = \mathbf{k} - \mathbf{K}. \quad (160)$$

Since the wavelength before and after the scattering is equivalent (otherwise the scattering would not have been elastic), the norm should remain the same

$$k = |\mathbf{k} - \mathbf{K}| \Rightarrow k^2 = k^2 - 2\mathbf{k} \cdot \mathbf{K} + K^2 \Rightarrow \mathbf{k} \cdot \mathbf{K} = \frac{1}{2}K^2, \quad (161)$$

which is the same result as for scattering of electrons. Note that the reciprocal lattice vectors for the planes in Fig. 29 is  $\mathbf{K} = n \frac{2\pi}{d} \hat{\mathbf{z}}$ , where the unit vector  $\hat{\mathbf{z}}$  is perpendicular to the lattice planes. We then obtain

$$\mathbf{k} \cdot \mathbf{K} = \frac{2\pi}{\lambda} n \frac{2\pi}{d} \cos\left(\frac{\pi}{2} - \theta\right) = \frac{1}{2}K^2 = \frac{1}{2} \left(n \frac{2\pi}{d}\right)^2 \Rightarrow 2d \sin \theta = n\lambda, \quad (162)$$

which reproduces Bragg's law.

There are several ways to do X-ray diffraction

- The Laue method. Here the scattering geometry is fixed, but the wavelength is varied or, alternatively, using not a monochromatic beam, but one containing X-rays with a certain bandwidth. If the crystal structure is complicated, it is often difficult to properly assign the Bragg peaks. However, it has the advantage that many Bragg peaks can be collected in a short period and is therefore interesting for time-dependent applications.
- More often used methods involve using monochromatic X-rays and changing the scattering condition. In these techniques, one can change the scattering angle (also known as  $\theta$ - $2\theta$  scan, see Fig. 30). However, this does not produce all the Bragg peaks, since one also needs to vary the different orientations of the planes. This can be done in two ways. When dealing with a single crystal, one can rotate the crystal to access the different orientations of the crystal (the rotating crystal method). An alternative method is to measure the X-ray diffraction of a powder. Note that a powder is not an amorphous system, but consists of many small crystallites. Therefore, the powder contains the different orientations of the crystal and an averaging occurs (this is not as the powder or Debye-Scherrer method).

#### XIV. THE RECIPROCAL LATTICE

By now, it has become clear that when dealing with solids the wavevectors related to the lattice often seem to play a more important role than the lattice in real space itself. This is a direct result of the fact that the wavevectors  $\mathbf{k}$

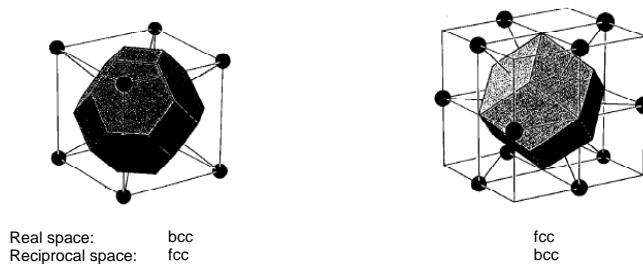


FIG. 31: The primitive unit cell for the bcc (left) and fcc (right) lattices. The spheres indicate the lattice points. Alternatively, these figures represent the first Brillouin zones of the fcc (left) and bcc (right) lattices. The spheres then represent the reciprocal lattice vectors.

are good quantum numbers due to the periodicity of the lattice. This is nothing unusual in physics. The periodicity in time of a wavefunction, makes the frequency  $\omega$  (and at the same time, the energy  $\hbar\omega$  a good quantum number. As we have also seen, it is also directly related to symmetry. That momentum is a good quantum number is inherently related to translational symmetry. Again, we have seen that in quantum mechanics. Angular momentum is a good quantum number for the hydrogen atom because of spherical symmetry. Also, no one is surprised that momentum is a good quantum number for a free particle. Conservation of momentum is a result of the translational symmetry of space. In a solid, however, not every point in space is equivalent to all the other points. Only discrete points are equivalent to each other. In this section, we take a closer look on how to go from real space to reciprocal space in three dimensions.

As we have seen before, reciprocal lattice vectors need to satisfy the condition  $e^{i\mathbf{K}\cdot\mathbf{R}} = 1$ . This can be done by defining the primitive vectors

$$\mathbf{b}_1 = 2\pi \frac{\mathbf{a}_2 \times \mathbf{a}_3}{\mathbf{a}_1 \cdot \mathbf{a}_2 \times \mathbf{a}_3}. \quad (163)$$

The vectors  $\mathbf{b}_2$  and  $\mathbf{b}_3$  can be obtained by cyclic rotation, i.e  $1 \rightarrow 2 \rightarrow 3 \rightarrow 1$ . Note that  $\mathbf{a}_2 \cdot \mathbf{b}_1 = 0$  and  $\mathbf{a}_3 \cdot \mathbf{b}_1 = 0$ , since the outer product makes  $\mathbf{b}_1$  perpendicular to  $\mathbf{a}_2$  and  $\mathbf{a}_3$ . In addition,  $\mathbf{a}_1 \cdot \mathbf{b}_1 = 2\pi$ , and therefore the condition  $e^{i\mathbf{K}\cdot\mathbf{R}} = 1$  is satisfied. The term  $V = \mathbf{a}_1 \cdot \mathbf{a}_2 \times \mathbf{a}_3$  is the volume of the parallelepiped spanned by the three primitive vectors.

The situation is relative straightforward for a simple cubic lattice which can be generated by the primitive vectors

$$\mathbf{a}_1 = a\hat{\mathbf{x}} \quad \text{and} \quad \mathbf{a}_2 = a\hat{\mathbf{y}} \quad \text{and} \quad \mathbf{a}_3 = a\hat{\mathbf{z}} \quad \Rightarrow \quad \mathbf{R} = n_1\mathbf{a}_1 + n_2\mathbf{a}_2 + n_3\mathbf{a}_3. \quad (164)$$

The reciprocal lattice vectors satisfying  $e^{i\mathbf{K}\cdot\mathbf{R}} = 1$  are also easily obtained

$$\mathbf{b}_1 = \frac{2\pi}{a}\hat{\mathbf{x}} \quad \text{and} \quad \mathbf{b}_2 = \frac{2\pi}{a}\hat{\mathbf{y}} \quad \text{and} \quad \mathbf{b}_3 = \frac{2\pi}{a}\hat{\mathbf{z}} \quad \Rightarrow \quad \mathbf{K} = n_1\mathbf{b}_1 + n_2\mathbf{b}_2 + n_3\mathbf{b}_3. \quad (165)$$

Let us now consider a somewhat more complicated lattice, such as the body-centered cube (bcc) as given in Eqn. (157). Let us first calculate  $V$ . Although we can start with the vectors in Eqn. (157), there is a somewhat simpler method. When considering the nonprimitive simple cube unit cell, the bcc structure can be described by a lattice and a basis. The volume of the simple cube is  $a^3$ . However, there are two atoms in the basis. Therefore, the primitive cell, containing only one atom, has a volume  $a^3/2$ . The first reciprocal lattice vector is then given by

$$\mathbf{b}_1 = 2\pi \frac{2}{a^3} \left(\frac{a}{2}\right)^2 (\hat{\mathbf{x}} - \hat{\mathbf{y}} + \hat{\mathbf{z}}) \times (\hat{\mathbf{x}} + \hat{\mathbf{y}} - \hat{\mathbf{z}}) = \frac{2\pi}{a}(\hat{\mathbf{y}} + \hat{\mathbf{z}}). \quad (166)$$

Similarly, the other two are given by

$$\mathbf{b}_2 = \frac{2\pi}{a}(\hat{\mathbf{x}} + \hat{\mathbf{z}}) \quad \text{and} \quad \mathbf{b}_3 = \frac{2\pi}{a}(\hat{\mathbf{x}} + \hat{\mathbf{y}}) \quad (167)$$

Interestingly, the reciprocal lattice of a bcc crystal structure is fcc. However, as we have seen, the more interesting physics often occurs at the regions in reciprocal space where the Bragg condition is satisfied. The condition  $\mathbf{k} \cdot \hat{\mathbf{K}} = \frac{1}{2}K$  defines a plane that has  $\hat{\mathbf{K}}$  as its normal vector. In addition, the vector  $\frac{1}{2}\mathbf{K}$  lies in the plane. The first Brillouin zone is defined as the smallest volume around a particular reciprocal lattice vector enclosed by the planes given by the Bragg condition. The first Brillouin zones for the bcc and fcc lattices are given in Fig. 31. We can use the same

procedure to define a primitive unit cell in real space using planes given by  $\mathbf{r} \cdot \hat{\mathbf{R}} = \frac{1}{2}R$ . These are called Wigner-Seitz cells and are given in Fig. 31 for the bcc and fcc lattices. However, in practice the Brillouin zone is of much greater importance than the Wigner-Seitz cell.

Essentially, in experiments such as X-ray and neutron diffraction, we are not measuring the real space distribution of the charge density, but the distribution in reciprocal space, which is the Fourier transform of the real space. Since the charge distribution is periodic due to the crystal symmetry, the Fourier transform is discrete

$$n(\mathbf{r}) = \sum_{\mathbf{K}} n_{\mathbf{K}} e^{i\mathbf{K} \cdot \mathbf{r}}, \quad (168)$$

where the Fourier coefficients are given by the inverse Fourier transform

$$n_{\mathbf{K}} = \frac{1}{V_c} \int_{\text{cell}} n(\mathbf{r}) e^{-i\mathbf{K} \cdot \mathbf{r}} d\mathbf{r}, \quad (169)$$

where the integration is over the volume  $V_c$  of a cell of the crystal. We have seen such a Fourier series before when introducing the periodic potential in the nearly free-electron model. Writing the density density as a Fourier transform directly makes it periodic since  $n(\mathbf{r} + \mathbf{R}) = n(\mathbf{r})$  since  $\exp(i\mathbf{K} \cdot \mathbf{R}) \equiv 1$  defines the reciprocal lattice.

For example, the interaction between light and matter is included by including the vector potential in the kinetic energy

$$H = \frac{(\mathbf{p} - e\mathbf{A})^2}{2m} = \frac{\mathbf{p}^2}{2m} + \frac{e}{2m}(\mathbf{p} \cdot \mathbf{A} + \mathbf{A} \cdot \mathbf{p}) + \frac{e^2 \mathbf{A}^2}{2m}. \quad (170)$$

The second term causes electronic transitions, such as absorption. For diffraction, we are interested in the third term. If we take the vector potential to be given by a plane wave  $\mathbf{A}(\mathbf{r}) = \mathbf{a} e^{i\mathbf{k} \cdot \mathbf{r}}$ , where  $\mathbf{a}$  gives the strength and direction of the potential, then to lowest order in perturbation theory, the scattering matrix element is given by

$$\langle \psi | \frac{e^2 \mathbf{A}^2(\mathbf{r})}{2m} | \psi \rangle = \frac{e^2 a^2}{2m} \int dV \psi^*(\mathbf{r}) e^{i(\mathbf{k} - \mathbf{k}') \cdot \mathbf{r}} \psi(\mathbf{r}) = \frac{e^2 a^2}{2m} \int dV n(\mathbf{r}) e^{-i\Delta\mathbf{k} \cdot \mathbf{r}} = \frac{e^2 a^2}{2m} F. \quad (171)$$

with  $\Delta\mathbf{k} = \mathbf{k}' - \mathbf{k}$  and  $F$  is the scattering amplitude

$$F = \int dV n(\mathbf{r}) e^{-i\Delta\mathbf{k} \cdot \mathbf{r}} = \sum_{\mathbf{K}} \int dV n_{\mathbf{K}} e^{i(\mathbf{K} - \Delta\mathbf{k}) \cdot \mathbf{r}}. \quad (172)$$

This only gives a strong contribution when

$$\Delta\mathbf{k} = \mathbf{K}, \quad (173)$$

when

$$F = V n_{\mathbf{K}} = N \int_{\text{cell}} n(\mathbf{r}) e^{-i\mathbf{K} \cdot \mathbf{r}} d\mathbf{r} = N S_{\mathbf{K}}, \quad (174)$$

where  $S_{\mathbf{K}}$  is the structure factor. If there is only one atom in the basis then  $S_{\mathbf{K}}$  is a number. However, if there is more than one atom in the basis it often makes sense to describe the charge distribution as a superposition of separate charge distributions (Note that this is not necessary and sometimes not even possible. One can just brute force compute  $S_{\mathbf{K}}$ , but separating it provides more insight),

$$n(\mathbf{r}) = \sum_j n_j(\mathbf{r} - \mathbf{r}_j), \quad (175)$$

where the position of the atoms in the basis are given by  $\mathbf{R} + \mathbf{r}_j$ . The structure factor is then given by

$$S_{\mathbf{K}} = \sum_j \int n_j(\mathbf{r} - \mathbf{r}_j) e^{-i\mathbf{K} \cdot \mathbf{r}} d\mathbf{r} = \sum_j e^{-i\mathbf{K} \cdot \mathbf{r}_j} \int n_j(\boldsymbol{\rho}) e^{-i\mathbf{K} \cdot \boldsymbol{\rho}} d\boldsymbol{\rho}, \quad (176)$$

where  $\boldsymbol{\rho} = \mathbf{r} - \mathbf{r}_j$ . If we define the atomic form factor as

$$f_i = \int n_j(\boldsymbol{\rho}) e^{-i\mathbf{K} \cdot \boldsymbol{\rho}} d\boldsymbol{\rho}, \quad (177)$$

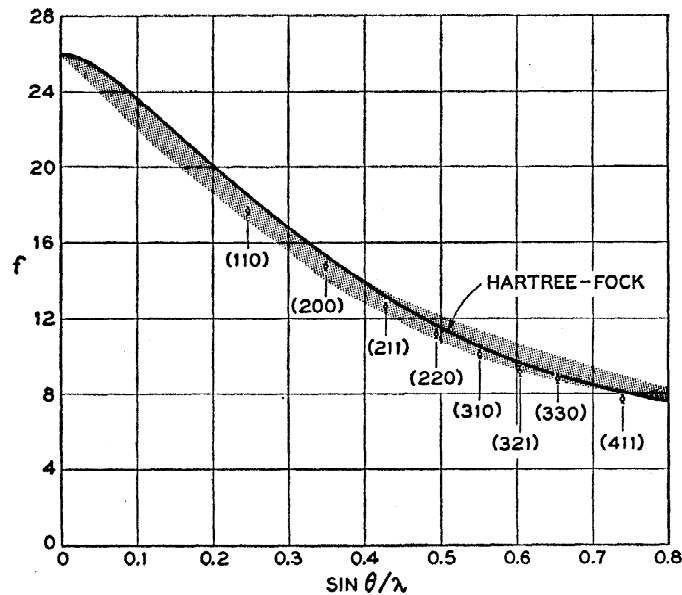


FIG. 32: Absolute experimental form factor for metallic Aluminium after Batterman, Chipman, and DeMarco. Al has a fcc structure.

then the structure factor can be written as

$$S_{\mathbf{K}} = \sum_j f_j e^{-i\mathbf{K}\cdot\mathbf{r}_j}. \quad (178)$$

Note that the scattering intensity is the square of the matrix element which involves  $S^*S$ .

*Structure factor of the bcc lattice.*— We already studied the reciprocal lattice of a bcc crystal using the primitive vectors, see Eqn. (166) and (167). However, we know that there is an alternative way of looking at the same lattice, namely as a simple cubic lattice plus a basis  $\mathbf{0}$  and  $\frac{a}{2}(\hat{\mathbf{x}} + \hat{\mathbf{y}} + \hat{\mathbf{z}})$  if the cube has sides of length  $a$ . The simple cubic basis vectors are given in Eqn. (165). The structure factor is then

$$S_{\mathbf{K}} = f_1 + f_2 e^{-i2\pi(n_1+n_2+n_3)}. \quad (179)$$

We can distinguish two distinct situations

$$S_{\mathbf{K}} = f_1 - f_2 \quad n_1 + n_2 + n_3 = \text{odd integer} \quad (180)$$

$$S_{\mathbf{K}} = f_1 + f_2 \quad n_1 + n_2 + n_3 = \text{even integer}. \quad (181)$$

For the situation that the atoms in the basis are equivalent  $f_1 = f_2$ . Let us look at the  $xy$  plane. For  $(0, 0, 0)$ ,  $(2, 0, 0)$ ,  $(0, 2, 0)$ ,  $(1, 1, 0)$ , and  $(2, 2, 0)$ , the structure factor is 2. For  $(1, 0, 0)$ ,  $(0, 1, 0)$ ,  $(2, 1, 0)$ , and  $(1, 2, 0)$ ,  $S_{\mathbf{K}} = 0$ . This forms a fcc reciprocal lattice as it should. However, the atoms in the basis can also be inequivalent. This is known as a CsCl structure. In that case, we can observe the reflections that are forbidden when the atoms are equivalent.

*Momentum dependence atomic form factor.*— We want to evaluate the atomic form factor. Let us take the classical limit

$$f_i = \int n_j(\mathbf{r}) e^{-i\mathbf{K}\cdot\mathbf{r}} d\mathbf{r}. \quad (182)$$

Let us take the angle between  $\mathbf{r}$  and  $\mathbf{K}$  to be  $\theta$  and assume that the charge distribution is spherically symmetric. The integral then becomes

$$f_i = \int dr \int_0^{2\pi} d\varphi \int_0^\pi d\theta r^2 \sin\theta n_j(r) e^{-iKr \cos\theta} = 2\pi \int dr r^2 n_j(r) \frac{e^{iKr} - e^{-iKr}}{iKr}, \quad (183)$$

where  $n_j(r)$  is the radial distribution of the charge density, giving

$$f_i = 4\pi \int dr r^2 n_j(r) \frac{\sin Kr}{Kr}. \quad (184)$$

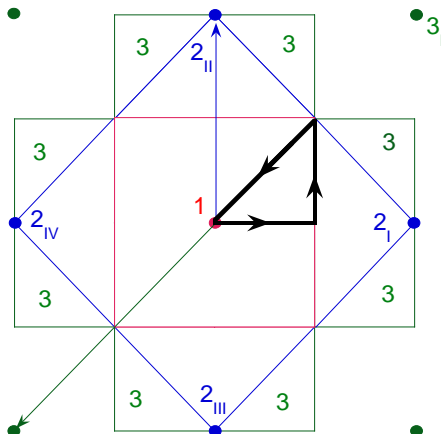


FIG. 33: The first three Brillouin zones for a square lattice.

In the limit that the charge density is close to the lattice point, i.e. much smaller than the distance between the atom,  $\sin Kr/Kr \cong 1$ . In this limit, we obtain

$$f_i = 4\pi \int dr r^2 n_j(r) = Z, \quad (185)$$

where  $Z$  is the number of atomic electrons. Figure 32 shows a comparison between calculated formfactors and experimental formfactors for metallic aluminium.

## XV. FREE ELECTRON IN TWO DIMENSIONS

Let us consider the nearly-free electron model in two dimensions for a square lattice. We will be calculating the electronic structure in the first Brillouin zone. Although we will consider the other Brillouin zones to try to connect to the free-electron model, it is important to get used to working in the first Brillouin with only the  $\mathbf{k}$  vectors that are good quantum numbers for the system. Virtually all sophisticated electronic structure programs work only in the first Brillouin zone. For the one-dimensional chain, the first Brillouin zone was the region  $[-\frac{\pi}{a}, \frac{\pi}{a}]$ , where the  $k$ -points  $\pm\frac{\pi}{a}$  satisfy the Bragg condition  $k = \frac{1}{2}K$ , see Eqn. (158). To find the first Brillouin zone in two dimensions, we need to find the  $k$  points that satisfy the Bragg condition. Obviously, we need to include the reciprocal lattice vector  $\mathbf{K} = 0$ . The next reciprocal lattice vectors are  $\pm\frac{2\pi}{a}\hat{\mathbf{x}}$  and  $\pm\frac{2\pi}{a}\hat{\mathbf{y}}$ . This leads to the following Bragg condition in the  $x$ -direction

$$\mathbf{k} \cdot (\pm\hat{\mathbf{x}}) = \frac{1}{2} \frac{2\pi}{a} \Rightarrow k_x = \pm\frac{\pi}{a}. \quad (186)$$

Note that there is no restriction on  $k_y$ . The Bragg condition is therefore satisfied for all points  $(0, \pm\frac{\pi}{a})$ . This point is more general. The condition  $\mathbf{k} \cdot \hat{\mathbf{K}} = \frac{1}{2}K$  always corresponds to a line perpendicular to  $\hat{\mathbf{K}}$  that crosses the vector  $\mathbf{K}$  at half of its length. The next reciprocal lattice vectors are  $(\pm\frac{2\pi}{a}\hat{\mathbf{x}}, \pm\frac{2\pi}{a}\hat{\mathbf{y}})$  and  $(\pm\frac{2\pi}{a}\hat{\mathbf{x}}, \mp\frac{2\pi}{a}\hat{\mathbf{y}})$ . The resulting lines where the Bragg condition is satisfied are shown in Fig. 33. The first Brillouin zones is the area around  $\mathbf{K} = 0$  up to the first line that satisfies a Bragg condition. Note that for a square lattice the first Brillouin zone is determined by the four shortest reciprocal lattice vectors (in general, it is not only determined by the shortest). We then calculate the values of the energies

$$\varepsilon_{\mathbf{k}-\mathbf{K}} = \frac{\hbar^2}{2m} (\mathbf{k} - \mathbf{K})^2 \quad (187)$$

inside the first Brillouin zone. In two dimensions, it is no longer practical to show the values for all  $k$  points. One therefore usually shows the bands in particular directions. A typical choice for two dimensions is  $(\frac{\pi}{a}, \frac{\pi}{a}) \rightarrow (0, 0) \rightarrow (\frac{\pi}{a}, 0)$ . The energies can be expressed in terms of  $\bar{\varepsilon} = \frac{\hbar^2}{2m} \frac{\pi^2}{a^2}$ . Let us first consider the direction from  $(0, 0) \rightarrow (0, \frac{\pi}{a})$ . The energy  $\varepsilon_{\mathbf{k}}$  goes from 0 to  $\bar{\varepsilon}$ . The energies of  $\varepsilon_{\mathbf{k}-\mathbf{K}}$  with  $\mathbf{K}$  equal to  $\pm\frac{2\pi}{a}\hat{\mathbf{x}}$  and  $\pm\frac{2\pi}{a}\hat{\mathbf{y}}$  are all equal at  $(0, 0)$  (often known as the  $\Gamma$  point). The energy is given by  $4\bar{\varepsilon}$ . These degeneracies are directly related to the high symmetry

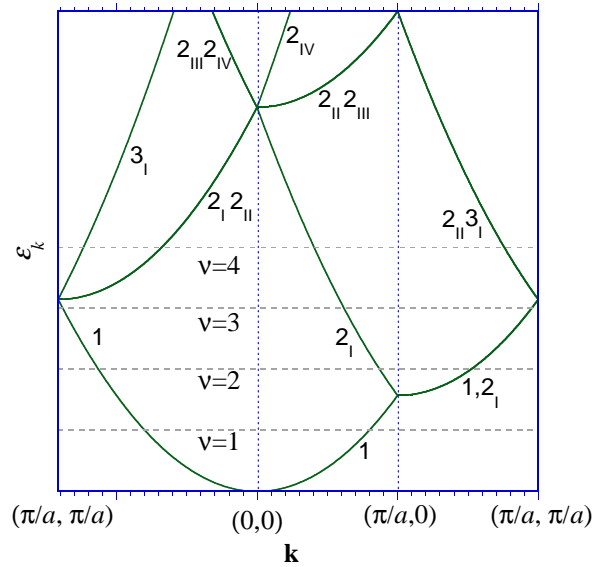


FIG. 34: The free-electron bands in two dimensions along particular directions indicated in Fig. 33.

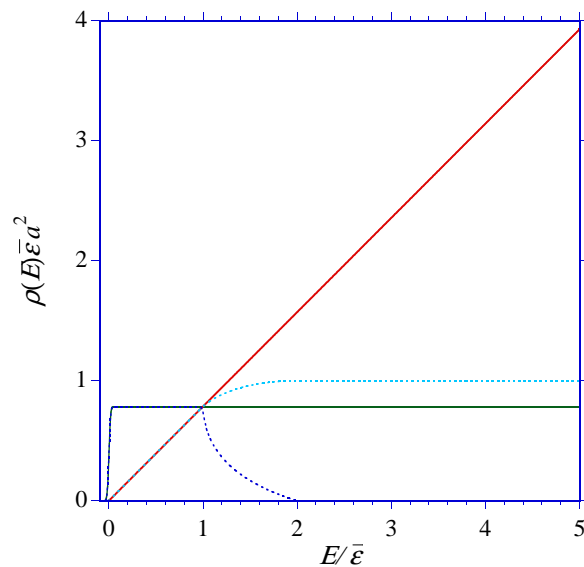


FIG. 35: The green line gives the density of states as a function of energy. The red line gives the integrated density of states. The dotted dark-blue line gives the density of states of the band from the first Brillouin zone (indicated by 1 in Fig. 34). The dotted light-blue gives its integral.

of the  $\Gamma$  point. Moving away from the  $\Gamma$ , the bands split:  $\varepsilon_{\mathbf{k}-\frac{\pi}{a}\hat{\mathbf{x}}}$  decreases to  $\bar{\varepsilon}$  and  $\varepsilon_{\mathbf{k}+\frac{\pi}{a}\hat{\mathbf{x}}}$  increases to  $9\bar{\varepsilon}$ . The bands  $\varepsilon_{\mathbf{k}\pm\frac{\pi}{a}\hat{\mathbf{y}}}$  remain degenerate and increase to  $5\bar{\varepsilon}$ . The point  $(\frac{\pi}{a}, \frac{\pi}{a})$  is again a special point in the Brillouin zone at the same distance from  $(0,0)$ ,  $(\frac{2\pi}{a}, \frac{2\pi}{a})$ ,  $(\frac{2\pi}{a}, 0)$ , and  $(0, \frac{2\pi}{a})$ . The lowest four bands are therefore degenerate with an  $2\bar{\varepsilon}$ . Moving towards  $(0,0)$ , with  $k_x = k_y$ ,  $\varepsilon_{\mathbf{k}}$  decreases to zero.  $\varepsilon_{\mathbf{k}-\frac{2\pi}{a}(\hat{\mathbf{x}}+\hat{\mathbf{y}})}$  increases to  $8\bar{\varepsilon}$ . The band  $\varepsilon_{\mathbf{k}-\frac{2\pi}{a}\hat{\mathbf{x}}/\hat{\mathbf{y}}}$  are degenerate and increase to  $4\bar{\varepsilon}$ .

*Density of states.*— For many physical quantities the exact dispersion is not important and one is more interested in the number of states at a particular energy.

*technical intermezzo:* Although, this density of states could have been calculated easily analytically, it was actually done numerically (useful when moving away from the free-electron model). How do you do this. There are several procedures to do this, some of them more efficient than others. Basically one discretizes the first Brillouin zone in a grid with a total of  $N_k$  points. and calculates the eigenvalues for each point (since the matrix is diagonal ( $U = 0$ ), this

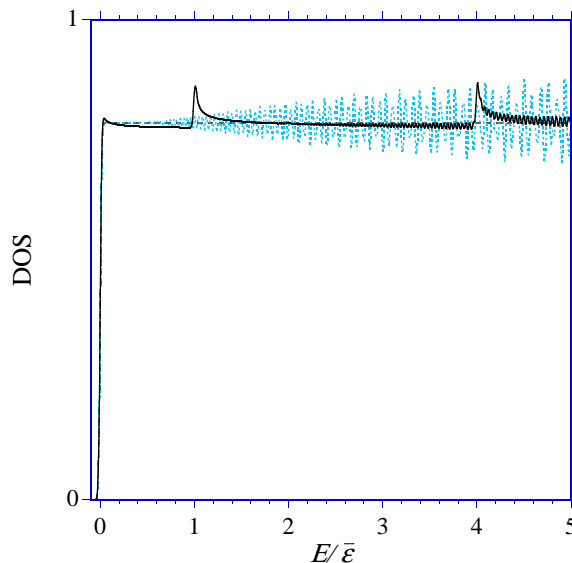


FIG. 36: Typical numerical problems in calculating the density of states. Dashed blue line: insufficient  $k$  points taken into account in the calculation. Black line: improper treatment of the edges of the Brillouin zone.

is trivial). One could have produced a simple histogram. This works wonders in case of a square density of states, but does not quickly produce nice results in other cases. Instead each  $k$  point has been broadened by a Gaussian

$$w(E) = \frac{\sqrt{\pi}}{N_k \sigma} e^{-\left(\frac{E - \varepsilon_{\mathbf{k}}}{\sigma}\right)^2}, \quad (188)$$

and all the Gaussians are added together. The Gaussian is normalized to give a weight of  $1/N_k$ . We have taken  $\sigma = 0.022\bar{\varepsilon}$ . The effect of broadening is visible at the edge of the density of states ( $E = 0$ ). In addition, we have used  $N_k = 200^2$ , which gives a nice smooth result. When  $N_k = 50$  is taken, one observes oscillations, see Fig. 36, due to the undersampling of the Brillouin zone. The black line in Fig. 36 shows the effect of an improper treatment of the edges of the Brillouin zone. The calculation uses only a quarter of the Brillouin zone (only positive  $k$ ), since the other parts are equivalent. In fact, we really only need  $1/8$  of the whole Brillouin zone due to symmetry. However, the  $k$  points at the edges are shared by different regions. For example, the  $k$  points at the edge of the first Brillouin zone lie for one half in the first and for the other half in the second Brillouin zone. When this is not taken into account properly (i.e. by scaling these  $k$  points by a factor of  $\frac{1}{2}$ ), one observes spikes in the density of states, see the black line in Fig. 36. Obviously, these would become irrelevant when  $N_k \rightarrow \infty$ , but for  $N_k = 100^2$  they are clearly visible. There exist more advanced and efficient methods to calculate the density of states (for example, the tetrahedron method, which effectively interpolates between the different  $k$ -points), but for a simple two-dimensional problem this works well enough.

The results are shown in Fig. 35. The end result looks simple: the density of states is constant. Obviously, we could have derived this more easily. However, in general this cannot be done, so this is certainly a useful check to see whether this routine works properly. Let us derive this density of states analytically. We ignore the spin of the electron for the moment. Although we have a discrete number of  $k$  states, the density is always large enough that we can approximate this by a continuous function. The amount of  $k$  space occupied by one  $k$  point is  $A_1 = \left(\frac{2\pi}{L}\right)^2$  following from the periodic boundary conditions in Eqn. (24) applied in both  $x$  and  $y$  directions. The number of  $k$  states in a certain area can then be obtained by dividing the area by  $A_1$ . For a free-electron model where the energy is given by  $\varepsilon_k = \frac{\hbar^2 k^2}{2m}$ , the areas of constant energy are circles. The number of electrons inside the circle is given by

$$N(k) = \pi k^2 / A_1 = \pi k^2 \left(\frac{L}{2\pi}\right)^2 = \frac{A}{4\pi} k^2, \quad (189)$$

where  $A$  is the area (i.e. the size) of the system. This number can be easily written in terms of energy

$$N(E) = \frac{A}{4\pi} \frac{2m}{\hbar^2} E \quad \text{or} \quad n(E) = \frac{N(E)}{A} = \frac{1}{4\pi} \frac{2m}{\hbar^2} E, \quad (190)$$

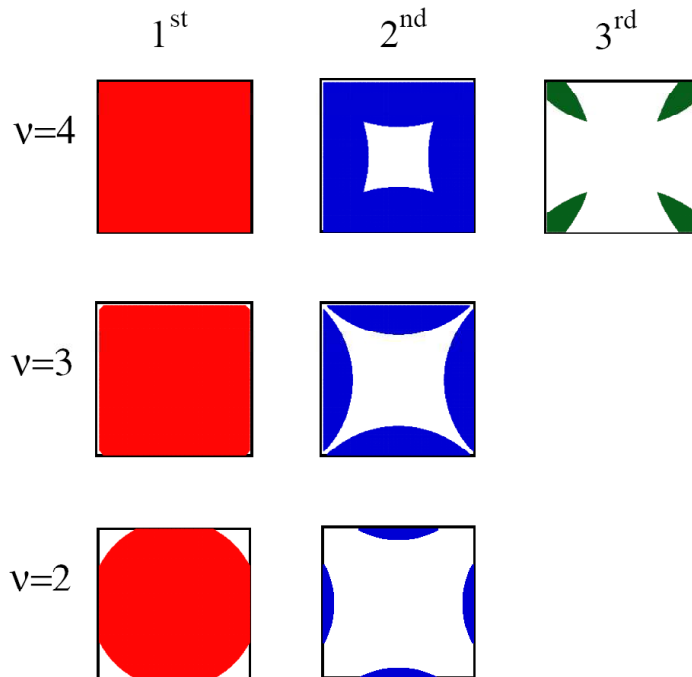


FIG. 37: The Fermi surfaces for different number of electrons  $\nu$  per site. The 1<sup>st</sup>, 2<sup>nd</sup>, and 3<sup>rd</sup> indicate from which Brillouin zone the bands originate.

where  $n(E)$  is the density of electrons. Often we are also interested in what the density is for a certain energy  $dn(E) = \rho(E)dE$ . This gives the density of states

$$\rho(E) = \frac{dn(E)}{dE} = \frac{1}{4\pi} \frac{2m}{\hbar^2}. \quad (191)$$

which is indeed a constant. The plot uses some normalizations. The energy is normalized to the value at  $(0, \frac{\pi}{a})$ , i.e.,  $\bar{\varepsilon} = \frac{\hbar^2}{2m} \left(\frac{\pi}{a}\right)^2$ . Figure 35 also shows the integrated intensities. Furthermore, if we had one electron per site, the electron density would be  $1/a^2$ . However, it is more convenient to think about 1 el/site, so let us multiply times  $a^2$ .

$$\rho(E)a^2\bar{\varepsilon} = a^2\bar{\varepsilon} \frac{1}{4\pi} \frac{2m}{\hbar^2} \left(\frac{a}{\pi}\right)^2 \left(\frac{\pi}{a}\right)^2 = \frac{\pi}{4} \cong 0.785, \quad (192)$$

which is the value of the constant density of states in the figure. It is interesting to look at only the band in the first Brillouin zone (see the dotted lines). Note that the density of states is no longer constant. You can easily observe this by drawing circles around the  $\Gamma$  point. For values of  $k > \frac{\pi}{a}$  these turn into arcs, up to  $k = \sqrt{2}\frac{\pi}{a}$  (with energy  $2\bar{\varepsilon}$ ), where only one point at the edge of the Brillouin zone is left (actually, there are four points, but since all four points are shared by four Brillouin zones there is only 1 point). The integral over the first Brillouin zone goes to one. The number of states in the first Brillouin zone can be easily calculated

$$N_{\text{first}} = \left(\frac{2\pi}{a}\right)^2 \left(\frac{L}{2\pi}\right)^2 = \frac{L^2}{a^2} = \frac{A}{a^2} = N. \quad (193)$$

Or exactly one state per site. This is not too much different from the tight-binding model we saw earlier. There we started from one state per site and filled up the entire first Brillouin zone (in one dimension). Again, by imposing the periodicity of the lattice, we are effectively creating orbitals on each site.

However, we have not applied any potential yet, so we are not going to fill up this orbital but fill up the free-electron bands. The  $k$ -value for  $\nu$  electrons per site is determined by

$$\nu N = 2\pi k^2 \left(\frac{L}{2\pi}\right)^2 \Rightarrow k_\nu = 2\sqrt{\frac{\nu}{2\pi}} \frac{\pi}{L} \sqrt{N} = \sqrt{\frac{2\nu}{\pi}} \frac{\pi}{a} \quad (194)$$



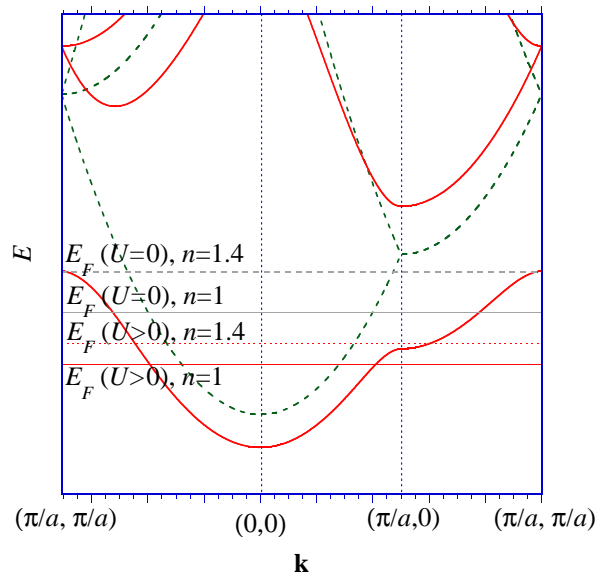


FIG. 38: The dashed lines show the free-electron model in two dimensions. The red lines indicate the effect of applying a potential  $U$ . The horizontal lines indicate the Fermi levels for 1.7 electrons per site.

where the factor 2 takes account of the fact that each state has spin-up and a spin-down component. The corresponding energy is given by

$$E_\nu = \frac{\hbar^2}{2m} k_\nu^2 = \frac{2\nu}{\pi} \bar{\epsilon}. \quad (195)$$

The maximum energy in the system (at least at  $T = 0$ ) is known as the Fermi energy  $E_F$ . For  $\nu = 1$  (1 electron per site), the Fermi energy is  $0.637\bar{\epsilon}$  with a corresponding Fermi wavevector of  $0.798\frac{\pi}{a}$ . This lies well inside the first Brillouin zone. This means that only the lowest band cross the Fermi level, see Fig. 34. This is essentially the Sommerfeld model, since the presence of nuclei can be essentially neglected. For  $\nu = 2$ ,  $E_F = 1.27\bar{\epsilon}$ . The corresponding wavevector  $k = 1.13\frac{\pi}{a}$  lies outside the first Brillouin zone. Although the pictures are easily constructed by drawing a circle through the different Brillouin zones in Fig. 33, it is important to learn to think in the first Brillouin zone, since no state-of-the-art calculations use free-electron approximations anymore. Things become more obvious when we compare the Fermi surfaces in Fig. 33 with the bands in Fig. 34. For  $\mathbf{k}$  from  $(0,0)$  to  $(\frac{\pi}{a}, 0)$ , we see that the band from the first Brillouin zone is entirely below  $E_F$  for  $\nu = 2$ . In Fig. 33, we see that in this direction there is no Fermi surface in for the bands coming from the first Brillouin zone (red), but we do see a Fermi surface in the bands coming from the second Brillouin zone (blue). However, when going from  $(0,0)$  to  $(\frac{\pi}{a}, \frac{\pi}{a})$ , we see that it is the band from the first Brillouin zone that crosses the Fermi level and we see that we have a Fermi surface in this direction. When going to three electrons per site ( $\nu = 3$ ), the part of the Fermi surface related to the bands from the second Brillouin zone increases, but the rest remain similar. Note that along the  $(0,0) \rightarrow (\frac{\pi}{a}, \frac{\pi}{a})$ , there is still a Fermi surface since  $\sqrt{\frac{6}{\pi}} < \sqrt{2}$ . When going to  $\nu = 4$ , we also start involving the band coming from the third Brillouin zone. Note that along the  $(0,0) \rightarrow (\frac{\pi}{a}, \frac{\pi}{a})$ , first the band from the second Brillouin zone crosses the Fermi level and then the band from the third Brillouin zone. Therefore in the direction, we have two Fermi surfaces (blue and green). However, along the  $(0,0) \rightarrow (\frac{\pi}{a}, 0)$  direction, there is only the band from the second Brillouin zone crossing the Fermi level.

## XVI. NEARLY-FREE ELECTRON IN TWO DIMENSIONS

So far, we have shown how the free-electron bands are folded back into the first Brillouin zone when the proper crystal symmetry is applied. However, in the end, this does not change anything. Without potential, you will simply end up with the Sommerfeld model. You cannot fool nature, you can pretend there are atoms, but without potential they are still free electrons. Obviously, there are potentials and even if they are small, they will have an effect close to the Bragg planes (okay, Bragg lines in two dimensions). For any finite  $U$  gaps will open up when the Bragg condition is satisfied. However, when  $U$  is small the effects will be small as well and the Fermi surfaces will not be too much

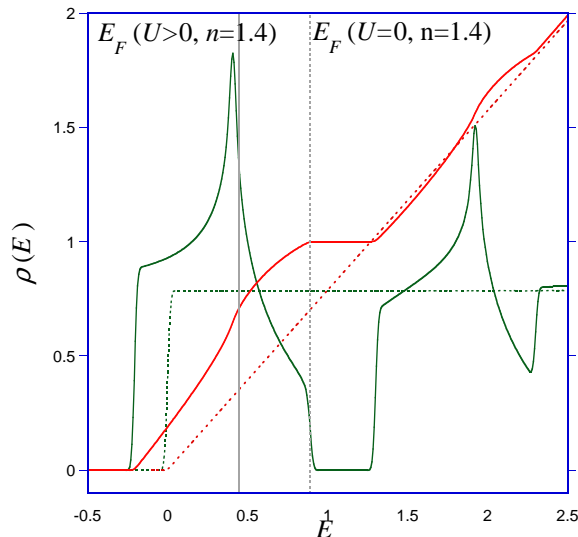


FIG. 39: The density of states  $\rho(E)$  (green) without (dotted) and with  $U$  (solid) in the (nearly) free electron model. The red lines give their integrated intensity. The vertical lines indicate the Fermi level for 1.4 electrons per site. Since the density of states is shown for only one spin degree of freedom, they occur when the integrated density of states equals 0.7. The density of states is shown for the same energy region as the band structure in Fig. 38.

different from the free-electron ones in Fig. 37. Let us consider a larger  $U$  value and a density of one electron per site ( $n = 1$ ). We directly observe a substantial change in the band structure. Degeneracies are lifted and gaps open up, Fig. 38. Since the band structure is more complicated, we can no longer easily determine the values of  $E_F$  and  $k_F$ . However, we can calculate them numerically, by determining the density of states  $\rho(E)$ , see Fig. 39.  $E_F$  is the energy for which the integral of  $\rho(E)$  with respect to energy equals the number of electrons (note that the density of states is plotted for one spin degree of freedom (up spin or down spin), so we need to integrate up to 0.5). The density of states is substantially different from the free electron one. First, we observe sharp peaks. They are called van Hove singularities. They are related to flat-band regions. The van Hove singularity just below the Fermi surface for  $U > 0$  is a result of the flat-band in the lowest band around  $(\frac{\pi}{a}, 0)$ . In addition, we observe gaps in the density of states. For those energies there are no states in the band structure. Note that the band structure is only given for particular directions. It is difficult to see from the bands if there is a gap for any  $\mathbf{k}$ . However,  $\rho(E)$  clearly shows the absence of states. The integrate intensity of  $\rho(E)$  up to the gap equals one (or two, if we take both spin degrees of freedom into account). Therefore, if there were two electrons per site in the system, the material would be a semiconductor. Figure 40 shows the Fermi surfaces for  $U = 0$  and  $U > 0$  with a density of  $n = 1$ . Note that they look very similar. The surface for  $U > 0$  has some slight distortion but it is close to a circle despite the relatively large value of  $U$ . The reason for that is that the states that are at the Fermi level are not close to satisfying the Bragg condition. This is the key ingredient for the surprising success of the Sommerfeld model for various materials. Let us see what happens if the Fermi was close to the states at the edges of the Brillouin zone by changing the number of free electrons to 1.4

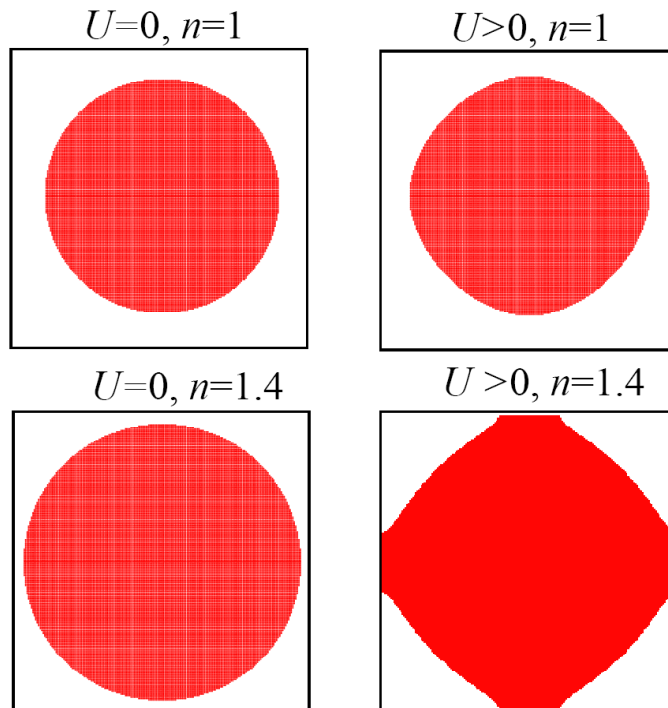


FIG. 40: The Fermi spheres for the band structures in Fig. 38 without (left) and with  $U$  (right).

per site. (This could be done with doping. However, the goal of this exercise is to demonstrate an effect that occurs in noble metals, where  $3d$  bands play an important role). As expected, when increasing  $U$ , gaps open up, see Fig. 38. However, let us consider 1.4 electrons per site. Figure 40 shows that for  $U = 0$ , the Fermi sphere is circular (as we would have expected). However, for  $U > 0$ , the Fermi surfaces touches the edges of the Brillouin zone (of course, the example is specifically chosen that this happens). At first, this looks comparable to what happens for the bands coming from the first Brillouin zone (red) in Fig. 37 for  $\nu = 2$ . You might expect a picture of the surface for bands coming from the second Brillouin zone (blue in 40). However, there is none. The trick to understand this is to follow the Fermi energy in different directions. Along the  $(0,0) \rightarrow (\frac{\pi}{a}, 0)$  directions for  $U = 0$ , we cross the free-electron band centered around  $(0,0)$  for a filling of 1.4 electrons per site, see Fig. 38. For  $U > 0$ , a gap opens up and this band is pushed below the Fermi level. For two electrons per site, the  $E_F$  is larger, see  $\nu = 2$  in Fig. 34, and the Fermi level crosses the free-electron band centered around  $(\frac{2\pi}{a}, 0)$ , i.e. there is a Fermi surface for bands coming from the second Brillouin zone, see Fig. 37. On the other hand, the second band for  $U > 0$  is at higher energy due to the opening of a gap, see Fig. 38. We can no longer identify this as the band coming from the second Brillouin zone, since the free-electron bands from the first and second Brillouin zone are mixed by the periodic potential  $U$ . Let us now look along the  $(\frac{\pi}{a}, 0) \rightarrow (\frac{\pi}{a}, \frac{\pi}{a})$  direction. For a filling of 1.7 electrons per site, the Fermi level does not cross a band, see Fig. 38. Since the Fermi surface lies entirely inside the first Brillouin zone, see Fig. 40, we do not expect a crossing since the direction  $(\frac{\pi}{a}, 0) \rightarrow (\frac{\pi}{a}, \frac{\pi}{a})$  lies at the edge of the Brillouin zone. For a filling of 2 electrons per site, see  $\nu = 2$  in Fig. 37, we do cross a band. In fact, two bands are crossed since the bands coming from the reciprocal lattice vectors  $\mathbf{K} = (0,0)$  and  $(\frac{2\pi}{a}, 0)$  are degenerate along the  $(\frac{\pi}{a}, 0) \rightarrow (\frac{\pi}{a}, \frac{\pi}{a})$  direction. This can be understood by noting that both  $\mathbf{K}$  are always at the same distance from the line  $(\frac{\pi}{a}, 0)$  and  $(\frac{\pi}{a}, \frac{\pi}{a})$ . Note that there is a Fermi surface in this direction for bands coming from the first (red) and second (blue) Brillouin zones in Fig. 37. For a finite  $U$ , this degeneracy is lifted, see Fig. 38. The Fermi level for a filling of 1.7 electrons per site just crosses the lowest band and the Fermi surface therefore lies entirely inside the first Brillouin zone. For the  $(0,0)$  and  $(\frac{\pi}{a}, \frac{\pi}{a})$  direction, the situation is still very similar for  $U = 0$  and  $U > 0$ , see Fig. 38.

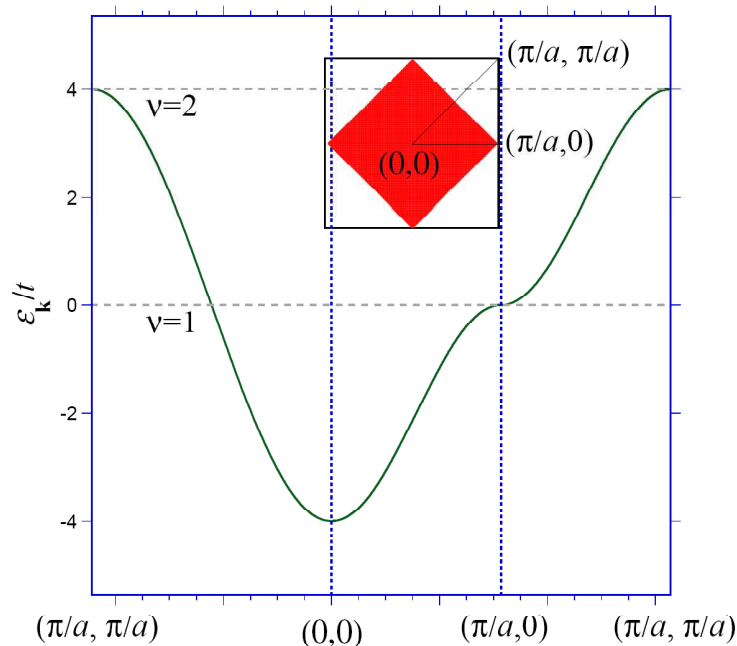


FIG. 41: The tight-binding dispersion  $\varepsilon_{\mathbf{k}}$  for a two-dimensional square lattice along particular directions in the Brillouin zone. The inset shows the Fermi surface in for a filling of one electron per site.

### XVII. TIGHT-BINDING IN TWO DIMENSIONS

The derivation of the tight-binding dispersion in two-dimension is very similar to that in one dimension in Eqn. (33)

$$\varepsilon_{\mathbf{k}} = -t \sum_{\delta} e^{i\mathbf{k}\cdot\delta} = -t(e^{ik_x a} + e^{-ik_x a} + e^{ik_y a} + e^{-ik_y a}) = -2t(\cos k_x a + \cos k_y a). \quad (196)$$

We can plot this curve by hand. Along the  $(0,0) \rightarrow (\frac{\pi}{a}, 0)$ , we have  $-2t \cos k_x a$ , equivalent to the one-dimensional dispersion; along the  $(\frac{\pi}{a}, 0) \rightarrow (\frac{\pi}{a}, \frac{\pi}{a})$ , we obtain  $-2t(1 + \cos k_y a)$ ; and along  $(0,0) \rightarrow (\frac{\pi}{a}, \frac{\pi}{a})$ , the dispersion is  $-4t \cos k a$  with  $k = k_x = k_y$ , see Fig. 41. The density of states  $\rho(E)$  is shown in Fig. 42. Since the band is made up of  $n$   $1s$  electron per site, the total band can accommodate two electrons (taking spin into account). The density of states is also symmetric around  $E = 0$ . This might not be directly obvious by looking at the dispersion curves in Fig. 41. However, displacing  $k$  by  $(\pi, \pi)$  has as result that  $\varepsilon_{\mathbf{k}} \rightarrow -\varepsilon_{\mathbf{k}}$ . This directly implies that the Fermi level for one electron per site is at  $E = 0$ . The inset in Fig. 41 shows that the Fermi surface is a square. This can be easily understood since  $E = 0$  implies  $\cos k_x + \cos k_y = 0$ , which is satisfied, for example when  $k_y = \pi - k_x$  and all the other straight lines on the Fermi surface.

Another interesting thing to note is the remarkable similarity between the tight-binding dispersion in Fig. 41 and the lowest band in the two-dimension nearly-free electron model in Fig. 38. Despite the entirely different starting points, the resulting physics is very similar.

### XVIII. THE PERIODIC TABLE

Up to now, we have seen discussed the nearly-free electron and the tight-binding approach to the electronic structure of solids. In the end, we found similar results even though we started from opposite points of view. We now would like to discuss the electronic structure of several elements. Even starting from a free-electron model, we noticed the formation of atomic-like structure around the nuclei in the solid. Let us briefly recapitulate some of the results from atomic physics. The eigenfunctions for the Hydrogen atom were obtained by solving the Schrödinger equation

$$-\frac{\hbar^2}{2m} \nabla^2 \psi(\mathbf{r}) + V(\mathbf{r})\psi(\mathbf{r}) = E\psi(\mathbf{r}), \quad (197)$$

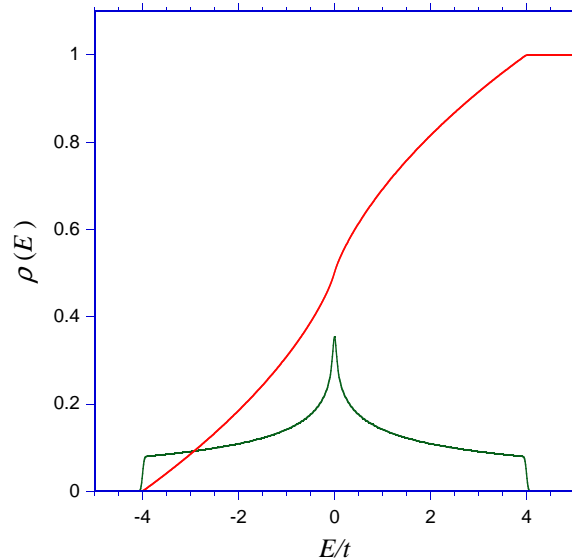


FIG. 42: The density of states  $\rho(E)$  for tight-binding dispersion  $\varepsilon_{\mathbf{k}}$ , shown in green. The red line shows its integral.

is the potential from the nucleus. This was solved by separation of variables leading to eigenfunctions that can be written as

$$\psi_{nlm}(r, \theta, \varphi) = R_{nl}(r)Y_{lm}(\theta, \varphi), \quad (198)$$

where  $R_{nl}$  are Laguerre polynomials and  $Y_{lm}(\theta, \varphi)$  spherical harmonics. The quantum numbers are given by  $n = 1, 2, 3, \dots$ ,  $l = 0, 1, \dots, n-1$ , and  $m = -l, -l+1, \dots, l$ . The orbitals are commonly denoted as  $s, p, d, f$  for  $l = 0, 1, 2, 3$ , respectively. Although the solution is exact for Hydrogen, the interactions between the electrons does not allow us to obtain exact solutions for larger atomic numbers. There are two approaches. We can try to do our best to treat the electron-electron interactions as well as possible. This leads to typical atomic physics (Hund's rule, local moments etc, see lecture notes from 560/1). However, this is many-body problem treating all the electrons explicitly and not a feasible approach for solid-state physics. The other approach is to assume that the electron only feels an average potential as a result of the presence of other electrons. This effectively modifies the potential  $V(\mathbf{r})$ . For example, one can easily understand stand that the  $3s$  electron does not feel the potential of the eleven protons in the nucleus (a  $\text{Na}^{11+}$  ion), but an effective potential due to the nucleus plus all the strongly bound electrons in the  $1s, 2s$ , and  $2p$  shells. However, we might not be able to calculate the exact shape of the potential and therefore the radial wavefunction  $R_{nl}(r)$ .

A phenomenological scheme of filling the orbitals is

$$\begin{array}{ccccccc}
 & 6s & & 6p & & & \\
 \swarrow & & \swarrow & & \swarrow & & \\
 & 5s & & 5p & & 5d & & 5f \\
 \swarrow & & \swarrow & & \swarrow & & \swarrow & \\
 & 4s & & 4p & & 4d & & 4f \\
 \swarrow & & \swarrow & & \swarrow & & \swarrow & \\
 & 3s & & 3p & & 3d & & \\
 \swarrow & & \swarrow & & \swarrow & & \swarrow & \\
 & 2s & & 2p & & & & \\
 \swarrow & & \swarrow & & \swarrow & & & \\
 & 1s & & & & & & 
 \end{array} . \quad (199)$$

How this works out for the periodic table is shown in Fig. 44.

When we look at solids, we can still observe the atomic character of the orbitals although often orbitals get mixed and we find states with, for example, both  $s$  and  $p$  character. Also, in solids we cannot easily determine the radial wavefunction  $R_{nl}$  without doing extensive calculations. However, some symmetry aspects still remain. For example, the  $1s$  and  $2s$  orbitals have the same spherical part of the wavefunction ( $Y_{00}(\theta, \varphi) = 1/\sqrt{4\pi}$ ). However, we know that

$\psi_{100}$  and  $\psi_{200}$  have to be orthogonal. This directly implies that the radial wavefunction of the  $2s$  orbital  $R_{20}$  must have a node (and positive and negative parts), since  $R_{10}$  does not have a node. This nodes make the orbitals more extended in space. This leads us to another simple rule of thumbs. The first orbitals of its kind are small. This means the  $1s$ ,  $2p$ ,  $3d$ , and  $4f$ . Of particular importance for condensed-matter physics are the compounds where the valence band contain  $3d$  and  $4f$  orbitals. Since the orbitals are small Coulomb interactions are important and we expect the nearly-free electron model to work less well.

## XIX. BAND STRUCTURE OF SELECTED MATERIALS: SIMPLE METALS AND NOBLE METALS

Let us first look at the situation of simple metals. Where can we find those in the periodic table? First, we do not want small orbitals, because then strong electron-electron interactions play an important role. This rules out all transition-metals (such as iron and cobalt), and all the rare earths. We want materials with  $s$  and  $p$  electrons. However, some of these are usually only present as gases (such as He) often in the form of molecules (such as  $H_2$ ,  $N_2$ , and  $O_2$ ). Certain combinations of  $s$  and  $p$  electrons have the tendency to form  $sp$  hybrids (for example in Si and carbon compounds such as graphene and diamond), which will be discussed later. We are therefore left with elements from groups 1A (Na, K, Rb), 2A (Mg, Ca), and 3A (Al). Let us consider Aluminum.

Al has a face-centered cubic lattice (fcc), see Fig. 45. The lattice vectors are

$$\mathbf{a}_1 = \frac{a}{2}(\hat{y} + \hat{z}), \quad \mathbf{a}_2 = \frac{a}{2}(\hat{z} + \hat{x}), \quad \mathbf{a}_3 = \frac{a}{2}(\hat{x} + \hat{y}). \quad (200)$$

The reciprocal lattice vectors can be obtained using Eqn. (57) and are

$$\mathbf{b}_1 = \frac{4\pi}{a} \frac{1}{2}(\hat{y} + \hat{z} - \hat{x}), \quad \mathbf{b}_2 = \frac{4\pi}{a} \frac{1}{2}(\hat{z} + \hat{x} - \hat{y}), \quad \mathbf{b}_3 = \frac{4\pi}{a} \frac{1}{2}(\hat{x} + \hat{y} - \hat{z}), \quad (201)$$

which corresponds to the lattice vectors of a body-centered cube (bcc). The first Brillouin is shown in Fig. 46. Bragg reflection occurs in planes perpendicular to the reciprocal lattice vectors at half the length of the vector. The

**PERIODIC TABLE OF THE ELEMENTS**

<http://www.kf-split.hr/periodni/en/>

Legend:

- Metal (Blue)
- Semimetal (Orange)
- Nonmetal (Green)
- Alkali metal (Light Blue)
- Alkaline earth metal (Light Orange)
- Transition metals (Yellow)
- Lanthanide (Light Purple)
- Actinide (Light Pink)
- Chalcogens element (Light Green)
- Halogens element (Light Red)
- Noble gas (Light Grey)

STANDARD STATE (100 °C; 101 kPa):  
 Ne - gas, Fe - solid, Ga - liquid, T - synthetic

(1) Pure Appl. Chem., 73, No. 4, 667-683 (2001)  
 Relative atomic mass is shown with five significant figures. For elements with no stable nuclides, the value enclosed in brackets indicates the mass number of the longest-lived isotope of the element.

However these such elements (Tl, Pa, and U) do have a characteristic terrestrial isotopic composition, and for these an atomic weight is tabulated.

Editor: Aditya Vardhan (advan@uafim.com)

FIG. 43: The periodic table of elements.

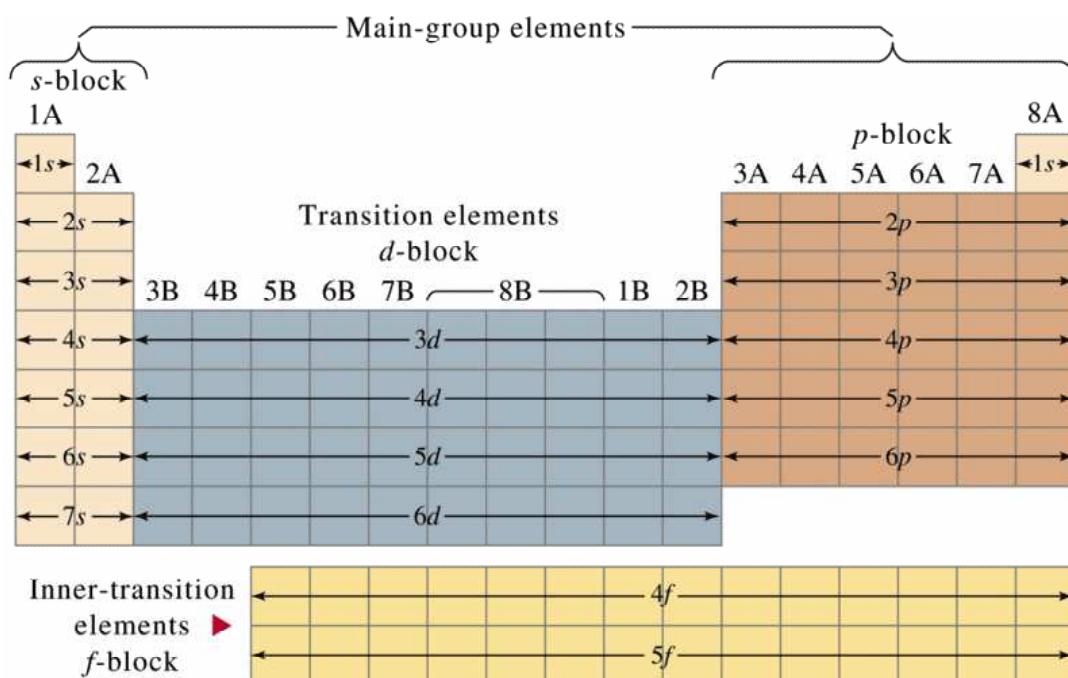


FIG. 44: The table shows which shell are being filled when going through the periodic table.

nearest-neighbors in reciprocal space are at the centers of the cube along the (111) directions, giving rise to the largest planes in the first Brillouin zone. The next-nearest neighbors are along the sides of the cube in the (100) directions. The electronic structure is shown in Fig. 47, where it is compared to a free-electron model. The periodic potential is smaller than we chose for the two-dimensional example. The gap at point X in reciprocal space is less than 0.1 Ry or of the order of one electron volt. We also observe (for example, along the XW direction), the lifting of degeneracies due to the periodic potential. However, despite the added complexity of dealing with a fcc lattice, the (nearly) free electron model is surprisingly successful.

There is another class of compounds, where the free-electron model is useful. These are the noble metals. Although

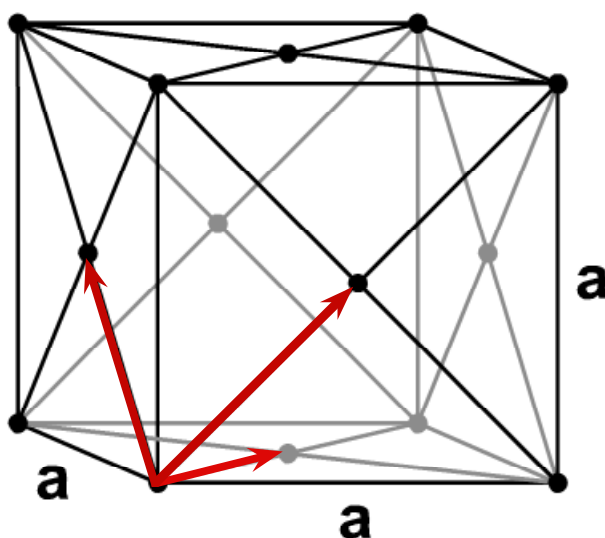


FIG. 45: The face-centered cubic lattice.

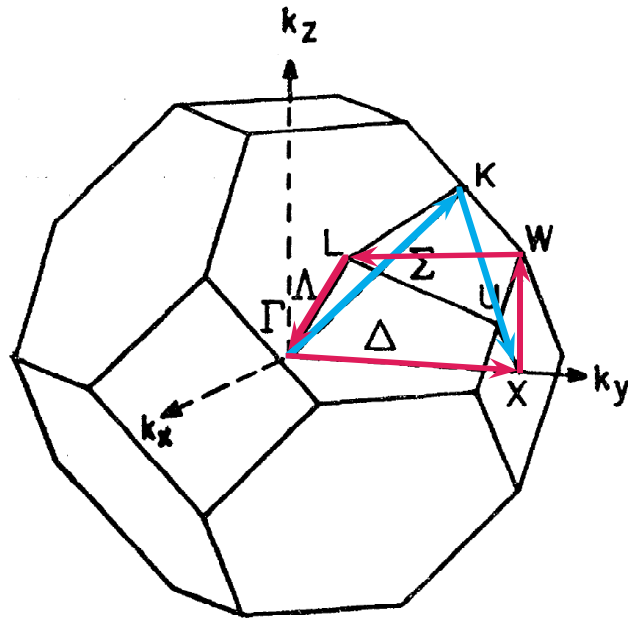


FIG. 46: The first Brillouin zone for Aluminum. Since Al is fcc, the reciprocal lattice vectors form a bcc lattice. The lines indicate the directions taken in plotting the electronic structure in Fig. 47.

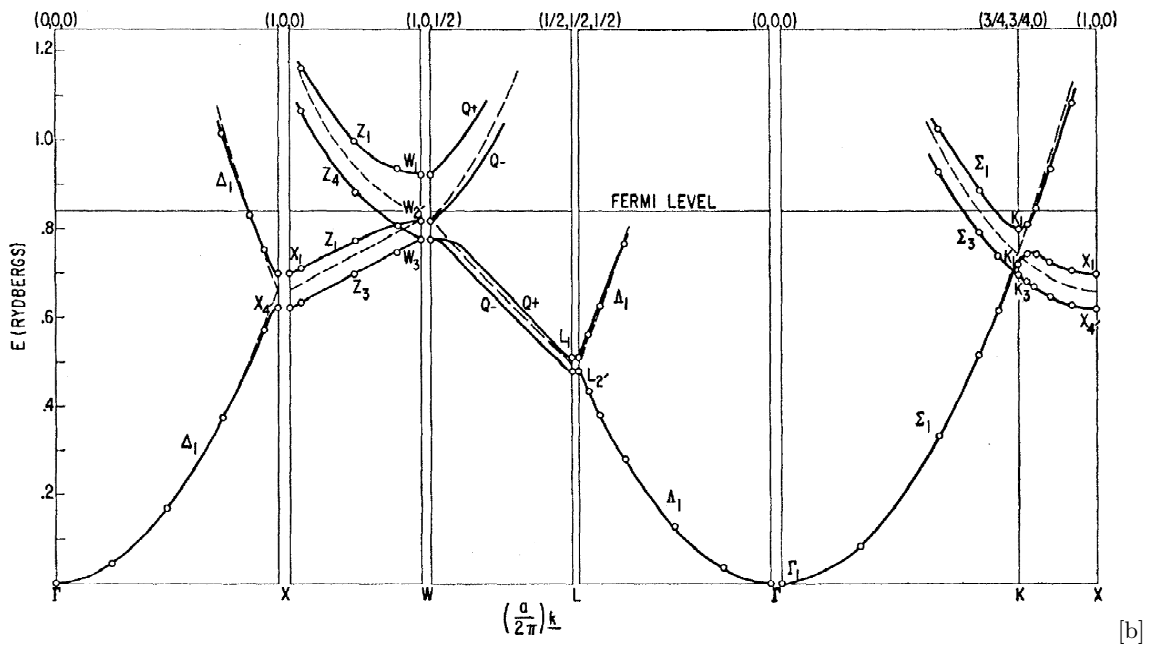


FIG. 47: The electronic structure of Aluminum along several directions. The dashed lines indicate the results for the free-electron model. From Segall, Phys. Rev. **124**, 1797 (1961).

transition metals, the  $d$  shell is full for the noble metals. For example, the atomic structure of copper is  $[\text{Ar}]3d^{10}4s^1$ , where  $[\text{Ar}]$  indicates the same shell as the noble element argon. These shells ( $1s$  to  $3p$ ) are all full and deep-lying core levels. The relevant shells are the  $3d$  and  $4s$  levels. Note that even for atomic copper, the  $3d$  shell is full. This is an exception to the phenomenological diagram that indicates that the  $4s$  shell is filled first. This is true for all the other  $3d$  transition metals that have a configuration  $3d^n4s^2$ . However, the filled  $3d$  shell is so stable, that it effectively “steals” an electron from the  $4s$  shell. Note that the next element, zinc, has a  $[\text{Ar}]3d^{10}4s^2$  configuration, again with the  $3d$  shell filled. When looking the electronic structure of copper, see Fig. 48, we expect significantly more bands due to the presence of the  $3d$  states. Since copper also has an fcc structure, we can try to compare it to Al, see Fig. 47. The first notable difference is the cluster of bands with relatively narrow dispersion. These are the five  $3d$





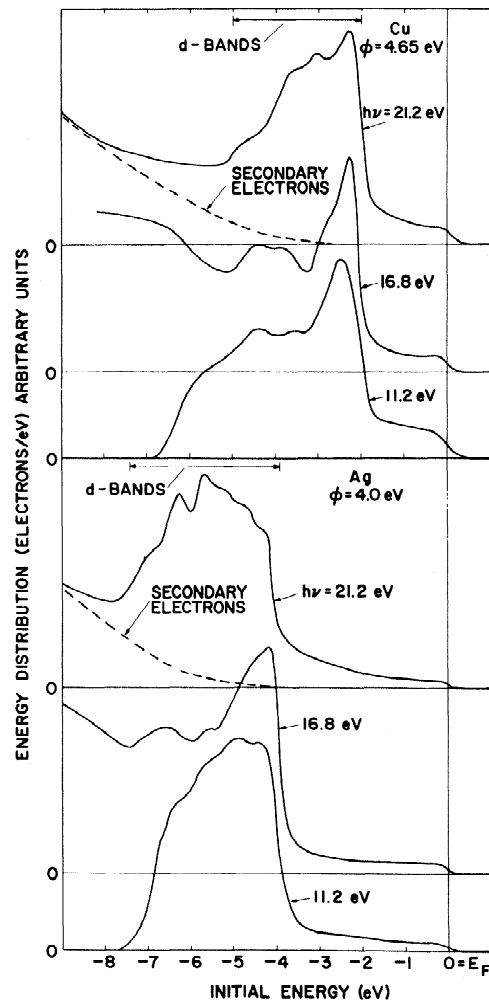


FIG. 50: Valence band photoemission of copper and silver from Eastman and Cashion, Phys. Rev. Lett. **24**, 310 (1970) using different energies for the incoming photon. Note the onset of the  $d$  band at 2 and 4 eV below the Fermi level for Cu ( $3d$ ) and Ag ( $4d$ ), respectively. The bands crossing the Fermi level are the  $4sp$  and  $5sp$  bands, respectively.

energies  $E_b$  via

$$E_{\text{kin}} = \hbar\omega - E_b, \quad (202)$$

where  $\hbar\omega$  (or  $h\nu$ ) is the energy of the photon. The spectra for copper and silver are given in Fig. 50. Different photon energies are used. The spectra look different due to changes in the matrix elements as a function of photon energy. What is clear is the strong emission from the  $d$  bands. The onset of is around 2 eV for copper and 4 eV for silver. The band width for copper is smaller than that of silver (this is most clearly seen in the spectra taken at 21.2 eV). This is in agreement with our notion that the  $3d$  bands are smaller and therefore more localized than the  $4d$  bands. The density of states at the Fermi level is rather small and due to the  $sp$  bands.

Another interesting effect occurs at the  $L$  point in the Brillouin zone. The Fermi surface lies just above the band at the edge of the Brillouin zone. This situation is very similar to our example for the nearly-free electron model in two dimensions for  $n = 1.4$  electrons per site, see Fig. 38 (in three dimensions, the  $\Gamma L$  direction is  $(111)$ , whereas in two dimensions the  $(0,0)$  ( $\Gamma$  in two dimensions) to  $(\frac{\pi}{a}, \frac{\pi}{a})$  direction is  $(1,1)$ . Note that the plot directions are opposite). We saw that in two dimensions a neck was formed touching the edge of the Brillouin zone. A comparable effect occurs in three dimension, see Fig. 49, where we find “neck” formation along the  $(111)$  directions.

## XX. THERMAL PROPERTIES

In this section, we are going to study the thermal properties of a solid. In particular, we will look at the specific heat

$$C = \frac{\partial U}{\partial t}. \quad (203)$$

Let us remind ourselves of the classical gas. For an ideal gas, we are dealing with the equipartition theorem that states that each particle has an energy  $\frac{1}{2}k_B T$ . For three dimension, we then have

$$U = \frac{3}{2}k_B T \quad \Rightarrow \quad C = \frac{\partial U}{\partial t} = \frac{3}{2}k_B, \quad (204)$$

which means a constant specific heat. In a solid, there are contributions to the specific heat due to phonons and electrons.

### A. Electrons

Up till now we have considered the (nearly) free-electron model in one and two dimensions. Let us have a look at the free-electron model in three dimensions. The Schrödinger equation is given by

$$H\psi(\mathbf{r}) = E\psi(\mathbf{r}) \quad \Rightarrow \quad -\frac{1}{2m}\nabla^2\psi(\mathbf{r}) = E\psi(\mathbf{r}). \quad (205)$$

The solutions are plane waves

$$\psi(\mathbf{r}) = \frac{1}{\sqrt{V}}e^{i\mathbf{k}\cdot\mathbf{r}} \quad \text{with} \quad \varepsilon_{\mathbf{k}} = \frac{\hbar^2\mathbf{k}^2}{2m}. \quad (206)$$

As is common in condensed-matter physics, we apply periodic boundary conditions in all three directions, which give

$$k_i = 0, \pm\frac{2\pi}{L}, \pm\frac{4\pi}{L}, \dots \quad (207)$$

where for simplicity we have assumed that the solid is a cube with sides  $L$ . For a sufficiently large systems, this reproduces the bulk properties. Whereas in the nineteenth century, first attempts by Drude at describing the electronic properties of a solid assumed that the electrons behaved as classical particles (no surprise, since quantum mechanics was not yet developed). However, this model fails in describing many properties and a treatment using quantum statistics is essential. The average occupation of a level  $i$  with energy  $\varepsilon_i$  is given by

$$\langle n_i \rangle = \frac{\sum_n n e^{-\beta n \varepsilon_i}}{\sum_n e^{-\beta n \varepsilon_i}} \quad (208)$$

with  $\beta = 1/k_B T$ . Electron are fermions and need to obey Pauli's principle. Therefore,  $n$  can only assume the values  $n = 0, 1$ .

$$\langle n_i \rangle = \frac{e^{-\beta \varepsilon_i}}{1 + e^{-\beta \varepsilon_i}} = \frac{1}{e^{\beta \varepsilon_i} + 1}. \quad (209)$$

However, this does not quite work. For  $T = 0$ , all states with  $\varepsilon_i < 0$  would be occupied and all states with  $\varepsilon_i > 0$  would be empty. However, at  $T = 0$ , the energy up to which the states are occupied is determined by the chemical potential (or the Fermi energy). Substituting  $\varepsilon_i \rightarrow E - \mu$  gives the Fermi-Dirac distribution function

$$f(E) = \frac{1}{e^{\frac{E-\mu}{k_B T}} + 1}, \quad (210)$$

where  $k_B$  is Boltzmann's constant and  $T$  is the temperature;  $\mu$  is the chemical potential. At  $T = 0$ , all the electron levels below the chemical potential are full and those above are empty. At all temperatures,  $f(\mu) = \frac{1}{2}$ . In a free-electron model, the position of the chemical potential or the Fermi energy at  $T = 0$  is determined by the number of electrons. To calculate this, we first need to find an expression for the number of levels or the density of states. The

$k$  values are quantized in all three directions, and one particular  $k$  point occupies a volume of  $(2\pi/L)^3$  in  $k$  space. Since the number of  $k$  states is very large (of the order of  $10^{23}$ ), the Fermi surface is essentially a sphere. The number of states is then

$$N = 2 \left( \frac{L}{2\pi} \right)^3 \frac{4}{3} \pi k_F^3 = \frac{V}{3\pi^2} k_F^3, \quad (211)$$

with  $V = L^3$  and where the factor two comes from the spin degrees of freedom for each state. The Fermi wavevector is then

$$k_F = \left( \frac{3\pi^2 N}{V} \right)^{1/3} \quad (212)$$

giving a Fermi energy of

$$E_F = \frac{\hbar^2 k_F^2}{2m} = \frac{\hbar^2}{2m} \left( \frac{3\pi^2 N}{V} \right)^{2/3}. \quad (213)$$

Using this expression, we can also find the number of states whose energy is less than  $E$

$$N = \frac{V}{3\pi^2 N} \left( \frac{2mE}{\hbar^2} \right)^{3/2}. \quad (214)$$

When changing the energy  $dE$ , the number of states change by

$$\rho(E) = \frac{dN}{dE} = \frac{V}{2\pi^2 N} \left( \frac{2m}{\hbar^2} \right)^{3/2} \sqrt{E}. \quad (215)$$

The Fermi-Dirac statistic are the major cause for the difference between the classical and quantum-mechanical specific heats. Classically, a change in temperature affects all particles. Quantum-mechanically, only the electrons close to the Fermi level are affected. Let us try to estimate the effect. The energy associated with the temperature ( $k_B T \cong 25$  meV at room temperature) is generally a lot smaller than the Fermi energy (typically of the order of electron volts). The percentage of electrons that are thermally excited is of the order of  $T/T_F$ . The change in energy is of the order of  $k_B T$ . The thermal kinetic energy (the kinetic energy at a finite temperature compared to the energy at  $T = 0$ ) is then

$$U \cong N \frac{T}{T_F} k_B T. \quad (216)$$

This leads to a specific heat of

$$C = \frac{\partial U}{\partial t} \cong N k_B \frac{T}{T_F}. \quad (217)$$

We note the difference between the specific heat for classical free particles, which is independent of energy. The specific heat using the Fermi-Dirac function is temperature dependent. In addition to the change in energy as a function of temperature, the number of electrons contributing to the specific heat also changes as a function of temperature. In addition, the specific heat is only on the order of a few percent of the classical specific heat. This is due to the ratio  $T/T_F$ . At room temperature  $k_B T \cong 25$  meV, so the thermal energy is of the order of meV. However, the Fermi energy is generally of the order of several electron volts.

Let us now derive a more quantitative expression for the electronic heat capacity valid at temperatures for which  $k_B T \ll E_F$ . The change in energy at finite temperatures is given by

$$\Delta U = \int_0^\infty dE E \rho(E) f(E) - \int_0^{E_F} dE E \rho(E), \quad (218)$$

where  $f(E)$  is the Fermi-Dirac function and  $\rho(E)$  is the density of states. We multiply the identity

$$N = \int_0^\infty dE \rho(E) f(E) = \int_0^{E_F} dE \rho(E) \quad (219)$$

by  $E_F$  to obtain

$$\left( \int_0^{E_F} + \int_{E_F}^{\infty} \right) dE E_F \rho(E) f(E) = \int_0^{E_F} E_F \rho(E). \quad (220)$$

We can use this to rewrite Eqn. (221)

$$\Delta U = \int_{E_F}^{\infty} dE (E - E_F) \rho(E) f(E) + \int_0^{E_F} (E_F - E) [1 - f(E)] \rho(E). \quad (221)$$

The first term is the energy needed to take electrons from the Fermi level to the states above the Fermi level; the second term is the energy needed to take electrons from below the Fermi to the Fermi level. Both terms are positive. The heat capacity can be found by taking the derivative with respect to the temperature  $T$ . The only temperature dependent term is the Fermi-Dirac function. Regrouping gives

$$C_{el} = \frac{d\Delta U}{dT} = \int_0^{\infty} dE (E - E_F) \rho(E) \frac{df(E)}{dT}. \quad (222)$$

At temperatures  $T \ll E_F$ , we see that the derivative is only large close to the Fermi level. Taking the density of states constant gives

$$C_{el} = \rho(E_F) \int_0^{\infty} dE (E - E_F) \frac{df(E)}{dT}. \quad (223)$$

There are some small difference between the Fermi energy  $E_F$  and the chemical potential  $\mu$ . The chemical potential is the point where  $f(\mu) = \frac{1}{2}$ . The Fermi energy is the energy where  $N = \int_0^{E_F} dE \rho(E) f(E)$ . However, for  $k_B T \ll E_F$ , this difference is negligible and we take  $\mu \cong E_F$ . Taking the derivative of the Fermi-Dirac function with  $\tau = k_B T$  gives

$$\frac{df(E)}{d\tau} = \frac{E - E_F}{\tau^2} \frac{\exp \frac{E - E_F}{\tau}}{(\exp \frac{E - E_F}{\tau} + 1)^2}. \quad (224)$$

Setting  $x = \frac{E - E_F}{\tau}$  and using  $\frac{d\tau}{dT} = k_B$ , we obtain

$$C_{el} = \rho(E_F) \int_0^{\infty} dE (E - E_F) \frac{df(E)}{d\tau} \frac{d\tau}{dT} \quad (225)$$

$$= \rho(E_F) \tau \int_0^{\infty} d \left( \frac{E - E_F}{\tau} \right) \frac{(E - E_F)^2}{\tau^2} \frac{\exp \frac{E - E_F}{\tau}}{(\exp \frac{E - E_F}{\tau} + 1)^2} k_B \quad (226)$$

$$= k_B^2 T \rho(E_F) \int_{-E_F/k_B T}^{\infty} dx x^2 \frac{e^x}{(e^x + 1)^2}. \quad (227)$$

We can safely replace the lower limit by  $-\infty$  since the integrand is negligible in this region. The integrand is given by

$$\int_{-\infty}^{\infty} dx x^2 \frac{e^x}{(e^x + 1)^2} = \frac{\pi^2}{3}. \quad (228)$$

This gives a heat capacity

$$C_{el} = \frac{\pi^2}{3} \rho(E_F) k_B^2 T. \quad (229)$$

The density of states at the Fermi level can be rewritten as

$$\rho(E_F) = \frac{3N}{2E_F} = \frac{3N}{2k_B T_F}, \quad (230)$$

giving

$$C_{el} = \frac{\pi^2}{2} N k_B \frac{T}{T_F}, \quad (231)$$

apart from a factor, in agreement with our earlier estimate.

## B. Phonons

In solids, there is also a heat capacity due to phonons. Let us start by calculating the density of states. The volume occupied by one  $k$  point is again given by

$$\left(\frac{2\pi}{L}\right)^3 = \frac{8\pi^3}{V}. \quad (232)$$

The number of states in a volume in reciprocal space around  $k = 0$ , is then given by

$$N = \frac{V}{8\pi^3} \frac{4}{3} \pi k^3 = \frac{V}{6\pi^2} k^3, \quad (233)$$

for each polarization. We obtain for the density of states

$$\rho(E) = \frac{dN}{d\omega} = \frac{V}{2\pi^2} k^2 \frac{dk}{d\omega}. \quad (234)$$

Although, in principle, it is possible to calculate numerically the density of states for any possible dispersion relationship, it is more insightful to obtain analytical results for some simplified dispersions. In our calculation of phonons in one dimension, we noticed that close to  $k \cong 0$ , the phonon dispersion for acoustic phonons was linear and can therefore be written as

$$\omega = vk, \quad (235)$$

where  $v$  is the constant velocity of sound. This is known as the Debye model. For systems with a basis, we also observed optical phonons. Their dispersion can be simplified by taking  $\omega = \omega_0$ , where  $\omega_0$  is a constant, i.e. there is no  $k$ -dependence. This is known as the Einstein model and is treated below.

*Debye model.*— For the Debye model the density of states is given by

$$\rho(E) = \frac{V}{2\pi^2 v^3} \omega^2. \quad (236)$$

A cut-off frequency  $\omega_D$  is determined from Eqn. (233)

$$\omega_D = \frac{6\pi^2 v^3 N}{V}. \quad (237)$$

We also need the occupation. The average occupation is given by

$$\langle n \rangle = \frac{\sum_n n e^{-\beta n \hbar \omega}}{\sum_n e^{-\beta n \hbar \omega}} = -\frac{1}{\beta} \frac{\partial}{\partial n} \ln \left( \sum_n e^{-\beta n \hbar \omega} \right). \quad (238)$$

The summation is a simple geometric series

$$\sum_n e^{-\beta n \hbar \omega} = 1 + e^{-\beta \hbar \omega} + e^{-2\beta \hbar \omega} + \dots = \frac{1}{1 - e^{-\beta \hbar \omega}} \quad (239)$$

This gives

$$\langle n(\omega) \rangle = -\frac{1}{\beta} \frac{\partial}{\partial \hbar \omega} \ln \frac{1}{1 - e^{-\beta \hbar \omega}} = \frac{1}{\beta} \frac{\partial}{\partial \hbar \omega} \ln(1 - e^{-\beta \hbar \omega}) = \frac{e^{-\beta \hbar \omega}}{1 - e^{-\beta \hbar \omega}} \quad (240)$$

or

$$\langle n \rangle = \frac{1}{e^{\beta \hbar \omega} - 1} \quad (241)$$

This is the well-known Planck distribution law.

We can now proceed with the calculation of the specific heat by noting that the thermal energy is given by

$$U = \int d\omega \rho(\omega) \langle n(\omega) \rangle \hbar \omega = \int_0^{\omega_D} d\omega \frac{V}{2\pi^2 v^3} \omega^2 \frac{\hbar \omega}{e^{\beta \hbar \omega} - 1}, \quad (242)$$

for each polarization type. For simplicity, we assume that all polarizations have the same dispersion and the total thermal energy is obtained by multiplying by a factor 3,

$$U = \frac{3V\hbar}{2\pi^2v^3} \int_0^{\omega_D} d\omega \frac{\omega^3}{e^{\beta\hbar\omega} - 1} = \frac{3V\hbar}{2\pi^2v^3} \left(\frac{k_B T}{\hbar}\right)^4 \int_0^{x_D} dx \frac{x^3}{e^x - 1}, \quad (243)$$

where  $x = \hbar\omega/k_B T$  and  $x_D = \hbar\omega_D/k_B T = T_D/T$  with the Debye temperature  $T_D = \hbar\omega_D/k_B$ . Using the expression for the Debye frequency in Eqn. (237), we can express

$$T_D = \frac{\hbar\omega_D}{k_B} = \left(\frac{6\pi^2 N}{V}\right)^{1/3} \frac{\hbar v}{k_B}. \quad (244)$$

This gives a total phonon energy of

$$U = 9Nk_B T \left(\frac{T}{T_D}\right)^3 \int_0^{x_D} dx \frac{x^3}{e^x - 1}. \quad (245)$$

The heat capacity is found from

$$C_{ph} = \frac{\partial U}{\partial T} = \frac{3V\hbar}{2\pi^2v^3} \frac{\partial}{\partial T} \left[ \int_0^{\omega_D} d\omega \frac{\omega^3}{e^{\beta\hbar\omega} - 1} \right] = \frac{3V\hbar}{2\pi^2v^3} \left[ - \int_0^{\omega_D} d\omega \frac{\omega^3}{(e^{\beta\hbar\omega} - 1)^2} \right] e^{\beta\hbar\omega} \hbar\omega \left( -\frac{1}{k_B T^2} \right) \quad (246)$$

$$= \frac{3V\hbar^2}{2\pi^2v^3 k_B T^2} \left(\frac{k_B T}{\hbar}\right)^5 \int_0^{x_D} dx \frac{x^4 e^x}{(e^x - 1)^2} \quad (247)$$

$$= 9Nk_B \left(\frac{T}{T_D}\right)^3 \int_0^{x_D} dx \frac{x^4 e^x}{(e^x - 1)^2} \quad (248)$$

For  $T \gg T_D$ , it approaches  $C_{ph} = 3Nk_B$ . The heat capacity approaches zero for  $T \ll T_D$ . In this limit, the upper limit of the integral approaches infinity and the integral becomes  $\pi^4/15$  and  $e^x \rightarrow 1$ . The thermal energy is then

$$U = \frac{3}{5} \pi^4 N k_B \frac{T^4}{T_D^3} \quad (249)$$

The specific heat is then

$$C_{ph} = \frac{12}{5} \pi^4 N k_B \left(\frac{T}{T_D}\right)^3. \quad (250)$$

This is known as the Debye  $T^3$  approximation. An intuitive understanding can be obtained by assuming that only a fraction of the total states are occupied. This volume fraction is determined by the temperature, where  $\hbar v k_T = k_B T$ , giving a thermal wavevector  $k_T = k_B T/\hbar v$ . The volume fraction is therefore determined by the excited states relative to the total number of states (determined by the Debye frequency) and is  $(T/T_D)^3$ . Each of the excited moments has a thermal energy  $k_B T$ . The total energy is then approximately  $\sim 3Nk_B T (T/T_D)^3$ . The specific heat is therefore  $\sim 12Nk_B (T/T_D)^3$ .

*Einstein model.*— The Einstein model assumes a dispersion that is constant as a function of  $k$ . Alternatively, one can view this as  $N$  independent oscillators. The thermal energy is then

$$U = N \langle n(\omega) \rangle \hbar\omega = \frac{N\hbar\omega}{e^{\frac{\hbar\omega}{k_B T}} - 1}, \quad (251)$$

where, for convenience, we write  $\omega$  instead of  $\omega_0$ . The heat capacity is then

$$C_{ph} = \frac{\partial U}{\partial T} = Nk_B \left(\frac{\hbar\omega}{k_B T}\right)^2 \frac{e^{\frac{\hbar\omega}{k_B T}}}{(e^{\frac{\hbar\omega}{k_B T}} - 1)^2}. \quad (252)$$

In three dimensions,  $N$  should be replaced by  $3N$ . In the high-temperature limit, we obtain again  $3Nk_B$  which is the Dulong-Petit value.

*Experimental heat capacity.*— At temperatures much below the Debye temperature and the Fermi temperature the heat capacity can be written as the sum of both the electron and phonon contributions

$$C = C_{el} + C_{ph} = \gamma T + AT^3. \quad (253)$$

It is often convenient to plot this as

$$\frac{C}{T} = \gamma + AT^2. \quad (254)$$

The observed values of the coefficient  $\gamma$  are of the expected magnitude but the effective electron masses do not correspond closely to the free-electron value. One often defines a thermal effective mass defined as

$$m_{th} = \frac{\gamma_{observed}}{\gamma_{free}} m. \quad (255)$$

The deviations in the electron model are directly related to the changes in dispersion as observed in the nearly-free electron model or the tight-binding model. The changes can be dramatic and up to two orders of magnitude for rare-earth compounds known as heavy-fermion systems.

## XXI. OPTICAL PROPERTIES

In a regular course on electricity and magnetism, the electronic structure is treated in a very approximate way (this section will, unlike AM, follow SI units). The assumption is that an external electric field induces a polarization  $\mathbf{P}$  counteracting the external field. The external field is given by the displacement  $\mathbf{D}$  which can be related to external charges that create the external field. The external field and the polarization together produce the electric field inside the solid

$$\mathbf{E} = \frac{1}{\epsilon_0} (\mathbf{D} - \mathbf{P}), \quad (256)$$

where  $\epsilon_0$  is the permittivity of free space (vacuum). We know from Gauss's law that  $\nabla \cdot \mathbf{E} = \rho/\epsilon_0$ , where  $\rho$  is the charge density. Taking the divergence of the above equation gives

$$\epsilon_0 \nabla \cdot \mathbf{E} = \nabla \cdot \mathbf{D} - \nabla \cdot \mathbf{P} \quad \Rightarrow \quad \rho = \rho_{free} + \rho_{ind}, \quad (257)$$

where we have used  $\nabla \cdot \mathbf{D} = \rho_{free}$  and  $\nabla \cdot \mathbf{P} = -\rho_{ind}$ , giving the free and induced charges, respectively. The assumption is now that the polarizability is directly proportional to the electric field

$$\mathbf{P} = \epsilon_0 \chi \mathbf{E}, \quad (258)$$

where  $\chi$  is known as the electric susceptibility. This quantity is supposed to represent all the electronic structure of the solid. Often the solid is represented as a simple electron gas. Although this assumption works often surprisingly well (it explains for example why light is reflected from metals, giving them the mirror-like appearance), it does not work well when considering more details (for example, why is copper reddish, silver silver, and gold yellow). To obtain some understanding about these details, we have to understand the interaction between light and solids in terms of transitions in the electronic structure. However, let us first continue with the standard E&M approach.

Inserting Eqn. (258) into (256), gives

$$\mathbf{E} = \frac{1}{\epsilon_0} (\mathbf{D} - \epsilon_0 \chi \mathbf{E}) \quad \Rightarrow \quad \mathbf{E} = \frac{1}{\epsilon_0(1 + \chi)} \mathbf{D} = \frac{\mathbf{D}}{\epsilon_0 \epsilon_r} = \frac{\mathbf{D}}{\epsilon}, \quad (259)$$

where we have introduced the relative permittivity  $\epsilon_r = 1 + \chi$ , also known as the dielectric constant. We see that once we have found  $\chi$ , we can also directly relate the electric field inside the solid to the externally applied field.

*The Lorentz oscillator.*— Let us first consider the example of a Lorentz oscillator. This classical model is useful since it can be related to quantum-mechanical interband transitions in a solid. We can also reduce it to the Drude model which quantum mechanically includes all intraband transitions (i.e. no scattering with reciprocal lattice vectors). The quantum-mechanical theory can therefore be seen as an extension of its classical analog. We start by considering Newton's equation for an electron in an electric field

$$\sum \mathbf{F} = m\mathbf{a} \quad \Rightarrow \quad -e\mathbf{E} - m\Gamma\mathbf{v} - m\omega_0^2\mathbf{r} = m\mathbf{a}. \quad (260)$$



Classically, this means that the electron feels an electric force  $-e\mathbf{E}$ . It is held in its place by an effective spring force  $-m\omega_0^2\mathbf{r}$  from the nucleus. In addition, it feels a viscous damping  $-m\Gamma\mathbf{v}$ . Quantum mechanically, we will see that  $\hbar\omega_0$  corresponds to the energy of inter/intraband transitions. The damping is due to scattering giving a finite lifetime (and therefore a broadening  $\Gamma$ ) to the electronic states. Eqn. (260) leads to a differential equation

$$\frac{d^2\mathbf{r}}{dt^2} + \Gamma\frac{d\mathbf{r}}{dt} + \omega_0^2\mathbf{r} = -\frac{e}{m}\mathbf{E}. \quad (261)$$

If the local electric field varies as  $e^{-i\omega t}$ , then  $\mathbf{r}$   $e^{-i\omega t}$  has a similar time dependence. Since  $\mathbf{r}$  gives the displacement of the electron with respect to the nucleus, this gives an induced dipole moment

$$\mathbf{r} = -\frac{e\mathbf{E}}{m} \frac{1}{\omega_0^2 - \omega^2 - i\Gamma\omega} \quad \Rightarrow \quad \mathbf{p} = -e\mathbf{r} = \alpha(\omega)\mathbf{E} \quad \text{with} \quad \alpha(\omega) = \frac{e^2}{m} \frac{1}{\omega_0^2 - \omega^2 - i\Gamma\omega}. \quad (262)$$

The total polarization per unit volume is given by

$$\mathbf{P} = \frac{N}{V}\mathbf{p} = n\alpha(\omega)\mathbf{E} \equiv \varepsilon_0\chi\mathbf{E} \quad \Rightarrow \quad \chi = \frac{n\alpha(\omega)}{\varepsilon_0}, \quad (263)$$

where  $n = N/V$  is the electron density. This gives for the dielectric constant

$$\varepsilon_r = 1 + \chi = 1 + \frac{n\alpha(\omega)}{\varepsilon_0} = 1 + \frac{ne^2}{m\varepsilon_0} \frac{1}{\omega_0^2 - \omega^2 - i\Gamma\omega}. \quad (264)$$

We can reduce this to the Drude result by realizing that the Drude model excludes the attractive potential of the nuclei ( $\omega_0 = 0$ ) and does not include scattering ( $\Gamma$ ). This gives

$$\varepsilon_r = 1 - \frac{ne^2}{m\varepsilon_0} \frac{1}{\omega^2} = 1 - \frac{\omega_p^2}{\omega^2}, \quad (265)$$

where  $\omega_p^2 = ne^2/\varepsilon_0m$  is the plasma frequency. This result basically has the electron gas moving along with the electric field.

Let us see what a typical value is for the plasma frequency. Let us consider aluminum. Al is face-centered cubic with a lattice constant  $a = 4.05 \text{ \AA}$ . Since this is fcc there are four atoms in the cube, see Fig. 45 (eight at the corners that count for 1/8 and six at the sides that count for a 1/2). Al has a  $3s^23p$  configuration, so each Al atom contributes three electrons. This gives a density  $n = 4 \times 3 / (4.05 \times 10^{-10})^3 = 1.8 \times 10^{29} \text{ m}^{-3}$ . Inserting the numbers gives  $\omega_p = 2.4 \times 10^{16} \text{ s}^{-1}$  or in energy  $\hbar\omega = 99 \text{ eV}$ . This is undoubtedly going to be too high since we know that the Drude model neglects the Fermi-Dirac statistics and therefore overestimates  $n$ .

*Interaction of light with a solid.*— This is all nice, but how does this affect the interaction of light with a solid, i.e. the optical properties of a solid? Let us go back to Maxwell equations. Two of them include the divergence of the electric and magnetic fields

$$\nabla \cdot \mathbf{D} = \rho_{\text{free}} \quad \rightarrow \quad \nabla \cdot (\varepsilon_R\mathbf{E}) = \rho_{\text{free}} = 0, \quad (266)$$

in the absence of an applied electric field. Some care should be taken here with the permittivity. We use here a real permittivity  $\varepsilon_R = \text{Re}[\varepsilon]$ . As we will see the complex part will be related to the currents. Furthermore, we also have for the magnetic induction  $\nabla \cdot \mathbf{B} = 0$ . The other two involve the rotation of the magnetic and electric fields.

$$\nabla \times \mathbf{E} + \frac{\partial \mathbf{B}}{\partial t} = 0 \quad \text{and} \quad \nabla \times \mathbf{H} - \frac{\partial \mathbf{D}}{\partial t} = \mathbf{J}_{\text{free}}, \quad (267)$$

where  $\mathbf{J}_{\text{free}}$  is the current due to the free charges. Since we are interested in the propagation of a wave in a solid, we want to transform these equations into a wave equation. This can be done by taking the rotation as follows

$$\nabla \times \nabla \times \mathbf{E} = \nabla(\nabla \cdot \mathbf{E}) - \nabla^2\mathbf{E} = -\nabla \times \frac{\partial \mathbf{B}}{\partial t}. \quad (268)$$

In an isotropic medium, we have the relation  $\mathbf{B} = \mu\mathbf{H}$  (similar to the relation  $\mathbf{D} = \varepsilon\mathbf{E}$ ). Since  $\nabla \cdot \mathbf{E} = 0$ , we obtain with the use of the other Maxwell equation

$$\nabla^2\mathbf{E} = \mu\nabla \times \frac{\partial \mathbf{H}}{\partial t} = \mu \frac{\partial}{\partial t}(\nabla \times \mathbf{H}) = \varepsilon_R\mu \frac{\partial^2\mathbf{E}}{\partial t^2} + \mu \frac{\partial \mathbf{J}_{\text{free}}}{\partial t}. \quad (269)$$

For the current, we have apply Ohm's law:  $\mathbf{J} = \sigma\mathbf{E}$ , where  $\sigma$  is the conductivity. This gives us the wave equation

$$\nabla^2\mathbf{E} - \varepsilon_R\mu\frac{\partial^2\mathbf{E}}{\partial t^2} = \mu\sigma\frac{\partial\mathbf{E}}{\partial t}. \quad (270)$$

The term with  $\sigma$  is related to the optical conductivity related to optical transitions accompanying photon absorption. Remember that the wave equation in free space is given by

$$\nabla^2\mathbf{E} - \varepsilon_0\mu_0\frac{\partial^2\mathbf{E}}{\partial t^2} = 0, \quad (271)$$

where  $\varepsilon_0\mu_0 = 1/c^2$ , where  $c$  is the speed of light in vacuum. We will now look for solution of the electric field in a solid of the form

$$\mathbf{E} = \mathbf{E}_0e^{i\mathbf{q}\cdot\mathbf{r}-i\omega t}. \quad (272)$$

Inserting into Eqn. (269) gives

$$-q^2 + \varepsilon_R\mu\omega^2 = -i\mu\sigma\omega \quad \Rightarrow \quad q^2 = \frac{\mu_r\varepsilon_1}{c^2}\omega^2 + i\mu_r\mu_0\sigma\omega = \mu_r\frac{\omega^2}{c^2}\left(\varepsilon_1 + i\frac{c^2\mu_0\sigma}{\omega}\right) = \mu_r\frac{\omega^2}{c^2}\left(\varepsilon_1 + i\frac{\sigma}{\varepsilon_0\omega}\right), \quad (273)$$

where  $\varepsilon_R \equiv \varepsilon_0\varepsilon_1$  and  $\mu_r = 1$  in a nonmagnetic solid. We can only find a solution if the wavevector is complex, which means we allow for evanescent waves. Let us define a complex diffractive index  $\hat{n}$ ,

$$q = \frac{\omega}{c}\hat{n} = \frac{\omega}{c}(n + i\kappa), \quad (274)$$

where  $n$  is the refractive index and  $\kappa$  is the extinction coefficient (many books use  $k$  or  $K$  here, but this notation is a bit confusing). Substituting gives

$$\frac{\omega^2}{c^2}(n + i\kappa)^2 = \frac{\omega^2}{c^2}(n^2 - \kappa^2 + 2in\kappa) \equiv \mu_r\frac{\omega^2}{c^2}\left(\varepsilon_1 + i\frac{\sigma}{\varepsilon_0\omega}\right), \quad (275)$$

or

$$\varepsilon_1 = \frac{n^2 - \kappa^2}{\mu_r} \quad \text{and} \quad \frac{\sigma}{\varepsilon_0\omega} = \frac{2n\kappa}{\mu_r}. \quad (276)$$

Often this is written as a complex dielectric function

$$\varepsilon_r = \varepsilon_1 + i\varepsilon_2 = \frac{\hat{n}^2}{\mu_r}, \quad (277)$$

giving

$$\varepsilon_1 = \varepsilon = \frac{n^2 - \kappa^2}{\mu_r} \quad \text{and} \quad \varepsilon_2 = \frac{\sigma}{\varepsilon_0\omega} = \frac{2n\kappa}{\mu_r}. \quad (278)$$

Let us consider nonmagnetic systems from now on, for which we have

$$\varepsilon_1 = \varepsilon = n^2 - \kappa^2 \quad \text{and} \quad \varepsilon_2 = 2n\kappa. \quad (279)$$

We can also invert these equations to find the expressions for  $n$  and  $\kappa$  in terms of  $\varepsilon_1$  and  $\varepsilon_2$ . Writing

$$n^2 - \left(\frac{\varepsilon_2}{2n}\right)^2 - \varepsilon_1 = 0 \quad \Rightarrow \quad n^4 - \varepsilon_1n^2 - \left(\frac{\varepsilon_2}{2}\right)^2 = 0 \quad (280)$$

This is a cubic equation in  $n^2$ , where the roots are given by

$$n^2 = \frac{1}{2}\varepsilon_1 + \frac{1}{2}\sqrt{\varepsilon_1^2 + 4\left(\frac{\varepsilon_2}{2}\right)^2}, \quad (281)$$

or

$$n = \sqrt{\frac{1}{2}\varepsilon_1 + \frac{1}{2}\sqrt{\varepsilon_1^2 + \varepsilon_2^2}}. \quad (282)$$

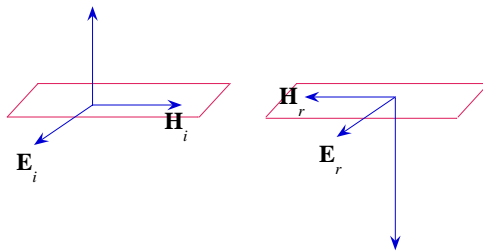


FIG. 51: The reflectance of light at the surface of a solid.

Similarly, we can find

$$\kappa = \sqrt{-\frac{1}{2}\varepsilon_1 + \frac{1}{2}\sqrt{\varepsilon_1^2 + \varepsilon_2^2}}. \quad (283)$$

We can split the dielectric constant that we obtained before into a real and imaginary part

$$\varepsilon_r = 1 + \frac{ne^2}{m\varepsilon_0} \frac{1}{\omega_0^2 - \omega^2 - i\Gamma\omega} = 1 + \frac{ne^2}{m\varepsilon_0} \frac{\omega_0^2 - \omega^2}{(\omega_0^2 - \omega^2)^2 + \Gamma^2\omega^2} + i \frac{ne^2}{m\varepsilon_0} \frac{\Gamma\omega}{(\omega_0^2 - \omega^2)^2 + \Gamma^2\omega^2}. \quad (284)$$

which gives

$$\varepsilon_1 = 1 + \frac{ne^2}{m\varepsilon_0} \frac{\omega_0^2 - \omega^2}{(\omega_0^2 - \omega^2)^2 + \Gamma^2\omega^2} \quad \text{and} \quad \varepsilon_2 = \frac{ne^2}{m\varepsilon_0} \frac{\Gamma\omega}{(\omega_0^2 - \omega^2)^2 + \Gamma^2\omega^2}. \quad (285)$$

As we will see later on,  $\varepsilon_2$  is related to the absorption. Note that the function is like a Lorentzian (it is plotted in Fig. 57), with a width related to  $\Gamma$ . Note that in the limit  $\Gamma \rightarrow 0$  this function becomes a  $\delta$ -function, going to zero for  $\omega \neq \omega_0$  and having a value of  $1/\omega\Gamma \rightarrow \infty$  for  $\omega = \omega_0$ . This means that the solid can only absorb light with energy  $\hbar\omega_0$ . Obviously, few solids have only one resonance frequency. However, we can easily generalize the Lorentz oscillator problem for many oscillators. Let us take  $n_j$  the density of electrons bound with resonance frequency  $\omega_j$

$$\varepsilon_r = 1 + \sum_j \frac{n_j e^2}{m\varepsilon_0} \frac{1}{\omega_j^2 - \omega^2 - i\Gamma_j\omega}, \quad (286)$$

with  $\sum_j n_j = n$ .

*Drude model and intraband transitions.*— Although the Drude model fails in a quantitative description of a solid (by grossly overestimating the number of electrons relevant for the conductivity and other properties, due to the neglect of Fermi-Dirac statistics), the idea that the conduction is determined by electrons that behave almost freely works rather well. This implies that  $\omega_0 = 0$ . The value of  $\Gamma$  is can be related to the inverse of the mean free time between collisions,  $\Gamma = 1/\tau$ . This gives for the dielectric functions

$$\varepsilon = 1 - \frac{\omega_p^2\tau}{\omega(\omega\tau + i)} \quad \Rightarrow \quad \varepsilon_1 = 1 - \frac{\omega_p^2\tau^2}{1 + \omega^2\tau^2} \quad \text{and} \quad \varepsilon_2 = \frac{\omega_p^2\tau}{\omega(1 + \omega^2\tau^2)} \quad (287)$$

*Reflectance.*— Although there are many different types of optical spectroscopies, one of the most intuitive ones is the reflectance. Let us consider an wave coming in perpendicular, see Fig. 51. Let us take the incident electric field along the  $x$ -direction,

$$\mathbf{E}_i = E_i e^{i\hat{q}z - i\omega t} \hat{\mathbf{x}}, \quad (288)$$

where  $\hat{q}$  can be complex. We can find the magnetic field from the Maxwell equation

$$\nabla \times \mathbf{E} = -\mu \frac{\partial \mathbf{H}}{\partial t} = i\mu\omega \mathbf{H}. \quad (289)$$

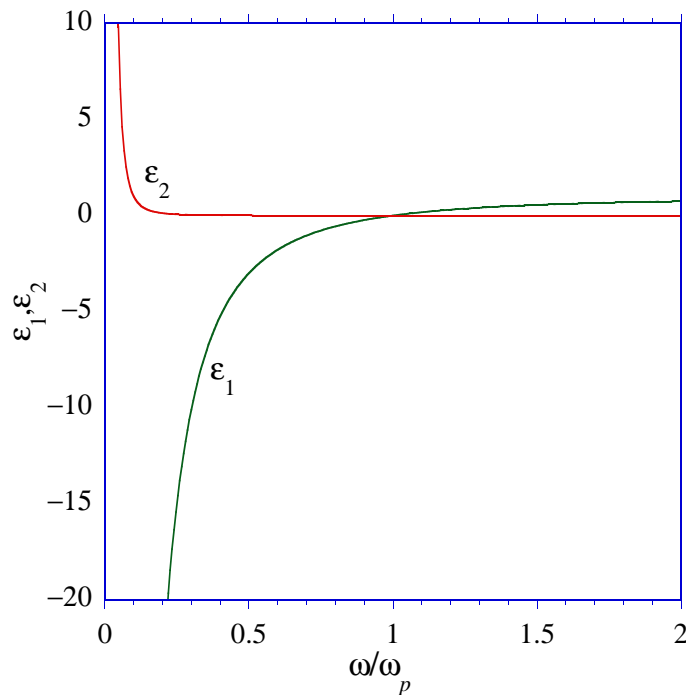


FIG. 52: The dependence of  $\varepsilon_1$  and  $\varepsilon_2$  as a function of  $\omega$  (normalized to the plasma frequency  $\omega_p$ ) of the Drude model. The scattering is small, i.e.  $\Gamma = \tau^{-1} \ll \omega_p$ .

The rotation can be obtained from

$$\nabla \times \mathbf{E} = \begin{vmatrix} \hat{\mathbf{x}} & \hat{\mathbf{y}} & \hat{\mathbf{z}} \\ \frac{\partial}{\partial x} & \frac{\partial}{\partial y} & \frac{\partial}{\partial z} \\ E_x & 0 & 0 \end{vmatrix} = \frac{\partial E_x}{\partial z} \hat{\mathbf{y}} = i\hat{q}E_x \hat{\mathbf{y}} \quad (290)$$

This gives

$$\mathbf{H}_i = \frac{\hat{q}}{\mu\omega} E_i e^{i\hat{q}z - i\omega t} \hat{\mathbf{y}}, \quad (291)$$

which means  $\mathbf{H}$  is perpendicular to  $\mathbf{E}$  (as it should be). At the surface part of the wave is reflected and part of it is transmitted. However, the other Maxwell equations impose continuity of the electric field

$$E_i + E_r = E_t, \quad (292)$$

where  $r$  and  $t$  stand for reflected and transmitted, respectively. For the magnetic field, we must satisfy

$$H_i - H_r = H_t, \quad (293)$$

where we should take care the the direction of the magnetic field changes for the reflected light, see Fig. 51. We can relate this to the electric field by

$$\frac{\hat{q}_1}{\mu_1\omega} (E_i - E_r) = \frac{\hat{q}_2}{\mu_2\omega} E_t, \quad (294)$$

Using that  $\hat{q} = \omega\hat{n}/c$  and that medium 1 is the vacuum for which we have  $\hat{n}_1 = 1$  and  $\mu_1 = \mu_0$  and, in addition, taking the solid nonmagnetic, which gives  $\mu_2 = \mu_0$ , we obtain

$$E_i - E_r = \hat{n}E_t. \quad (295)$$

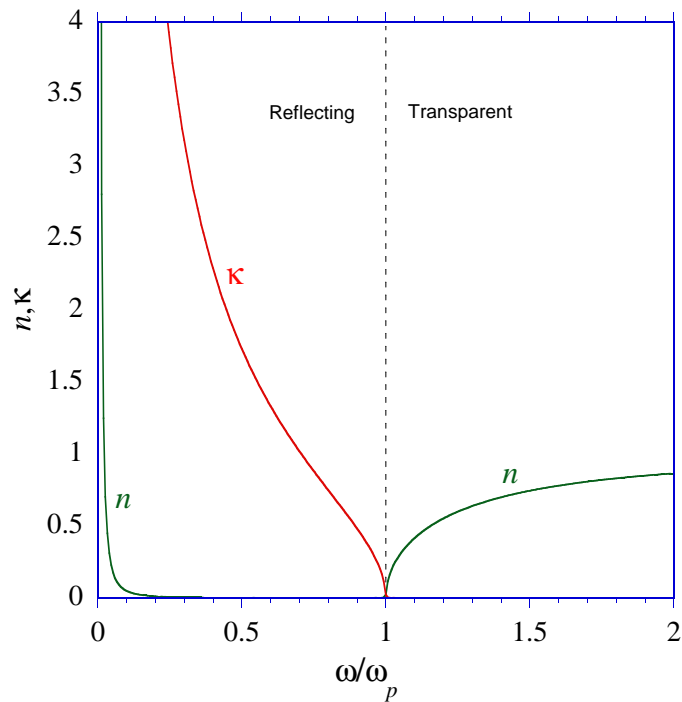


FIG. 53: The dependence of  $n$  and  $\kappa$  as a function of  $\omega$  (normalized to the plasma frequency  $\omega_p$ ) for the Drude model. Same  $\Gamma$  as in Fig. 52.

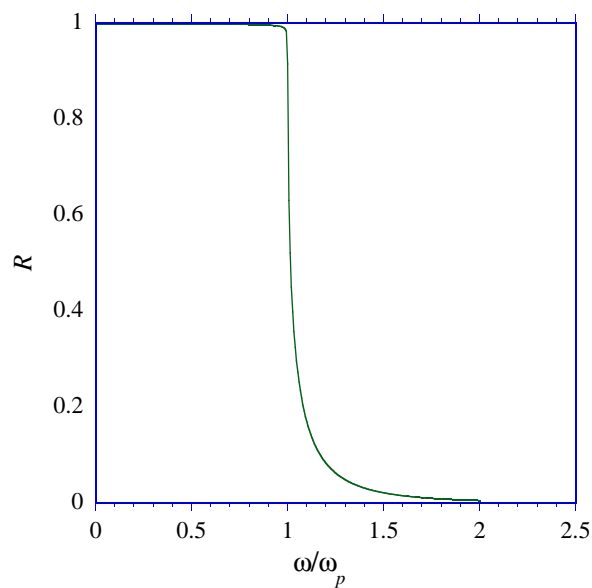


FIG. 54: The dependence of the reflectivity  $R$  as a function of  $\omega$  (normalized to the plasma frequency  $\omega_p$ ) for the Drude model. Same  $\Gamma$  as in Fig. 52.

Combining this with Eqn. (292) gives

$$(\hat{n} - 1)E_i + (1 + \hat{n})E_r = 0 \quad \Rightarrow \quad r = \frac{E_r}{E_i} = \frac{1 - \hat{n}}{1 + \hat{n}}. \quad (296)$$

The reflectivity is then given by

$$R = r^*r = \left| \frac{1 - \hat{n}}{1 + \hat{n}} \right|^2 = \frac{(1 - n)^2 + \kappa^2}{(1 + n)^2 + \kappa^2} \quad (297)$$

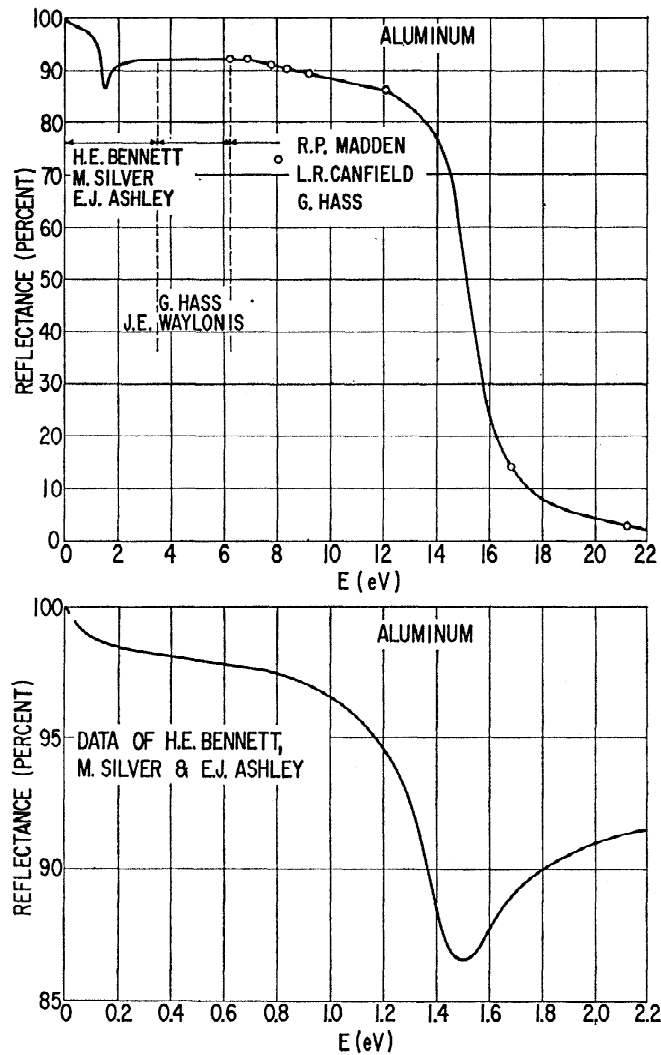


FIG. 55: The reflectance of aluminum. The plasma frequency is given by  $\hbar\omega_p = 14.7$  eV. The decrease in reflectance around 1.4 eV is due to a weak interband transition.

Given the expressions for  $\varepsilon_1$  and  $\varepsilon_2$ , see Fig. 52, for the Drude model, it is straightforward to calculate the index of refraction  $\hat{n} = n + i\kappa$  and the reflectivity, see Fig. 53 and 54. Let us first look at the most intuitive one: the reflectivity, see Fig. 54. In the Drude, we see that the reflectivity is close 100% up to the plasma frequency  $\omega_p$ . How does this work out for our “prototype” nearly-free electron system Al? Figure 55 shows that there is a remarkable agreement in the reflectivity. Close to 90% of the light is reflected up to the plasma frequency. The wavelength of visible light ranges from 380 (violet) to 750 (red) nm. This corresponds to an energy of 1.66-3.27 eV. The value of  $\hbar\omega_p$  for Al is 14.7 eV. Therefore all the visible light is reflected, explaining why aluminum foil has the mirror-like look. The difference in the two sides of the aluminum foil has to do with the manufacturing process. Since aluminum foil is so thin, two sheet of foil are placed on top of each other in the final rolling. When separated after rolling the inside is duller than the outside due to different surface roughness. The reflectance is 88% for the shiny side and 80% for the dull side. There is a decrease in reflectance deviating from the Drude-like behavior around 1.4 eV due to weak interband transitions. The plasma frequency is  $\omega_p = 3.5$  s<sup>-1</sup>. This corresponds to a density of  $n = 3.9 \times 10^{27}$  m<sup>-3</sup>. So when neglecting the Fermi-Dirac distribution, we overestimate  $n$  by a factor 50. This is roughly the overestimation of the conductivity in the Drude model, which is given by  $\sigma = ne^2\tau/m$ , where  $\tau$  is the time between scattering events. The Drude model assumes that the electrons are free, but does not take into account the Fermi-Dirac statistics. However, even though the model completely misses the actual value of  $\omega_p$ , it gives a very nice description of the reflectivity.

The reflectance for frequencies less than the plasma frequency also manifests itself in other quantities. For  $\omega < \omega_p$ , the extinction coefficient is finite, indicating that light does not penetrate the solid. For  $\omega > \omega_p$  we obtain no extinction and obtain a finite index of refraction. Thus aluminum will become transparent in the ultraviolet. We also observe a

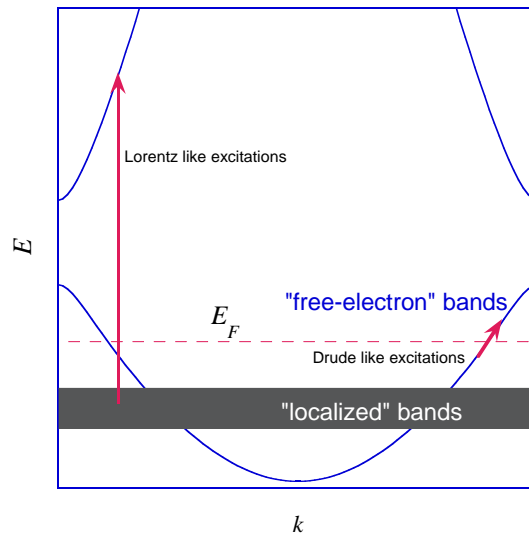


FIG. 56: Schematic figure of the possible transitions. The Drude model describes intraband transition. For free electron like systems and noble metals that would be in the free electron like bands that cross the Fermi level. The minimum energy needed for these transitions is zero. However, for noble metals, one also has to consider interband transitions from the more localized  $3d$  bands. These occur at a finite energy.

finite refractive index  $n$  close to  $\omega = 0$ . This is due to absorption related to the fact that  $\omega_0 = 0$  for the Drude model. *Lorentz oscillators and interband transitions.*—

However, the Drude model appears to fail for noble metals, such as copper (reddish) and gold (yellow), although it works reasonably well for silver. The electron density of copper is  $n = 4 \times 1/(3.61 \times 10^{-10})^3 = 8.5 \times 10^{28} \text{ m}^{-3}$ . This about a factor two smaller than that of aluminum (although the absolute densities fail to predict the plasma frequency, your first order guess for the ratio of the plasma frequencies would be the ratio of the electron densities). Naively one can expect the plasma frequency to be about a factor  $\sqrt{2}$  smaller. This would be of the order of 10 eV, sufficiently high to reflect all visible light. However, to obtain absorption in the visible light we need a plasma frequency around 2 eV, about seven times smaller. Since  $\omega_p \sim \sqrt{n}$ , this would correspond to an electron density which is about a factor 50 smaller. Although we might be willing to swallow a factor two, this is a bit too much. To understand the difference one needs to take a closer look at the electronic structure. The Drude model describes intraband transition. For free electron like systems like aluminum, these occur in the bands that cross the Fermi level. The minimum energy needed for these transitions is zero. However, for noble metals, one also has to consider interband transitions from the more localized  $d$  bands. These occur at a finite energy.

Let us therefore return to the original expressions for  $\epsilon$ , see Eqn. (264). The real and imaginary part of the dielectric function,  $\epsilon_1$  and  $\epsilon_2$  are plotted in Fig. 57. The refractive index  $n$ , extinction coefficient  $\kappa$ , and the reflectivity  $R$  are shown in Fig. 58 for  $\omega_0 = \omega_p/2$ . Again, let us first look at the reflectivity. In the limit that  $\Gamma \rightarrow 0$ , we see again that a decrease in reflectivity around  $\omega_p$ . This transition occurs when  $\epsilon_1 = 0$ , or, for  $\Gamma = 0$ ,

$$\epsilon_1 = 1 + \frac{\omega_p^2}{\omega_0^2 - \omega^2} = 0 \quad \Rightarrow \quad \omega = \sqrt{\omega_p + \omega_0^2}. \quad (298)$$

This gives for our example  $\omega_p \sqrt{1 + (\frac{1}{2})^2} \cong 1.12 \omega_p$ . Above this energy, the solid is transparent. Below this energy the solid is reflecting down to the energy  $\omega_0$ . Below that energy, the system becomes transparent again. This situation is very comparable to what is found for semiconductors or insulators. For a wide-band insulator (for example, diamond, see Fig. 59) an optical transition occurs at a finite energy, i.e. the energy needed to excite an electron from the valence band into the conduction band. Below that energy, the system becomes transparent. For diamond, the minimum excitation energy is greater than 5 eV, larger than the energy of visible light. This makes diamond transparent for visible light giving it a glass light appearance. However, the reflectance is not entirely zero and some of the light will therefore be reflected. Diamonds can also have a color. This is due to impurities. These impurities create energy states inside the insulating gap. In Fig. 58, the optical properties are divided into four regions. These regions roughly indicate the dominant aspect of the material. For  $\omega$  less than roughly  $0.4\omega_0$ , the material is mainly transparent with

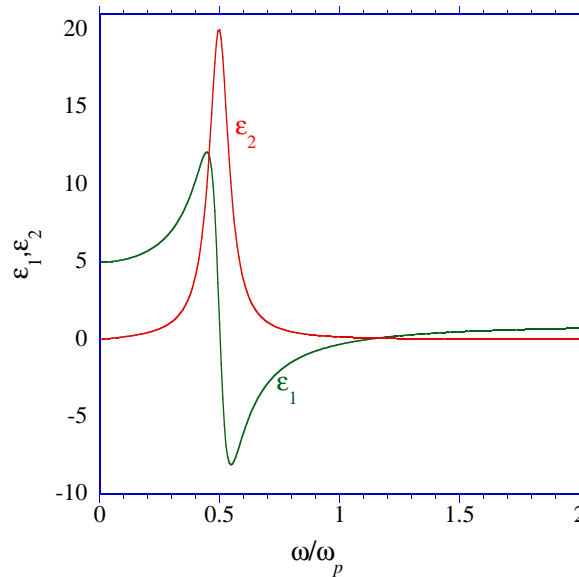


FIG. 57: The coefficients  $\varepsilon_1$  and  $\varepsilon_2$  as a function of  $\omega/\omega_p$  with  $\omega_0 = \omega_p/2$  and  $\Gamma = 0.1\omega_p$ .

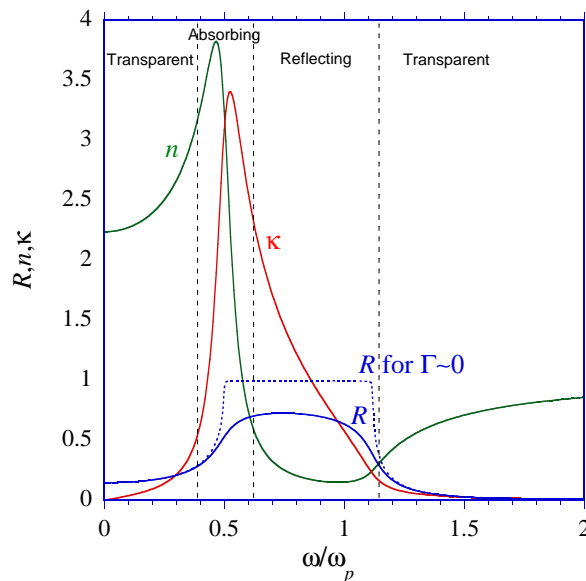


FIG. 58: The refractive index  $n$ , extinction coefficient  $\kappa$ , and the reflection coefficient  $R$  for a Lorentz oscillator as a function of  $\omega/\omega_p$  with  $\omega_0 = \omega_p/2$  and  $\Gamma = 0.1\omega_p$ .

a finite refractive index  $n$  and a small extinction coefficient  $\kappa$ . Around  $\omega_0$ , the material is predominantly absorbing, where the incoming light causes transitions of energy  $\hbar\omega$ . Between  $0.6\hbar\omega_0$  and  $\omega_p$ , the system is reflecting with a large  $R$ . For energies greater than  $\omega_p$ , we again observe transparent behavior.

When considering the reflectance of noble metal such as copper and silver, see Fig. 60, one has to consider a combination of both Drude and Lorentz excitations. The Drude excitations related to excitations in the  $4sp$  bands crossing the Fermi level dominate the reflectance for low energies. However at approximately 2 and 4 eV for Cu and Ag, respectively, we observe Lorentz-like excitations related to transitions from the occupied  $3d$  band into the empty  $4sp$  states, see also Fig. 50. To describe the reflectance we cannot consider a single Lorentz oscillator, but we have to take into account a large number of Lorentz oscillators of different energy. This causes a sharp drop in reflectance. For Ag, this hardly affects the reflectance in the visible light, since 4 eV is in the ultraviolet. However, for copper, the decrease in reflectance occur in the visible region, cutting of the blue part of the spectrum, giving copper its reddish



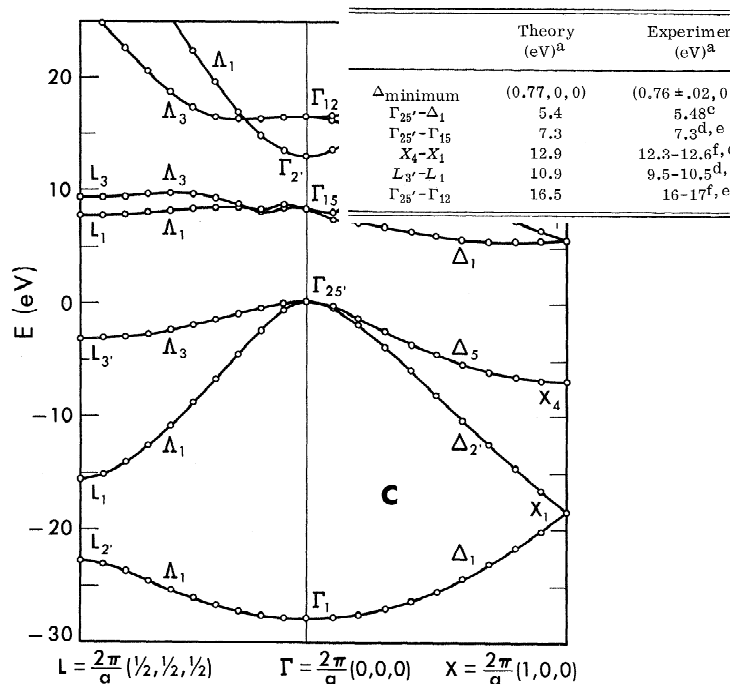


FIG. 59: The band structure of diamond after Saslow, Bergstresser, and Cohen, Phys. Rev. Lett. **16**, 354 (1966). The inset shows the values of several optical transitions.

color. Note that another drop of occurs at higher energies, clearly visible in Ag around 7-8 eV. This drop-off is related to the plasma frequency at an energy about half that in Al, in agreement with our simple estimate of the relative plasma frequencies of Al and Ag/Cu.

## XXII. QUANTUM-MECHANICAL TREATMENT OF OPTICAL SPECTROSCOPY

We now want to interpret optical spectroscopy in term of quantum mechanics and relate the Lorentz oscillators to interband and intraband transitions. We can write our eigenstates in the absence of light as

$$H_0 = |\mathbf{k}n\rangle = E_{\mathbf{k}n}|\mathbf{k}n\rangle, \quad (299)$$

where  $H_0$  is the Hamiltonian describing the solid and  $E_{\mathbf{k}n}$  are the eigenenergies that describe the electronic structure. We want to study how the solid reacts to light and we therefore add a time-dependent perturbation to the Hamiltonian,

$$H = H_0 + H'(t). \quad (300)$$

The wave function as a function of time can now be found from the time-dependent Schrödinger equation

$$i\hbar \frac{\partial}{\partial t} |\psi(t)\rangle = [H_0 + H'(t)] |\psi(t)\rangle. \quad (301)$$

The question is now, what states are involved in the wavefunction  $|\psi(t)\rangle$ ? We have to make some approximations here. Obviously, we want to include the ground state, which is the Fermi sea, i.e. all the states filled up to the Fermi level following Pauli's principle (we assume that  $T = 0$  K). For the Fermi sea, which we denote by  $|0\rangle$ , we have

$$H_0|0\rangle = E_0|0\rangle \quad \text{with} \quad E_0 = \sum_{E_{\mathbf{k}n} \leq E_F} E_{\mathbf{k}n}. \quad (302)$$

Let us now consider the excited states. To lowest order, the light will create electron-hole pair excitations with respect to the Fermi sea. Let us denote these states by

$$|m\rangle = |\mathbf{k}'n'; \mathbf{k}n\rangle \quad (303)$$

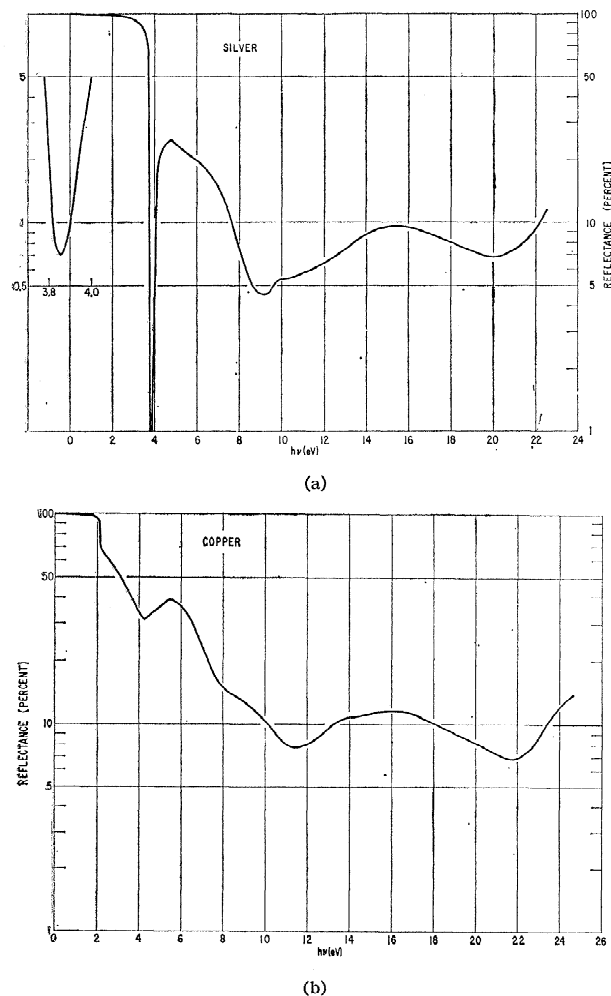


FIG. 60: The reflectance of copper and silver, see Ehrenreich and Philipp, Phys. Rev. **128**, 1622 (1962).

where the state  $|\mathbf{k}'n'; \mathbf{k}n\rangle$  indicates a Fermi sea, but with an electron with wave vector  $\mathbf{k}'$  and band index  $n'$  above the Fermi level and a hole (or missing electron) with wavevector  $\mathbf{k}$  and band index  $n$  below the Fermi level. The energy of this state is given by

$$H_0|m\rangle = E_m|m\rangle = (\hbar\omega_m + E_0)|m\rangle \quad \text{with} \quad \hbar\omega_m = E_{\mathbf{k}'n'} - E_{\mathbf{k}n}. \quad (304)$$

We can now write the time-dependent wavefunction as

$$|\psi(t)\rangle = \sum_m a_m(t) e^{-iE_m t/\hbar} |m\rangle. \quad (305)$$

Inserting this into the Schrödinger equation gives

$$i\hbar \sum_m \left\{ \frac{da_m(t)}{dt} - \frac{i}{\hbar} E_m a(t) \right\} e^{-iE_m t/\hbar} |m\rangle = \sum_m \{E_m + H'(t)\} a_m(t) e^{-iE_m t/\hbar} |m\rangle. \quad (306)$$

We see that the terms with  $E_m$  cancel, giving

$$i\hbar \sum_m \frac{da_m(t)}{dt} e^{-iE_m t/\hbar} |m\rangle = \sum_m H'(t) a_m(t) e^{-iE_m t/\hbar} |m\rangle. \quad (307)$$

We can multiply this on the left by  $\langle m'|e^{iE_m t/\hbar}$ , giving

$$i\hbar \frac{da_{m'}(t)}{dt} = \sum_m \langle m'|H'(t)|m\rangle a_m(t) e^{i(E_{m'} - E_m)t/\hbar}. \quad (308)$$

If we take the system to be initially in the ground state,

$$a_m = \delta_{m,0}, \quad t = 0, \quad (309)$$

we obtain  $E_{m'} - E_m = E_{m'} - E_0 = \hbar\omega_m$ . Using

$$H'_{m'} = \langle m'|H'(t)|0\rangle = \int d\mathbf{r}\varphi_{\mathbf{k}'n'}^* H' \varphi_{\mathbf{k}n}, \quad (310)$$

we can write, in first order approximation theory,

$$i\hbar \frac{da_{m'}(t)}{dt} = H'_{m'} e^{i\omega_{m'}t}. \quad (311)$$

Note that the summation has disappeared since we only consider one transition, from the ground state  $|0\rangle$  to an excited state  $|m'\rangle$ .

So far we have not really specified the perturbation  $H'(t)$ . For a classical oscillator, we can write

$$H'(t) = e\mathbf{E}(t) \cdot \mathbf{r}. \quad (312)$$

We are concerned with the situation that the wavelength of the light is much larger than the dimension of the atom. So we can therefore approximate the electric field by its value at the nucleus. Let us consider monochromatic light with a cosine dependence (we can always express other light in these components),

$$\mathbf{E}(t) = \mathbf{E} \cos \omega t = \frac{1}{2}\mathbf{E}(e^{i\omega t} + e^{-i\omega t}). \quad (313)$$

We can then express

$$H(t) = \frac{1}{2}e\mathbf{E} \cdot \mathbf{r}(e^{i\omega t} + e^{-i\omega t}) \quad \Rightarrow \quad H'_m = \frac{1}{2}e\mathbf{E} \cdot \langle \mathbf{r} \rangle_m (e^{i\omega t} + e^{-i\omega t}), \quad (314)$$

where

$$\langle \mathbf{r} \rangle_m = \langle m|\mathbf{r}|0\rangle = \int d\mathbf{r}\varphi_{\mathbf{k}'n'} r \varphi_{\mathbf{k}n} \quad (315)$$

is the dipole matrix element, which follows the usual dipole selection rules. Let us drop the prime in Eqn. (311) and integrate the time from  $t = 0$  to a particular time  $t$

$$a_m(t) = \frac{1}{i\hbar} \frac{1}{2} e\mathbf{E} \cdot \langle \mathbf{r} \rangle_m \int_0^t dt' [e^{i(\omega_m+\omega)t'} + e^{i(\omega_m-\omega)t'}] \quad (316)$$

$$= \frac{e\mathbf{E} \cdot \langle \mathbf{r} \rangle_m}{2\hbar} \left[ \frac{1 - e^{i(\omega_m+\omega)t}}{\omega_m + \omega} + \frac{1 - e^{i(\omega_m-\omega)t}}{\omega_m - \omega} \right]. \quad (317)$$

We are interested in comparing the classical with the quantum-mechanical dielectric function. We obtained the classical dielectric function by studying the induced dipole moment due to the electric field. Let us consider calculate the induced dipole moment which can be directly related to the expectation value of  $\mathbf{r}$ ,

$$\mathbf{p} = -e\langle \psi(t)|\mathbf{r}|\psi(t)\rangle. \quad (318)$$

However, we just obtained the expression for  $|\psi(t)\rangle$  within first-order perturbation theory. Using this, we have

$$\mathbf{p} = -e \sum_{m,m'} a_{m'}^*(t) a_m(t) \langle m'|\mathbf{r}|m\rangle e^{i(E_{m'}-E_m)t/\hbar}. \quad (319)$$

However, we expect that the coefficients  $a_m$  with  $m \neq 0$  are relatively small. Therefore, the major contributions will come from the terms where either  $m = 0$  or  $m' = 0$ . Renaming one of the dummy arguments gives

$$\mathbf{p} = -e \sum_m [a_m^*(t) \langle m|\mathbf{r}|0\rangle e^{i\omega_m t} + a_m(t) \langle 0|\mathbf{r}|m\rangle e^{-i\omega_m t}] = -e \sum_m [a_m^*(t) \langle \mathbf{r} \rangle_m e^{i\omega_m t} + a_m(t) \langle \mathbf{r} \rangle_m^* e^{-i\omega_m t}] \quad (320)$$

Let us now also assume that the excited states have a finite lifetime. This means that they obtain a complex frequency

$$\omega_m \rightarrow z_m = \omega_m + \frac{i}{2}\Gamma_m, \quad (321)$$

giving a time dependence  $e^{i\omega t - \frac{1}{2}\Gamma_m t}$ , showing a decay of the wavefunction. In the remainder, we neglect the  $m$  dependence of  $\Gamma$ . We are now dealing with terms

$$a_m(t)e^{-iz_m t} = \frac{e\mathbf{E} \cdot \langle \mathbf{r} \rangle_m}{2\hbar} \left[ \frac{e^{-iz_m t} - e^{i\omega t}}{z_m + \omega} + \frac{e^{-iz_m t} - e^{-i\omega t}}{z_m - \omega} \right] \rightarrow -\frac{e\mathbf{E} \cdot \langle \mathbf{r} \rangle_m}{2\hbar} \left[ \frac{e^{i\omega t}}{z_m + \omega} + \frac{e^{-i\omega t}}{z_m - \omega} \right], \quad (322)$$

where in the last step we have used the fact that only the terms with the same frequency as the driving force remain when taking a time average. Let us for simplicity also take the electric field along the  $x$  direction, with  $\mathbf{E} = E\hat{\mathbf{x}}$ . This gives also a dipole moment  $p_x$  along the  $x$  direction. Using  $x_m = \langle m|x|0\rangle$ , we find for the dipole moment

$$p = \sum_m \frac{e^2 E |x_m|^2}{2\hbar} (z_m + z_m^*) \left[ \frac{e^{i\omega t}}{(z_m + \omega)(z_m^* - \omega)} + \frac{e^{-i\omega t}}{(z_m - \omega)(z_m^* + \omega)} \right], \quad (323)$$

where  $z_m + z_m^* = 2\omega_m$  and

$$(z_m \pm \omega)(z_m^* \mp \omega) = (\omega_m + \frac{i}{2}\Gamma \pm \omega)(\omega_m - \frac{i}{2}\Gamma \mp \omega) \quad (324)$$

$$= (\omega_m \pm \omega)(\omega_m \mp \omega) + \frac{i}{2}\Gamma[\omega_m \mp \omega - (\omega_m \pm \omega)] - \frac{1}{4}\Gamma^2 \quad (325)$$

$$= \omega_m^2 - \omega^2 - \frac{1}{4}\Gamma^2 \mp i\Gamma\omega \rightarrow \omega_m^2 - \omega^2 \mp i\Gamma\omega, \quad (326)$$

where in the last step we assumed that the broadening is small relatively to the excitation energy  $\omega_m$ . This gives for the dipole moment

$$p = \sum_m \frac{e^2 E |x_m|^2}{\hbar} \left[ \frac{\omega_m e^{i\omega t}}{\omega_m^2 - \omega^2 - i\Gamma\omega} + \frac{\omega_m e^{-i\omega t}}{\omega_m^2 - \omega^2 + i\Gamma\omega} \right]. \quad (327)$$

The polarization is then given by

$$P = \frac{N}{V} p = \sum_m \frac{2e^2 n |x_m|^2}{\hbar} \left[ \frac{\omega_m(\omega_m^2 - \omega^2)}{(\omega_m^2 - \omega^2)^2 + \Gamma^2 \omega^2} \cos \omega t + \frac{\omega_m \Gamma \omega}{(\omega_m^2 - \omega^2)^2 + \Gamma^2 \omega^2} \sin \omega t \right] E. \quad (328)$$

In order to relate this to the dielectric function, we need to look at the response to a cosine wave. We know that for an electric field  $\mathbf{E} e^{-i\omega t}$ , the polarization is given by  $\mathbf{P} = \chi(\omega)\varepsilon_0\mathbf{E}$ . To construct a cosine, we also need  $\chi(-\omega)$ . From Eqn. (264), we can see that replacing  $\omega$  by  $-\omega$  gives  $\varepsilon(-\omega) = \varepsilon^*(-\omega)$ . We therefore have for a cosine

$$\mathbf{P} = \frac{1}{2}\varepsilon_0 E (\chi e^{-i\omega t} + \chi^* e^{i\omega t}) = \frac{1}{2}\varepsilon_0 E [(\varepsilon_1 - 1)(e^{-i\omega t} + e^{i\omega t}) + i\varepsilon_2(e^{-i\omega t} - e^{i\omega t})] \quad (329)$$

$$= \varepsilon_0(\varepsilon_1 - 1)E \cos \omega t + \varepsilon_0 \varepsilon_2 E \sin \omega t. \quad (330)$$

This means that the cosine term is related to  $\varepsilon_1$ ,

$$\varepsilon_1 = 1 + \sum_m \frac{2e^2 n |x_m|^2}{\varepsilon_0 \hbar} \frac{\omega_m(\omega_m^2 - \omega^2)}{(\omega_m^2 - \omega^2)^2 + \Gamma^2 \omega^2} \quad (331)$$

and the sine term to  $\varepsilon_2$ ,

$$\varepsilon_2 = \sum_m \frac{2e^2 n |x_m|^2}{\varepsilon_0 \hbar} \frac{\omega_m \Gamma \omega}{(\omega_m^2 - \omega^2)^2 + \Gamma^2 \omega^2}. \quad (332)$$

We can also write this in its complex form

$$\varepsilon_r = 1 + \frac{ne^2}{m\varepsilon_0} \sum_m \frac{f_m}{\omega_m^2 - \omega^2 - i\Gamma\omega}, \quad (333)$$

with the oscillator strength given by

$$f_m = \hbar\omega_m \frac{2m}{\hbar^2} |x_m|^2. \quad (334)$$

### XXIII. RELATION TO ABSORPTION

Earlier it was mentioned that  $\varepsilon_2$  was related to absorption. This might not be directly obvious. We are used to relating absorption and emission in terms of Fermi's Golden Rule

$$I(\omega) \sim \sum_m |\langle m|H'|0\rangle|^2 \delta(\omega - \omega_m), \quad (335)$$

where  $I(\omega)$  is the absorption intensity. However, we want to rewrite the  $\delta$ -function. Using

$$-i \int_0^\infty e^{i(\omega - \omega_m)t - \eta t} dt = \frac{1}{\omega - \omega_m + i\eta} = \frac{\omega - \omega_m}{(\omega - \omega_m)^2 + \eta^2} - i \frac{\eta}{(\omega - \omega_m)^2 + \eta^2} \quad (336)$$

Note that the imaginary part works as a  $\delta$ -function in the limit  $\eta \rightarrow 0$ , when it is zero for  $\omega \neq \omega_m$  and  $1/\eta \rightarrow \infty$  for  $\omega = \omega_m$ . The integral over this function, known as a Lorentzian, is equal to  $\pi$ . Normalizing the  $\delta$ -function to unity, we have

$$\delta(\omega - \omega_m) = \frac{1}{\pi} \frac{\eta}{(\omega - \omega_m)^2 + \eta^2} = -\frac{1}{\pi} \text{Im} \frac{1}{\omega - \omega_m + i\eta}. \quad (337)$$

The function  $(\omega - \omega_m + i\eta)^{-1}$  is also known as a Green's function. Therefore we can also write Fermi's golden rule as

$$I(\omega) \sim -\frac{1}{\pi} \sum_m |x_m|^2 \text{Im} \frac{1}{\omega - \omega_m + i\eta} = -\frac{1}{\pi} \sum_m |x_m|^2 \text{Im} \frac{1}{\omega - z_m^*}, \quad (338)$$

where we have used  $x_m = \langle m|H'|0\rangle$ . We can also do the inverse process and emit a photon

$$I(\omega) \sim \sum_m |\langle 0|H'|m\rangle|^2 \delta(\omega_m + \omega). \quad (339)$$

This term requires some closer consideration. The conservation of energy says that we start in an initial state and end up with an excitation with energy  $\hbar\omega_m$  and a photon with energy  $\hbar\omega$ . Since energy is conserved this implies that  $\hbar\omega = -\hbar\omega_m$ . Since the photon energy is always positive, this implies that  $\hbar\omega_m < 0$ . However, we saw before that the  $\hbar\omega_m$  corresponded to an electron-hole pair excitation, which is always positive. However, we can have this term if there are excitations in the initial state, which can be present at finite temperature or due to laser excitations. Then the energy  $\hbar\omega_m$  corresponds to the deexcitation of an electron-hole pair. We can also rewrite this in an integral form

$$i \int_{-\infty}^0 e^{i(\omega_m + \omega)t + \eta t} dt = -\frac{1}{\omega_m + \omega + i\eta} = -\frac{1}{\omega + z_m} \quad (340)$$

This gives for the intensity

$$I(\omega) \sim -\frac{1}{\pi} \sum_m |x_m|^2 \text{Im} \frac{1}{\omega + z_m}, \quad (341)$$

Adding the two terms together gives

$$\frac{1}{\omega - z_m^*} - \frac{1}{z_m + \omega} = -\frac{z_m + z_m^*}{(\omega - z_m^*)(\omega + z_m)}, \quad (342)$$

which reproduces the  $e^{i\omega t}$  term in Eqn. (326).

### XXIV. THOMAS-FERMI SCREENING

As we have seen in the previous sections, the electrons respond to an externally applied electric field. In the same way, one can envision the electron cloud corresponding to the electric field produced by an electron. This is called screening. We can understand screening physically by noting that the electron cloud reacts to the electron and will move as a result of the potential created by the electron. However, in a system in equilibrium we assume that the

chemical potential  $\mu = E_F(\mathbf{r}) - U(\mathbf{r})$  remains constant. Thus the change in potential has to be compensated by a change in number of electrons

$$\frac{dE_F}{dn} \Delta n - U = 0. \quad (343)$$

In a free electron model, the Fermi energy is given by

$$N = 2 \frac{V}{(2\pi)^3} \frac{4}{3} \pi k_F^3 \Rightarrow k_F = (3\pi^2 n)^{1/3} \Rightarrow E_F = \frac{\hbar^2 k_F^2}{2m} = \frac{\hbar^2}{2m} (3\pi n)^{2/3}, \quad (344)$$

giving  $dE_F/dn = \frac{2}{3} E_F/n$ . The induced charge is therefore

$$\rho_{\text{ind}} = e \Delta n = \frac{3}{2} \frac{enU}{E_F} = \frac{3}{2} \frac{e^3 n}{E_F \epsilon_0 q^2} \quad (345)$$

where use has been made of Laplace's equation to calculate the potential from the point charge  $e$ :  $\nabla^2 V = e/\epsilon_0$  (which also follows from Gauss's equation  $\nabla \cdot \mathbf{E} = -e/\epsilon_0$  and  $\mathbf{E} = -\nabla V$ , or in momentum space  $-q^2 V = e/\epsilon_0$  or  $V = -e/\epsilon_0 q^2$ ). The potential energy is then  $U = -eV = e^2/\epsilon_0 q^2$ . An alternative way of obtaining the same result is to make a Fourier transform of the Coulomb potential

$$U(r) = \frac{1}{4\pi\epsilon_0} \frac{e^2}{r}. \quad (346)$$

The use of this alternative way becomes clear in a little while. The Fourier transform gives

$$U_q = \frac{e^2}{4\pi\epsilon_0} \int_0^{2\pi} d\varphi \int_0^\infty dr \int_0^\pi d\theta r^2 \sin\theta e^{iqr \cos\theta} \frac{1}{r} \quad (347)$$

$$= \frac{e^2}{2\epsilon_0} \int_0^\infty dr \int_{-1}^1 d\cos\theta r e^{iqr \cos\theta} = \frac{e^2}{2iq\epsilon_0} \int_0^\infty dr (e^{iqr} - e^{-iqr}) \quad (348)$$

Here we have a small problem with the convergence of the integration. This can be solved by making the oscillation damp out by  $e^{-\lambda r}$ , and in the end take  $\lambda = 0$

$$\begin{aligned} U_q &= \frac{e^2}{2iq\epsilon_0} \int_0^\infty dr (e^{iqr} - e^{-iqr}) e^{-\lambda r} = \frac{e^2}{2iq\epsilon_0} \int_0^\infty dr (e^{i(q+i\lambda)r} - e^{-i(q-i\lambda)r}) = \frac{e^2}{2q\epsilon_0} \left[ \frac{1}{q+i\lambda} + \frac{1}{q-i\lambda} \right] \\ &= \frac{e^2}{\epsilon_0} \frac{1}{q^2 + \lambda^2} \end{aligned} \quad (349)$$

where a  $\lambda$  has been introduced to let the oscillations damp out slowly. In the limit  $\lambda \rightarrow 0$ , we obtain  $U_q = e^2/\epsilon_0 q^2$ .

For the dielectric function we then find

$$\epsilon_r = 1 + \chi = 1 - \frac{\rho_{\text{ind}}}{\rho_{\text{free}}} = 1 - \frac{\rho_{\text{ind}}}{-e} = 1 + \frac{3e^2 n}{2E_F \epsilon_0 q^2} = 1 + \frac{q_{TF}^2}{q^2} \quad (350)$$

with  $q_{TF} = \sqrt{3ne^2/2\epsilon_0 E_F}$ . We therefore find an effective Coulomb potential

$$U_q = \frac{1}{\epsilon} \frac{e^2}{q^2} = \frac{1}{\epsilon + 0} \frac{e^2}{\epsilon_r q^2} = \frac{1}{4\pi\epsilon_0} \frac{e^2}{q^2 + q_{TF}^2}. \quad (351)$$

One might wonder to what potential this corresponds in real space. However, we see that the form is exactly the same as the form obtained in deriving the Fourier transform of the potential. We can therefore write the effective screened potential as

$$U(r) = \frac{1}{4\pi\epsilon_0} \frac{e^2}{r} e^{-q_{TF} r}, \quad (352)$$

which look like a Coulomb potential but with a reduced range.

## XXV. MANY-PARTICLE WAVEFUNCTIONS

In quantum mechanics, particles are indistinguishable. This means that we should be able to interchange two particles without seeing any effect on the probability function. We can distinguish two fundamentally different types of particles, namely those with a symmetric and antisymmetric wavefunction. Under permutation between particle  $i$  and  $j$  for a  $N$  particle wavefunction, one has the following possibilities

$$P_{ij}\psi_{n_1\dots n_N}^{\pm}(\mathbf{r}_1, \dots, \mathbf{r}_i, \dots, \mathbf{r}_j, \dots, \mathbf{r}_N) = \pm\psi_{n_1\dots n_N}^{\pm}(\mathbf{r}_1, \dots, \mathbf{r}_j, \dots, \mathbf{r}_i, \dots, \mathbf{r}_N) \quad (353)$$

where  $k_i$  means that a particle is in a certain quantum state  $n_i$  (for example a particle in a box where the quantum numbers are  $n_i = n_x, n_y, n_z$ , but it could also refer to the quantum numbers of an atom  $n_i = nlm\sigma$ ). At first sight one might think it does not make any difference since the real properties are related to the square of the wavefunction and a plus or minus sign should not make too much of a difference. However, the sign has drastic consequences for the statistics. Let us look at the wavefunction for two particles:

$$\psi_{k_1, k_2}^{\pm}(\mathbf{r}_1, \mathbf{r}_2) = \frac{1}{\sqrt{2}}(\varphi_{k_1}(\mathbf{r}_1)\varphi_{k_2}(\mathbf{r}_2) \pm \varphi_{k_2}(\mathbf{r}_1)\varphi_{k_1}(\mathbf{r}_2)). \quad (354)$$

where  $\phi_k$  are eigenfunctions of the Hamiltonian. The symmetric and antisymmetric wavefunctions give two fundamentally different particles. Particles whose wavefunction is symmetric are bosons, particles with antisymmetric wavefunctions are called fermions. Examples of bosons are photons,  $\pi$  and  $K$  mesons. These are particles with integral spin. Also the harmonic oscillator and lattice vibrations (also known as phonons) behave like a “boson”-like particle. Particles with half integral spin behave like fermions. Examples are electrons, protons, and neutrons. The antisymmetric wavefunctions have a very special characteristic. Let us take two particle in the same quantum state

$$\psi_{k, k}^{-}(\mathbf{r}_1, \mathbf{r}_2) = \frac{1}{\sqrt{2}}(\varphi_k(\mathbf{r}_1)\varphi_k(\mathbf{r}_2) - \varphi_k(\mathbf{r}_1)\varphi_k(\mathbf{r}_2)) = 0. \quad (355)$$

Therefore, it is impossible to have two fermions with the same quantum numbers. Note that the spin is also considered a quantum number. Therefore, we can have two electrons in the same wavefunction (say the same plane wave or the same atomic orbital), but with opposite spins. The occupation of each fermion state is therefore 0 or 1.

Let us now generalize the wavefunctions for an arbitrary number of particles. For bosons the general wavefunction is

$$\Psi_{k_1, \dots, k_N} = \sqrt{\frac{\prod_i n_{k_i}!}{N!}} \sum_P \psi_{k_1}(\mathbf{r}_1) \cdots \psi_{k_N}(\mathbf{r}_N), \quad (356)$$

where the summations runs over all the possible permutations of *different* indices  $k_i$ . This gives the normalization constant.  $n_{k_i}$  indicates how many  $k$ -values are  $k_i$ . Note that the  $\sum_i n_{k_i} = N$ . For two particles with  $S = 0$ , we have

$$\Psi_{k_1, k_2} = \frac{1}{\sqrt{2}} \{ \psi_{k_1}(\mathbf{r}_1)\psi_{k_2}(\mathbf{r}_2) + \psi_{k_2}(\mathbf{r}_1)\psi_{k_1}(\mathbf{r}_2) \}. \quad (357)$$

For  $k_1 = k_2 = k$ , we find

$$\Psi_{k_1, k_2} = \sqrt{\frac{2!}{2!}} \psi_k(\mathbf{r}_1)\psi_k(\mathbf{r}_2) = \psi_k(\mathbf{r}_1)\psi_k(\mathbf{r}_2), \quad (358)$$

using the fact that  $n_k = 2$ . We see that it is possible to put two bosons in the same quantum state. In fact, we can put any arbitrary number of bosons in a particle quantum state. From a statistical point of view, we therefore have for the occupation numbers of a particular quantum state  $i$

$$n_i = 0, 1 \quad \text{fermions} \quad (359)$$

$$n_i = 0, 1, 2, 3, \dots \quad \text{bosons} \quad (360)$$

This is an important aspect that we have to include in our quantum statistics. Up till now the only aspect that we have used is the indistinguishability.

The situation for electrons (and other spin-1/2 particles) is fact a bit more complicated since the total wavefunction, i.e., orbital and spin, has to be asymmetric. This means  $\psi_S(\mathbf{r}_1, \mathbf{r}_2)\xi_A(1, 2)$  or  $\psi_A(\mathbf{r}_1, \mathbf{r}_2)\xi_S(1, 2)$ , where  $\xi(1, 2)$  is the wavefunction for the spin. There are four ways to combine two spins  $\xi_{\uparrow}(1)\xi_{\uparrow}(2)$ ,  $\xi_{\uparrow}(1)\xi_{\downarrow}(2)$ ,  $\xi_{\downarrow}(1)\xi_{\uparrow}(2)$ , and  $\xi_{\downarrow}(1)\xi_{\downarrow}(2)$ .

$\xi_{\uparrow}(1)\xi_{\uparrow}(2)$  and  $\xi_{\downarrow}(1)\xi_{\downarrow}(2)$  are clearly symmetric spin functions, since interchange of the particles does not change the sign of the wave function. These are the  $\xi_{11}(1, 2)$  and  $\xi_{1,-1}(1, 2)$  components of the triplet ( $S = 1$ ). Since  $S_z = 1, 0, -1$  for  $S = 1$ , there should also be a  $S = 0$  component. This can be obtained by using the step operator for the spin

$$S_- \xi_{11} = \sqrt{(1+1)(1-1+1)} \xi_{10} = \sqrt{2} \xi_{10} = \xi_{\uparrow}(1)\xi_{\downarrow}(2) + \xi_{\downarrow}(1)\xi_{\uparrow}(2) \quad (361)$$

$$\Rightarrow \xi_{10} = \frac{1}{\sqrt{2}} [\xi_{\uparrow}(1)\xi_{\downarrow}(2) + \xi_{\downarrow}(1)\xi_{\uparrow}(2)] \quad (362)$$

where we have used

$$S_{\pm} \xi_{S S_z} = \sqrt{(S \mp S_z)(S \pm S_z + 1)} \xi_{S, S_z \pm 1} \quad (363)$$

Note that this is also a symmetric wavefunction. The remaining wave function has to be orthogonal to the previous one

$$\xi_{00}(1, 2) = \frac{1}{\sqrt{2}} [\xi_{\uparrow}(1)\xi_{\downarrow}(2) - \xi_{\downarrow}(1)\xi_{\uparrow}(2)] \quad (364)$$

which is antisymmetric. Since there is only one component (called a singlet), this has to be  $S = 0$ . The four total wavefunctions for two electrons are therefore  $\Psi_{1S_z}(\mathbf{r}_1, \mathbf{r}_2) = \psi_A(\mathbf{r}_1, \mathbf{r}_2)\xi_{1S_z}(1, 2)$  with  $S_z = 1, 0, -1$  and  $\Psi_{00}(\mathbf{r}_1, \mathbf{r}_2) = \psi_S(\mathbf{r}_1, \mathbf{r}_2)\xi_{00}(1, 2)$ . The  $S = 1$  and  $S_z = 1$  is given by

$$\Psi_{11}(\mathbf{r}_1, \mathbf{r}_2) = \psi_A(\mathbf{r}_1, \mathbf{r}_2)\xi_{11}(1, 2) = \frac{1}{\sqrt{2}} [\varphi_{k_1}(\mathbf{r}_1)\varphi_{k_2}(\mathbf{r}_2) - \varphi_{k_2}(\mathbf{r}_1)\varphi_{k_1}(\mathbf{r}_2)] \xi_{\uparrow}(1)\xi_{\uparrow}(2) \quad (365)$$

$$= \frac{1}{\sqrt{2}} [\varphi_{k_1}(\mathbf{r}_1)\xi_{\uparrow}(1)\varphi_{k_2}(\mathbf{r}_2)\xi_{\uparrow}(2) - \varphi_{k_2}(\mathbf{r}_1)\xi_{\uparrow}(1)\varphi_{k_1}(\mathbf{r}_2)\xi_{\uparrow}(2)] \quad (366)$$

$$= \frac{1}{\sqrt{2}} \begin{vmatrix} \varphi_{k_1}(\mathbf{r}_1)\xi_{\uparrow}(1) & \varphi_{k_1}(\mathbf{r}_2)\xi_{\uparrow}(2) \\ \varphi_{k_2}(\mathbf{r}_1)\xi_{\uparrow}(1) & \varphi_{k_2}(\mathbf{r}_2)\xi_{\uparrow}(2) \end{vmatrix} \quad (367)$$

The  $S = 0$  and  $S_z = 0$  wavefunction is given by

$$\Psi_{00}(\mathbf{r}_1, \mathbf{r}_2) = \psi_S(\mathbf{r}_1, \mathbf{r}_2)\xi_{00}(1, 2) = \frac{1}{\sqrt{2}} [\varphi_{k_1}(\mathbf{r}_1)\varphi_{k_2}(\mathbf{r}_2) + \varphi_{k_2}(\mathbf{r}_1)\varphi_{k_1}(\mathbf{r}_2)] \frac{1}{\sqrt{2}} [\xi_{\uparrow}(1)\xi_{\downarrow}(2) - \xi_{\downarrow}(1)\xi_{\uparrow}(2)] \quad (368)$$

$$= \frac{1}{2} [\varphi_{k_1}(\mathbf{r}_1)\xi_{\uparrow}(1)\varphi_{k_2}(\mathbf{r}_2)\xi_{\downarrow}(2) - \varphi_{k_2}(\mathbf{r}_1)\xi_{\downarrow}(1)\varphi_{k_1}(\mathbf{r}_2)\xi_{\uparrow}(2) \quad (369)$$

$$- \varphi_{k_1}(\mathbf{r}_1)\xi_{\downarrow}(1)\varphi_{k_2}(\mathbf{r}_2)\xi_{\uparrow}(2) + \varphi_{k_2}(\mathbf{r}_1)\xi_{\uparrow}(1)\varphi_{k_1}(\mathbf{r}_2)\xi_{\downarrow}(2)] \quad (370)$$

Note that this can also be written as a combination of Slater determinants

$$\Psi_{00}(\mathbf{r}_1, \mathbf{r}_2) = \frac{1}{\sqrt{2}} \left( \frac{1}{\sqrt{2}} \begin{vmatrix} \varphi_{k_1}(\mathbf{r}_1)\xi_{\uparrow}(1) & \varphi_{k_1}(\mathbf{r}_2)\xi_{\uparrow}(2) \\ \varphi_{k_2}(\mathbf{r}_1)\xi_{\downarrow}(1) & \varphi_{k_2}(\mathbf{r}_2)\xi_{\downarrow}(2) \end{vmatrix} - \frac{1}{\sqrt{2}} \begin{vmatrix} \varphi_{k_1}(\mathbf{r}_1)\xi_{\downarrow}(1) & \varphi_{k_1}(\mathbf{r}_2)\xi_{\downarrow}(2) \\ \varphi_{k_2}(\mathbf{r}_1)\xi_{\uparrow}(1) & \varphi_{k_2}(\mathbf{r}_2)\xi_{\uparrow}(2) \end{vmatrix} \right) \quad (371)$$

$$= \frac{1}{\sqrt{2}} [\psi_{k_1\uparrow, k_2\downarrow}(\mathbf{r}_1, \mathbf{r}_2) - \psi_{k_1\downarrow, k_2\uparrow}(\mathbf{r}_1, \mathbf{r}_2)] \quad (372)$$

Note that in general we can built up antisymmetric states from Slater determinants

$$\psi_{k_1\sigma_1, \dots, k_N\sigma_N}(\mathbf{r}_1 \cdots \mathbf{r}_N) = \frac{1}{\sqrt{N!}} \begin{vmatrix} \varphi_{k_1}(\mathbf{r}_1)\xi_{\sigma_1}(1) & \cdots & \varphi_{k_1}(\mathbf{r}_N)\xi_{\sigma_1}(N) \\ \vdots & & \vdots \\ \varphi_{k_N}(\mathbf{r}_1)\xi_{\sigma_N}(1) & \cdots & \varphi_{k_N}(\mathbf{r}_N)\xi_{\sigma_N}(N) \end{vmatrix} \quad (373)$$

where  $\sigma_i = \uparrow, \downarrow$ . As a result of the properties of the determinant, having two columns with the same  $k$  and  $\sigma$  implies that the determinant is zero, just as for the exclusion principle. Interchange of two columns also leads to a change in sign of the determinant, giving us directly the antisymmetry. This is obvious for the  $S_z = 1, -1$  states of the triplet. For the  $S_z = 0$  states, one needs a combination of Slater determinants

$$\Psi_{k_1 k_2, 00} = \frac{1}{\sqrt{2}} (\psi_{k_1\uparrow, k_2\downarrow} - \psi_{k_1\downarrow, k_2\uparrow}) \quad \text{and} \quad \Psi_{k_1 k_2, 10} = \frac{1}{\sqrt{2}} (\psi_{k_1\uparrow, k_2\downarrow} + \psi_{k_1\downarrow, k_2\uparrow}). \quad (374)$$

You may have noticed that dealing with the statistic of many particles using wavefunction is quite cumbersome. This is due to the fact that we have to permute all the different particles (or the different coordinates  $\mathbf{r}_i$  over all the



different wavefunctions. The statistics for fermions and bosons can greatly simplify if we start out with something indistinguishable. This can be done by using operators. You probably remember that the analytical solution of the harmonic oscillator involved the step up/down operators  $a^\dagger$  and  $a$ , which had the relations

$$a^\dagger|n\rangle = \sqrt{n+1}|n+1\rangle \quad \text{and} \quad a|n\rangle = \sqrt{n}|n-1\rangle. \quad (375)$$

Now forget for the moment the relation of  $a^\dagger$  with  $x$  and  $p$ , since this result is far more general. Note that  $a^\dagger$  effectively put adds one to the quantum state, whereas  $a$  removes one from the quantum state. Let us now identify this with bosons.  $a^\dagger$  creates a boson in the quantum state, whereas  $a$  removes a boson from the quantum state. Now the harmonic oscillator is only one quantum state. We can in principle have many different quantum states  $k$  in which we can put bosons. So we can generalize it to

$$a_k^\dagger|n_1, n_2, \dots, n_k, \dots\rangle = \sqrt{n_k+1}|n_1, n_2, \dots, n_k+1, \dots\rangle \quad \text{and} \quad (376)$$

$$a_k|n_1, n_2, \dots, n_k, \dots\rangle = \sqrt{n_k}|n_1, n_2, \dots, n_k-1, \dots\rangle. \quad (377)$$

These operators have some nice characteristics: they are indistinguishable. In addition, they are symmetric. This follows from the generalized commutation relations

$$[a_k, a_{k'}^\dagger] = \delta_{k,k'} \quad \text{and} \quad [a_k^\dagger, a_{k'}^\dagger] = 0 \quad \text{and} \quad [a_k, a_{k'}] = 0 \quad (378)$$

Thus for  $k \neq k'$ , we can write

$$a_k^\dagger a_{k'}^\dagger = a_{k'}^\dagger a_k^\dagger. \quad (379)$$

Therefore, interchange of two particles does not change the sign of the wavefunction.

The wavefunction for a single harmonic oscillator could be written as

$$|n\rangle = \frac{1}{\sqrt{N!}}(a^\dagger)^N|0\rangle. \quad (380)$$

For more than one  $k$  value, we can generalize the wavefunction as

$$|\{n_{k_i}\}\rangle = \frac{1}{\sqrt{\prod_i n_{k_i}}} \prod_i (a_{k_i}^\dagger)^{n_{k_i}} |0\rangle. \quad (381)$$

Let us look at the two-particle wavefunctions. If the two particles are in the same state (i.e. have the same quantum number) then the wavefunction should be similar to that of the harmonic oscillator:

$$|kk\rangle = \frac{1}{\sqrt{2}} a_k^\dagger a_k^\dagger |0\rangle. \quad (382)$$

This wavefunction is now properly normalized since

$$\langle k k | k k \rangle = \frac{1}{2} \langle 0 | a_k a_k a_k^\dagger a_k^\dagger | 0 \rangle = \frac{1}{2} \langle 0 | a_k (1 + a_k^\dagger a_k) a_k^\dagger | 0 \rangle \quad (383)$$

$$= \frac{1}{2} \langle 0 | a_k a_k^\dagger | 0 \rangle + \frac{1}{2} \langle 0 | a_k a_k^\dagger a_k a_k^\dagger | 0 \rangle \quad (384)$$

$$= \frac{1}{2} \langle 0 | (1 + a_k^\dagger a_k) | 0 \rangle + \frac{1}{2} \langle 0 | (1 + a_k^\dagger a_k) (1 + a_k^\dagger a_k) | 0 \rangle = 1 \quad (385)$$

$$(386)$$

since  $a_k|0\rangle = 0$ . For two different wavevectors, we have

$$|k_1 k_2\rangle = a_{k_1}^\dagger a_{k_2}^\dagger |0\rangle. \quad (387)$$

This gives the right normalization since

$$\langle k_1 k_2 | k_1 k_2 \rangle = \langle 0 | a_{k_1} a_{k_2} a_{k_2}^\dagger a_{k_1}^\dagger | 0 \rangle = \langle 0 | a_{k_1} (1 + a_{k_2}^\dagger a_{k_2}) a_{k_1}^\dagger | 0 \rangle = \langle 0 | a_{k_1} a_{k_1}^\dagger | 0 \rangle = \langle 0 | (1 + a_{k_1}^\dagger a_{k_1}) | 0 \rangle = 1 \quad (388)$$

Working with Slater determinants becomes quite elaborate. We can however do the same trick with operators to account for the statistics as with bosons. The operator  $c_k^\dagger$  creates a fermion in a certain quantum state  $k$ , whereas  $c_k$  removes it from this quantum state, i.e.

$$c_k^\dagger|0_k\rangle = |1_k\rangle \quad \text{and} \quad c_k|1_k\rangle = |0_k\rangle, \quad (389)$$

where  $|0_k\rangle$  and  $|1_k\rangle$  denote the states with 0 and 1 electron in quantum state  $k$ , respectively. However, unlike bosons that satisfy commutation relations, fermions satisfy anticommutation relations

$$\{c_k, c_{k'}^\dagger\} = \delta_{k,k'}, \quad \{c_k^\dagger, c_{k'}^\dagger\} = 0, \quad \{c_k, c_{k'}\} = 0, \quad (390)$$

where the term in braces is defined as

$$\{A, B\} = AB + BA. \quad (391)$$

However, we cannot put two particles in the same state, since

$$c_k^\dagger c_k^\dagger |0\rangle = \frac{1}{2} \{c_k^\dagger, c_k^\dagger\} |0\rangle = 0. \quad (392)$$

We can put them in different quantum states, thus for  $k \neq k'$

$$c_k^\dagger c_{k'}^\dagger |0\rangle = -c_{k'}^\dagger c_k^\dagger |0\rangle. \quad (393)$$

Note that the operators directly take care of the antisymmetry of the wavefunctions. Including spin, we can write the wavefunctions  $|k_1 k_2, SS_z\rangle$  for two particles in states labeled with quantum numbers  $k_1$  and  $k_2$  with different spin  $S$  and  $S_z$  as

$$|k_1 k_2, 11\rangle = c_{k_2\uparrow}^\dagger c_{k_1\uparrow}^\dagger |0\rangle, \quad |k_1 k_2, 10\rangle = \frac{1}{\sqrt{2}} (c_{k_2\downarrow}^\dagger c_{k_1\uparrow}^\dagger + c_{k_2\uparrow}^\dagger c_{k_1\downarrow}^\dagger) |0\rangle, \quad |k_1 k_2, 1, -1\rangle = c_{k_2\downarrow}^\dagger c_{k_1\downarrow}^\dagger |0\rangle \quad (394)$$

$$|k_1 k_2, 00\rangle = \frac{1}{\sqrt{2}} (c_{k_2\downarrow}^\dagger c_{k_1\uparrow}^\dagger - c_{k_2\uparrow}^\dagger c_{k_1\downarrow}^\dagger) |0\rangle. \quad (395)$$

In general, we can write the many-body Fermion wavefunction as

$$|\{n_{k_i}\}\rangle = \Pi_i (c_{k_i}^\dagger)^{n_{k_i}} |0\rangle. \quad (396)$$

Note, that the normalization is unity since we can never have more than one fermion in the same quantum state.

Summarizing, we have seen that the a symmetric and antisymmetric wavefunction corresponds to particles with completely different statistics. Bosons have a symmetric wavefunction that allows any number of bosons in a particular quantum state. Fermions have antisymmetric wavefunctions and the occupation numbers are restricted to 0 and 1. We also saw that these statistic can be closely related to operators and their corresponding commutation relationships. Bosons commute, whereas fermions anticommute.

## XXVI. MAGNETISM

From quantum mechanics, we learned that the electrons in an atom can have an orbital moment  $\mathbf{L}$  and a spin  $\mathbf{S}$ . This is not only true for a single electron but also for many electrons on an atom. In addition, we saw that the orbital and spin moment can be coupled through the spin-orbit coupling forming a total momentum  $\mathbf{J}$ . This creates an effective magnetic moment on a site. Magnetism is the phenomenon that the moments are aligned in the solid. This can happen in several ways. First, we can apply a magnetic field which, through its interaction with the orbital and spin moment wants to align the magnetic moments. This is called diamagnetism and paramagnetism. Even more interesting, is the spontaneous alignment of the magnetic moments below a particular temperature. There are several types: ferromagnetism, antiferromagnetism, and ferrimagnetism.

### A. Diamagnetism

Many atoms in a have magnetic moments. However, it is not essential to obtain a magnetization of a solid in a magnetic field. The magnetic field will make the electrons precess in addition to their regular motion. This gives rise to an orbital moment, which is aligned with the magnetic field.

*Classical derivation.*— Classically, the frequency of this precession is given by

$$\omega = \frac{eB}{2m}, \quad (397)$$

where  $B$  is the magnetic field and  $m$  the mass of the electron. (note that this is comparable to the frequency of a sphere around its axis and not that of an electron turning around in circles with a frequency  $eB/m$ , also known as the cyclotron frequency). This frequency should be much lower than the frequency of the original motion in the field of the atom. This is generally satisfied, since atomic potential are a lot stronger than the change in frequency due to the magnetic field.

The rotation causes a current. For an atom with  $Z$  electrons, this gives

$$I = \frac{-Ze}{T} = -Ze \frac{\omega}{2\pi} = -Ze \frac{1}{2\pi} \frac{eB}{2m}. \quad (398)$$

This current in itself creates a magnetic field opposing the externally applied field as in the case of the Biot-Savart law. The magnetic field is proportional to the magnetic moment given by the current times the area of the effective loop

$$\mu = I \times \pi \langle \rho^2 \rangle = -Ze \frac{1}{2\pi} \frac{eB}{2m} \pi \langle \rho^2 \rangle = -\frac{Ze^2 B}{4m} \langle \rho^2 \rangle. \quad (399)$$

Note that  $\langle \rho^2 \rangle$  is the area perpendicular to the magnetic field. Taking the magnetic field along the  $z$ -axis, one has  $\langle \rho^2 \rangle = \langle x^2 \rangle + \langle y^2 \rangle$ . For a uniform charge distribution, this can be related to the radius  $\langle r^2 \rangle = \langle x^2 \rangle + \langle y^2 \rangle + \langle z^2 \rangle = \frac{2}{3} \langle \rho^2 \rangle$  if  $\langle x^2 \rangle = \langle y^2 \rangle = \langle z^2 \rangle$ . This gives for the magnetic moment

$$\mu = -\frac{Ze^2 B}{6m} \langle r^2 \rangle. \quad (400)$$

For a solid with  $N$  equivalent atoms, the total magnetization is given by  $\mathbf{M} = N\boldsymbol{\mu}$ .

We see that the induced magnetic moment is directly proportional to the magnetic field. It is therefore useful to define a susceptibility

$$\chi = \frac{\mu_0 M}{B}, \quad (401)$$

where  $\mu_0 = 4\pi \times 10^{-7}$  N/A<sup>2</sup> is the magnetic constant or the permeability of vacuum. For diamagnetism, one has

$$\chi = \frac{N\boldsymbol{\mu}}{B} = -\frac{NZ\mu_0 e^2}{6m} \langle r^2 \rangle. \quad (402)$$

This is the classical Langevin result.

In general, the magnetization does not have to be linearly proportional to the magnetic field and we need to define the susceptibility as

$$\chi = \mu_0 \frac{\partial M}{\partial B}. \quad (403)$$

The susceptibility is a typical response function. It demonstrates how much the magnetization changes due to a change in the magnetic field.

*Quantum-mechanical derivation.*— We can include the effect of the magnetic field by replacing the momentum by

$$\mathbf{p} \rightarrow \mathbf{p} + e\mathbf{A}. \quad (404)$$

$\mathbf{A}$  is the vector potential and the magnetic field is given by  $\mathbf{B} = \nabla \times \mathbf{A}$ . The kinetic part of the Hamiltonian then becomes

$$H\psi \frac{(\mathbf{p} + e\mathbf{A})^2}{2m} \psi = \frac{\mathbf{p}^2}{2m} \psi + \frac{e}{2m} (\mathbf{p} \cdot \mathbf{A} + \mathbf{A} \cdot \mathbf{p}) \psi + \frac{e^2 \mathbf{A}^2}{2m} \psi. \quad (405)$$

The first term is the kinetic energy in the absence of a vector potential. The second term describes the interaction between the electron and the vector potential. In general, we cannot take these two terms together since  $\mathbf{p}$  is acting on both the wavefunction  $\psi$  and the vector potential  $\mathbf{A}$ . We can take them together if we use the Lorentz gauge for which  $\nabla \cdot \mathbf{A} = 0$ . The last term describes the scattering of the vector potential. Let us consider the case of a uniform magnetic field along the  $z$  direction. The vector field is then

$$A_x = -\frac{1}{2}yB_z \quad \text{and} \quad A_y = \frac{1}{2}xB_z \quad \text{and} \quad A_z = 0. \quad (406)$$

This vector potential satisfies the Lorentz gauge. The only nonzero component is then

$$B_z = (\nabla \times \mathbf{A})_z = \frac{\partial A_y}{\partial x} - \frac{\partial A_x}{\partial y} = B_z, \quad (407)$$

as it should be. We can then write

$$\frac{e}{m} \mathbf{A} \cdot \mathbf{p} + \frac{e^2 \mathbf{A}^2}{2m} = \frac{-i\hbar e B_z}{2m} \left( x \frac{\partial}{\partial y} - y \frac{\partial}{\partial x} \right) + \frac{e^2 B_z^2}{8m} (x^2 + y^2). \quad (408)$$

The second term gives a change in energy

$$E' = \frac{e^2 B_z^2}{8m} (\langle x^2 \rangle + \langle y^2 \rangle) = \frac{e^2 B_z^2}{12m} \langle r^2 \rangle, \quad (409)$$

using the same relation as used earlier for a homogenous charge distribution. The magnetic moment is given by

$$\boldsymbol{\mu} = \frac{\partial E'}{\partial B} = \frac{e^2 \langle r^2 \rangle}{6m} B_z, \quad (410)$$

which reproduces the classical Langevin result.

## B. Paramagnetism

The first term can be rewritten as

$$\frac{-i\hbar e B_z}{2m} \left( x \frac{\partial}{\partial y} - y \frac{\partial}{\partial x} \right) = \frac{e\hbar}{2m} L_z B_z = \mu_B (\mathbf{L} \cdot \mathbf{B})_z, \quad (411)$$

where  $\mu_B = e\hbar/2m$  is the Bohr magneton. The angular momentum is defined as dimensionless (as opposed to the often-used definition of units of  $\hbar$ ).

Let us consider the simple example of two electrons in a  $p$  shell. The different electron configurations are shown in Table ???. We use the notation for a configuration  $(m^\pm m'^\pm)$ , where the  $\pm$  indicates  $\sigma = \pm \frac{1}{2}$ . For the Coulomb interaction  $L, M_L, S$ , and  $M_S$  are good quantum numbers. The different terms can be found by looking at the extreme  $M_L$  and  $M_S$ . The configuration  $(1^+1^-)$  belongs to the term with  $L = 2$  and  $S = 0$ . This is denoted by  ${}^1D$  (say singlet  $D$ ). The letter indicates the value of  $L$ , which corresponds to the notation. The different values for  $l$  are often denoted by

$$\begin{array}{cccccc} L : & 0 & 1 & 2 & 3 & 4 \\ & S & P & D & F & G \end{array} \quad (412)$$

The superscript is  $2S + 1$ . Note that the  ${}^1D$  term appears in the configurations with  $M_L = 2, \dots, -2$  and  $M_S = 0$ . This energy level is  $(2L + 1)(2S + 1)$  fold degenerate. The configuration  $(1^+0^+)$  belongs to a  ${}^3P$  term (say triplet  $P$ ). Then there is only one term unaccounted for with  $M_L = M_S = 0$ , i.e., a  ${}^1S$ .

The diagonal matrix elements are given by

$$\sum_k [c^k(lm, lm)c^k(l'm', l'm')F^k - \delta_{\sigma\sigma'}(c^k(lm, l'm'))^2 G^k], \quad (413)$$

where for  $p^2$ , we have  $l = l' = 1$ . For  ${}^1D$ , we find

$$E({}^1D) = E(1^+1^-) = \sum_k (c^k(11, 11))^2 F^k = F^0 + \frac{1}{25} F^2, \quad (414)$$

where the values of  $c^k$  are given in Table ???. In the case of  ${}^3P$ , there is also an exchange contribution

$$\begin{aligned} E({}^3P) = E(1^+0^+) &= \sum_k [c^k(11, 11)c^k(10, 10)F^k - (c^k(11, 10))^2 G^k] \\ &= F^0 - \frac{2}{25} F^2 - (0G^0 + \frac{3}{25} G^2) = F^0 - \frac{5}{25} F^2, \end{aligned} \quad (415)$$

where use has been made of the fact that within one shell  $G^k = F^k$ . The energy of the  $^1S$  term cannot be calculated this way. However, here we can make use of the fact that the sum of the diagonal energies is unchanged when transforming from our basis set into the  $LS$  states,

$$E(1^+ - 1^-) + E(1^- - 1^+) + E(0^+0^-) = 2 \sum_k c^k(11, 11)c^k(1-1, 1-1)F^k + \sum_k c^k(10, 10)F^k \quad (416)$$

$$= 2(F^0 + \frac{1}{25}F^2) + F^0 + \frac{4}{25}F^2 \quad (417)$$

$$= E(^1S) + E(^3P) + E(^1D) = E(^1S) + \frac{2}{25}F^0 - \frac{4}{25}F^2,$$

which gives  $E(^1S) = F^0 + \frac{10}{25}F^2$ .

Generally, one finds that for electrons in one shell the lowest term is the one with first, the highest spin multiplicity, and, secondly, the highest orbital multiplicity. In the case of  $p^2$ , the  $^3P$  term. This can be understood by noting that for the highest spin electrons have to occupy different orbitals, therefore reducing the Coulomb interaction. The same applies, in a more complicated manner for the angular momentum.

Thus we find in general that that

$$^2P \otimes ^2P = ^{1,3}D + ^{1,3}P + ^{1,3}S \quad (418)$$

giving a total degeneracy of  $1 \times 5 + 3 \times 5 + 1 \times 3 + 3 \times 3 + 1 \times 1 + 3 \times 1 = 36$ , which is equal to  $6 \times 6$ . This would be the case for two electrons in different  $p$  shells, i.e.  $pp$ . However, for  $p^2$ , the Pauli exclusion principle states that electrons cannot be in the same orbital. This makes matters a bit more complicated. We can easily see that  $^3D$  is forbidden, since this would require a configuration  $(1^+1^+)$ . We know that the total number of configurations is 15. So we still have 10 left. The other terms are 3, 9, 3, and 1 fold degenerate. Apparently the only way to make 10 is to take the  $^3P$  and the  $^1S$  configurations, being 9 and 1-fold degenerate.

## XXVII. FERROMAGNETISM

??

## XXVIII. ANTIFERROMAGNETISM

??

## XXIX. PHONONS

Although this is the most convenient way to obtain the dispersion, it is often useful to derive this in a different fashion. Let us consider again the Hamiltonian.

$$H = \sum_n \frac{\mathbf{P}_{\mathbf{R}_n}^2}{2M} + V(\mathbf{r}_{\mathbf{R}_1}, \dots, \mathbf{r}_{\mathbf{R}_N}), \quad (419)$$

TABLE II: Different configurations for  $p^2$ .

$p^2$	$M_S = 1$	0	-1
$M_L = 2$		$(1^+1^-)$	
1	$(1^+0^+)$	$(1^+0^-)(1^-0^+)$	$(1^-0^-)$
0	$(1^+ - 1^+)$	$(1^+ - 1^-)(1^- - 1^+)(0^+0^-)$	$(1^- - 1^-)$
-1	$(0^+ - 1^+)$	$(0^+ - 1^-)(0^- - 1^+)$	$(0^- - 1^-)$
-2		$(-1^+ - 1^-)$	

where  $\mathbf{r}_{\mathbf{R}_n}$  and  $\mathbf{p}_{\mathbf{R}_n}$  are the position and momentum, respectively, of the  $n$ 'th atom. We can expand the potential in a Taylor series around the equilibrium positions  $\mathbf{r}_{\mathbf{R}_n} = 0$ ,

$$V(\mathbf{r}_{\mathbf{R}_1}, \dots, \mathbf{r}_{\mathbf{R}_N}) = V(0, 0, \dots) + \sum_{\mathbf{R}} \mathbf{r}_{\mathbf{R}} \cdot \nabla_{\mathbf{R}} V|_{\{\mathbf{r}_n=0\}} + \frac{1}{2} \sum_{\mathbf{R}, \mathbf{R}'} (\mathbf{r}_{\mathbf{R}'} \cdot \nabla_{\mathbf{R}'}) (\mathbf{r}_{\mathbf{R}} \cdot \nabla_{\mathbf{R}}) V + \dots \quad (420)$$

The first term is a simple shift of the energy, which we can ignore. The second term contains

$$\nabla_{\mathbf{R}} V = \frac{\partial V}{\partial x_{\mathbf{R}}} \hat{\mathbf{x}} + \frac{\partial V}{\partial y_{\mathbf{R}}} \hat{\mathbf{y}} + \frac{\partial V}{\partial z_{\mathbf{R}}} \hat{\mathbf{z}} \quad (421)$$

is zero, since we have taken  $\mathbf{r}_{\mathbf{R}} = 0$  as the equilibrium position, i.e.  $V$  is in a minimum. The third term is a sum over second partial derivatives

$$\sum_{\mathbf{R}, \mathbf{R}'} (\mathbf{r}_{\mathbf{R}'} \cdot \nabla_{\mathbf{R}'}) (\mathbf{r}_{\mathbf{R}} \cdot \nabla_{\mathbf{R}}) V = \sum_{\mathbf{R}, \mathbf{R}'} \sum_{\alpha, \alpha' = x, y, z} \alpha_{\mathbf{R}'} \frac{\partial^2 V}{\partial \alpha_{\mathbf{R}'} \partial \alpha_{\mathbf{R}}} \alpha_{\mathbf{R}}. \quad (422)$$

When we denote  $V_{\mathbf{R}'\mathbf{R}}^{\alpha'\alpha} = \partial^2 V / \partial \alpha_{\mathbf{R}'} \partial \alpha_{\mathbf{R}}$ , we can also write this in matrix form

$$V = \frac{1}{2} \sum_{\mathbf{R}, \mathbf{R}'} \mathbf{r}_{\mathbf{R}'}^T V_{\mathbf{R}'\mathbf{R}} \mathbf{r}_{\mathbf{R}} = \frac{1}{2} \sum_{\mathbf{R}, \mathbf{R}'} (x_{\mathbf{R}'}, y_{\mathbf{R}'}, z_{\mathbf{R}'}) \begin{pmatrix} V_{\mathbf{R}'\mathbf{R}}^{xx} & V_{\mathbf{R}'\mathbf{R}}^{xy} & V_{\mathbf{R}'\mathbf{R}}^{xz} \\ V_{\mathbf{R}'\mathbf{R}}^{yx} & V_{\mathbf{R}'\mathbf{R}}^{yy} & V_{\mathbf{R}'\mathbf{R}}^{yz} \\ V_{\mathbf{R}'\mathbf{R}}^{zx} & V_{\mathbf{R}'\mathbf{R}}^{zy} & V_{\mathbf{R}'\mathbf{R}}^{zz} \end{pmatrix} \begin{pmatrix} x_{\mathbf{R}} \\ y_{\mathbf{R}} \\ z_{\mathbf{R}} \end{pmatrix}. \quad (423)$$

Since we are dealing with a crystal, we obviously do not want to stay in real space, but make a Fourier transform over the positions of the nuclei in the solid to momentum space

$$\mathbf{r}_{\mathbf{R}} = \frac{1}{\sqrt{N}} \sum_{\mathbf{q}} e^{i\mathbf{q} \cdot \mathbf{R}} \mathbf{r}_{\mathbf{q}} \quad \text{and} \quad \mathbf{p}_{\mathbf{R}} = \frac{1}{\sqrt{N}} \sum_{\mathbf{q}} e^{-i\mathbf{q} \cdot \mathbf{R}} \mathbf{p}_{\mathbf{q}}. \quad (424)$$

The Hamiltonian then becomes

$$H = \sum_{\mathbf{q}} \frac{\mathbf{p}_{\mathbf{q}}^\dagger \mathbf{p}_{\mathbf{q}}}{2M} + \frac{1}{2} \sum_{\mathbf{q}} \mathbf{r}_{\mathbf{q}}^\dagger V_{\mathbf{q}} \mathbf{r}_{\mathbf{q}}, \quad (425)$$

where  $\mathbf{r}_{\mathbf{q}}$  is a complex number so we need to take  $\mathbf{r}_{\mathbf{q}}^\dagger$  as opposed to simply transposing it. The interaction matrix is now given by

$$V_{\mathbf{q}} = \begin{pmatrix} V_{\mathbf{q}}^{xx} & V_{\mathbf{q}}^{xy} & V_{\mathbf{q}}^{xz} \\ V_{\mathbf{q}}^{yx} & V_{\mathbf{q}}^{yy} & V_{\mathbf{q}}^{yz} \\ V_{\mathbf{q}}^{zx} & V_{\mathbf{q}}^{zy} & V_{\mathbf{q}}^{zz} \end{pmatrix}. \quad (426)$$

Note that whereas there are cross terms  $V_{\mathbf{R}'\mathbf{R}}$  in real space (giving a double sum of  $\mathbf{R}$  and  $\mathbf{R}'$ ), the interaction is diagonal in  $\mathbf{q}$ , since it only depends on the  $\mathbf{R} - \mathbf{R}'$ ,

$$V_{\mathbf{q}}^{\alpha'\alpha} = \sum_{\delta'} e^{-i\mathbf{q} \cdot \delta} V_{\mathbf{R}+\delta, \mathbf{R}}^{\alpha'\alpha}, \quad (427)$$

where  $\delta$  runs over the lattice sites around the site  $\mathbf{R}$ . Note that this is equivalent for each site  $\mathbf{R}$ . Let us go back to one dimension, to see what our next step is in solving the problem. In one dimension, the Fourier transform of the Hamiltonian

$$H = \sum_{\mathbf{R}} \frac{p_{\mathbf{R}}^2}{2M} + \sum_{\mathbf{R}\mathbf{R}'} V_{\mathbf{R}'\mathbf{R}} x_{\mathbf{R}'} x_{\mathbf{R}}, \quad (428)$$

with  $V_{\mathbf{R}'\mathbf{R}} = \frac{\partial^2 V}{\partial x_{\mathbf{R}'} \partial x_{\mathbf{R}}}$ , becomes

$$H = \sum_{\mathbf{q}} \left[ \frac{p_{\mathbf{q}}^\dagger p_{\mathbf{q}}}{2M} + \frac{1}{2} m \omega_{\mathbf{q}}^2 x_{\mathbf{q}}^\dagger x_{\mathbf{q}} \right], \quad (429)$$

with

$$\omega_q = \sqrt{\frac{V_q}{M}} \quad \text{with} \quad V_q = \sum_{\delta} e^{-iq\delta} V_{R+\delta,R}, \quad (430)$$

and the Fourier transforms

$$x_R = \frac{1}{\sqrt{N}} \sum_q e^{iqR} x_q \quad \text{and} \quad p_R = \frac{1}{\sqrt{N}} \sum_q e^{-iqR} p_q \quad \text{or, inversely} \quad x_q = \frac{1}{\sqrt{N}} \sum_R e^{-iqR} x_R \quad \text{and} \quad p_q = \frac{1}{\sqrt{N}} \sum_R e^{iqR} p_R$$

However, apart from the summation over  $q$ , we readily recognize Eqn. (429) as the Hamiltonian for a harmonic oscillator. We can diagonalize this by introducing the operators

$$a_q = \frac{1}{\sqrt{2M\hbar\omega_q}} (M\omega_q x_R + ip_q^\dagger) \quad \text{and} \quad a_q^\dagger = \frac{1}{\sqrt{2M\hbar\omega_q}} (M\omega_q x_R^\dagger - ip_q), \quad (431)$$

leading to

$$H = \sum_q \hbar\omega_q \left( a_q^\dagger a_q + \frac{1}{2} \right). \quad (432)$$

We would now like to determine the value of  $\omega_q$ . Let us consider only nearest-neighbor interactions. The interaction is then

$$V = \sum_R \frac{1}{2} K (x_R - x_{R+a})^2 = \sum_R K (x_R^2 - x_R x_{R+a}) = K \sum_R x_R^2 - \frac{K}{2} \sum_R \sum_{\delta=\pm a} x_{R+\delta} x_R \quad (433)$$

Since this should be equivalent to  $V = \frac{1}{2} \sum_{RR'} V_{RR'} x_{R'} x_R$ , we have  $V_{RR} = 2K$ ,  $V_{R\pm a,R} = -K$ , and  $V_{R'R} = 0$  for  $|R - R'| \geq 2a$ . The Fourier transform is then

$$V_q = \sum_{\delta} e^{-iq\delta} V_{R+\delta,R} = 2K - K(e^{-iqa} + e^{iqa}) = 2K(1 - \cos qa) = 4K \sin^2 \frac{qa}{2}, \quad (434)$$

and

$$\omega_q = \sqrt{\frac{V_q}{M}} = 2\sqrt{\frac{K}{M}} \sin \frac{qa}{2} = \omega_m \sin \frac{qa}{2}, \quad (435)$$

with  $\omega_m = \sqrt{\frac{K}{M}}$ . reproducing the result at the beginning of the chapter. We can also express the position and momentum in terms of the step operators

$$x_q = \sqrt{\frac{\hbar}{2M\omega_q}} (a_{-q}^\dagger + a_q) \quad \text{and} \quad p_q = i\sqrt{\frac{2M\omega_q}{\hbar}} (a_q^\dagger - a_{-q}), \quad (436)$$

making use of the relations  $x_q^\dagger = x_{-q}$  and  $p_q^\dagger = p_{-q}$  and  $\omega_q = \omega_{-q}$ .

Let us now return to three dimensions, where life is complicated by the fact that the interaction between the nuclei is now a matrix, see Eqn. (426). However, we can turn this effectively into three independent one-dimensional problems by diagonalizing  $V_{\mathbf{q}}$ . This gives three eigenvalues  $V_{\mathbf{q}}^s$ . There are three mutually perpendicular eigenvectors. We can write those as unit vectors  $\hat{\mathbf{e}}_1$ ,  $\hat{\mathbf{e}}_2$ , and  $\hat{\mathbf{e}}_3$  in real space. These vectors are known as polarization vectors. The direction of these vectors depend on the wavevectors which we omit here. If one of the polarization vectors is parallel to  $\mathbf{q}$  then there are longitudinally polarized phonons. Since the other two vectors are orthogonal, we also have two transversely polarized phonons. However, this usually only occurs when  $\mathbf{q}$  is along certain symmetry direction in the crystal. Equation (425) then becomes

$$H = \sum_{\mathbf{q}s} \left[ \frac{p_{\mathbf{q}s}^\dagger p_{\mathbf{q}s}}{2M} + \frac{1}{2} V_{\mathbf{q}}^s r_{\mathbf{q}s}^\dagger r_{\mathbf{q}s} \right], \quad (437)$$

where the subscript  $s$  indicated that we are dealing with the component along a particular polarization vectors, i.e.  $r_{\mathbf{q}s} = \mathbf{r}_{\mathbf{q}s} \cdot \hat{\mathbf{e}}_s$  and  $p_{\mathbf{q}s} = \mathbf{p}_{\mathbf{q}s} \cdot \hat{\mathbf{e}}_s$ . The frequencies are given by

$$\omega_{\mathbf{q}s} = \sqrt{\frac{V_{\mathbf{q}}^s}{M}}. \quad (438)$$

The step operators are given by

$$a_{\mathbf{q}s} = \frac{1}{\sqrt{2M\hbar\omega_{\mathbf{q}s}}}(M\omega_{\mathbf{q}s}\mathbf{r}_{\mathbf{q}} + i\mathbf{p}_{\mathbf{q}}) \cdot \hat{\mathbf{e}}_s \quad (439)$$

$$a_{\mathbf{q}s}^\dagger = \frac{1}{\sqrt{2M\hbar\omega_{\mathbf{q}s}}}(M\omega_{\mathbf{q}s}\mathbf{r}_{\mathbf{q}} - i\mathbf{p}_{\mathbf{q}}) \cdot \hat{\mathbf{e}}_s \quad (440)$$

leading to the Hamiltonian

$$H = \sum_{\mathbf{q}s} \hbar\omega_{\mathbf{q}s} (a_{\mathbf{q}s}^\dagger a_{\mathbf{q}s} + \frac{1}{2}). \quad (441)$$

### XXX. ELECTRON-PHONON INTERACTION

In this section, we discuss the electron phonon interaction. The electrons are treated as a simple electron gas feeling the potential of the nuclei. The unperturbed Hamiltonian is given by

$$H = \sum_{\mathbf{k}} \varepsilon_{\mathbf{k}} c_{\mathbf{k}}^\dagger c_{\mathbf{k}} + \sum_{\mathbf{q}s} \hbar\omega_{\mathbf{q}s} a_{\mathbf{q}s}^\dagger a_{\mathbf{q}s}. \quad (442)$$

We then add the potential of the atoms. Unlike what we considered before (as in the free-electron model), the nuclei. We assume that the potential of the ion depends only on the distance from the equilibrium position of the ion. The periodic potential is then described in second quantization as

$$H_U = \frac{1}{N} \sum_{\mathbf{k}\mathbf{k}'\mathbf{R}} \langle \mathbf{k}' | U(\mathbf{r} - \mathbf{R} - \mathbf{r}_{\mathbf{R}}) | \mathbf{k} \rangle c_{\mathbf{k}}^\dagger c_{\mathbf{k}} \quad (443)$$

$$= \frac{1}{N} \sum_{\mathbf{k}\mathbf{q}\mathbf{R}} e^{-i\mathbf{q} \cdot (\mathbf{R} + \mathbf{r}_{\mathbf{R}})} U_{\mathbf{q}} c_{\mathbf{k}+\mathbf{q}}^\dagger c_{\mathbf{k}} \quad (444)$$

with  $\mathbf{q} = \mathbf{k}' - \mathbf{k}$ . We assume that the displacements  $\mathbf{r}_{\mathbf{R}}$  from the equilibrium positions are small so that we can write

$$e^{-i\mathbf{q} \cdot \mathbf{r}_{\mathbf{R}}} = 1 - i\mathbf{q} \cdot \mathbf{r}_{\mathbf{R}}. \quad (445)$$

The first term gives the Bloch periodic potential

$$U = \frac{1}{N} \sum_{\mathbf{k}\mathbf{k}'\mathbf{R}} e^{-i\mathbf{q} \cdot \mathbf{R}} U_{\mathbf{q}} c_{\mathbf{k}+\mathbf{q}}^\dagger c_{\mathbf{k}} \quad (446)$$

$$U = \sum_{\mathbf{k}\mathbf{K}} U_{\mathbf{K}} c_{\mathbf{k}+\mathbf{K}}^\dagger c_{\mathbf{k}} \quad (447)$$

$$(448)$$

The second term gives the electron-phonon interaction

$$H_{ep} = -i \frac{1}{N} \sum_{\mathbf{k}\mathbf{q}\mathbf{R}} e^{-i\mathbf{q} \cdot \mathbf{R}} \mathbf{q} \cdot \mathbf{r}_{\mathbf{R}} U_{\mathbf{q}} c_{\mathbf{k}+\mathbf{q}}^\dagger c_{\mathbf{k}} = -i \frac{1}{N} \sum_{\mathbf{k}\mathbf{q}\mathbf{R}} e^{-i\mathbf{q} \cdot \mathbf{R}} \frac{1}{\sqrt{N}} \sum_{\mathbf{q}'} e^{i\mathbf{q}' \cdot \mathbf{R}} \mathbf{q} \cdot \mathbf{r}_{\mathbf{q}'} U_{\mathbf{q}} c_{\mathbf{k}+\mathbf{q}}^\dagger c_{\mathbf{k}} \quad (449)$$

$$= -i \frac{1}{\sqrt{N}} \frac{1}{N} \sum_{\mathbf{k}\mathbf{q}\mathbf{q}'\mathbf{R}} e^{-i(\mathbf{q}-\mathbf{q}') \cdot \mathbf{R}} \mathbf{q} \cdot \mathbf{r}_{\mathbf{q}'} U_{\mathbf{q}} c_{\mathbf{k}+\mathbf{q}}^\dagger c_{\mathbf{k}} \quad (450)$$

$$= -i \frac{1}{\sqrt{N}} \sum_{\mathbf{k}\mathbf{q}} \mathbf{q} \cdot \mathbf{r}_{\mathbf{q}} U_{\mathbf{q}} c_{\mathbf{k}+\mathbf{q}}^\dagger c_{\mathbf{k}}. \quad (451)$$



Expressing the displacement in creation and annihilation operators using

$$\mathbf{r}_{\mathbf{q}} = \sum_s \sqrt{\frac{\hbar}{2M\omega_{\mathbf{q}}}} (a_{-\mathbf{q}s}^\dagger + a_{\mathbf{q}s}) \hat{\mathbf{e}}_s \quad (452)$$

gives

$$H_{ep} = -i \sum_{\mathbf{k}\mathbf{q}s} \sqrt{\frac{\hbar}{2NM\omega_{\mathbf{q}s}}} \mathbf{q} \cdot \hat{\mathbf{e}}_s U_{\mathbf{q}} (a_{-\mathbf{q}s}^\dagger + a_{\mathbf{q}s}) c_{\mathbf{k}+\mathbf{q}}^\dagger c_{\mathbf{k}}. \quad (453)$$

For simplicity, we shall assume that the phonon spectrum is isotropic. This implies that phonons are either longitudinally or transversely polarized. In that case, only the longitudinal phonon with the polarization vector parallel to the wavevector contribute. In the following, we will also neglect the effects of the periodic potential  $U$ . We are then left with the Fröhlich Hamiltonian

$$H = \sum_{\mathbf{k}} \varepsilon_{\mathbf{k}} c_{\mathbf{k}}^\dagger c_{\mathbf{k}} + \sum_{\mathbf{q}} \hbar\omega_{\mathbf{q}} c_{\mathbf{q}}^\dagger c_{\mathbf{q}} + \sum_{\mathbf{k}\mathbf{q}} M_{\mathbf{q}} (a_{-\mathbf{q}}^\dagger + a_{\mathbf{q}}) c_{\mathbf{k}+\mathbf{q}}^\dagger c_{\mathbf{k}}, \quad (454)$$

where the matrix element is given by

$$M_{\mathbf{q}} = i \sum_{\mathbf{k}\mathbf{q}s} \sqrt{\frac{\hbar}{2NM\omega_{\mathbf{q}}}} q U_{\mathbf{q}}. \quad (455)$$

The Hamiltonian consists of two components. In one case,  $a_{\mathbf{q}} c_{\mathbf{k}+\mathbf{q}}^\dagger c_{\mathbf{k}}$ , the electron is scattered by the absorption of a phonon with momentum  $\mathbf{q}$ , in the other case,  $a_{-\mathbf{q}}^\dagger c_{\mathbf{k}+\mathbf{q}}^\dagger c_{\mathbf{k}}$  the electron is scattered by emission of a phonon with momentum  $-\mathbf{q}$ . Note that the total momentum of the creation operators equals that of the annihilation operators (in principle, they could differ by a reciprocal lattice vector  $\mathbf{K}$  but we will neglect this and reduce everything to the first Brillouin zone). We now want to consider the change of the ground state energy due to the presence of electron-phonon interactions. This will modify the excitation spectra and even result in an effective attractive interaction between the electrons mediated by the phonons.

Let us study the change in total energy up to second-order perturbation theory, this gives

$$E = E_0 + \langle \Phi | H_{ep} | \Phi \rangle + \langle \Phi | H_{ep} \frac{1}{E_0 - H_0} H_{ep} | \Phi \rangle, \quad (456)$$

where  $|\Phi\rangle$  is the unperturbed state characterized by the occupation numbers  $n_{\mathbf{q}}$  for phonons and  $n_{\mathbf{k}}$  for electrons. Since  $H_{ep}$  involves the creation or annihilation of a phonon, the first term is zero. The second term gives

$$E_2 = \langle \Phi | \sum_{\mathbf{k}\mathbf{q}} M_{\mathbf{q}} (a_{-\mathbf{q}}^\dagger + a_{\mathbf{q}}) c_{\mathbf{k}+\mathbf{q}}^\dagger c_{\mathbf{k}} \frac{1}{E_0 - H_0} \sum_{\mathbf{k}'\mathbf{q}'} M_{\mathbf{q}'} (a_{-\mathbf{q}'}^\dagger + a_{\mathbf{q}'}) c_{\mathbf{k}'+\mathbf{q}'}^\dagger c_{\mathbf{k}'} | \Phi \rangle. \quad (457)$$

Since we start with the state  $|\Phi\rangle$  and end with the same state, the  $H_{ep}$ 's have to cancel each others excitations. This is achieved for  $\mathbf{q}' = -\mathbf{q}$ . The terms that remain

$$E_2 = \sum_{\mathbf{k}\mathbf{q}} |M_{\mathbf{q}}|^2 \left[ \langle \Phi | a_{-\mathbf{q}}^\dagger c_{\mathbf{k}}^\dagger c_{\mathbf{k}-\mathbf{q}} \frac{1}{E_0 - H_0} a_{-\mathbf{q}} c_{\mathbf{k}-\mathbf{q}}^\dagger c_{\mathbf{k}} | \Phi \rangle + \langle \Phi | a_{\mathbf{q}} c_{\mathbf{k}}^\dagger c_{\mathbf{k}-\mathbf{q}} \frac{1}{E_0 - H_0} a_{\mathbf{q}}^\dagger c_{\mathbf{k}-\mathbf{q}}^\dagger c_{\mathbf{k}} | \Phi \rangle \right]. \quad (458)$$

We see that the combinations of creation and annihilation operators form number operators  $n_{\mathbf{k}} = c_{\mathbf{k}}^\dagger c_{\mathbf{k}}$ . Note that  $c_{\mathbf{k}} c_{\mathbf{k}}^\dagger = 1 - n_{\mathbf{k}}$ . It is also straightforward to obtain the difference in energy between the excited state and  $E_0$ . This leads to the expression

$$E_2 = \sum_{\mathbf{k}\mathbf{q}} |M_{\mathbf{q}}|^2 \langle n_{\mathbf{k}} (1 - n_{\mathbf{k}-\mathbf{q}}) \rangle \left[ \frac{\langle n_{-\mathbf{q}} \rangle}{\varepsilon_{\mathbf{k}} - \varepsilon_{\mathbf{k}-\mathbf{q}} + \hbar\omega_{-\mathbf{q}}} + \frac{\langle n_{\mathbf{q}} + 1 \rangle}{\varepsilon_{\mathbf{k}} - \varepsilon_{\mathbf{k}-\mathbf{q}} - \hbar\omega_{\mathbf{q}}} \right], \quad (459)$$

where  $\langle \dots \rangle$  gives the expectation value. Since we considered an isotropic system, we can assume that  $\omega_{\mathbf{q}} = \omega_{-\mathbf{q}}$  and  $\langle n_{\mathbf{q}} \rangle = \langle n_{-\mathbf{q}} \rangle$ . The second term in the above equation can be split into two terms. We then obtain

$$E_2 = \sum_{\mathbf{k}\mathbf{q}} |M_{\mathbf{q}}|^2 \langle n_{\mathbf{k}} (1 - n_{\mathbf{k}-\mathbf{q}}) \rangle \left[ \frac{2(\varepsilon_{\mathbf{k}} - \varepsilon_{\mathbf{k}-\mathbf{q}}) \langle n_{\mathbf{q}} \rangle}{(\varepsilon_{\mathbf{k}} - \varepsilon_{\mathbf{k}-\mathbf{q}})^2 - (\hbar\omega_{\mathbf{q}})^2} + \frac{1}{\varepsilon_{\mathbf{k}} - \varepsilon_{\mathbf{k}-\mathbf{q}} - \hbar\omega_{\mathbf{q}}} \right], \quad (460)$$

FIG. 61: Schematic plot of the Kohn anomaly. The energy is given by  $E = q + \alpha \ln \sqrt{(1 - 2q/k_F)^2 + \gamma^2}$  with  $\alpha = 0.1$  and  $\gamma = 0.03$ . In the absence of electron-phonon interactions, the phonon energy would be a straight line  $E = q$ . The presence of these interactions gives rise to an anomaly around  $q/k_F = 2$ .

The total energy is given by  $E_0 + E_2$ . Note that the phonon part of the ground state energy can be given  $\sum_{\mathbf{q}} \hbar\omega_{\mathbf{q}} \langle n_{\mathbf{q}} \rangle$ . We can find the change in the phonon energy due to the electron-phonon interaction by determining the change in energy with respect to a change in the phonon occupation number  $n_{\mathbf{q}}$ , giving

$$\hbar\omega'_{\mathbf{q}} = \frac{\partial}{\partial \langle n_{\mathbf{q}} \rangle} (E_0 + E_2) = \hbar\omega_{\mathbf{q}} + \sum_{\mathbf{k}} |M_{\mathbf{q}}|^2 \frac{2 \langle n_{\mathbf{k}} (1 - n_{\mathbf{k}-\mathbf{q}}) \rangle (\varepsilon_{\mathbf{k}} - \varepsilon_{\mathbf{k}-\mathbf{q}})}{(\varepsilon_{\mathbf{k}} - \varepsilon_{\mathbf{k}-\mathbf{q}})^2 - (\hbar\omega_{\mathbf{q}})^2} \quad (461)$$

Since phonon energies are generally small, let us have a look at this result when we neglect  $\hbar\omega_{\mathbf{q}}$  in the denominator:

$$\hbar\omega'_{\mathbf{q}} = \hbar\omega_{\mathbf{q}} + \sum_{\mathbf{k}} |M_{\mathbf{q}}|^2 \frac{2 \langle n_{\mathbf{k}} (1 - n_{\mathbf{k}-\mathbf{q}}) \rangle}{\varepsilon_{\mathbf{k}} - \varepsilon_{\mathbf{k}-\mathbf{q}}}. \quad (462)$$

We can interpret this expression as follows. A phonon will be absorbed under the creation of an electron-hole pair with energy  $\varepsilon_{\mathbf{k}} - \varepsilon_{\mathbf{k}-\mathbf{q}}$ . The electron-hole pair is then annihilated under the emission of a phonon. We expect the largest change in the phonon energy to occur when the energy of the electron-hole pair approaches zero. Let us suppose that  $\mathbf{q}$  is in the  $x$  direction. An electron-hole pair of zero energy can be created by scattering across the Fermi surface with  $q = 2k_F$ . Integrating over  $\mathbf{k}$  leads to a logarithmic divergence. This leads to an infinite group velocity of the phonons, known as the Kohn anomaly.

Let us try to make a very simple of the Kohn anomaly and assume a one-dimensional system with a band with a linear dispersion. Obviously, this is not very realistic, but the underlying idea is that the presence of an anomaly should not depend too much on the details of the electronic structure. The dispersion is then given by  $\varepsilon_k = \alpha|k|$ . We are interested in what happens if the energy of the electron-hole pair is close to zero. This occurs for scattering from  $-k_F$  to  $k_F$ , i.e. for  $q = 2k_F$ . Let us consider scattering from negative  $k$ -values to positive  $k$  values (the other way will be equivalent). An electron at  $-k$  (with  $k > 0$ ) scatters to  $q - k$ . We have to be careful with the integration. When  $k_F < q < 2k_F$ , not all  $q$ -values give allowed transitions due to the Fermi-Dirac distribution. At  $T = 0$ , the maximum allowed value is  $q - k_F$ . The integration over momentum then becomes

$$\int_0^{q-k_F} dk \frac{1}{\alpha(q-k) - \alpha k} = \frac{1}{\alpha} \int_0^{q-k_F} dk \frac{1}{q-2k} = \ln(q - 2(q - k_F)) - \ln q = \ln\left(\frac{2k_F}{q} - 1\right) \quad (463)$$

For  $q > 2k_F$ , we can always scatter from the negative  $k$  values to positive  $k$  values. The maximum  $k$  value is then  $k_F$ , since we cannot remove electrons from above the Fermi level. For  $q > 2k_F$ , the momentum is always sufficiently large to scatter the electrons and the upper bound is given by  $k_F$

$$\frac{1}{\alpha} \int_0^{k_F} dk \frac{1}{q-2k} = \ln(q - 2k_F) - \ln q = \ln\left(\frac{1 - 2k_F}{q}\right). \quad (464)$$

We can combine the two result, giving

$$\hbar\omega'_{\mathbf{q}} = \hbar\omega'_{\mathbf{q}} + \text{const} \times \ln \left| 1 - \frac{2k_F}{q} \right| \quad (465)$$

where the constant defines the strength of the interaction. We clearly see the Kohn anomaly at  $q = 2k_F$ . Figure 61 shows a schematic picture of the Kohn anomaly. A broadening  $\gamma$  of the divergence has been included by using

$$\hbar\omega'_{\mathbf{q}} = \hbar\omega'_{\mathbf{q}} + \text{const} \times \ln \sqrt{\left(1 - \frac{2k_F}{q}\right)^2 + \gamma^2}. \quad (466)$$

We can also do it the other way around and look at the change in electron energies due to the phonons. This can be obtained by calculating the change in energy due to a change in electron occupation of the electron state with momentum  $\mathbf{k}$  in Eqn. (459). For simplicity, we assume that we are at low temperatures where the number of phonons

is small, i.e.  $\langle n_{\mathbf{q}} \rangle$ . This gives

$$\varepsilon'_{\mathbf{k}} = \frac{\partial}{\partial \langle n_{\mathbf{k}} \rangle} (E_0 + E_2) \quad (467)$$

$$= \frac{\partial}{\partial \langle n_{\mathbf{k}} \rangle} \left[ \sum_{\mathbf{k}} \varepsilon_{\mathbf{k}} \langle n_{\mathbf{k}} \rangle + \sum_{\mathbf{k}\mathbf{k}'} |M_{\mathbf{k}'-\mathbf{k}}|^2 \langle n_{\mathbf{k}}(1-n_{\mathbf{k}'}) \rangle \frac{1}{\varepsilon_{\mathbf{k}} - \varepsilon_{\mathbf{k}'} - \hbar\omega_{\mathbf{q}}} \right] \quad (468)$$

$$= \varepsilon_{\mathbf{k}} + \sum_{\mathbf{k}'} |M_{\mathbf{k}'-\mathbf{k}}|^2 \left[ \frac{1 - \langle n_{\mathbf{k}'} \rangle}{\varepsilon_{\mathbf{k}} - \varepsilon_{\mathbf{k}'} - \hbar\omega_{\mathbf{q}}} - \frac{\langle n_{\mathbf{k}'} \rangle}{\varepsilon_{\mathbf{k}'} - \varepsilon_{\mathbf{k}} - \hbar\omega_{\mathbf{q}}} \right], \quad (469)$$

where  $\mathbf{q} = \mathbf{k}' - \mathbf{k}$  and the momenta  $\mathbf{k}$  and  $\mathbf{k}'$  have been interchanged in the second term.

$$\varepsilon'_{\mathbf{k}} = \varepsilon_{\mathbf{k}} + \sum_{\mathbf{q}} |M_{\mathbf{q}}|^2 \left[ \frac{1}{\varepsilon_{\mathbf{k}} - \varepsilon_{\mathbf{k}+\mathbf{q}} - \hbar\omega_{\mathbf{q}}} - \frac{2\hbar\omega_{\mathbf{q}} \langle n_{\mathbf{k}+\mathbf{q}} \rangle}{(\varepsilon_{\mathbf{k}+\mathbf{q}} - \varepsilon_{\mathbf{k}})^2 - (\hbar\omega_{\mathbf{q}})^2} \right]. \quad (470)$$

The first term is independent of  $\langle n_{\mathbf{k}+\mathbf{q}} \rangle$ . We can see it as a single electron moving around in a lattice. It will create phonons while scattering temporarily to a different state  $\mathbf{k} + \mathbf{q}$ . It will then reabsorb the phonon. Effectively, the electron is moving around with a phonon cloud around it. This cloud will increase the effective mass of the particle. This interaction can be very strong. We only treat it up to second-order perturbation. One can imagine that the electron can emit more than one phonon at the time. The electron plus its accompanying phonon cloud is known as a polaron. The name arises from the contraction of the lattice around the negatively-charged electron leading to a polarization of the lattice.

The second term gives the change in the energy of the electron due to the presence of the other electrons. This term gives a change in the group velocity of the electron. Note that for a free electron, the group velocity is given by

$$\hbar\mathbf{v}_{\mathbf{k}}^0 = \frac{\partial}{\partial \mathbf{k}} \varepsilon_{\mathbf{k}} = \frac{\partial}{\partial \mathbf{k}} \frac{\hbar^2 \mathbf{k}^2}{2m} = \hbar \frac{\hbar \mathbf{k}}{m} = \hbar \frac{\mathbf{p}}{m}. \quad (471)$$

Taking the first and third term in  $\varepsilon_{\mathbf{k}'}$  and differentiating with respect to  $\mathbf{k}$  gives

$$\hbar\mathbf{v}_{\mathbf{k}} = \frac{\partial \varepsilon'_{\mathbf{k}}}{\partial \mathbf{k}} = \frac{\partial \varepsilon'_{\mathbf{k}}}{\partial \varepsilon_{\mathbf{k}}} \frac{\partial \varepsilon_{\mathbf{k}}}{\partial \mathbf{k}} \quad (472)$$

$$= \frac{\partial \varepsilon_{\mathbf{k}}}{\partial \mathbf{k}} \left[ 1 - \frac{\partial}{\partial \varepsilon_{\mathbf{k}}} \sum_{\mathbf{q}} |M_{\mathbf{q}}|^2 \frac{2\hbar\omega_{\mathbf{q}} \langle n_{\mathbf{k}+\mathbf{q}} \rangle}{(\varepsilon_{\mathbf{k}+\mathbf{q}} - \varepsilon_{\mathbf{k}})^2 - (\hbar\omega_{\mathbf{q}})^2} \right]. \quad (473)$$

We now argue that the major contribution in the summation comes from the derivative of fast variation of  $\langle n_{\mathbf{k}+\mathbf{q}} \rangle$  around the Fermi energy  $E_F$ . We replace the summation by an integration and approximate  $M_{\mathbf{q}}$  and  $\omega_{\mathbf{q}}$  by their averages  $\bar{M}$  and  $\bar{\omega}$ . For the density of states, we take the value at  $E_F$ . This gives

$$\hbar\mathbf{v}_{\mathbf{k}} \cong \hbar\mathbf{v}_{\mathbf{k}}^0 \left[ 1 - 2\hbar\bar{\omega}\rho(E_F)|\bar{M}|^2 \frac{d}{d\varepsilon_{\mathbf{k}}} \int \frac{\langle n(E) \rangle}{(\varepsilon_{\mathbf{k}} - E)^2 - (\hbar\bar{\omega})^2} dE \right]. \quad (474)$$

At low temperatures the occupation number is a step function and its derivative is therefore a  $\delta$ -function at the Fermi energy

$$\frac{d\langle n(E) \rangle}{d\varepsilon_{\mathbf{k}}} = -\delta(E - E_F), \quad (475)$$

where the minus arises from the fact that  $n(E)$  goes from 1 to 0.

$$\hbar\mathbf{v}_{\mathbf{k}} \cong \hbar\mathbf{v}_{\mathbf{k}}^0 \left[ 1 + \frac{2\hbar\bar{\omega}\rho(E_F)|\bar{M}|^2}{(\varepsilon_{\mathbf{k}} - E_F)^2 - (\hbar\bar{\omega})^2} \right]. \quad (476)$$

The infinities around  $\varepsilon_{\mathbf{k}} = E_F \pm \hbar\bar{\omega}$  are a spurious result of our averaging procedure. We are often more interested in how the group velocity around the Fermi level is affected by the interaction of the electron with the phonons. For  $\varepsilon_{\mathbf{k}} = E_F$ , we have

$$\mathbf{v}_{\mathbf{k}} = \mathbf{v}_{\mathbf{k}}^0 (1 - \alpha), \quad (477)$$

with

$$\alpha = \frac{2\rho(E_F)|\bar{M}|^2}{\hbar\bar{\omega}}. \quad (478)$$

An alternative way to look at it is by trying to reexpress  $\varepsilon_{\mathbf{k}'}$  as an effective free-electron dispersion

$$\mathbf{v}_{\mathbf{k}} = \frac{\hbar\mathbf{k}}{m^*} = \mathbf{v}_{\mathbf{k}}^0(1 - \alpha) = \frac{\hbar\mathbf{k}}{m}(1 - \alpha), \quad (479)$$

giving an effective mass of

$$m^* = \frac{m}{1 - \alpha}. \quad (480)$$

The electron-phonon interaction therefore gives a mass enhancement.

### XXXI. ATTRACTIVE POTENTIAL

We now want to see if there is an effective attractive potential between electrons. We therefore look for a term proportional to  $\langle n_{\mathbf{k}}n_{\mathbf{k}-\mathbf{q}} \rangle$  in Eqn. (459). Originally, we had ascribed this term to the scattering of an electron under the emission of a phonon, followed by the recapturing of the phonon by the same electron. We want to reinterpret this term as the interaction between two electrons through the mediation of a phonon. We can write the term proportional to  $\langle n_{\mathbf{k}}n_{\mathbf{k}-\mathbf{q}} \rangle$  in the limit  $\langle n_{\mathbf{q}} \rangle \rightarrow 0$  as

$$E_c = - \sum_{\mathbf{k}\mathbf{q}} |M_{\mathbf{q}}|^2 \frac{\langle n_{\mathbf{k}}n_{\mathbf{k}-\mathbf{q}} \rangle}{\varepsilon_{\mathbf{k}} - \varepsilon_{\mathbf{k}-\mathbf{q}} - \hbar\omega_{\mathbf{q}}} \quad (481)$$

We can rewrite this by splitting up the summation and relabeling the second summation

$$E_c = -\frac{1}{2} \sum_{\mathbf{k}\mathbf{q}} |M_{\mathbf{q}}|^2 \frac{\langle n_{\mathbf{k}}n_{\mathbf{k}-\mathbf{q}} \rangle}{\varepsilon_{\mathbf{k}} - \varepsilon_{\mathbf{k}-\mathbf{q}} - \hbar\omega_{\mathbf{q}}} - \frac{1}{2} \sum_{\mathbf{k}\mathbf{q}} |M_{\mathbf{q}}|^2 \frac{\langle n_{\mathbf{k}-\mathbf{q}}n_{\mathbf{k}} \rangle}{\varepsilon_{\mathbf{k}-\mathbf{q}} - \varepsilon_{\mathbf{k}} - \hbar\omega_{-\mathbf{q}}} \quad (482)$$

$$= \frac{1}{2} \sum_{\mathbf{k}\mathbf{q}} |M_{\mathbf{q}}|^2 \frac{2\hbar\omega_{\mathbf{q}}}{(\varepsilon_{\mathbf{k}-\mathbf{q}} - \varepsilon_{\mathbf{k}})^2 - \hbar\omega_{\mathbf{q}}} \langle -n_{\mathbf{k}}n_{\mathbf{k}-\mathbf{q}} \rangle, \quad (483)$$

where we have used  $\omega_{-\mathbf{q}} = \omega_{\mathbf{q}}$ . If we define

$$V_{\mathbf{q}} = |M_{\mathbf{q}}|^2 \frac{2\hbar\omega_{\mathbf{q}}}{(\varepsilon_{\mathbf{k}-\mathbf{q}} - \varepsilon_{\mathbf{k}})^2 - \hbar\omega_{\mathbf{q}}}, \quad (484)$$

we obtain an effective interaction

$$V = \frac{1}{2} \sum_{\mathbf{k}\mathbf{q}} V_{\mathbf{q}} \langle -n_{\mathbf{k}}n_{\mathbf{k}-\mathbf{q}} \rangle. \quad (485)$$

In general, we can write interaction between two particles as

$$V = \sum_{\mathbf{k}\mathbf{k}'\mathbf{q}} V_{\mathbf{q}} c_{\mathbf{k}+\mathbf{q}}^\dagger c_{\mathbf{k}'-\mathbf{q}}^\dagger c_{\mathbf{k}'} c_{\mathbf{k}}. \quad (486)$$

We can distinguish two contributions that are nonzero working on a Fermi sphere. We can take  $\mathbf{q} = 0$ .

$$V = \frac{1}{2} \sum_{\mathbf{k}\mathbf{k}'} V_{\mathbf{q}} \langle n_{\mathbf{k}}n_{\mathbf{k}'} \rangle. \quad (487)$$

This is called the Hartree or direct terms. If  $V_{\mathbf{q}}$  was a Coulomb interaction this would correspond to the interaction of the electrons with each other. Another possibility is that  $\mathbf{k} = \mathbf{k}' - \mathbf{q}$

$$V = \frac{1}{2} \sum_{\mathbf{k}'\mathbf{q}} V_{\mathbf{q}} \langle c_{\mathbf{k}'}^\dagger c_{\mathbf{k}'-\mathbf{q}}^\dagger c_{\mathbf{k}'} c_{\mathbf{k}'-\mathbf{q}} \rangle = -\frac{1}{2} \sum_{\mathbf{k}\mathbf{q}} V_{\mathbf{q}} \langle c_{\mathbf{k}}^\dagger c_{\mathbf{k}} c_{\mathbf{k}-\mathbf{q}}^\dagger c_{\mathbf{k}-\mathbf{q}} \rangle = \frac{1}{2} \sum_{\mathbf{k}\mathbf{q}} V_{\mathbf{q}} \langle -n_{\mathbf{k}}n_{\mathbf{k}-\mathbf{q}} \rangle, \quad (488)$$

where the prime has been dropped on the right-hand side. Although usually the electron energies are significantly larger than the phonon energies, it is always possible to find values for which  $|\varepsilon_{\mathbf{k}-\mathbf{q}} - \varepsilon_{\mathbf{k}}| < \hbar\omega_{\mathbf{q}}$ . This means that the matrix element is negative. Although a negative matrix element in momentum space does not always guarantee a negative interaction in real space, it does offer the possibility of an attractive interaction.

We can also obtain the attractive interaction by performing a canonical transformation on the Fröhlich Hamiltonian.

*Intermezzo: canonical transformation.*— We want to derive the effective interaction with a canonical transformation. Let us first review what a canonical transformation was. Let us consider a displaced harmonic oscillator

$$H = H_0 + H_{e-p} = \hbar\omega a^\dagger a + M(a^\dagger + a), \quad (489)$$

where we call the second term  $H_{e-p}$  to draw the parallel with the electron-phonon interaction. Note that this Hamiltonian has similarities with the one we are considering. We can diagonalize this by taking displaced operators

$$A = a + \lambda \quad \text{and} \quad A^\dagger = a^\dagger + \lambda. \quad (490)$$

We can then write

$$\hbar\omega A^\dagger A = \hbar\omega a^\dagger + \hbar\omega\lambda(a^\dagger + a) + \hbar\omega\lambda^2. \quad (491)$$

This means we can write our Hamiltonian as

$$H = \hbar\omega A^\dagger A - \Delta, \quad (492)$$

using  $M = \hbar\omega\lambda$  or  $\lambda = M/\hbar\omega$  this gives  $\Delta = \hbar\omega\lambda^2 = M^2/\hbar\omega$  for the shift in energy. In order to treat a more complicated Hamiltonian, we want to take a more systematic approach using a canonical transformation. We are looking for a transformation of the form

$$H' = e^{-S} H e^S, \quad (493)$$

that will eliminate  $H_{e-p}$  to lowest order. Expanding the exponentials gives

$$H' = (1 - S + \frac{1}{2}S^2 - \dots)H(1 + S + \frac{1}{2}S^2 + \dots) \quad (494)$$

$$= H_0 + H_{e-p} + [H_0, S] + [H_{e-p}, S] + \frac{1}{2}[[H_0, S], S] + \dots \quad (495)$$

We neglect the higher-order terms and choose  $S$  such that the commutator with  $H_0$  cancels  $H_{e-p}$ . If we achieve that, we end up with

$$H' = H_0 + [H_{e-p}, S] \dots \quad (496)$$

Let us try  $S$  of the form using

$$S = \lambda(a - a^\dagger). \quad (497)$$

We can now make a unitary transformation of  $a^\dagger a$ ,

$$[a^\dagger a, S] = \lambda[a^\dagger a, a] - \lambda[a^\dagger a, a] \quad (498)$$

$$= \lambda(a^\dagger a a - a a^\dagger a) - \lambda(a^\dagger a a^\dagger - a^\dagger a^\dagger a) \quad (499)$$

$$= \lambda[a^\dagger, a]a - \lambda a^\dagger[a, a^\dagger] \quad (500)$$

$$= -\lambda(a + a^\dagger) \quad (501)$$

The idea for solving the electron-phonon interaction is very similar, except now we have  $\mathbf{k}$  dependence and  $M$  is no longer a simple constant, but contains  $c^\dagger c$  operators. However, in the end we want to look at the final change in electron energy, which is proportional to  $M^2$  which would then become a  $c^\dagger c^\dagger c c$  term, which is an effective electron-electron interaction. We write

$$H = H_0 + H_{e-p}. \quad (502)$$

Now since

$$H_0 = \sum_{\mathbf{k}} \varepsilon_{\mathbf{k}} c_{\mathbf{k}}^\dagger c_{\mathbf{k}} + \sum_{\mathbf{q}} \hbar\omega_{\mathbf{q}} a_{\mathbf{q}}^\dagger a_{\mathbf{q}} \quad (503)$$

and

$$H' = \sum_{\mathbf{k}\mathbf{q}} M_{\mathbf{q}}(a_{-\mathbf{q}}^\dagger + a_{\mathbf{q}})c_{\mathbf{k}+\mathbf{q}}^\dagger c_{\mathbf{k}} \quad (504)$$

we try

$$S = \sum_{\mathbf{k}\mathbf{q}} M_{\mathbf{q}}(Aa_{-\mathbf{q}}^\dagger + Ba_{\mathbf{q}})c_{\mathbf{k}+\mathbf{q}}^\dagger c_{\mathbf{k}}. \quad (505)$$

In order to obtain

$$H_{e-p} + [H_0, S] = 0, \quad (506)$$

we need

$$A = -\frac{1}{\varepsilon_{\mathbf{k}-\mathbf{q}} - \varepsilon_{\mathbf{k}} + \hbar\omega_{-\mathbf{q}}} \quad \text{and} \quad B = -\frac{1}{\varepsilon_{\mathbf{k}-\mathbf{q}} - \varepsilon_{\mathbf{k}} - \hbar\omega_{\mathbf{q}}}. \quad (507)$$

This can be seen by working the relation on the ground state  $|E_0\rangle$ . Let us consider the term with  $A$ , which gives

$$(H_0S - SH_0)|E_0\rangle = \sum_{\mathbf{k}\mathbf{q}} M_{\mathbf{q}}A(H_0a_{-\mathbf{q}}^\dagger c_{\mathbf{k}+\mathbf{q}}^\dagger c_{\mathbf{k}} - a_{-\mathbf{q}}^\dagger c_{\mathbf{k}+\mathbf{q}}^\dagger c_{\mathbf{k}}H_0)|E_0\rangle \quad (508)$$

$$= \sum_{\mathbf{k}\mathbf{q}} M_{\mathbf{q}}A(E_0 + \varepsilon_{\mathbf{k}-\mathbf{q}} - \varepsilon_{\mathbf{k}} + \hbar\omega_{-\mathbf{q}} - E_0)a_{-\mathbf{q}}^\dagger c_{\mathbf{k}+\mathbf{q}}^\dagger c_{\mathbf{k}}|E_0\rangle \quad (509)$$

$$= -\sum_{\mathbf{k}\mathbf{q}} M_{\mathbf{q}}a_{-\mathbf{q}}^\dagger c_{\mathbf{k}+\mathbf{q}}^\dagger c_{\mathbf{k}}|E_0\rangle, \quad (510)$$

where in the last step we have used the value of  $A$ . Combined with the term with  $B$ , this will cancel  $H_{e-p}$ .

The transformed Hamiltonian then becomes

$$H' = H_0 - \frac{1}{2} \left[ \sum_{\mathbf{k}\mathbf{q}} M_{\mathbf{q}}(a_{-\mathbf{q}}^\dagger + a_{\mathbf{q}})c_{\mathbf{k}+\mathbf{q}}^\dagger c_{\mathbf{k}}, \sum_{\mathbf{k}\mathbf{q}} M_{\mathbf{q}} \left( \frac{a_{-\mathbf{q}}^\dagger}{\varepsilon_{\mathbf{k}-\mathbf{q}} - \varepsilon_{\mathbf{k}} + \hbar\omega_{-\mathbf{q}}} + \frac{a_{\mathbf{q}}}{\varepsilon_{\mathbf{k}-\mathbf{q}} - \varepsilon_{\mathbf{k}} - \hbar\omega_{\mathbf{q}}} \right) c_{\mathbf{k}+\mathbf{q}}^\dagger c_{\mathbf{k}} \right]. \quad (511)$$

Of the many terms in the Hamiltonian we pay special attention to those that arise from commuting the phonon operators. This gives the effective Hamiltonian

$$H' = H_0 + \sum_{\mathbf{k}\mathbf{q}} |M_{\mathbf{q}}|^2 \frac{\hbar\omega_{\mathbf{q}}}{(\varepsilon_{\mathbf{k}} - \varepsilon_{\mathbf{k}-\mathbf{q}}) - (\hbar\omega_{\mathbf{q}})^2} c_{\mathbf{k}-\mathbf{q}}^\dagger c_{\mathbf{k}}^\dagger c_{\mathbf{k}-\mathbf{q}} c_{\mathbf{k}}. \quad (512)$$

## XXXII. SUPERCONDUCTIVITY AND THE BCS HAMILTONIAN

Although the possibility of an attractive interaction between electrons is exciting, that it leads to such a surprising phenomena as superconductivity is really startling. At most temperatures, conventional superconductors (i.e., not high-temperature superconductors such as the cuprates) behave pretty much like normal metals. At the transition temperature  $T_c$ , the materials undergoes a phase transition which the spectacular effect that the resistivity goes to zero. In addition, there is a discontinuity in the specific heat. Below  $T_c$ , it has a dependence  $e^{-\Delta/k_B T}$ , thereby providing an indication of an energy gap  $\Delta$  in the excitation spectra. One also observes that magnetic fields are expelled from the superconductor. This is known as the Meissner effect and can be used to levitate the superconductor.

Since the discovery of superconductivity in 1911 by Heike Kamerlingh Onnes, physicists have been looking for an origin of the effect. Convincing evidence that the electron-phonon interaction is involved came from the discovery of the isotope effect, where it was found that the critical temperature depended on the mass of the nuclei. Our starting point is a Hamiltonian that includes the attractive interaction described in the preceding section

$$H = H_0 + \sum_{\mathbf{k}\mathbf{k}'\mathbf{q}\sigma\sigma'} W_{\mathbf{k}\mathbf{q}} c_{\mathbf{k}-\mathbf{q},\sigma}^\dagger c_{\mathbf{k}\sigma'}^\dagger c_{\mathbf{k}-\mathbf{q},\sigma'} c_{\mathbf{k}\sigma}, \quad (513)$$

where  $H_0$  describes the Hamiltonian in the absence of electron-phonon interactions,  $\sigma, \sigma' = \pm\frac{1}{2} = \uparrow, \downarrow$  is the spin. The matrix element is given by

$$W_{\mathbf{k}\mathbf{q}} = |M_{\mathbf{q}}|^2 \frac{\hbar\omega_{\mathbf{q}}}{(\varepsilon_{\mathbf{k}} - \varepsilon_{\mathbf{k}-\mathbf{q}}) - (\hbar\omega_{\mathbf{q}})^2}. \quad (514)$$

We will not solve this problem according to the methods of Bardeen, Cooper, and Schrieffer who used a variational technique. We follow the method of Bogoliubov. Bogoliubov's assumption was that the condensate should have zero momentum. This implies that the electrons that couple with each other have opposite momentum, directly giving  $\mathbf{q} = 2\mathbf{k}$ . We shall also assume that  $\sigma' = -\sigma$ . It can be shown (which we will not do) that the ground state for opposite spins (singlet pairing) is in fact lower in energy than the ground state for parallel spins (triplet pairing). This leads to the effective Hamiltonian

$$H_{\text{BCS}} = \sum_{\mathbf{k}\sigma} \varepsilon_{\mathbf{k}} c_{\mathbf{k}\sigma}^\dagger c_{\mathbf{k}\sigma} - \sum_{\mathbf{k}\mathbf{k}'} V_{\mathbf{k}\mathbf{k}'} c_{\mathbf{k}'\uparrow}^\dagger c_{-\mathbf{k}'\downarrow}^\dagger c_{-\mathbf{k}\downarrow} c_{\mathbf{k}\uparrow}, \quad (515)$$

Where we have taken  $V_{\mathbf{k}\mathbf{k}'} = -2W_{\mathbf{k},\mathbf{k}'-\mathbf{k}}$ , i.e. the interaction is attractive when  $V_{\mathbf{k}}$  is positive. The factor 2 comes from the summation over  $\sigma$ .

We will now look for effective operators that help diagonalize the Hamiltonian. The operators suggested by Bogoliubov are

$$\gamma_{\mathbf{k}\uparrow} = u_{\mathbf{k}} c_{\mathbf{k}\uparrow} - v_{\mathbf{k}} c_{-\mathbf{k}\downarrow}^\dagger \quad \text{and} \quad \gamma_{-\mathbf{k}\downarrow} = u_{\mathbf{k}} c_{-\mathbf{k}\downarrow} + v_{\mathbf{k}} c_{\mathbf{k}\uparrow}^\dagger, \quad (516)$$

with conjugates

$$\gamma_{\mathbf{k}\uparrow}^\dagger = u_{\mathbf{k}} c_{\mathbf{k}\uparrow}^\dagger - v_{\mathbf{k}} c_{-\mathbf{k}\downarrow} \quad \text{and} \quad \gamma_{-\mathbf{k}\downarrow}^\dagger = u_{\mathbf{k}} c_{-\mathbf{k}\downarrow}^\dagger + v_{\mathbf{k}} c_{\mathbf{k}\uparrow}. \quad (517)$$

The constants  $u_{\mathbf{k}}$  and  $v_{\mathbf{k}}$  are real and positive and satisfy

$$u_{\mathbf{k}}^2 + v_{\mathbf{k}}^2 = 1. \quad (518)$$

With this condition, the operators satisfy the commutation relations

$$\{\gamma_{\mathbf{k}\uparrow}, \gamma_{\mathbf{k}'\uparrow}\} = \{\gamma_{\mathbf{k}\uparrow}, \gamma_{-\mathbf{k}'\downarrow}\} = \{\gamma_{\mathbf{k}\uparrow}, \gamma_{-\mathbf{k}'\downarrow}^\dagger\} = 0 \quad (519)$$

$$\{\gamma_{\mathbf{k}\uparrow}^\dagger, \gamma_{\mathbf{k}'\uparrow}\} = \{\gamma_{-\mathbf{k}\downarrow}, \gamma_{-\mathbf{k}'\downarrow}^\dagger\} = \delta_{\mathbf{k},\mathbf{k}'}. \quad (520)$$

Using the Bogoliubov transformation does not allow us to diagonalize the Hamiltonian entirely. It will contain two-particle term (including four operators). However, we hope that an appropriate choice of  $u_{\mathbf{k}}$  and  $v_{\mathbf{k}}$  will remove the dominant terms.

We can rewrite  $H_{\text{BCS}}$ , using the inverse operators

$$c_{\mathbf{k}\uparrow} = u_{\mathbf{k}} \gamma_{\mathbf{k}\uparrow} + v_{\mathbf{k}} \gamma_{-\mathbf{k}\downarrow}^\dagger \quad \text{and} \quad c_{-\mathbf{k}\downarrow} = u_{\mathbf{k}} \gamma_{-\mathbf{k}\downarrow} - v_{\mathbf{k}} \gamma_{\mathbf{k}\uparrow}^\dagger \quad (521)$$

$$c_{\mathbf{k}\uparrow}^\dagger = u_{\mathbf{k}} \gamma_{\mathbf{k}\uparrow}^\dagger + v_{\mathbf{k}} \gamma_{-\mathbf{k}\downarrow} \quad \text{and} \quad c_{-\mathbf{k}\downarrow}^\dagger = u_{\mathbf{k}} \gamma_{-\mathbf{k}\downarrow}^\dagger - v_{\mathbf{k}} \gamma_{\mathbf{k}\uparrow} \quad (522)$$

Let us first rewrite the kinetic part of the Hamiltonian. Substituting the expressions for  $c$  and  $c^\dagger$  gives

$$H_0 = \sum_{\mathbf{k}\sigma} \varepsilon_{\mathbf{k}} c_{\mathbf{k}\sigma}^\dagger c_{\mathbf{k}\sigma} = \sum_{\mathbf{k}\sigma} \varepsilon_{\mathbf{k}} [c_{\mathbf{k}\uparrow}^\dagger c_{\mathbf{k}\uparrow} + c_{\mathbf{k}\downarrow}^\dagger c_{\mathbf{k}\downarrow}] \quad (523)$$

$$= \sum_{\mathbf{k}} \varepsilon_{\mathbf{k}} [u_{\mathbf{k}}^2 \gamma_{\mathbf{k}\uparrow}^\dagger \gamma_{\mathbf{k}\uparrow} + v_{\mathbf{k}}^2 \gamma_{-\mathbf{k}\downarrow}^\dagger \gamma_{-\mathbf{k}\downarrow} + u_{\mathbf{k}} v_{\mathbf{k}} (\gamma_{\mathbf{k}\uparrow}^\dagger \gamma_{-\mathbf{k}\downarrow}^\dagger + \gamma_{-\mathbf{k}\downarrow} \gamma_{\mathbf{k}\uparrow})] \quad (524)$$

$$+ v_{\mathbf{k}}^2 \gamma_{\mathbf{k}\uparrow} \gamma_{\mathbf{k}\uparrow}^\dagger + u_{\mathbf{k}}^2 \gamma_{-\mathbf{k}\downarrow} \gamma_{-\mathbf{k}\downarrow}^\dagger - u_{\mathbf{k}} v_{\mathbf{k}} (\gamma_{-\mathbf{k}\downarrow}^\dagger \gamma_{\mathbf{k}\uparrow}^\dagger + \gamma_{\mathbf{k}\uparrow} \gamma_{-\mathbf{k}\downarrow}). \quad (525)$$

$H_0$  can be simplified by introducing the number operators

$$m_{\mathbf{k}\uparrow} = \gamma_{\mathbf{k}\uparrow}^\dagger \gamma_{\mathbf{k}\uparrow}; \quad m_{-\mathbf{k}\downarrow} = \gamma_{-\mathbf{k}\downarrow}^\dagger \gamma_{-\mathbf{k}\downarrow}, \quad (526)$$

and making use of the commutation relationships of the  $\gamma$ 's. We then obtain

$$H_0 = \sum_{\mathbf{k}} \varepsilon_{\mathbf{k}} [2v_{\mathbf{k}}^2 + (u_{\mathbf{k}}^2 - v_{\mathbf{k}}^2)(m_{\mathbf{k}\uparrow} + m_{-\mathbf{k}\downarrow}) + 2u_{\mathbf{k}} v_{\mathbf{k}} (\gamma_{\mathbf{k}\uparrow}^\dagger \gamma_{-\mathbf{k}\downarrow}^\dagger + \gamma_{-\mathbf{k}\downarrow} \gamma_{\mathbf{k}\uparrow})]. \quad (527)$$

There are three different types of terms here: a constant, a term containing the number operators  $m$ , and a term containing creation and annihilation of pairs of quasi particles.

The interaction part of the Hamiltonian can now be written as

$$H_V = - \sum_{\mathbf{k}} V_{\mathbf{k}\mathbf{k}'} (u_{\mathbf{k}'} \gamma_{\mathbf{k}'\uparrow}^\dagger + v_{\mathbf{k}'} \gamma_{-\mathbf{k}'\downarrow}) (u_{\mathbf{k}'} \gamma_{-\mathbf{k}'\downarrow}^\dagger - v_{\mathbf{k}'} \gamma_{\mathbf{k}'\uparrow}) (u_{\mathbf{k}} \gamma_{-\mathbf{k}\downarrow} - v_{\mathbf{k}} \gamma_{\mathbf{k}\uparrow}^\dagger) (u_{\mathbf{k}} \gamma_{\mathbf{k}\uparrow} + v_{\mathbf{k}} \gamma_{-\mathbf{k}\downarrow}^\dagger) \quad (528)$$

$$= - \sum_{\mathbf{k}} V_{\mathbf{k}} [u_{\mathbf{k}'} v_{\mathbf{k}'} u_{\mathbf{k}} v_{\mathbf{k}} (1 - m_{\mathbf{k}'\uparrow} - m_{-\mathbf{k}'\downarrow}) (1 - m_{\mathbf{k}\uparrow} - m_{-\mathbf{k}\downarrow}) \quad (529)$$

$$+ u_{\mathbf{k}'} v_{\mathbf{k}'} (u_{\mathbf{k}}^2 - v_{\mathbf{k}}^2) (1 - m_{-\mathbf{k}'\downarrow} - m_{\mathbf{k}'\uparrow}) (\gamma_{\mathbf{k}\uparrow}^\dagger \gamma_{-\mathbf{k}\downarrow}^\dagger + \gamma_{-\mathbf{k}\downarrow} \gamma_{\mathbf{k}\uparrow})] + \text{higher order terms.} \quad (530)$$

We now want to eliminate all the off-diagonal terms to obtain a Hamiltonian of independent fermions  $\gamma$ . The first assumption is that there are the occupations  $m_{\mathbf{k}\uparrow}$  and  $m_{-\mathbf{k}\downarrow}$  are zero in the ground state. We can later verify this assumption. The off-diagonal terms that remain are

$$\sum_{\mathbf{k}} 2\varepsilon_{\mathbf{k}} u_{\mathbf{k}} v_{\mathbf{k}} (\gamma_{\mathbf{k}\uparrow}^\dagger \gamma_{-\mathbf{k}\downarrow}^\dagger + \gamma_{-\mathbf{k}\downarrow} \gamma_{\mathbf{k}\uparrow}) + \sum_{\mathbf{k}\mathbf{k}'} V_{\mathbf{k}\mathbf{k}'} u_{\mathbf{k}'} v_{\mathbf{k}'} (u_{\mathbf{k}}^2 - v_{\mathbf{k}}^2) (\gamma_{\mathbf{k}\uparrow}^\dagger \gamma_{-\mathbf{k}\downarrow}^\dagger + \gamma_{-\mathbf{k}\downarrow} \gamma_{\mathbf{k}\uparrow}) + \text{higher order terms.} \quad (531)$$

If we neglect the higher-order contributions, we are left with

$$2\varepsilon_{\mathbf{k}} u_{\mathbf{k}} v_{\mathbf{k}} + (u_{\mathbf{k}}^2 - v_{\mathbf{k}}^2) \sum_{\mathbf{k}'} V_{\mathbf{k}\mathbf{k}'} u_{\mathbf{k}'} v_{\mathbf{k}'} = 0. \quad (532)$$

However,  $u_{\mathbf{k}}$  and  $v_{\mathbf{k}}$  are not independent due to the condition  $u_{\mathbf{k}}^2 + v_{\mathbf{k}}^2 = 1$ , and we can express them in a single variable  $x_{\mathbf{k}}$ ,

$$u_{\mathbf{k}} = \sqrt{\frac{1}{2} - x_{\mathbf{k}}} \quad \text{and} \quad v_{\mathbf{k}} = \sqrt{\frac{1}{2} + x_{\mathbf{k}}}. \quad (533)$$

This transforms the equation into

$$2\varepsilon_{\mathbf{k}} \sqrt{\frac{1}{4} - x_{\mathbf{k}}^2} + 2x_{\mathbf{k}} \sum_{\mathbf{k}'} V_{\mathbf{k}\mathbf{k}'} \sqrt{\frac{1}{4} - x_{\mathbf{k}'}^2} = 0. \quad (534)$$

If we define a new quantity

$$\Delta_{\mathbf{k}} = \sum_{\mathbf{k}'} V_{\mathbf{k}\mathbf{k}'} \sqrt{\frac{1}{4} - x_{\mathbf{k}'}^2}, \quad (535)$$

then we obtain

$$2\varepsilon_{\mathbf{k}} \sqrt{\frac{1}{4} - x_{\mathbf{k}}^2} + 2x_{\mathbf{k}} \Delta_{\mathbf{k}} = 0 \quad \Rightarrow \quad \varepsilon_{\mathbf{k}}^2 \left( \frac{1}{4} - x_{\mathbf{k}}^2 \right) = x_{\mathbf{k}}^2 \Delta_{\mathbf{k}}^2 \quad (536)$$

$$\Rightarrow \quad x_{\mathbf{k}}^2 (\Delta_{\mathbf{k}}^2 + \varepsilon_{\mathbf{k}}^2) = \frac{1}{4} \varepsilon_{\mathbf{k}}^2 \quad (537)$$

or

$$x_{\mathbf{k}} = \frac{\varepsilon_{\mathbf{k}}}{2\sqrt{\Delta_{\mathbf{k}}^2 + \varepsilon_{\mathbf{k}}^2}} \quad (538)$$

Substituting  $x_{\mathbf{k}}$  in the expression for  $\Delta_{\mathbf{k}}$ , leads to the following integral equation

$$\Delta_{\mathbf{k}} = \sum_{\mathbf{k}'} V_{\mathbf{k}\mathbf{k}'} \frac{\Delta_{\mathbf{k}}}{\sqrt{\varepsilon_{\mathbf{k}}^2 + \Delta_{\mathbf{k}}^2}}, \quad (539)$$

if  $V_{\mathbf{k}\mathbf{k}'}$  is known, we can use this to solve for  $\Delta_{\mathbf{k}}$ . Let us make a simple assumption for  $V_{\mathbf{k}\mathbf{k}'}$ . We know that the matrix element is given by

$$V_{\mathbf{k}\mathbf{k}'} = -2|M_{\mathbf{k}'-\mathbf{k}}|^2 \frac{\hbar\omega_{\mathbf{k}'-\mathbf{k}}}{(\varepsilon_{\mathbf{k}} - \varepsilon_{\mathbf{k}'}) - (\hbar\omega_{\mathbf{k}'-\mathbf{k}})^2}. \quad (540)$$



We want  $V_{\mathbf{k}\mathbf{k}'}$  to be positive for an attractive interaction. This is the region that  $|\varepsilon_{\mathbf{k}} - \varepsilon_{\mathbf{k}'}| < \hbar\omega_{\mathbf{k}'-\mathbf{k}}$ . In general, phonon frequencies have an energy significantly smaller than the Fermi energy.  $E_F$  is generally of the order of a few electron volts, whereas phonon frequencies are in the region of several tenths of meV. Let us denote the maximum phonon frequency  $\omega_D$ , known as the Debye frequency. Let us for mathematical simplicity (and also for lack of information of a better  $\mathbf{k}$  dependence) assume

$$V_{\mathbf{k}\mathbf{k}'} = \begin{cases} V & \text{if } |\varepsilon_{\mathbf{k}}| < \hbar\omega_D \\ 0 & \text{otherwise} \end{cases} \quad (541)$$

Replacing the sum over momentum by an integral over energy, we obtain

$$\Delta = \frac{1}{2} \int_{-\infty}^{\infty} \rho(E) \frac{\Delta}{\sqrt{E^2 + \Delta^2}} V(E) = \frac{1}{2} V \rho(E_F) \int_{-\hbar\omega_D}^{\hbar\omega_D} \frac{\Delta}{\sqrt{E^2 + \Delta^2}} dE, \quad (542)$$

where we have assumed that the density of states does not vary too much in a region  $\hbar\omega_D$  around the Fermi surface. This equation has the solution

$$\Delta = \frac{\hbar\omega_D}{\sinh[1/V\rho(E_F)]}. \quad (543)$$

An estimate of the magnitude of  $V\rho(E_F)$  can be obtained by noting that

$$V \cong \frac{|M_{\mathbf{q}}|^2}{\hbar\omega_D}. \quad (544)$$

Earlier we had seen that

$$|M_{\mathbf{q}}|^2 \cong \frac{\hbar k_F}{MN\omega_D} |U_{\mathbf{k}}|^2 \cong \frac{m}{M} \frac{E_F}{N\hbar\omega_D} |U_{\mathbf{k}}|^2. \quad (545)$$

For a constant density of states, we can roughly estimate  $\rho(E_F) = N/E_F$ . This leaves us with

$$|M_{\mathbf{q}}|^2 \cong \frac{m}{M} \frac{1}{\rho(E_F)\hbar\omega_D} |U_{\mathbf{k}}|^2, \quad (546)$$

and hence

$$V\rho(E_F) \cong \frac{m}{M} \left( \frac{U_{\mathbf{k}}}{\hbar\omega_D} \right)^2. \quad (547)$$

The value of  $\hbar\omega_D$  is of the order of  $10^{-2}$  eV, whereas the screened Coulomb potential can be several eV. The mass ratio  $m/M$  is about  $10^{-5}$ . This makes  $V\rho(E_F)$  roughly equal to 0.1. We can therefore write

$$\Delta = 2\hbar\omega_D e^{-1/V\rho(E_F)}. \quad (548)$$

This rough estimate shows that the  $\Delta$  is a small quantity, about 1% of the Debye energy and hence corresponding to thermal energies of about 1 K.

Note that the total number of electrons is given by

$$N = \sum_{\mathbf{k}\sigma} \varepsilon_{\mathbf{k}} c_{\mathbf{k}\sigma}^\dagger c_{\mathbf{k}\sigma} \quad (549)$$

$$= \sum_{\mathbf{k}} [2v_{\mathbf{k}}^2 + (u_{\mathbf{k}}^2 - v_{\mathbf{k}}^2)(m_{\mathbf{k}\uparrow} + m_{-\mathbf{k}\downarrow}) + 2u_{\mathbf{k}}v_{\mathbf{k}}(\gamma_{\mathbf{k}\uparrow}^\dagger \gamma_{-\mathbf{k}\downarrow}^\dagger + \gamma_{-\mathbf{k}\downarrow} \gamma_{\mathbf{k}\uparrow})] \quad (550)$$

which reduces to

$$\langle N \rangle = \sum_{\mathbf{k}} 2v_{\mathbf{k}}^2. \quad (551)$$

In the absence of interactions this would be

$$\langle N \rangle = \sum_{\mathbf{k}} 2, \quad (552)$$

where the factor 2 comes from the spin. The presence of  $\Delta$  will cause a disturbance around the Fermi level given by

$$v_{\mathbf{k}}^2 = \frac{1}{2} - \frac{\varepsilon_{\mathbf{k}}}{2\sqrt{\varepsilon_{\mathbf{k}}^2 + \Delta_{\mathbf{k}}^2}}, \quad (553)$$

which basically causes a smoothing of the electron density around  $E_F$ , of the order of  $\Delta$ .

### XXXIII. BCS GROUND STATE WAVEFUNCTION AND ENERGY GAP

First, we would like to see how the ground state energy is changed by the presence of an attractive electron-phonon coupling. By performing a Bogliubov transformation, we have removed the off-diagonal terms. In addition, we have assumed that  $m_{\mathbf{k}\uparrow} = m_{-\mathbf{k}\downarrow} = 0$ . We can then write the ground state energies as

$$E_S = \sum_{\mathbf{k}} 2\varepsilon_{\mathbf{k}} v_{\mathbf{k}}^2 - \sum_{\mathbf{k}\mathbf{k}'} V_{\mathbf{k}\mathbf{k}'} u_{\mathbf{k}'} v_{\mathbf{k}'} u_{\mathbf{k}} v_{\mathbf{k}} \quad (554)$$

$$= \sum_{\mathbf{k}} \varepsilon_{\mathbf{k}} (1 + 2x_{\mathbf{k}}) - \sum_{\mathbf{k}\mathbf{k}'} V_{\mathbf{k}\mathbf{k}'} \sqrt{\left(\frac{1}{4} - x_{\mathbf{k}'}^2\right)\left(\frac{1}{4} - x_{\mathbf{k}}^2\right)}. \quad (555)$$

In the normal state, we have  $x_{\mathbf{k}}^2 = \frac{1}{4}$ . We want to find the difference between the energy in the superconducting state and the energy in the normal state, known as the condensation energy

$$E_c = E_S - E_N = \sum_{k < k_f} \varepsilon_{\mathbf{k}} (2x_{\mathbf{k}} - 1) + \sum_{k > k_f} \varepsilon_{\mathbf{k}} (2x_{\mathbf{k}} + 1) - \sum_{\mathbf{k}} \sqrt{\frac{1}{4} - x_{\mathbf{k}}^2} \Delta \quad (556)$$

$$= 2\rho(E_F) \int_0^{\hbar\omega_D} \left[ E - \frac{2E^2 + \Delta^2}{2\sqrt{E^2 + \Delta^2}} \right] dE \quad (557)$$

$$= D(E_F) \left[ (\hbar\omega_D)^2 - \hbar\omega_D \sqrt{(\hbar\omega_D)^2 + \Delta^2} \right] \quad (558)$$

$$= (\hbar\omega_D)^2 \rho(E_F) \left[ 1 - \coth \left( \frac{1}{V\rho(E_F)} \right) \right]. \quad (559)$$

In the weak coupling regime, this becomes

$$E_c \cong -2(\hbar\omega_D)^2 \rho(E_F) e^{-2/V\rho(E_F)} = -\frac{1}{2} \rho(E_F) \Delta^2. \quad (560)$$

This condensation energy is very small, only of the order of  $10^{-7}$  eV per electron, equivalent to about a millidegree Kelvin. Obviously, these are all the electrons and only the electrons in the region  $E_F - \Delta$  to  $E_F + \Delta$  are acutally affected by the attractive interaction, i.e. only a fraction  $\Delta/E_F$  of the whole number. Note that we cannot expand  $\Delta$  in terms of the interaction  $V$ , since it appears as  $1/V$  and has a singularity as  $V \rightarrow 0$ . Therefore, superconductivity cannot be understood in terms of perturbation theory.

In our derivation of the ground state, we had assumed that  $m_{\mathbf{k}\uparrow}$  and  $m_{-\mathbf{k}\downarrow}$  are zero for all  $\mathbf{k}$ . This means that there are no quasiparticles in the ground state and

$$\gamma_{\mathbf{k}\uparrow}|0\rangle = \gamma_{-\mathbf{k}\downarrow}|0\rangle = 0 \quad (561)$$

Since the  $\gamma$ 's are fermions, we have  $\gamma_{\mathbf{k}\uparrow}\gamma_{\mathbf{k}\uparrow} = 0$  and  $\gamma_{-\mathbf{k}\downarrow}\gamma_{-\mathbf{k}\downarrow} = 0$ , we can satisfy the above criterium by creating a ground state by working with the  $\gamma$ 's on the vacuum

$$\left( \prod_{\mathbf{k}} \gamma_{\mathbf{k}\uparrow} \gamma_{-\mathbf{k}\downarrow} \right) |0\rangle = \left[ \prod_{\mathbf{k}} (u_{\mathbf{k}} c_{\mathbf{k}\uparrow} - v_{\mathbf{k}} c_{-\mathbf{k}\downarrow}^\dagger) (u_{\mathbf{k}} c_{-\mathbf{k}\downarrow} + v_{\mathbf{k}} c_{\mathbf{k}\uparrow}^\dagger) \right] |0\rangle \quad (562)$$

$$= \left[ \prod_{\mathbf{k}} (u_{\mathbf{k}} v_{\mathbf{k}} + v_{\mathbf{k}}^2 c_{\mathbf{k}\uparrow}^\dagger c_{-\mathbf{k}\downarrow}^\dagger) \right] |0\rangle. \quad (563)$$

We see that this is not normalized. We can do this by dividing by  $v_{\mathbf{k}}$ ,

$$|\Psi_0\rangle = \left[ \prod_{\mathbf{k}} (u_{\mathbf{k}} + v_{\mathbf{k}} c_{\mathbf{k}\uparrow}^\dagger c_{-\mathbf{k}\downarrow}^\dagger) \right] |0\rangle. \quad (564)$$

We see that this ground state does not conserve the total number of particles. However, we need to be sure that the average number of particles is still equal to  $N$ .

The quasi-particle excitation of the system are created by the operators  $\gamma_{\mathbf{k}\uparrow}^\dagger$  and  $\gamma_{-\mathbf{k}\downarrow}^\dagger$ . We can look again at the Hamiltonian and look at the terms with  $m_{\mathbf{k}\uparrow}$  and  $m_{-\mathbf{k}\downarrow}$ . This gives

$$H_{\text{BCS}} = E_S + \sum_{\mathbf{k}} (m_{\mathbf{k}\uparrow} + m_{-\mathbf{k}\downarrow}) [(u_{\mathbf{k}}^2 - v_{\mathbf{k}}^2) \varepsilon_{\mathbf{k}} + 2u_{\mathbf{k}} v_{\mathbf{k}} \sum_{\mathbf{k}'} V_{\mathbf{k}\mathbf{k}'} u_{\mathbf{k}'} v_{\mathbf{k}'}] + \text{higher order terms}, \quad (565)$$

which becomes

$$H_{\text{BCS}} = E_S + \sum_{\mathbf{k}} \sqrt{\varepsilon_{\mathbf{k}}^2 + \Delta^2} (m_{\mathbf{k}\uparrow} + m_{-\mathbf{k}\downarrow}) + \dots \quad (566)$$

We see that the energy to make an elementary excitation is

$$E_{\mathbf{k}} = \sqrt{\varepsilon_{\mathbf{k}}^2 + \Delta^2}. \quad (567)$$

Note that this energy is always larger than  $\Delta$ . This is the opening of a superconducting gap.

Let us try to make an excitation with respect to the superconducting ground state. We now that

$$\gamma_{\mathbf{k}\uparrow} |\Psi_0\rangle = \gamma_{-\mathbf{k}\downarrow} |\Psi_0\rangle = 0, \quad (568)$$

which therefore do not produce excitations. However, operating with their conjugates does

$$\gamma_{\mathbf{k}\uparrow}^\dagger |\Psi_0\rangle = (u_{\mathbf{k}} c_{\mathbf{k}\uparrow}^\dagger - v_{\mathbf{k}} c_{-\mathbf{k}\downarrow}) \prod_{\mathbf{k}} (u_{\mathbf{k}} + v_{\mathbf{k}} c_{\mathbf{k}\uparrow}^\dagger c_{-\mathbf{k}\downarrow}^\dagger) |0\rangle \quad (569)$$

$$= (u_{\mathbf{k}}^2 c_{\mathbf{k}\uparrow}^\dagger + u_{\mathbf{k}} v_{\mathbf{k}} c_{\mathbf{k}\uparrow}^\dagger c_{\mathbf{k}\uparrow}^\dagger c_{-\mathbf{k}\downarrow}^\dagger - u_{\mathbf{k}} v_{\mathbf{k}} c_{-\mathbf{k}\downarrow} - v_{\mathbf{k}}^2 c_{-\mathbf{k}\downarrow} c_{\mathbf{k}\uparrow}^\dagger c_{-\mathbf{k}\downarrow}^\dagger) \prod_{\mathbf{k}' \neq \mathbf{k}} (u_{\mathbf{k}'} + v_{\mathbf{k}'} c_{\mathbf{k}'\uparrow}^\dagger c_{-\mathbf{k}'\downarrow}^\dagger) |0\rangle. \quad (570)$$

The second term and third term are zero because of the  $c_{\mathbf{k}\uparrow}^\dagger c_{\mathbf{k}\uparrow}^\dagger$  and  $c_{-\mathbf{k}\downarrow}$  working on the vacuum, respectively. The fourth term can be rewritten as  $-v_{\mathbf{k}}^2 c_{-\mathbf{k}\downarrow} c_{\mathbf{k}\uparrow}^\dagger c_{-\mathbf{k}\downarrow}^\dagger = v_{\mathbf{k}}^2 c_{\mathbf{k}\uparrow}^\dagger c_{-\mathbf{k}\downarrow} c_{-\mathbf{k}\downarrow}^\dagger = v_{\mathbf{k}}^2 c_{\mathbf{k}\uparrow}^\dagger$ , since  $c_{-\mathbf{k}\downarrow} c_{-\mathbf{k}\downarrow}^\dagger$  working on the vacuum gives unity. Combining the two remaining terms and making use of the fact that  $u_{\mathbf{k}}^2 + v_{\mathbf{k}}^2 = 1$ , gives

$$\gamma_{\mathbf{k}\uparrow}^\dagger |\Psi_0\rangle = c_{\mathbf{k}\uparrow}^\dagger \prod_{\mathbf{k}' \neq \mathbf{k}} (u_{\mathbf{k}'} + v_{\mathbf{k}'} c_{\mathbf{k}'\uparrow}^\dagger c_{-\mathbf{k}'\downarrow}^\dagger) |0\rangle, \quad (571)$$

which therefore creates an electron in a superconducting back ground. Similarly we can find

$$\gamma_{-\mathbf{k}\downarrow}^\dagger |\Psi_0\rangle = c_{-\mathbf{k}\downarrow}^\dagger \prod_{\mathbf{k}' \neq \mathbf{k}} (u_{\mathbf{k}'} + v_{\mathbf{k}'} c_{\mathbf{k}'\uparrow}^\dagger c_{-\mathbf{k}'\downarrow}^\dagger) |0\rangle. \quad (572)$$

Apparently, the onset of superconductivity has changed the density of states. However, we see that there is a one-to-one correspondence between the quasiparticle excitations and the electrons. We should therefore also have a unique correspondence between the superconducting density of states  $\rho_s(E)$  and  $\rho_n(\varepsilon)$  (note the energies are related to  $E_{\mathbf{k}}$  and  $\varepsilon_{\mathbf{k}}$ , respectively)

$$\rho_s(E) dE = \rho_n(\varepsilon) d\varepsilon. \quad (573)$$

Since we are only interested in the changes in density of states very close to the Fermi level, we can assume that  $\rho(\varepsilon)$  is approximately constant. We then find

$$\frac{\rho_s(E)}{\rho_n(\varepsilon)} = \frac{d\varepsilon}{dE} = \begin{cases} \frac{E}{\sqrt{E^2 - \varepsilon^2}} & E > \Delta \\ 0 & E < \Delta \end{cases}, \quad (574)$$

where we have used  $E = \sqrt{\varepsilon^2 + \Delta^2}$  and the fact that no density of states is associated with energies less than the gap energy  $\Delta$ .

#### XXXIV. TRANSITION TEMPERATURE

We managed to diagonalize the BCS Hamiltonian by choosing  $u_{\mathbf{k}}$  and  $v_{\mathbf{k}}$  such that the off-diagonal matrix elements were zero. The resulting equation was of the form

$$\sum_{\mathbf{k}} [2\varepsilon_{\mathbf{k}} u_{\mathbf{k}} v_{\mathbf{k}} - \sum_{\mathbf{k}'} V_{\mathbf{k}\mathbf{k}'} u_{\mathbf{k}'} v_{\mathbf{k}'} (1 - m_{-\mathbf{k}\downarrow} - m_{\mathbf{k}\uparrow}) (u_{\mathbf{k}}^2 - v_{\mathbf{k}}^2)] (\gamma_{\mathbf{k}\uparrow}^\dagger \gamma_{-\mathbf{k}\downarrow}^\dagger + \gamma_{-\mathbf{k}\downarrow} \gamma_{\mathbf{k}\uparrow}) = 0, \quad (575)$$

which we solved by putting  $m_{-\mathbf{k}\downarrow} = m_{\mathbf{k}\uparrow} = 0$ . Although this works well when few quasi-particle excitations are present, it obviously fails when the number of excitations becomes higher which occurs when  $k_B T$  becomes comparable

with the gap energy  $\Delta$ . We will sort this difficulty by assuming that we are still able to remove the off-diagonal terms. We are then left with the BCS Hamiltonian without off-diagonal matrix elements but with nonzero quasiparticle numbers:

$$H_{\text{BCS}} = \sum_{\mathbf{k}} 2\varepsilon_{\mathbf{k}} v_{\mathbf{k}}^2 + \sum_{\mathbf{k}} (u_{\mathbf{k}}^2 - v_{\mathbf{k}}^2) \varepsilon_{\mathbf{k}} (m_{\mathbf{k}\uparrow} + m_{-\mathbf{k}\downarrow}) - \sum_{\mathbf{k}\mathbf{k}'} V_{\mathbf{k}\mathbf{k}'} u_{\mathbf{k}'} v_{\mathbf{k}'} u_{\mathbf{k}} v_{\mathbf{k}} (1 - m_{\mathbf{k}'\uparrow} - m_{-\mathbf{k}'\downarrow}) (1 - m_{\mathbf{k}\uparrow} - m_{-\mathbf{k}\downarrow}).$$

The energy to create a quasi-particle excitation is then given by

$$E_{\mathbf{k}} = \frac{\partial \langle H_{\text{BCS}} \rangle}{\partial \langle m_{\mathbf{k}} \rangle} = (u_{\mathbf{k}}^2 - v_{\mathbf{k}}^2) \varepsilon_{\mathbf{k}} + 2u_{\mathbf{k}} v_{\mathbf{k}} \sum_{\mathbf{k}'} V_{\mathbf{k}\mathbf{k}'} u_{\mathbf{k}'} v_{\mathbf{k}'} (1 - \langle m_{\mathbf{k}'\uparrow} \rangle - \langle m_{-\mathbf{k}'\downarrow} \rangle). \quad (576)$$

Since the quasiparticles are effective fermions, they should obey Fermi-Dirac statistics

$$\langle m_{\mathbf{k}'\uparrow} \rangle = \langle m_{-\mathbf{k}'\downarrow} \rangle = \frac{1}{\exp(E_{\mathbf{k}'} / k_B T) + 1}. \quad (577)$$

There is no chemical potential since the quasiparticles are excitations with respect to the ground state. We can obtain an approximate solution by replacing the number operators by the Fermi function

$$\sum_{\mathbf{k}} [2\varepsilon_{\mathbf{k}} u_{\mathbf{k}} v_{\mathbf{k}} - (u_{\mathbf{k}}^2 - v_{\mathbf{k}}^2) \sum_{\mathbf{k}'} V_{\mathbf{k}\mathbf{k}'} u_{\mathbf{k}'} v_{\mathbf{k}'} [1 - 2f(E_{\mathbf{k}'})]] = 0. \quad (578)$$

The only difference with the original condition of Eqn. (532) is the presence of the Fermi functions in the factor  $(1 - 2f(E_{\mathbf{k}'}))$ . We again make the substitution for the gap energy but now including the Fermi function

$$\Delta_{\mathbf{k}}(T) = \sum_{\mathbf{k}'} V_{\mathbf{k}\mathbf{k}'} \sqrt{\frac{1}{4} - x_{\mathbf{k}'}^2} [1 - 2f(E_{\mathbf{k}'})]. \quad (579)$$

and obtain again

$$x_{\mathbf{k}} = \frac{\varepsilon_{\mathbf{k}}}{2\sqrt{\Delta_{\mathbf{k}}^2(T) + \varepsilon_{\mathbf{k}}^2}}. \quad (580)$$

The temperature-dependent gap equation is then

$$\Delta_{\mathbf{k}}(T) = \sum_{\mathbf{k}'} V_{\mathbf{k}\mathbf{k}'} \frac{\Delta_{\mathbf{k}}(T)}{\sqrt{\varepsilon_{\mathbf{k}}^2 + \Delta_{\mathbf{k}}^2(T)}} [1 - 2f(E_{\mathbf{k}'})] \quad (581)$$

and by taking the thermal average of the energy The energy to create a quasi-particle excitation is then given by

$$E_{\mathbf{k}} = (u_{\mathbf{k}}^2 - v_{\mathbf{k}}^2) \varepsilon_{\mathbf{k}} + 2u_{\mathbf{k}} v_{\mathbf{k}} \sum_{\mathbf{k}'} V_{\mathbf{k}\mathbf{k}'} u_{\mathbf{k}'} v_{\mathbf{k}'} [1 - 2f(E_{\mathbf{k}'})] = \sqrt{\varepsilon_{\mathbf{k}}^2 + \Delta_{\mathbf{k}}^2(T)}, \quad (582)$$

which is equivalent to the quasiparticle excitation energy except that the gap is now temperature dependent.

Now since

$$1 - 2f(E_{\mathbf{k}}) = 1 - 2 \frac{1}{e^{\frac{E_{\mathbf{k}}}{k_B T}} + 1} = \frac{e^{\frac{E_{\mathbf{k}}}{k_B T}} + 1 - 2}{e^{\frac{E_{\mathbf{k}}}{k_B T}} + 1} = \frac{e^{\frac{E_{\mathbf{k}}}{2k_B T}} - e^{-\frac{E_{\mathbf{k}}}{2k_B T}}}{e^{\frac{E_{\mathbf{k}}}{2k_B T}} + e^{-\frac{E_{\mathbf{k}}}{2k_B T}}} = \tanh \frac{E_{\mathbf{k}}}{2k_B T}, \quad (583)$$

we obtain for the gap equation

$$\Delta_{\mathbf{k}}(T) = \sum_{\mathbf{k}'} V_{\mathbf{k}\mathbf{k}'} \frac{\Delta_{\mathbf{k}}(T)}{\sqrt{\varepsilon_{\mathbf{k}}^2 + \Delta_{\mathbf{k}}^2(T)}} \tanh \frac{\sqrt{\varepsilon_{\mathbf{k}}^2 + \Delta_{\mathbf{k}}^2(T)}}{2k_B T}. \quad (584)$$

Using the approximations of a constant density of states and an constant interaction limited to a region of width  $2\hbar\omega_D$  around the Fermi level, we obtain the equation

$$V\rho(E_F) \int_0^{\hbar\omega} dE \frac{\tanh \frac{\sqrt{E^2 + \Delta(T)}}{2k_B T}}{\sqrt{E^2 + \Delta(T)}} = 1. \quad (585)$$

At  $T = 0$ , the argument of the tanh, which contains  $1/T$  goes to infinity, and hence the tanh approaches 1 and we recover the original gap equation. For finite temperatures, the numerator decreases, which implies that the denominator should decrease as well. This means that the value of  $\Delta$  decreases. At first, this decrease is very slow, until  $k_B T$  becomes comparable to the gap energy  $\Delta$ . We obtain a rapid increase in quasiparticle excitations. We then obtain a more rapid drop in  $\Delta$  until it vanishes at the transition temperature. For  $\Delta(T_c) = 0$ , we have

$$V\rho(E_F) \int_0^{\hbar\omega} dE \frac{\tanh \frac{E}{k_B T_c}}{E} = 1 \quad (586)$$

or

$$V\rho(E_F) \int_0^{\hbar\omega} dx \frac{\tanh x}{x} = 1. \quad (587)$$

The integral is somewhat annoying but partial integration gives

$$[\ln x \tanh x]_0^{\hbar\omega_D} - \int_0^{\hbar\omega_D} \frac{1}{\cosh^2 x} \ln x dx = \frac{1}{V\rho(E_F)}. \quad (588)$$

In the weak coupling limit,  $k_B T_c$  is expected to be small compared to  $\hbar\omega_D$ . This means that the tanh will be close to unity and that we can take the integral to infinity:

$$\ln \frac{\hbar\omega_D}{2k_B T_c} - \int_0^{\infty} \frac{1}{\cosh^2 x} \ln x dx = \frac{1}{V\rho(E_F)}. \quad (589)$$

The integral turn out to be 0.44 (???0.56?), which gives

$$\frac{\hbar\omega_D}{2k_B T_c} = e^{0.44 + \frac{1}{V\rho(E_F)}} \Rightarrow k_B T_c = 2\hbar\omega_D e^{-0.44} e^{-\frac{1}{V\rho(E_F)}} = 1.14\hbar\omega_D e^{-\frac{1}{V\rho(E_F)}}. \quad (590)$$

Comparing this with the equation for the gap in the weak-coupling limit gives

$$\frac{2\Delta(0)}{k_B T_c} = 3.50. \quad (591)$$

This is reasonable agreement with most experimentally observed values for BCS-type superconductors.

### XXXV. GINZBURG-LANDAU THEORY

Ginzburg-Landau theory is a phenomenological theory which was developed before BCS theory. Ginzburg and Landau suggested a pseudowavefunction  $\psi(\mathbf{r})$  and suggested a free energy expanded in terms of  $|\psi|^2$  and  $|\nabla\psi|^2$ . Although relatively successful in explaining a number of phenomena, the lack of microscopic derivation led to an initial neglect of the work in the Western literature. However, in 1959, Gor'kov demonstrated that the Ginzburg-Landau theory can be directly related to BCS theory in the limit that the spatial variations of  $\psi(\mathbf{r})$  are not too rapid and that the temperature are close to the transition temperature. The pseudowavefunction turns out to be directly related to the gap parameter  $\Delta(\mathbf{r})$ . The derivation is however rather lengthy and will be omitted.

The basic postulate of Ginzburg and Landau is that the free energy in the superconducting state  $F_s$  can be expanded in a series of the form

$$F_s = F_n + \alpha|\psi|^2 + \frac{\beta}{2}|\psi|^4 + \frac{1}{2m^*} |(-i\hbar\nabla - e\mathbf{A})\psi|^2, \quad (592)$$

where  $F_n$  is the free energy in the normal state;  $m^*$  is the effective mass. If we identify  $\psi$  with the superconducting current, we can take as  $m^* = 2m$  corresponding to the Cooper pairs in the supercurrent. However, the mass might be different from  $2m$  due to mass renormalization related to the electron-phonon interactions. When the spatial variations are small and in the absence of external fields, the difference is given by

$$F_s - F_n = \alpha|\psi|^2 + \frac{\beta}{2}|\psi|^4. \quad (593)$$

As is obvious, we have to different cases. Either  $|\psi|^2 = 0$ , in which case we have the normal state, or

$$|\psi|^2 = |\psi_\infty|^2 = -\frac{\alpha}{\beta}, \quad (594)$$

where by  $\psi_\infty$ , we imply the pseudowavefunction deep inside the superconductor or for an infinite system where the effects of external fields are negligible. Since  $|\psi|^2$  is always positive,  $\frac{\alpha}{\beta}$  should be negative to find a non zero solution for  $|\psi|^2$ . This means that either  $\alpha$  or  $\beta$  is negative. We impose that the difference in free energy goes to infinity for  $|\psi|^2 \rightarrow \infty$ , so that we do not obtain an enormous energy gain by increasing the pseudowavefunction. This leaves the parameter  $\alpha$ . Then, when  $\alpha > 0$ , we do not find a superconducting state since the minimum lies at  $|\psi|^2 = 0$ . We do find a finite value for  $|\psi|^2$  if  $\alpha < 0$ . Substituting the value back into the difference of the free energy gives

$$F_s - F_n = -\frac{\alpha^2}{2\beta}. \quad (595)$$

This energy can be related to the Meissner effect found in 1933. Meissner and Ochsenfeld discovered the the magnetic field is excluded from a superconductor. In addition, not only is the magnetic field excluded from a superconductor, which might be explained by a perfect conductor, the magnetic field is also expelled from the superconductor when going through the transition temperature. This cannot be explained by perfect conductivity which would trap the flux lines inside the superconductor. When can define the critical field as the work done by the magnetic field to destroy the superconductivity, i.e.

$$\frac{1}{2}\mu_0 H^2 = F_n - F_s = \frac{\alpha^2}{2\beta}. \quad (596)$$

Apparently  $\alpha$  should change sign at the transition temperature. If we only take the leading term, we have

$$\alpha = \alpha_0 \left( \frac{T}{T_c} - 1 \right). \quad (597)$$

This directly says that

$$|\psi|^2 \sim \left( 1 - \frac{T}{T_c} \right) \Rightarrow \Delta \sim \sqrt{1 - \frac{T}{T_c}}, \quad (598)$$

where we have made use of the Gor'kov's result that  $\psi$  and  $\Delta$  are related. Using variational methods, we can also write the problem in the celebrated Ginzburg-Landau differential equation

$$\alpha\psi + \beta|\psi|^2\psi + \frac{1}{2m^*} |(-i\hbar\nabla - e\mathbf{A})|^2 \psi = 0. \quad (599)$$

To gain some insight into this equation let us consider it in one dimension and in the absence of external fields and introduce a normalized wavefunction  $f = \psi/\psi_\infty$  with  $\psi_\infty^2 = -\alpha/\beta$ , giving

$$-\frac{\hbar^2}{2m^*} \frac{d^2\psi}{dx^2} + \alpha\psi + \beta\psi^3 = 0 \Rightarrow -\frac{\hbar^2}{2m^*\alpha\psi_\infty} \frac{d^2\psi}{dx^2} + \frac{\psi}{\psi_\infty} + \frac{\beta}{\alpha} \frac{\psi^3}{\psi_\infty^3} = 0, \quad (600)$$

which gives

$$\frac{\hbar^2}{2m^*|\alpha|} \frac{d^2f}{dx^2} + f - f^3 = 0. \quad (601)$$

This makes it natural to introduce a characteristic length  $\xi(T)$  given by

$$\xi(T)^2 = \frac{\hbar^2}{2m^*|\alpha|} \Rightarrow \xi(T) \sim \frac{1}{\sqrt{1 - \frac{T}{T_c}}}. \quad (602)$$

$\xi(T)$  is known as the coherence length. Note that it diverges as the temperature approaches  $T_c$ . This means that the superconducting state becomes very sensitive to minor disturbances. Compare this to ferromagnetism, where the

susceptibility diverges close to the critical temperature. Although the magnetization is small, the magnetism is very sensitive to external effects such as an applied magnetic field. We can then rewrite the differential equation as

$$\xi(T)^2 \frac{d^2 f}{dx^2} + f - f^3 = 0. \quad (603)$$

Let us consider the situation where the  $f$  is close to unity. We can then write  $f(x) = 1 + g(x)$ , where  $g(x) \ll 1$ . To lowest order we can write

$$\xi(T)^2 \frac{d^2 g}{dx^2} + (1 + g + \dots) - (1 + 3g + \dots) = 0 \quad (604)$$

or

$$\frac{d^2 g}{dx^2} = \frac{2}{\xi(T)^2} g, \quad (605)$$

which has a solution

$$g(x) \sim \exp\left(\pm \frac{\sqrt{2}x}{\xi(T)}\right). \quad (606)$$

This means that a small disturbance of  $\psi$  from  $\psi_\infty$  we decay exponentially over a characteristic length of order  $\xi(T)$ .

### XXXVI. FLUX QUANTIZATION AND THE JOSEPHSON EFFECT

Let us first consider the effects of the magnetic field on the current carried by an electron. The Hamiltonian of a free particle in the presence of a magnetic field given by  $\mathbf{B} = \nabla \times \mathbf{A}$  is of the form

$$H = \frac{(\mathbf{p} - e^* \mathbf{A})^2}{2m^*}, \quad (607)$$

where  $m^*$  and  $e^*$  are the effective mass and charge of the Cooper pairs, respectively. However, if the vector potential is of the form

$$\mathbf{A} = (A, 0, 0), \quad (608)$$

where  $A$  is a constant, then  $\nabla \times \mathbf{A}$  would vanish and there would be no magnetic field. The eigenstates would be

$$\psi(\mathbf{r}) = \exp[i(k_x x + k_y y + k_z z)] \quad (609)$$

with energies

$$E = \frac{\hbar^2}{2m^*} \left[ \left(k_x - \frac{e^* A}{\hbar}\right)^2 + k_y^2 + k_z^2 \right]. \quad (610)$$

Let us now consider a superconducting ring. The energy in the  $x$  direction is then given by

$$E = \frac{\hbar^2}{2m^*} \left(k_x - \frac{2eA}{\hbar}\right)^2, \quad (611)$$

where we have introduced the effective charge  $2e$  for superconducting pairs. We have defined an effective mass  $m^*$  (which could in principle also include some bandstructure effects). The wavevector in the  $x$  direction is quantized giving

$$E = \frac{\hbar^2}{2m^*} \left(\frac{2\pi n}{L} - \frac{2eA}{\hbar}\right)^2, \quad (612)$$

Although the Meissner effect will remove the magnetic field inside the superconductor, there can still be flux inside the ring. This magnetic flux is given by

$$\Phi = \int \mathbf{B} \cdot d\mathbf{a} = \int \nabla \times \mathbf{A} \cdot d\mathbf{a} = \int \mathbf{A} \cdot d\mathbf{l} = AL, \quad (613)$$

where  $L$  is the circumference of the ring. We can then write the energy as

$$E = \frac{2\hbar^2}{m^*L^2} \left( \pi n - \frac{eAL}{\hbar} \right)^2 = \frac{2\hbar^2}{m^*L^2} \left( \pi n - \frac{e\Phi}{\hbar} \right)^2. \quad (614)$$

The total energy of the system as a function of the flux then becomes a periodic function of  $\Phi$ . The energy is given by parabola centered around  $n\Phi_0$ . If  $n = 0$ , there will be a minimum in the energy around zero. If the flux increases the energy increases. However, if the flux exceeds  $\pi\hbar/e$ , then it becomes energetically favorable for the electron to make a transition to  $n = 1$ . The new energy minimum then lies around  $\Phi = \pi\hbar/e$ , and so on. This leads us to the conclusion that the flux prefers to be quantized in flux quanta  $\Phi_0$ , i.e.

$$\Phi = n\Phi_0 = n \frac{\pi\hbar}{e}. \quad (615)$$

We can also look at the current as a function of the flux. The current is related to the flux as follows

$$I m \frac{d\mathbf{r}}{dt} = \hbar\mathbf{k} - 2e\mathbf{A} = \frac{2\pi n}{L} - \frac{2e\Phi}{\hbar L} \frac{\partial E}{\partial \Phi}. \quad (616)$$

The current is therefore directly proportional to  $\Phi$ . It crosses zero at  $n\Phi_0$  and makes discrete jumps around  $(n + \frac{1}{2})\Phi_0$ .

The concepts above can be applied to an interesting device known as a Josephson junction. Let us consider a ring with a narrow insulating layer somewhere in the ring. This layer should be thin enough that it allows tunneling of superconducting pairs. Let us first envision an experiment where the flux is held constant. Since  $E = -\frac{\partial A}{\partial t} = -\frac{1}{L} \frac{\partial \Phi}{\partial t}$ , the electric field is zero and hence  $V = EL = 0$ . However, we saw that for  $\Phi \neq n\Phi_0$ , there is a finite current. Therefore, there must be a current at zero voltage. This is known as the DC (direct current) Josephson effect.

The other experiment that we can envision is keeping the voltage constant. This implies that the flux is  $\Phi = Vt$ . Therefore the current will be a sawtooth as a function of time. The current will be alternating with a frequency

$$\Phi_0 = VT \quad \Rightarrow \quad \omega = \frac{2\pi}{T} = \frac{2\pi V}{\Phi_0} = \frac{2eV}{\hbar}, \quad (617)$$

which is of the order of  $\frac{1}{2}$  GHz per microvolt. This is known as the AC Josephson effect.

## APPENDIX A: 666

The number 666 has a pretty bad reputation, related to its mentioning in the Book of Revelation 13:17-18:

And that no man might buy or sell, save he that had the mark, or the name of the beast, or the number of his name. Here is wisdom. Let him that hath understanding count the number of the beast: for it is the number of a man; and his number is six hundred threescore and six.

Many scholars believe that the number 666 stands for the emperor Nero. In Hebrew gematria, every letter corresponds to a number. The Hebrew transliteration of the Greek "Nerōn Kaisar" adds up to 666.

It has some other nice properties as well:

$$\sum_{i=1}^{6 \times 6} i = 666, \quad (A1)$$

so the number on the roulette table add up to 666. In Roman numerals, we have

$$666 = DCLXVI, \quad (A2)$$

so 666 uses every Roman numeral symbol (except  $M$ ). Also, 666 is the sum of the first seven prime numbers

$$2^2 + 3^2 + 5^2 + 7^2 + 11^2 + 13^2 + 17^2 = 666. \quad (A3)$$

If you are afraid of the symbolic meanings behind the number 666, you might be suffering from hexakosioihexekonta-hexaphobia. (If the number 13 worries you, it is called triskaidekaphobia.)

And poor 667?  $23 \times 29$ ?



**Homework 9/24/09**

We want to consider the formation of a  $sp$  hybrid between carbon and hydrogen atoms. We take the  $z$ -axis along the carbon-hydrogen bond.

1a. Let us consider the  $\sigma$  bonding orbitals. Denote the carbon  $2s$ , carbon  $2p_z$ , and hydrogen  $1s$  as  $|C_{2s}\rangle$ ,  $|C_{2p_z}\rangle$ , and  $|H_{1s}\rangle$ , respectively. (the carbon  $1s$  orbitals are strongly bound and can be neglected). Write the Hamiltonian as a matrix, using

$$T_{ss} = \langle C_{2s}|H|H_{1s}\rangle, \quad T_{ps} = \langle C_{2p_z}|H|H_{1s}\rangle, \quad \varepsilon_C = \langle C_{2s}|H|C_{2s}\rangle = \langle C_{2p_z}|H|C_{2p_z}\rangle, \quad \varepsilon_H = \langle H_{1s}|H|H_{1s}\rangle$$

1b. We see that the carbon  $2s$  and  $2p_z$  both couple to the hydrogen. Combine these two orbitals into  $sp$  hybrids and calculate the coupling between the hybrids and the hydrogen.

1c. Write down the  $3 \times 3$  matrix for the carbon  $sp$  hybrids and hydrogen and determine the eigenenergies for  $T_{ss} = T_{sp}$ .

Let us consider a infinite one-dimensional chain of hydrogen atoms with interatomic distance  $a$ . Apply periodic boundary conditions. We only consider the  $1s$  orbitals.

2a. Derive the eigenenergies for a nearest-neighbor matrix element  $t_1$  (distance  $a$ ) and a next-nearest-neighbor matrix elements  $t_2$  (distance  $2a$ ).

2b. Plot the eigenvalues as a function of momentum  $k$  with  $-\frac{\pi}{a} \leq k \leq \frac{\pi}{a}$ . Take  $t_2 = \frac{1}{2}t_1 < 0$ .

2c. For what  $k$ -values are the eigenvalues maximum.

### Answers Homework 9/24/09

1a.

$$H = \begin{pmatrix} \varepsilon_O & 0 & T_{ss} \\ 0 & \varepsilon_O & T_{sp} \\ T_{ss} & T_{sp} & \varepsilon_H \end{pmatrix} \quad (\text{A4})$$

1b. The  $sp$  hybrids are given by

$$|O_{sp}^{\pm}\rangle = \frac{1}{\sqrt{2}}(|O_{2s}\rangle \pm |O_{2p_z}\rangle). \quad (\text{A5})$$

The coupling to the Hydrogen is now

$$\langle H_{1s}|H|O_{sp}^{\pm}\rangle = \langle H_{1s}|H\frac{1}{\sqrt{2}}(|O_{2s}\rangle \pm |O_{2p_z}\rangle) = \frac{1}{\sqrt{2}}(T_{ss} \pm T_{sp}) \quad (\text{A6})$$

1c.

$$H = \begin{pmatrix} \varepsilon_O & 0 & \frac{1}{\sqrt{2}}(T_{ss} - T_{sp}) \\ 0 & \varepsilon_O & \frac{1}{\sqrt{2}}(T_{ss} + T_{sp}) \\ \frac{1}{\sqrt{2}}(T_{ss} - T_{sp}) & \frac{1}{\sqrt{2}}(T_{ss} + T_{sp}) & \varepsilon_H \end{pmatrix} \quad (\text{A7})$$

when  $T = T_{ss} = T_{sp}$ , the eigenvalue problem becomes

$$H = \begin{pmatrix} \varepsilon_O - E & 0 & 0 \\ 0 & \varepsilon_O - E & \sqrt{2}T \\ 0 & \sqrt{2}T & \varepsilon_H - E \end{pmatrix} \quad (\text{A8})$$

This has one eigenvalue  $E = \varepsilon_O$ , the other two eigenvalues are given by the determinant of the remaining  $2 \times 2$  matrix:

$$(\varepsilon_O - E)(\varepsilon_H - E) - 2T^2 = E^2 - (\varepsilon_O + \varepsilon_H)E + \varepsilon_O\varepsilon_H - 2T^2 \quad (\text{A9})$$

giving

$$E_{1,2} = \frac{1}{2}(\varepsilon_O + \varepsilon_H) \pm \frac{1}{2}\sqrt{(\varepsilon_O + \varepsilon_H)^2 - 4(\varepsilon_O\varepsilon_H - 2T^2)} = \frac{1}{2}(\varepsilon_O + \varepsilon_H) \pm \frac{1}{2}\sqrt{(\varepsilon_O - \varepsilon_H)^2 + 8T^2} \quad (\text{A10})$$

2a.

$$\varepsilon_k = 2t_1 \cos ka + 2t_2 \cos 2ka. \quad (\text{A11})$$

2c.

$$\frac{d\varepsilon_k}{dk} = -2t_1 \sin ka - 4t_2 \sin 2ka = -2t_1 \sin ka - 8t_2 \sin ka \cos ka \quad (\text{A12})$$

$$= -2 \sin ka(t_1 + 4t_2 \cos ka). \quad (\text{A13})$$

This gives

$$\cos ka = -\frac{t_1}{4t_2} = -\frac{1}{2} \Rightarrow k = \frac{2\pi}{3a} \quad (\text{A14})$$

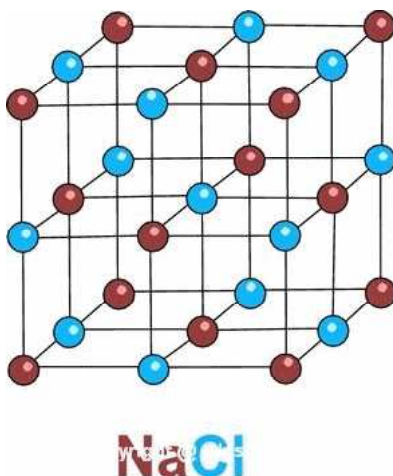


FIG. 62: The NaCl lattice.

**Homework 10/15/09**

- 1a. Figure 62 shows the lattice for sodium chloride (NaCl). Express the lattice in lattice vectors plus a basis.
  - 1b. Calculate the structure factor  $S_{\mathbf{K}}$ .
  - 1c. Show for what wave vectors Bragg diffraction occurs. What type of lattice do these (reciprocal) wavevectors form?
  - 1d. Calculate the intensities of the Bragg peaks.
- 2a. An atom is surrounded by four other atoms in planar symmetry, see Fig. 63. We are considering the  $2p$  orbitals ( $p_\eta$  with  $\eta = x, y, z$ ) on the central atom. On the surrounding atom we consider only the  $1s$  orbitals (denoted as  $s_i$ , where  $i = 1, 2, 3, 4$  numbers the surrounding atoms). The  $2p$  orbitals hybridize with the neighboring  $1s$  orbitals. In other words, there are finite matrix elements  $\langle p_\eta | H | s_i \rangle$ . However, due to symmetry not all matrix are finite. What combinations of  $\eta$  and  $i$  give a nonzero matrix element?
  - 2b. Calculate the eigenenergies (denote the value of the nonzero matrix elements as  $t$ ).
  - 2c. The hybridization has split the  $2p$  level. Is the splitting what you would expect from symmetry considerations? (Explain).

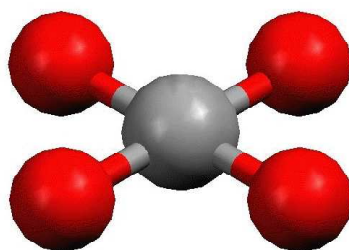


FIG. 63: A central atom is surrounded by four atoms in a planar symmetry.